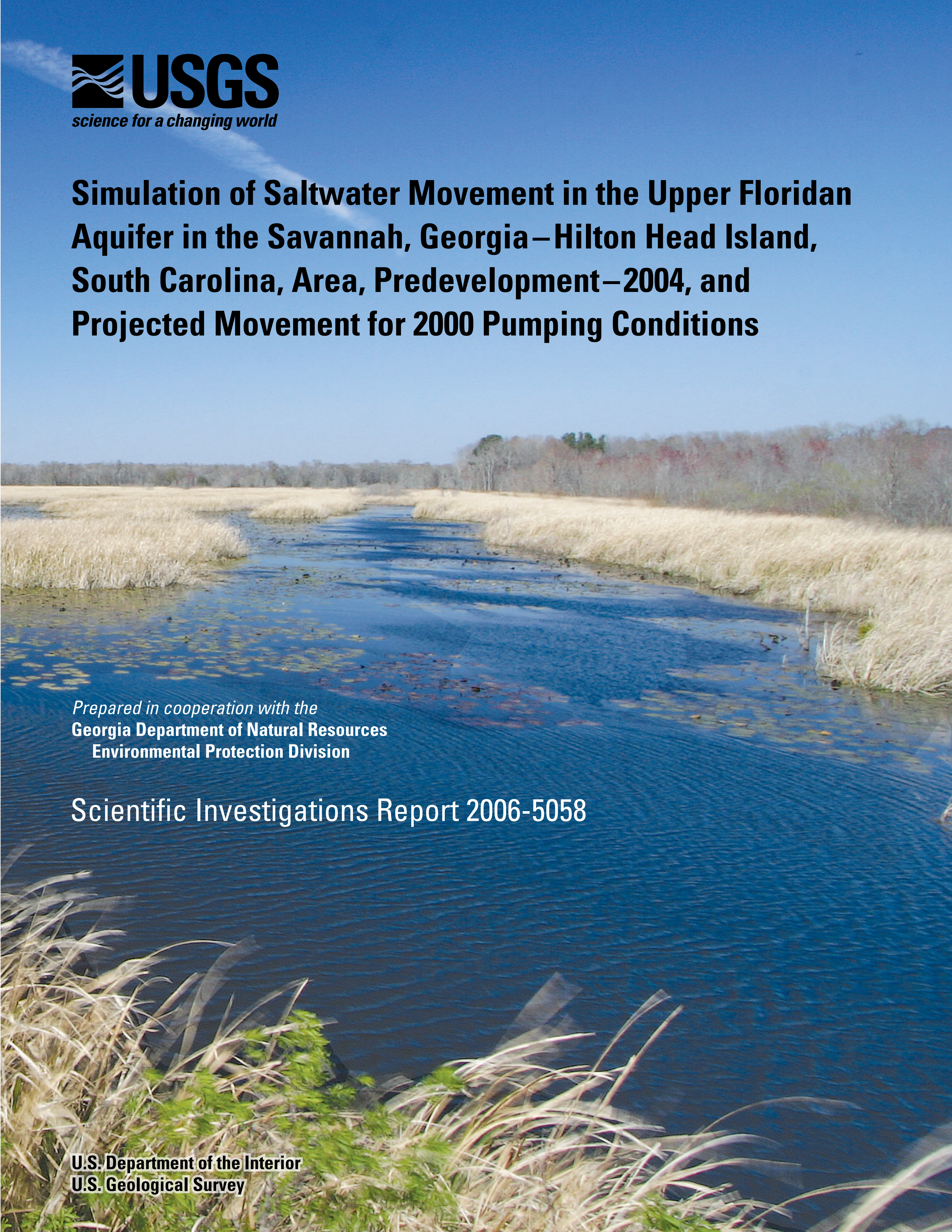

Simulation of Saltwater Movement in the Upper Floridan Aquifer in the Savannah, Georgia–Hilton Head Island, South Carolina, Area, Predevelopment–2004, and Projected Movement for 2000 Pumping Conditions

Prepared in cooperation with the
Georgia Department of Natural Resources
Environmental Protection Division

Scientific Investigations Report 2006-5058

U.S. Department of the Interior
U.S. Geological Survey

Cover photograph: Savannah National Wildlife Refuge, near Savannah, Georgia

Photograph by Alan M. Cressler, U.S. Geological Survey, 2006

Simulation of Saltwater Movement in the Upper Floridan Aquifer in the Savannah, Georgia–Hilton Head Island, South Carolina, Area, Predevelopment–2004, and Projected Movement for 2000 Pumping Conditions

By Alden M. Provost, Dorothy F. Payne, and Clifford I. Voss

Prepared in cooperation with the
Georgia Department of Natural Resources,
Environmental Protection Division

Scientific Investigations Report 2006-5058

U.S. Department of the Interior
U.S. Geological Survey

U.S. Department of the Interior
Gale A. Norton, Secretary

U.S. Geological Survey
Charles G. Groat, Director

U.S. Geological Survey, Reston, Virginia: 2006

This report is a Web-only publication: *pubs.usgs.gov/sir/2006/5058/*

For more information about the USGS and its products:
Telephone: 1-888-ASK-USGS
World Wide Web: *http://www.usgs.gov/*

Suggested citation:
Provost, A.M., Payne, D.F., and Voss, C.I., 2006, Simulation of saltwater movement in the Upper Floridan aquifer in the Savannah, Georgia–Hilton Head Island, South Carolina, area, predevelopment–2004, and projected movement for 2000 pumping conditions: U.S. Geological Survey SIR 2006-5058, 132 p.

Contents

Figures

Tables

Conversion Factors, Datum, and Abbreviations

Multiply	By	To obtain
	Length	
foot (ft)	0.3048	meter (m)
mile (mi)	1.609	kilometer (km)
	Area	
square mile (mi^2)	2.590	square kilometer (km^2)
	Volume	
million gallons (Mgal)	3,785	cubic meter (m^3)
	Flow rate	
cubic foot per second (ft^3/s)	0.02832	cubic meter per second (m^3/s)
cubic foot per day (ft^3/d)	0.02832	cubic meter per day (m^3/d)
inch per year (in/yr)	25.4	millimeter per year
kilogram per second (kg/s)	3,051	cubic meter per second (m^3/s)
million gallons per day (Mgal/d)	0.04381	cubic meter per second (m^3/s)
	Hydraulic conductivity	
foot per day (ft/d)	0.3048	meter per day (m/d)
	Transmissivity*	
foot squared per day (ft^2/d)	0.09290	meter squared per day (m^2/d)
	Permeability	
meter squared (m^2)	10.76	foot squared (ft^2)

Temperature in degrees Celsius (°C) may be converted to degrees Fahrenheit (°F) as follows:

$$°F = (1.8 \times °C)+32$$

Temperature in degrees Fahrenheit (°F) may be converted to degrees Celsius (°C) as follows:

$$°C = (°F–32)/1.8$$

Vertical coordinate information is referenced to the North American Vertical Datum of 1988 (NAVD 88).

Horizontal coordinate information is referenced to the North American Datum of 1983 (NAD 83).

Altitude, as used in this report, refers to distance above the vertical datum.

*Transmissivity: The standard unit for transmissivity is cubic foot per day per square foot times foot of aquifer thickness $[(ft^3/d)/ft^2]ft$. In this report, the mathematically reduced form, foot squared per day (ft^2/d), is used for convenience.

Specific conductance is given in microsiemens per centimeter at 25 degrees Celsius (µS/cm at 25 °C).

Concentrations of chemical constituents in water are given either in milligrams per liter (mg/L) or micrograms per liter (µg/L).

Additional abbreviated units and symbols used in this report:

ft^{-2}	foot to the negative 2
$[kg/(m \cdot s^2)]^{-1}$	kilogram per meter second squared to the negative one
kg/kg	kilogram per kilogram
kg/m^3	kilogram per cubic meter
m^2/s	meter squared per second
mS/cm	millisiemens per centimeter

Abbreviations used in this report:

CSSI	Coastal Sound Science Initiative
GaEPD	Georgia Environmental Protection Division
MODFLOW	Modular Ground-Water Model
RASA	Regional Aquifer System Analysis
RMSE	root-mean-square error
SCDHEC	South Carolina Department of Health and Environmental Control
SUTRA	Saturated-Unsaturated Transport Simulator
UCODE	Universal Inverse Modeling Simulator
USEPA	U.S. Environmental Protection Agency
USGS	U.S. Geological Survey

Simulation of Saltwater Movement in the Upper Floridan Aquifer in the Savannah, Georgia–Hilton Head Island, South Carolina, Area, Predevelopment–2004, and Projected Movement for 2000 Pumping Conditions

By Alden M. Provost, Dorothy F. Payne, and Clifford I. Voss

Abstract

A digital model was developed to simulate ground-water flow and solute transport for the Upper Floridan aquifer in the Savannah, Georgia–Hilton Head Island, South Carolina, area. The model was used to (1) simulate trends of saltwater intrusion from predevelopment to the present day (1885–2004), (2) project these trends from the present day into the future, and (3) evaluate the relative influence of different assumptions regarding initial and boundary conditions and physical properties. The model is based on a regional, single-density ground-water flow model of coastal Georgia and adjacent parts of South Carolina and Florida.

Variable-density ground-water flow and solute transport were simulated using the U.S. Geological Survey finite-element, variable-density solute-transport simulator SUTRA, 1885–2004. The model comprises seven layers: the surficial aquifer system, the Brunswick aquifer system, the Upper Floridan aquifer, the Lower Floridan aquifer, and the intervening confining units.

The model was calibrated to September 1998 water levels, for single-density freshwater conditions, then refined using variable density and chloride concentration to give a reasonable match to the trend in the chloride distribution in the Upper Floridan aquifer inferred from field measurements of specific conductance made during 2000, 2002, 2003, and 2004. The model was modified to simulate solute transport by allowing saltwater to enter the system through localized areas near the northern end of Hilton Head Island, at Pinckney Island, and near the Colleton River, and was calibrated to match chloride concentrations inferred from field measurements of specific conductance. This simulation is called the “Base Case.” Water-level residuals ranged from –5.3 to 23.4 feet for September 1998 conditions and single-density freshwater conditions. When chloride transport was simulated, water-level residuals ranged from –12.5 to 23.3 feet. The simulated chloride distribution captures the general trends in the field data. Chloride transport is sensitive to the permeabilities assigned to the confining units in the source areas and the porosity assigned to the Upper Floridan aquifer.

Results of the study indicate that

1. if present-day (year 2000) pumping conditions are maintained, plumes of saltwater in the Upper Floridan aquifer will continue to expand and move toward Savannah and across Hilton Head Island;

2. the rate of movement of the 250-mg/L (milligram per liter) isochlor toward Savannah is between 144 feet per year and 190 feet per year and that the 250-mg/L isochlor could reach the pumping center at Savannah in 800 years;

3. if effective porosities are lower than those used in the model, as is likely, higher rates of solute transport would result; and

4. plumes may have occurred along the northern shore of Hilton Head Island before substantial development began in the mid-1960s, and lesser amounts of intrusion may have already occurred prior to the onset of pumping during 1885.

Model limitations include uncertainty in (1) field data, (2) the conceptual model, (3) the physical properties and representation of the hydrogeologic framework, and (4) uncertainty in the boundary and initial conditions. Results of simulations projected far into the future must be interpreted with caution because they are based on an assumed future pumping distribution and fixed boundary conditions, and because these conditions may differ substantially from those for which the model is calibrated.

Introduction

Saltwater contamination has occurred in the Upper Floridan aquifer in South Carolina in the Parris Island and Beaufort areas since the early 1900s, and in the Hilton Head Island area since the late 1970s. During the last century, increased ground-water pumpage because of population growth, increased tourism, and sustained industrial activity in the coastal area of Georgia and South Carolina have resulted in water-level declines and increased potential for saltwater contamination. A period of drought during 1998–2002 also increased stresses on the coastal ground-water system. The coastal population is projected to increase during the next several decades, resulting in increased, competing ground-water demands.

The Upper Floridan aquifer is the principal source of water in the coastal area. It is an extremely permeable, high-yielding aquifer that was first developed in the late 1800s, and has been used extensively ever since. Pumping from the Upper Floridan aquifer has resulted in substantial water-level decline in Savannah, Georgia, and local declines on Hilton Head Island, South Carolina. Saltwater contamination in South Carolina has constrained further development of the Upper Floridan aquifer in the coastal area of South Carolina and has created competing demands for the available supply of water. As part of the 1997–2005 interim water-management strategy, the Georgia Environmental Protection Division (GaEPD) capped permitted withdrawal from the Upper Floridan aquifer in the study area at 1997 rates in Chatham County and in southern Effingham and Bryan Counties, and permitted only an additional 36 million gallons per day (Mgal/d) in coastal counties to limit further saltwater contamination. In South Carolina, the South Carolina Department of Health and Environmental Control (SCDHEC) has been monitoring pumping rates since the mid-1980s in Beaufort and Jasper Counties.

To provide information required for development of a water-management strategy to address these problems and the effect of projected future coastal water-resource needs, during 1997 the GaEPD implemented the Georgia Coastal Sound Science Initiative (CSSI), a series of scientific and feasibility investigations designed to assess coastal-area ground-water resources and address issues of saltwater intrusion and resource sustainability. As part of this initiative, the GaEPD, Skidaway Institute of Oceanography, SCDHEC, the U.S. Army Corps of Engineers, and the U.S. Geological Survey (USGS), as well as private consulting firms, collected and analyzed hydrogeologic data to refine the conceptual models of ground-water flow and saltwater transport. The USGS then synthesized this information into digital models that describe the ground-water flow system and movement of saltwater. The GaEPD will use these digital models to help design a coastal ground-water permitting strategy.

The USGS developed the digital models as part of the CSSI to satisfy multiple objectives at varying scales. Objectives include simulation of (1) regional ground-water flow, including the Brunswick aquifer system and the Lower Floridan aquifer, in addition to the Upper Floridan aquifer; (2) subregional flow and localized seawater intrusion in the Savannah, Ga.–Hilton Head Island, S.C., area (this report); and (3) localized saltwater intrusion at Brunswick, Ga. To satisfy these objectives, the USGS developed a consistent set of ground-water flow and solute-transport models that update and expand upon earlier digital models for the area.

This report is the second in a series describing ground-water models and simulations of the Floridan aquifer system and shallower confined aquifers in coastal Georgia, northern Florida, and southern South Carolina. This report documents the simulation of ground-water flow and variable-density solute transport in the Savannah–Hilton Head Island, area. This model will serve as a tool for future evaluations of hypothetical pumping distribution scenarios used to guide ground-water permitting in the coastal area.

Purpose and Scope

This report documents a digital ground-water flow and variable-density solute-transport model for the Upper Floridan aquifer in the Savannah, Ga.–Hilton Head Island, S.C., area. The model accounts for the hypothesized downward leakage of saltwater from marine and estuarine sources through the Upper Floridan confining unit and the predominantly lateral flow along the hydraulic gradient in the Upper Floridan aquifer. Specifically, the model is intended to simulate the observed occurrence of saltwater intrusion in the Upper Floridan aquifer at the northern end of Hilton Head Island, at Pinckney Island, and near the Colleton River, although the model does not preclude the simulated occurrence of saltwater intrusion in other areas. The model was used to (1) simulate trends of saltwater intrusion from predevelopment to the present day (1885–2004), (2) project these trends from the present day into the future, and (3) evaluate the relative influence of different assumptions regarding initial and boundary conditions and physical properties. The analysis focuses on evaluating a conceptual model for saltwater intrusion in which saline surface water enters the Upper Floridan aquifer through localized areas where the upper confining units are thin or absent. The model is based on and refined from a regional, single-density ground-water flow model developed as part of the CSSI (Payne and others, 2005).

Discussions in this report include modeling approach and construction, including refinements made to a precursory regional ground-water flow model; calibration approach and calibrated model results and model-fit characteristics; sensitivity testing and analysis; alternative realizations of the conceptual model; simulated future chloride distributions for sustained current conditions; and limitations of the model. Data acquired as part of the CSSI were integrated with available data from USGS databases, publications, and a variety of other sources to create model input and calibration datasets that are as current and consistent as practicable. While the model is constructed based on the best available information, many aspects of model uncertainty are discussed throughout. The purpose in describing the uncertainty is to guide the interpretation of model results.

Approach

The model was developed using the USGS finite-element variable-density solute-transport simulator SUTRA (Voss and Provost, 2002), hereinafter referred to as the SUTRA simulator. The SUTRA simulator calculates the pressure and concentration distribution throughout the model volume using a hybrid finite-element and integrated finite-difference method. The computer code for this simulator was modified for this study to allow irregular mesh structure, output of simulated pressure and concentration at points other than nodes (corners of finite elements), and time-dependent pumping (appendix A). The model, referred to as the SUTRA model to distinguish it from other models, was refined from a previously developed regional ground-water flow model (Payne and others, 2005), which was calibrated to 1980 and 2000 conditions, by increasing the mesh density in the Savannah–Hilton Head Island area and reducing the mesh density outside of this area. Generally, the same or similar hydrogeologic framework, hydraulic properties, and boundary conditions were applied to both models. Permeabilities of the Upper Floridan aquifer and the overlying confining units were recalibrated to September 1998 conditions in the Savannah–Hilton Head Island area. The pumping history from predevelopment to 2000 was estimated for the SUTRA model. Throughout this report, mathematical units of physical properties, distances, and rates are presented in either metric or imperial units, primarily depending on most-common usage. A conversion table has been provided for the reader.

Description of Study Area

The Savannah–Hilton Head Island study area encompasses about 3,000 square miles (mi^2), including Chatham and parts of Bryan and Effingham Counties in Georgia, and Beaufort County and part of Jasper County in South Carolina and the adjacent offshore area (fig. 1). The study area lies within a larger, 42,155-mi^2 model area (fig. 1), which extends to some natural hydrologic boundaries that enable a more realistic simulation of the ground-water flow system in the area of interest.

The study area is in the Coastal Plain physiographic province. Altitudes range from 0 feet (ft) along the coast to 150 ft above NAVD 88 in the northernmost part of the study area. Land use is largely urban residential in Savannah; outside of this area, land use is largely a mix of forestland, grassland, wetland, and cropland or pastureland (accessed November 4, 2004, at *http://landcover.usgs.gov/natllandcover.asp*). Mean-annual temperature in Savannah is about 77 degrees Fahrenheit (°F) for the period 1971–2000 (National Oceanic and Atmospheric Administration, 2002). Mean-annual precipitation, based on the period 1971–2000, is about 50 inches per year (in/yr) at Savannah (Priest, 2004). Rainfall is not evenly distributed throughout the year. Maximum rainfall generally occurs during the months of June, July, and August. Estimated evapotranspiration is about 34 in/yr in the study area (Krause and Randolph, 1989). Payne and others (2005) describe the topography, physiography and climate for the entire model region in more detail.

Previous Investigations

Several ground-water flow investigations of the Floridan aquifer system have been conducted in the study area, some of which incorporated digital modeling. These include Bush and Johnston (1988), Clarke and Krause (2000), Johnston and others (1980), Krause (1982), Krause and Randolph (1989), and Randolph and others (1991). Payne and others (2005) give a more complete description of these models.

Several smaller-scale models have been developed, focusing on the Savannah–Chatham County, Ga., area. Counts and Krause (1976) developed a model that simulated the "principal artesian aquifer" (which incorporated both the Upper and Lower Floridan aquifers) as a single layer calibrated for steady-state predevelopment conditions, then for transient conditions in 1956, 1960 and 1970, using time steps of variable length. A combination of source-sink and no-flow boundary conditions was used for both lateral and top boundaries, with a no-flow boundary condition at the bottom. This model was subsequently expanded and refined (with modifications to the boundary conditions) and calibrated to 1980 conditions, using a steady-state approximation (Randolph and Krause, 1984). These two models were used to simulate hypothetical changes in ground-water levels responding to possible changes in pumping distribution. Another model for this area was developed to simulate the water-supply potential of both the Upper and Lower Floridan aquifers (Garza and Krause, 1996). That model was "telescoped" within the area of the larger Regional Aquifer System Analysis (RASA) model of Krause and Randolph (1989). Vertical boundaries are identical to those of the RASA model, and lateral boundaries were derived from the RASA model.

Two solute-transport models (Bush, 1988; Smith, 1994) were previously developed to evaluate the potential for saltwater intrusion in the Hilton Head Island, S.C., area. Both models used the SUTRA simulator (Voss, 1984) to simulate flow and solute transport in northeast-southwest cross sections extending from the northern part of Hilton Head Island across Port Royal Sound, S.C. In both models, the bottom boundaries are no-flow boundaries, a specified pressure condition represents either the water table or sea level at the top boundary, and the seaward boundary has a concentration of seawater along the entire vertical profile. Both models were run to steady-state pressure and solute distribution for predevelopment conditions to establish initial conditions for subsequent transient simulations. Flux at the landward vertical boundary was estimated during calibration of each model to allow the best match of observed concentrations and heads. The permeabilities assigned to both the Upper Floridan aquifer and the overlying confining unit, respectively, within each model were generally within the same order of magnitude in both models. Both models assumed isotropic permeability for the confining units. The thickness of each layer was assumed constant across each cross-sectional model.

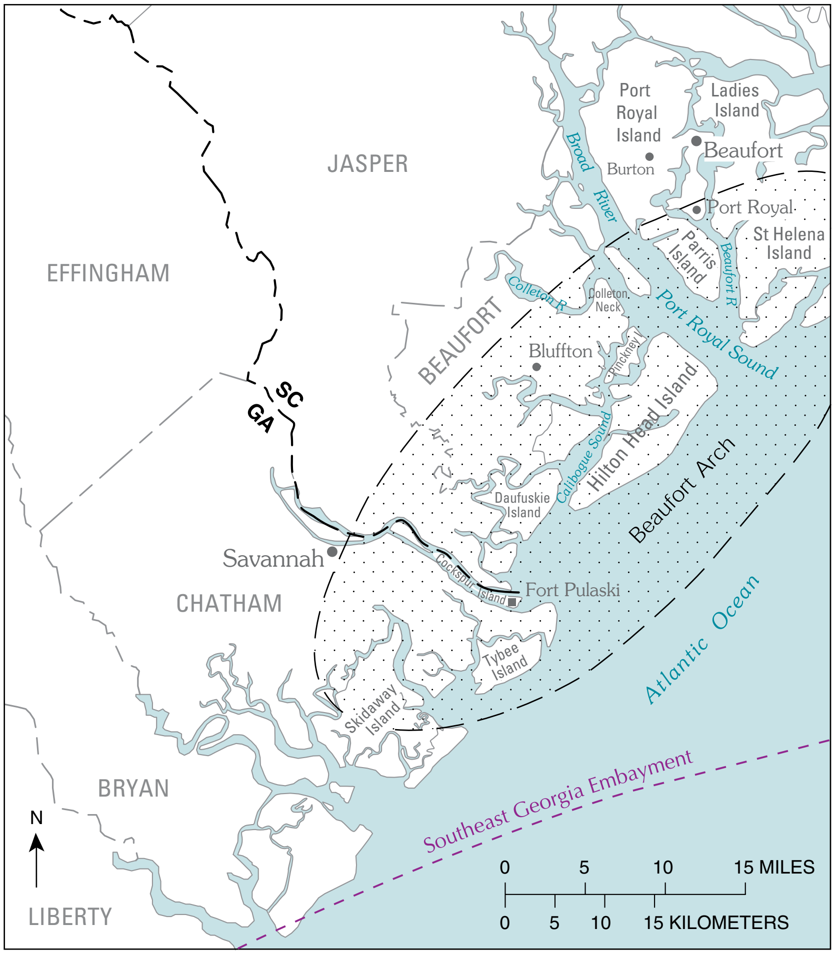

Base from U.S. Geological Survey
1:100,000 and 1:250,000-scale data

Structural feature from
Weems and Edwards, 2001

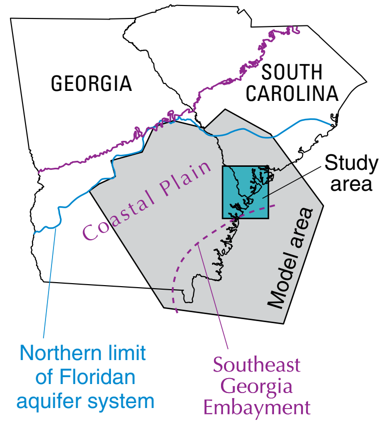

Figure 1. Location of solute-transport model study area, model area, and major structural features, Savannah, Georgia–Hilton Head Island, South Carolina, area.

These two solute-transport models differ in many ways. Bush (1988) simulated the upper permeable zone and the lower part of the Upper Floridan aquifer, Lower Floridan aquifer, and overlying confining units of each; each unit had constant properties across the model. Smith (1994) simulated the Upper Floridan aquifer (the upper permeable zone of Bush [1988]) and the overlying confining unit, each with variable permeability. The permeabilities for both aquifer and confining units were lower and the porosities were higher in the Smith (1994) model than in the Bush (1988) model. The element dimensions, dispersivities, and pumping periods also differed. Bush (1988) simulated an average flow velocity in the upper permeable zone of the Upper Floridan aquifer of 68 feet per year (ft/yr), and 14 ft/yr in the lower permeable zone. Smith (1994) simulated flow velocity in the freshwater-saltwater transition zone of 115 ft/yr, and a maximum velocity of 230 ft/yr beneath Hilton Head Island where the hydraulic gradient was highest.

The models also differed in sensitivity to physical properties and boundary conditions. The Bush (1988) model was most sensitive to lateral permeability in the aquifer units, whereas the Smith (1994) model showed greater sensitivity to the permeability of the Upper Floridan confining unit. Unlike the Bush (1988) model, the Smith (1994) model was sensitive to the pressure and concentration conditions at the seaward boundary. On the other hand, the Bush (1988) model showed a moderate sensitivity to the flow rates at the landward boundary, unlike the Smith (1994) model. The Bush (1988) model was sensitive to the transverse dispersivity value of the upper permeable zone of the Upper Floridan aquifer, but the Smith (1994) model was sensitive only to very large changes (greater than 50 percent) in this parameter.

Bush (1988) suggested that the saltwater-freshwater interface had moved little between predevelopment and 1983 and that there was little likelihood of saltwater intrusion into the upper permeable zone of the Upper Floridan aquifer between 1983 and 2034 if pumping levels did not change. Furthermore, the results indicated that if the decline in head continued at the 1983 rate, the chloride concentration beneath Hilton Head Island would remain below 250 milligrams per liter (mg/L) during this period. Smith (1994), on the other hand, suggested that the saltwater-freshwater transition zone had moved on the order of thousands of feet toward Hilton Head Island from predevelopment to 1984, and that the transition zone would continue to move toward Hilton Head Island even if pumping ceased.

Acknowledgments

The authors want to thank Caryl J. Wipperfurth of the U.S. Geological Survey for preparation of illustrations and Patricia L. Nobles of the U.S. Geological Survey for preparation of the manuscript. Jack Childress, Robert Logan, and Camille Ransom III of the South Carolina Department of Health and Environmental Control provided water-level and water-chemistry data. Robert Logan and Camille Ransom of the South Carolina Department of Health and Environmental Control, and James E. Landmeyer of the U.S. Geological Survey participated in valuable discussions regarding the conceptual model.

Hydrogeology

Coastal Plain sediments of varying permeability comprise the aquifer and confining units in the study area. These sediments were differentiated into geologic units based on their geologic characteristics and into aquifers and confining units based on their water-bearing characteristics (fig. 2).

Geologic Setting

Coastal Plain strata consist of consolidated to unconsolidated layers of sand and clay, and semiconsolidated to very dense layers of limestone and dolomite. These sediments range in age from Late Cretaceous to Holocene, and unconformably overlie igneous, metamorphic, and sedimentary Paleozoic to Mesozoic rocks. On a regional scale, the sedimentary units generally strike southwest-northeast, and dip and thicken to the southeast, where they reach a maximum thickness of 5,500 ft in Camden County, Ga. (Wait and Davis, 1986).

The Beaufort Arch (fig. 1) is a prominent structural feature centered near Beaufort, S.C., that interrupts the regional southeastward dip of the sediments in that area (fig. 3). The Coastal Plain strata become thin and shallow over the Beaufort Arch. Beneath Port Royal Sound and the northern end of Hilton Head Island, sediments dip toward the southeast on the seaward flank of the arch. Under the southern end of Hilton Head Island and landward parts of Beaufort and Jasper Counties, sediments dip toward the southwest, toward a regional structural low called the Southeast Georgia Embayment (fig. 1). The Southeast Georgia Embayment is a shallow east-to-northeast-plunging syncline centered in the southern coastal counties of Georgia (Miller, 1986); the thickness of the Coastal Plain deposits is greatest near the embayment. North of Port Royal Sound, sediments dip toward the north. Within the area influenced by the Beaufort Arch, the Coastal Plain deposits are thinner and at shallower depths than near the Southeast Georgia Embayment.

The Floridan aquifer system is composed primarily of carbonate sediments deposited in a shallow tropical marine environment from the middle Eocene through Oligocene (Miller, 1986), from about 55 to 25 million years ago. Unconformably overlying these units are the primarily siliciclastic Miocene sediments (25–5 million years ago) (Clarke and others, 1990; Weems and Edwards, 2001). These units are generally less permeable than the underlying carbonates and primarily function as a confining unit to the Floridan aquifer system. During the last 2 million years, sea level has changed, rising and lowering more than several hundred feet (Foyle and others, 2001). During sea level low stands, sediments at the surface of the Continental Shelf were exposed and eroded.

Series		Geologic unit[1]	Hydrogeologic unit[2] (Savannah, Ga. / Hilton Head Island, S.C.)		Model unit
Post-Miocene		Undivided	Water-table zone	SURFICIAL AQUIFER SYSTEM	1
Miocene	Upper	Ebenezer Formation	Confining unit	SURFICIAL AQUIFER SYSTEM	1
Miocene	Middle	Coosawhatchie Formation	Confining unit	BRUNSWICK AQUIFER SYSTEM	2
Miocene	Middle / Lower	Coosawhatchie Formation; Marks Head Formation	Upper Brunswick aquifer	BRUNSWICK AQUIFER SYSTEM	3
Miocene	Lower	Parachucla Formation		BRUNSWICK AQUIFER SYSTEM	3
Miocene	Lower	Tiger Leap Formation	Lower Brunswick aquifer	BRUNSWICK AQUIFER SYSTEM	3
Oligocene		Lazaretto Creek Formation	Upper Floridan confining unit		4
Oligocene		Suwannee Limestone	Upper Floridan aquifer[3]	FLORIDAN AQUIFER SYSTEM	5
Eocene	Upper	Ocala Limestone	Upper Floridan aquifer[3]	FLORIDAN AQUIFER SYSTEM	5
Eocene	Middle	Avon Park Formation[4]	Lower Floridan confining unit[3]	FLORIDAN AQUIFER SYSTEM	6
Eocene	Lower	Oldsmar Formation[5]	Lower Floridan aquifer[6]	FLORIDAN AQUIFER SYSTEM	7
Paleocene		Cedar Keys Formation[5]	Lower Floridan aquifer[6]	FLORIDAN AQUIFER SYSTEM	7
Upper Cretaceous		Undivided	Confining unit		Not modeled

[1] Modified from Randolph and others, 1991; Weems and Edwards, 2001

[2] Modified from Randolph and others, 1991; Clarke and Krause, 2000; Clarke, 2003

[3] In the Hilton Head Island, S.C., area, these units contain the *middle confining unit* and the *middle Floridan aquifer*, but the exact correlation is uncertain

[4] The equivalent age unit in South Carolina is the Santee Limestone

[5] The equivalent age unit in South Carolina is the Black Mingo Formation

[6] The presence of the Lower Floridan aquifer at Hilton Head Island, S.C., is uncertain

Figure 2. Generalized correlation of geologic, hydrogeologic, and model units.

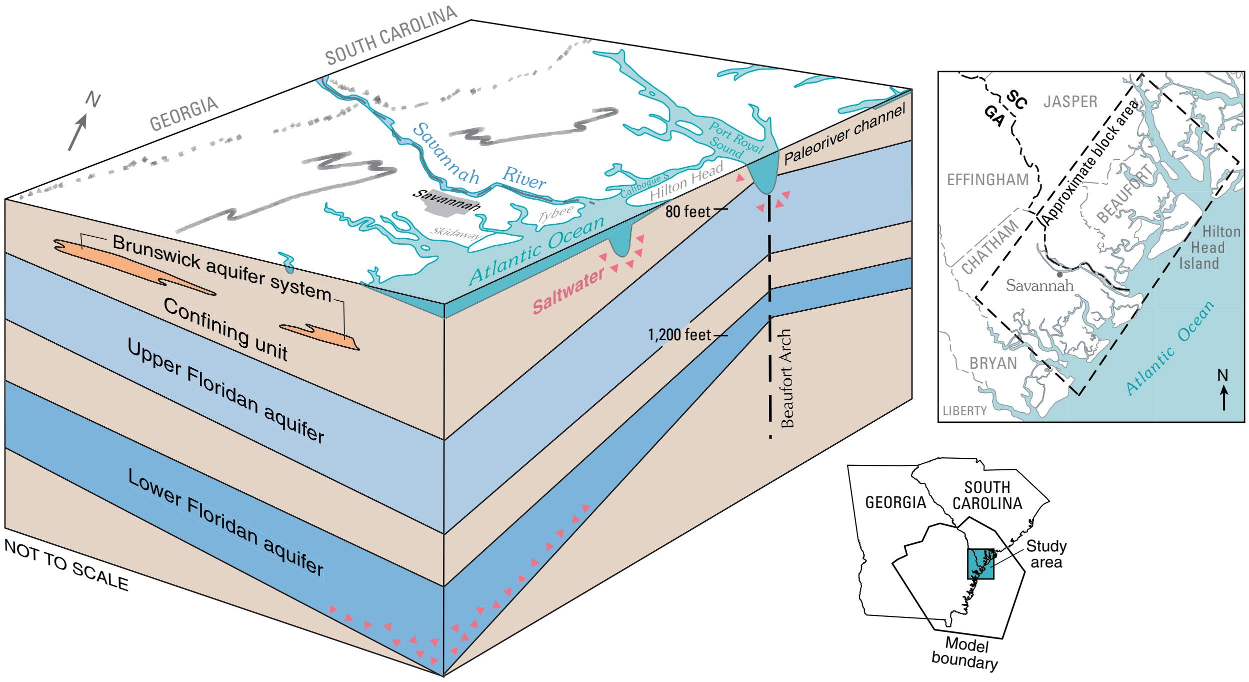

Figure 3. Schematic block diagram showing major structural and hydrostratigraphic features and their influence on the distribution of hydrogeologic units.

About 18,000 years ago, sea level was at a low stand, about 300 ft below present-day sea level, and the coast was located about 60 miles (mi) offshore (Foyle and others, 2001). Before and since then, rivers and creeks have cut into and locally eroded the Miocene sediments where exposed; and, with transgression, these areas have been filled in with more recent sediments of varying permeability (Falls and others, 2005b). At present, currents in coastal creeks and sounds may be eroding the Miocene sediments. This continued erosion has resulted in a thinning of the Miocene and younger units, and thus a reduction in the confinement above the Upper Floridan aquifer. This thinningoccurs particularly where the aquifer is shallow, for example in the Beaufort Arch area (figs. 1 and 4) (Foyle and others, 2001).

Hydrogeologic Units

The principal source of water for all uses in the coastal area is the Floridan aquifer system, consisting primarily of the Upper and Lower Floridan aquifers (Miller, 1986; Krause and Randolph, 1989). Secondary sources of water include the surficial and Brunswick aquifer systems (Clarke, 2003), consisting of sand of Miocene to Holocene age. Confining units of relatively lower permeability separate these water-bearing units. For a more complete description of the hydrogeologic units in the "simulated" region, see Payne and others (2005).

Surficial and Brunswick Aquifer Systems

The surficial aquifer system (model unit 1; fig. 2) consists of Miocene to Holocene interlayered sand, clay, and thin limestone beds (Clarke, 2003; Dale, 1995). At Skidaway Island, Chatham County, Ga., and on Hilton Head Island, S.C., two permeable zones have been identified: an unconfined zone (water table) and a confined or semiconfined zone (Clarke and others, 1990; Dale, 1995). The thickness of the surficial aquifer system at Skidaway Island is about 65 ft (Clarke and others, 1990), and reaches a maximum depth of 67 ft below NAVD 88 on the northern end of Hilton Head Island (Dale, 1995). Reported transmissivity of the unconfined zone at Skidaway Island ranges from 14 to 1,100 feet squared per day (ft^2/d), with a hydraulic conductivity ranging from 2 to 65 feet per day (ft/d); reported transmissivity of the confined zone ranges from 150 to 6,000 ft^2/d, with a hydraulic conductivity ranging from 40 to 400 ft/d (Clarke and others, 1990). On Hilton Head Island, the transmissivity of the surficial aquifer ranges from 80 to 1,200 ft^2/d, with a hydraulic conductivity ranging from 4 to 65 ft/d (Dale, 1995). Offshore seismic data indicate that many in-filled paleoriver channels caused by migrating fluvial channels and changing sea level comprise the stratigraphic units of the surficial aquifer system (Foyle and others, 2001). In this study, undifferentiated sediments comprising the confined zones of the surficial aquifer system are grouped into the uppermost model unit (unit 1).

The surficial aquifer system is separated from the underlying Brunswick aquifer system (where present), or the Floridan aquifer system by a confining unit consisting of silty clay and dense, phosphatic limestone of Miocene to Oligocene age (model units 2, 3, and 4; fig. 2). Vertical hydraulic conductivity data of this confining unit obtained from cores from the Hilton Head Island, Port Royal Sound, and offshore areas range from 2.3×10^{-4} to 3.0 ft/d (Smith, 1994; Clarke and others, 2004). Furlow (1969) reported an average vertical hydraulic conductivity of 1.0×10^{-3} ft/d in eastern Chatham County, Ga. In the area, including and surrounding Hilton Head Island, offshore and just landward in South Carolina, the Miocene sediments that comprise the confining unit are from 0 to 50 ft thick. Foyle and others (2001) mapped several locations where this confining unit is thin or absent as a result of erosion—offshore of Hilton Head Island, at Calibogue Sound, at Pinckney Island, and at the Colleton River (fig. 4). To the south and southwest of the study area, where the Brunswick aquifer system may be present, and to the west the thickness of these sediments may be greater than 100 ft (Clarke and others, 1990; Foyle and others, 2001; Waddell, 1989).

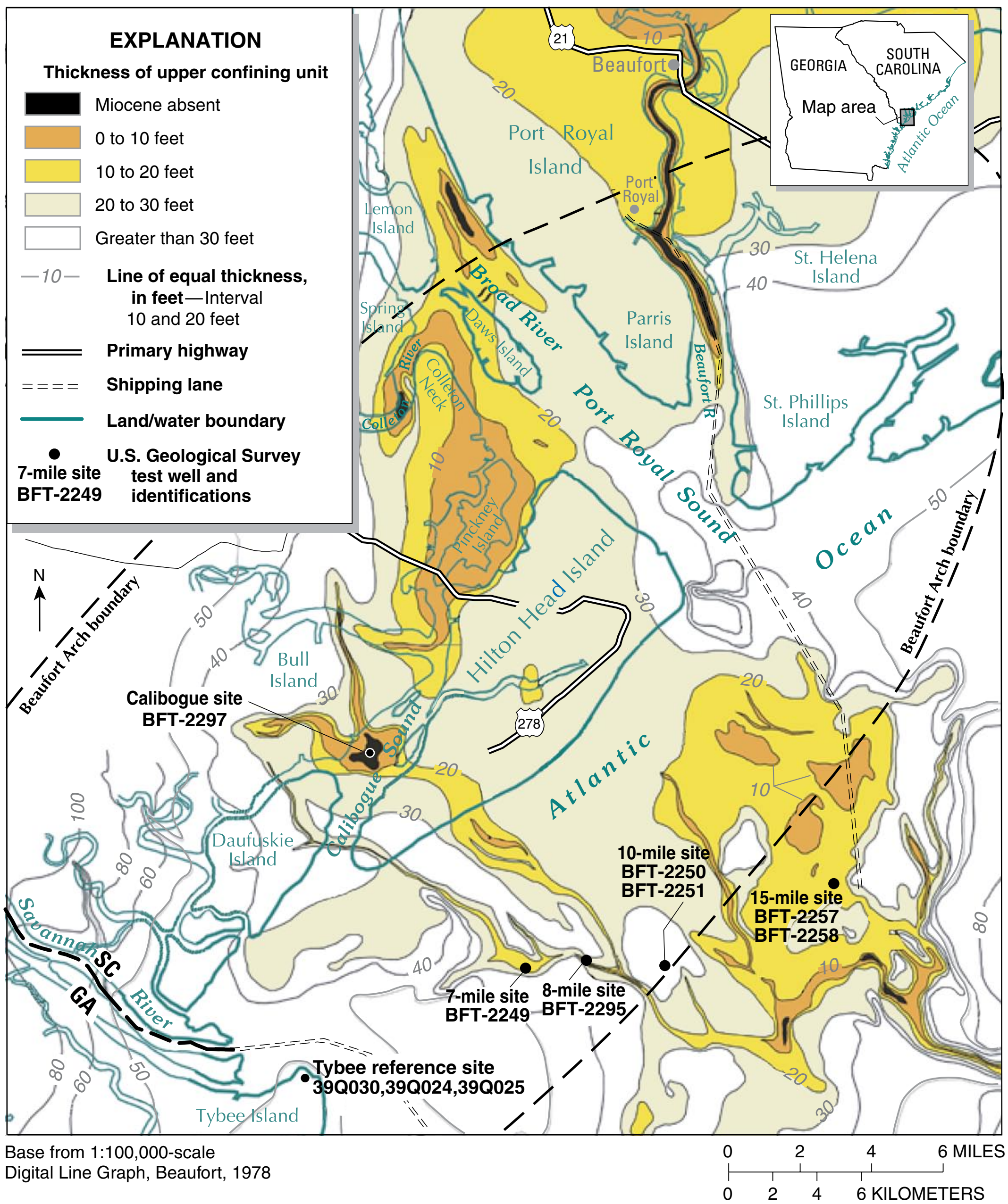

Figure 4. Thickness of the upper (Miocene) confining unit and location of onshore Georgia and offshore Coastal Sound Science Initiative wells (modified from Foyle and others, 2001; Falls and others, 2005b).

Where present in the study area, the Brunswick aquifer system consists of one low permeability water-bearing zone—the Upper Brunswick aquifer (Weems and Edwards, 2001). The Upper Brunswick aquifer consists of poorly sorted, fine to coarse, slightly phosphatic and dolomitic quartz sand and dense phosphatic limestone (Clarke and others, 1990). Reported hydraulic conductivity of the Upper Brunswick aquifer in Chatham and Effingham Counties is less than 15 ft/d, and in southern Bryan County is as much as 100 ft/d (Golder Associates, Inc., 2003). Farther south, within the area of the Southeast Georgia Embayment, the Brunswick aquifer system is thicker and more permeable, and is composed of the Upper and Lower Brunswick aquifers (Clarke, 2003). Outside and along the margins of the Southeast Georgia Embayment (fig. 1), permeable sediments comprising the Brunswick aquifer system are discontinuous, and the aquifer system has a higher percentage of lower permeability, clayey deposits than inside the Southeast Georgia Embayment (Clarke, 2003). In this study, sediments comprising the Upper and Lower Brunswick aquifers are considered as a single unit, with combined thickness and composite hydraulic properties used to represent the unit.

Floridan Aquifer System

The Floridan aquifer system, consisting of the Upper and Lower Floridan aquifers (Miller, 1986; Krause and Randolph, 1989) and locally the *middle Floridan aquifer* near Hilton Head Island, S.C. (Gawne and Park, 1992; Ransom and White, 1999), is comprised mostly of Paleocene to Oligocene carbonate rocks that locally include Upper Cretaceous rocks (fig. 2). The aquifer system extends from the Coastal Plain of South Carolina, westward into Georgia and Alabama, and southward throughout Florida. The thickness of the Floridan aquifer system in the study area ranges from less than 100 ft where it is shallow and thin in Beaufort County, S.C., to about 1,000 ft in southern Chatham and Bryan Counties, Ga. (Miller, 1986).

The Upper Floridan aquifer (model unit 5; fig. 2) is highly productive and consists of Eocene to Oligocene limestone and dolomite. Reported transmissivities of the Upper Floridan aquifer in the study area range from 5,000 to 55,000 ft^2/d in Beaufort County, S.C. (Newcome, 2000); from 2,800 to 32,000 ft^2/d in Effingham County, Ga. (Kellam and Gorday, 1990); and about 70,000 ft^2/d in Bryan County, S.C. (Harrelson and Falls, 2003). Estimated hydraulic conductivity in the study area varies from 10 to 1,250 ft/d. Reported Upper Floridan aquifer transmissivity for the entire model area is as high as 600,000 ft^2/d (Clarke and others, 2004). The Upper Floridan aquifer ranges in thickness from about 20 ft at the northeasternmost part of the study area to about 600 ft in southern Chatham County, Ga. Reported maximum thickness of the Upper Floridan aquifer for the entire model area is 2,800 ft (Miller, 1986).

In some areas, several distinct water-bearing zones have been identified within the Upper Floridan aquifer. McCollum and Counts (1964) identified five water-bearing zones near the Savannah–Hilton Head Island area in strata that would be defined later as part of the Floridan aquifer system, the upper four of which define the Upper Floridan aquifer (Falls and others, 2005b; Miller, 1986; Clarke and others, 1990). In the Hilton Head Island area, only one permeable unit defines the Upper Floridan aquifer (Ransom and White, 1999; Hayes, 1979). In Beaufort County, S.C., the middle Floridan aquifer is about 250–550 ft below land surface and is separated from the Upper Floridan aquifer by the *middle confining unit*. The middle Floridan aquifer has been correlated with zone 3 or zone 4 of McCollum and Counts (1964) (Falls and others, 2005b; Gawne and Park, 1992). The extent of the middle Floridan aquifer, however, is uncertain, and likely is limited to the Hilton Head Island area. Transmissivities of 2,300–26,700 ft^2/d (hydraulic conductivity of 60–460 ft/d) have been reported for the middle Floridan aquifer on and near Hilton Head Island, S.C.

The Upper Floridan aquifer is underlain by a middle to late Eocene confining unit (model unit 6; fig. 2) of dense, recrystallized limestone and dolomite that hydraulically separate the aquifer to varying degrees from the Lower Floridan aquifer (fig. 2). The confining unit thickness in the Savannah area is about 160–280 ft. Laboratory permeability analysis of a sample in Chatham County (Counts and Donsky, 1963) indicates a vertical hydraulic conductivity for this unit of 0.0007 ft/d.

The Lower Floridan aquifer (model unit 7; fig. 2) is composed mainly of dolomitic limestone of early to middle Eocene. In Chatham County, the lowermost water-bearing zone of McCollum and Counts (1964) is included in the Lower Floridan aquifer (Falls and others, 2005b). In southeastern South Carolina, some Paleocene and early Eocene units contain permeable beds, and production wells are commonly screened in these zones and in the overlying Santee Limestone (Newcome, 2000). In this report, these productive zones and the Santee Limestone are considered part of the Lower Floridan aquifer. On Hilton Head Island, the aquifer units below the middle Floridan aquifer are used little, and the presence of the Lower Floridan aquifer as a permeable unit is uncertain (Gawne and Park, 1992). Hydraulic-property data specifically for the Lower Floridan aquifer are limited in the study area. Reported transmissivity of the Lower Floridan aquifer in Bryan County, S.C., in the southernmost part of the study area, is 8,300 ft^2/d (Harrelson and Falls, 2003). For the entire model area, reported transmissivity values range from 170 to 43,000 ft^2/d (Clarke and others, 2004). In Effingham County, the reported thickness of the Lower Floridan aquifer is 157 ft; and in Bryan County, south of the Chatham County line, the reported thickness is 140 ft (Falls and others, 2005b).

Ground-Water Flow System

Ground-water flow is controlled mainly by rates and distribution of recharge to and discharge from the system, the extent and effects of confinement, the ability of the aquifers to transmit and store water, ground-water withdrawal, and the dips of the water-bearing and confining units. Recharge to the water-table zone of the surficial aquifer system occurs directly from precipitation throughout the study area; recharge to confined aquifers from precipitation occurs outside the study area at outcrop areas, or from downward leakage through adjacent semiconfining units. Natural discharge occurs directly into some stream reaches and estuarine areas, or indirectly through upward leakage into adjacent units.

Ground-water flow in the Upper Floridan aquifer is illustrated on a potentiometric-surface map for May 1998 (Peck and others, 1999) and September 1998 (Ransom and White, 1999), as well as for predevelopment (Krause and Randolph, 1989) (fig. 5). Northwest of the study area, where the aquifer is shallow or exposed at land surface, the Floridan aquifer system receives recharge. Because the units in the northwest are shallow and the area is characterized by greater topographic relief, some aquifer discharge is directly to streams, as indicated by potentiometric contours that bend upstream. From these northern areas, ground water flows mostly southeastward toward the coast into the study area and discharges into overlying units and surface-water bodies—major streams, estuaries, and the Atlantic Ocean.

Toward the southwestern part of the study area in the western part of Chatham County and southern Beaufort County, the Upper Floridan aquifer deepens and is overlain by thick confining units and the Brunswick aquifer system (figs. 1–3). Water may enter or discharge from the aquifer through leaky confining units.

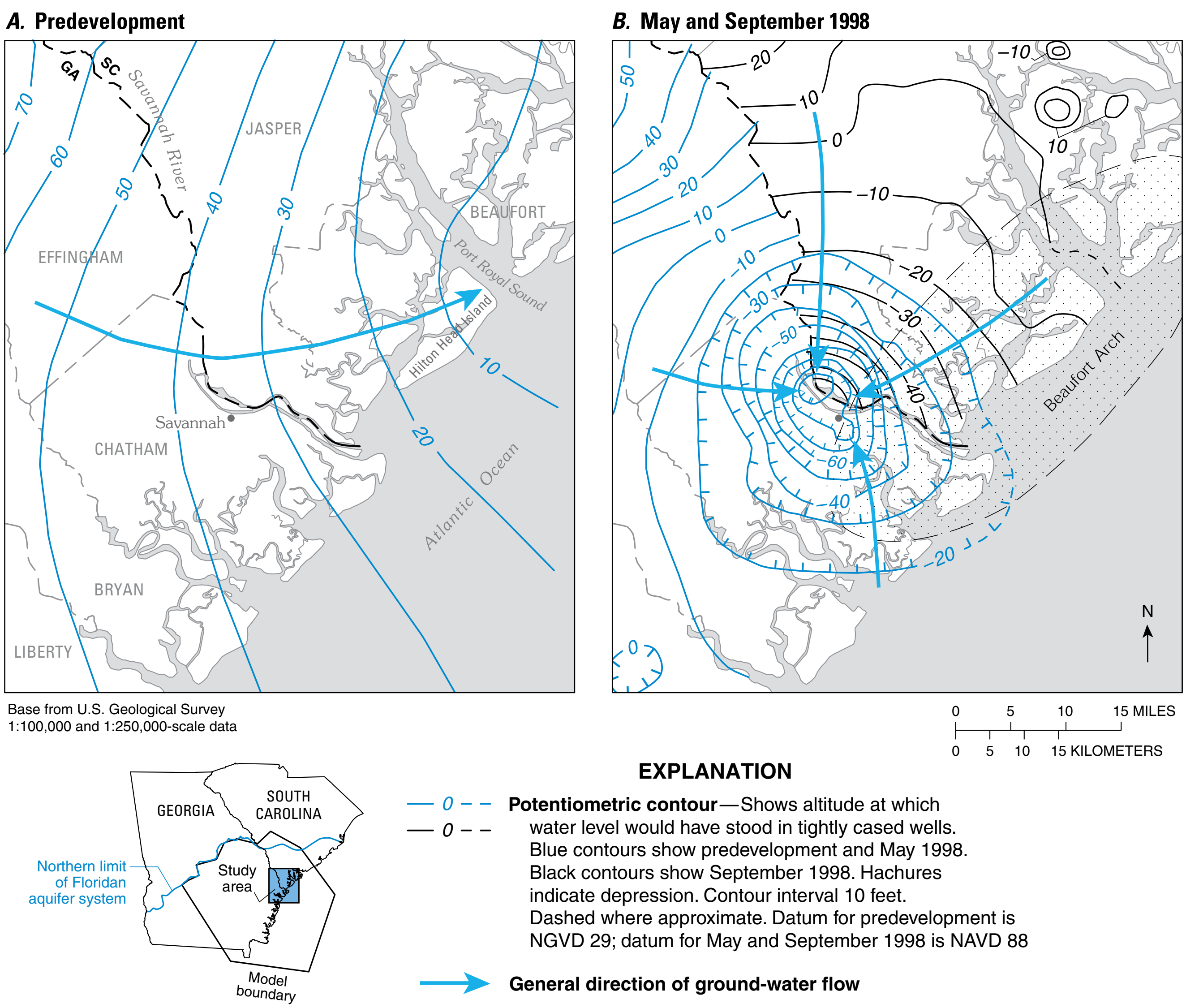

Figure 5. Potentiometric surface of the Upper Floridan aquifer in the Savannah, Georgia–Hilton Head Island, South Carolina, area (*A*) predevelopment and (*B*) May and September 1998 (modified from Krause and Randolph, 1989; Peck and others, 1999; and Ransom and White, 1999).

In the eastern part of the study area near Port Royal Sound, the Upper Floridan aquifer thins and is shallow in depth; in localized areas, there is little or no confinement above the aquifer (fig. 3). Potentiometric mounds northeast of Port Royal Sound on St. Helena Island, on Ladies Island, and near Burton, S.C. (figs. 1 and 5), indicate local recharge areas for the Upper Floridan aquifer (Ransom and White, 1999). Geochemical data showing a meteoric component in ground water, combined with potentiometric data and lithologic information, indicate that freshwater recharge occurs on the northern part of Hilton Head Island (Back and others, 1970). Recharge on the northern end of Hilton Head Island may provide a natural boundary that inhibits the movement of high-salinity ground water toward the center of Hilton Head Island from the northeastern shore (Camille Ransom III, South Carolina Department of Health and Environmental Control, oral commun., 2004). Because water-level trends for the two aquifers within the model area are similar (Falls and others, 2005a), and little is known about ground-water flow in the Lower Floridan aquifer in the study area, it is assumed that the regional flow characteristics of the Lower Floridan aquifer are similar to those of the Upper Floridan aquifer.

Predevelopment

Prior to the initiation of ground-water pumping during the 1880s, recharge to the Floridan aquifer system was offset by natural discharge to springs (both on land and offshore), rivers, and other surface-water bodies, and by diffuse upward leakage. The hydraulic head in the Upper Floridan aquifer was sufficiently high that the earliest wells flowed at land surface throughout much of the coastal area, with water levels at Savannah ranging from 30 to 40 ft above NAVD 88 (Krause and Clarke, 2001) (fig. 6A). Recharge occurred northwest of the study area, and water flowed downgradient toward the coast (fig. 5A). Within the study area, flow was eastward, with a local potentiometric mound near Burton, S.C. (Hughes and others, 1989; Johnston and others, 1980).

Present Day: 1980–2000

The present-day flow system reflects changes that have occurred as a result of ground-water development (withdrawal) (figs. 5 and 6B). Ground-water withdrawal has lowered water levels, induced additional recharge, reduced natural discharge, and increased the chloride concentration in ground water along the coast. An extensive cone of depression in the Upper Floridan aquifer potentiometric surface is centered in the Savannah, Ga., area (fig. 5B) and is the result of large pumping rates and decreasing transmissivity of the aquifer as it thins toward the Beaufort Arch. Increased pumping has resulted in a reversal of the seaward head gradient east and north of Savannah. The zero-foot potentiometric contour for the cone of depression is mostly offshore and extends to the middle of Port Royal Sound, which has resulted in a downward hydraulic gradient that facilitates potential intrusion of seawater into the aquifer.

The hydraulic gradient has steepened near the cone of depression and from the recharge area downgradient toward the coast. The steeper gradient has resulted in high ground-water flow velocities and large quantities of water infiltrating into the Upper Floridan aquifer, both vertically and laterally. The cone of depression has "captured" ground-water flow, which prior to development, may have discharged offshore. In addition, diffuse upward leakage of water from the Upper Floridan aquifer into overlying units, streams, and wetlands may have decreased or ceased, and wells no longer flow at land surface (fig. 6B).

Recharge and Discharge

Recharge to the hydrologic system is from rainfall, which is estimated to be 50 inches per year (in/yr) in Savannah based on mean-annual precipitation for the 30-year period, 1971–2000 (Priest, 2004). Potentiometric mounds in the Upper Floridan aquifer indicate areas of more or less direct recharge in the study area. Most of the recharge is discharged from shallow, local flow systems into small streams or is lost as evapotranspiration. A smaller percentage of recharge infiltrates through clayey confining units and enters the deeper, confined regional flow system. During 2000, total simulated recharge to the confined part of the aquifer system in the onshore part of the model area was 0.35 inches (Payne and others, 2005). Some ground water from the Upper Floridan aquifer may have discharged into the Atlantic Ocean through the overlying confining unit or submarine outcrops (Counts and Donsky, 1963). Landmeyer and Belval (1996) suggested the historical presence of submarine springs in Calibogue Sound, and anecdotal evidence indicates the presence of submarine springs in the Beaufort River (Counts and Donsky, 1963). Some ground water may also discharge to major streams and wetlands.

Estimates of mean-annual ground-water discharge to streams (baseflow) determined using hydrograph-separation methods are considered to approximate a large percentage of the long-term average recharge to the ground-water flow system (Clarke and West, 1998). There are no baseflow estimates within the study area because of tidal influence. Priest (2004), however, used hydrograph-separation techniques to estimate mean-annual baseflow during 1971–2000 for 14 streamflow gaging stations in coastal Georgia (fig. 7). Estimated baseflow at the 14 stations ranged from 4.4 in/yr along the Little Satilla River to 10 in/yr along the Altamaha River.

A portion of the estimated long-term average recharge based on hydrograph separation flows into and out of the shallow, unconfined surficial aquifer system, allowing only a fraction to recharge the regional flow system. Thus, the estimated baseflow values are likely substantially larger than recharge to the regional flow system and may be considered to be an upper limit to regional recharge simulated by the model. Priest (2004) reported drought estimates of baseflow that eliminate much of the discharge from the local flow system and may represent a more reasonable estimate of recharge to the regional aquifer system; values range from 0 to 2.4 in/yr.

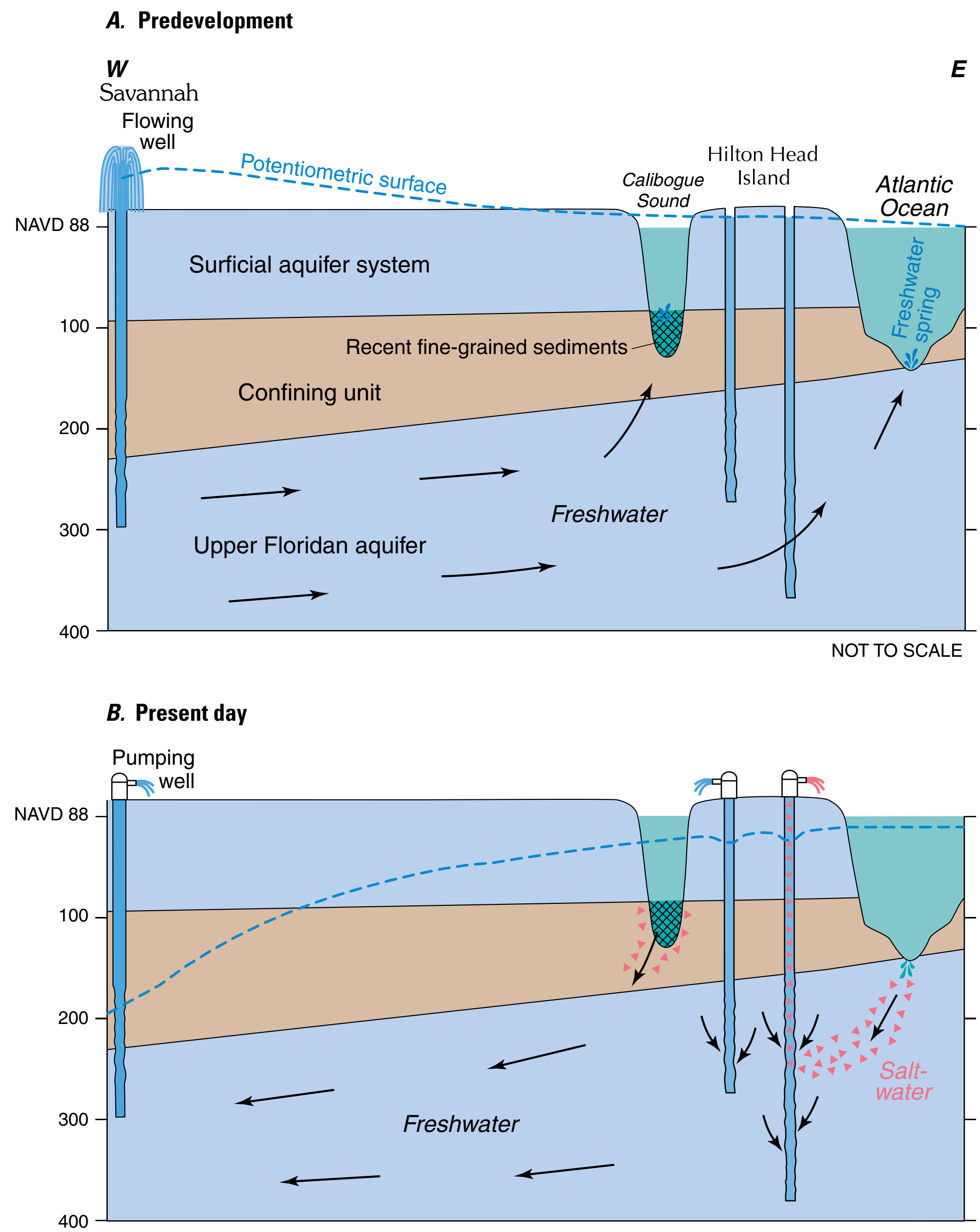

Figure 6. Schematic cross sections showing the (*A*) predevelopment and (*B*) present-day flow system in the study area (modified from Krause and Clarke, 2001). Arrows indicate general direction of ground-water flow.

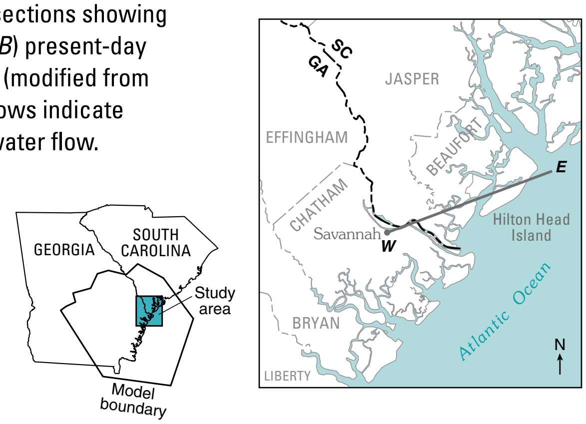

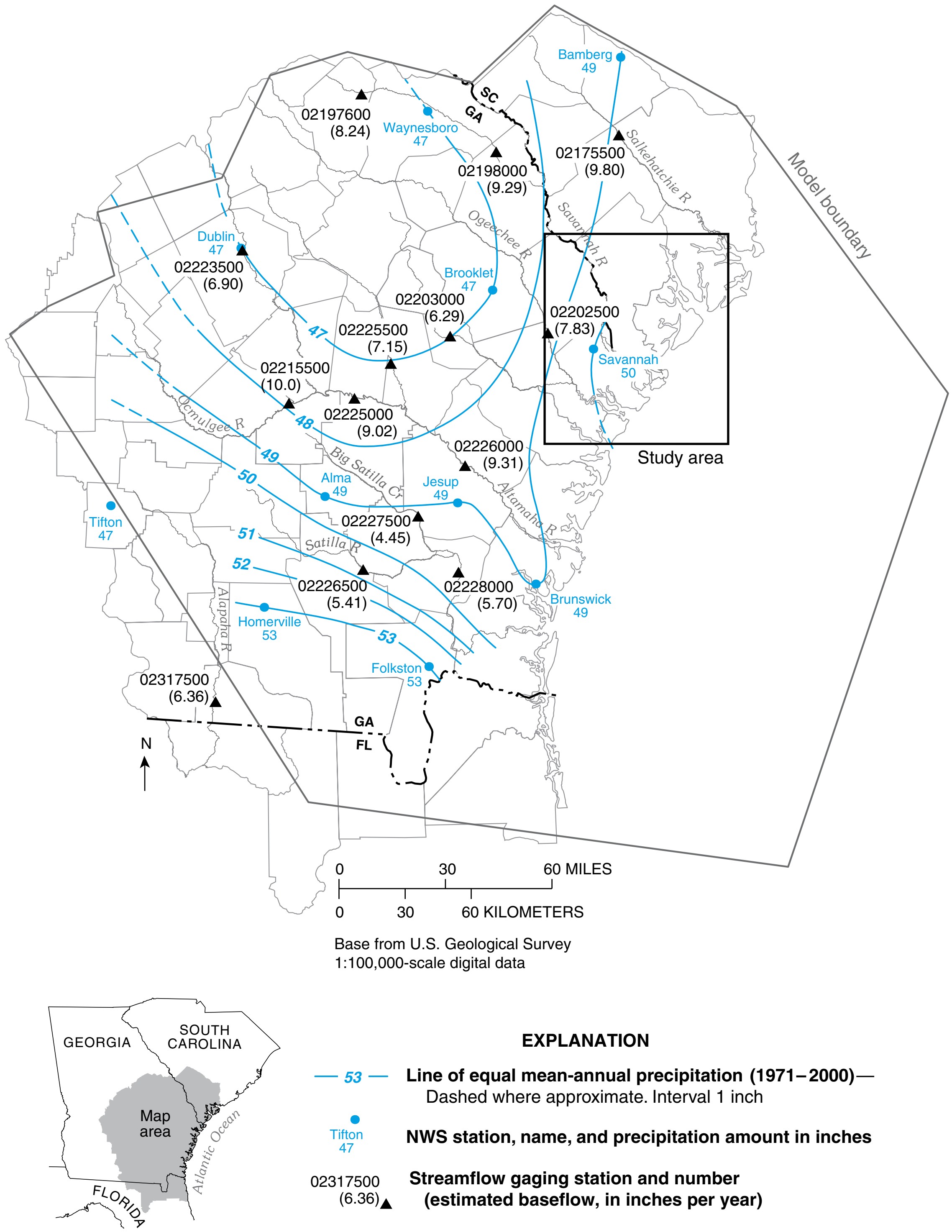

Figure 7. Mean-annual precipitation for selected National Weather Service (NWS) stations and mean-annual baseflow computed using hydrograph-separation analysis in the model area, 1971–2000 (modified from Priest, 2004).

Ground-Water Pumpage

The locations of ground-water pumping centers and quantities of water withdrawn from these centers may substantially affect ground-water levels in the study area. For the long term, changes in pumping rates and the addition of new pumping centers may alter the configuration of potentiometric surfaces, reverse ground-water flow directions, and increase seasonal and long-term water-level fluctuations in the aquifers. Payne and others (2005) discuss the methods used to distribute pumping for the entire model area.

Apparent inconsistencies in pumping rates between years shown in tables 1, 2, and 3 are the result of different data sources and changes in data collection and estimation methods. Estimates before the early 1980s were generally made using values reported in publications and were largely based on estimates from major industrial users or public suppliers. Starting around the early 1980s, pumpage data collection became more thorough and consistent, and estimated values of pumpage were based on permitted pumping. In addition, estimates were made for unpermitted pumping. Because accounting of pumping rates and distribution has improved since the early 1980s, recent estimates of pumpage distribution are more accurate. Although observed and simulated water levels in the study area respond rapidly to abrupt changes in pumping rates, solute-transport processes generally respond less rapidly. Because the calibration years for the SUTRA model are 1998 and later, the inconsistencies in the pumpage data for earlier years likely have a minor effect on simulation results.

The earliest recorded supply well was drilled at Savannah during 1885, and by 1891, 25 wells were in use for public supply (Warren, 1944). These early artesian wells supplied about 6 Mgal/d by the turn of the century (Counts and Donsky, 1963). During 1899, supply wells were drilled on Parris Island, S.C., but several were abandoned within 4 years because of high salinity (Landmeyer and Belval, 1996).

From the late 1800s until the 1980s, ground-water pumpage increased continuously, although at an unsteady rate (tables 1–3). Reported ground-water pumping rates increased markedly in Savannah from about 20 Mgal/d during the mid- to late 1930s to more than 40 Mgal/d by 1940; pumping rates increased sharply again to about 60 Mgal/d by 1958 (Counts and Donsky, 1963). Pumping continued to increase in the Savannah area through the 1960s and 1970s. By 1980, pumping in Chatham County was about 75 Mgal/d, and peaked during 1990 when pumping was 89 Mgal/d (Fanning, 2003). A graph showing estimated pumpage in the study area for selected years between 1915 and 2000 is shown in figure 8.

Until the 1960s, much of the pumping in coastal Beaufort and Jasper Counties, S.C., was in and around Parris Island. During the 1920s, several supply wells were drilled around Port Royal Island, some of which had high salinities initially; by the 1940s, about 0.15 Mgal/d were being pumped in the area (Landmeyer and Belval, 1996). During the 1940s, ground-water pumpage increased markedly, and in Beaufort salinity levels started to increase. By 1960, pumpage at Beaufort ranged from about 0.5 to 0.75 Mgal/d and 0.05 Mgal/d at the city of Port Royal. During 1965, Beaufort and Port Royal switched to surface water for public supply (Landmeyer and Belval, 1996). With rapid residential and recreational development during the 1960s, ground-water withdrawals from the Floridan aquifer system on Hilton Head Island increased markedly; and from the late 1970s to early 1980s, almost 10 Mgal/d was being pumped at Hilton Head Island (Hayes, 1979; Smith, 1994). Estimated peak pumpage in Beaufort County was greater than 20 Mgal/d during 2000 (Whitney Stringfield, U.S. Geological Survey, written commun., 2002).

From the early 1980s to the early 1990s, total pumping in the five counties comprising most of the study area increased, and then started to decline (Julia Fanning, U.S. Geological Survey, written commun., 2001; Whitney Stringfield, U.S. Geological Survey, written commun., 2002). This trend is due largely to changes in industrial pumpage in Chatham County, Ga.

The Upper Floridan aquifer provides the largest volume of ground water in the study area. The Lower Floridan aquifer is used to a lesser extent in the Savannah area, and the middle Floridan aquifer is used locally in the Hilton Head Island area. There also is some localized use of the surficial aquifer system across the study area. Withdrawal from the Brunswick aquifer system is generally less than 0.25 Mgal/d across the entire model area, and limited to the southern parts of the study area where permeability and thickness are greatest. In Bryan, Chatham, and Effingham Counties during 2000, the Upper Floridan aquifer comprised about 95 percent of permitted pumping for industrial and public-supply uses, whereas the Lower Floridan comprised about 5 percent. In Beaufort and Jasper Counties during 2000, about 81 percent of monitored pumping was attributed to the Upper Floridan aquifer, about 15 percent to the middle Floridan aquifer, and the remainder to the surficial and Lower Floridan aquifers.

Ground-Water Level Trends

Ground-water levels are affected by precipitation, evapotranspiration, and ground-water withdrawal. Water levels generally are highest in the winter and early spring when evapotranspiration is lowest and irrigation withdrawals are minimal; water levels are lowest during summer and fall when evapotranspiration and withdrawals are greatest. Water levels may respond to pumping from an adjacent aquifer where aquifer interconnection occurs as a result of discontinuous or leaky confining units.

During 1980–2000, water levels showed a combination of rises and declines in response to changing pumping patterns and a prolonged drought during 1998–2000. During 1980–2000, there was an increase in total ground-water use of about 4 Mgal/d in the study area. This increase included ground-water use in Beaufort and Jasper Counties, S.C., and Bryan and Effingham Counties, Ga.; there was, however, a net decrease in Chatham County, Ga., of about 12 Mgal/d (fig 8). Total ground-water use in these five counties increased to a maximum of about 144 Mgal/d until 1990, and then generally decreased until 2000.

Table 1. Estimated ground-water pumpage for all simulated aquifers in selected counties, pre-1980.

[<, less than; selected counties are those for which specific industrial or public-supply data are available. Data from Counts and Donsky, 1963; Counts and Krause, 1976; Gregg and Zimmerman, 1974; Hayes, 1979; Landmeyer and Belval, 1996; Smith, 1994; Wait, 1965; and Wait and Gregg, 1973]

State	County	Estimated pumpage in million gallons per day								
		1915	1920	1930	1937	1940	1955	1965	1970	1975
Florida	Duval	<0.1	0.1	0.2	0.6	37.2	71.3	52.6	66.9	55.1
	Nassau	<0.1	<0.1	0.2	0.5	34.7	55.7	44.7	58.2	63.0
Georgia	Bryan	<0.1	<0.1	0.1	0.3	0.9	2.2	2.7	2.7	2.8
	Camden	<0.1	<0.1	0.1	0.4	1.3	26.4	40.4	35.2	40.4
	Chatham	1.4	1.4	1.5	21.7	29.6	44.9	53.7	61.2	71.4
	Effingham	<0.1	<0.1	0.1	0.3	1.1	2.5	3.5	3.8	4.0
	Evans	<0.1	<0.1	<0.1	0.1	0.2	0.7	0.9	0.8	0.8
	Glynn	<0.1	1.3	11.5	15.3	28.1	56.9	93.6	84.4	88.8
	Liberty	<0.1	<0.1	0.1	0.3	1.1	5.3	13.9	12.4	13.2
	Wayne	<0.1	<0.1	0.2	0.5	1.5	27.0	46.0	54.0	59.3
South Carolina	Beaufort	<0.1	<0.1	0.2	0.4	1.5	3.6	4.7	5.2	10.5

Table 2. Estimated ground-water pumpage from the Upper Floridan aquifer, in the coastal area of Georgia and adjacent parts of South Carolina and Florida, 1980–2000.

[Values with * are interpolated; modified from Payne and others, 2005]

State	County	Pumpage, in million gallons per day						
		1980	1985	1990	1995	1997	Sept. 1998	2000
Florida	Baker	1.72	2.88	3.68	2.11	2.11	2.11*	2.11
	Columbia	3.05	4.79	5.07	6.92	6.57	6.39*	6.04
	Duval	46.86	50.21	50.86	48.12	50.53	49.89*	48.61
	Hamilton	0.10	0.30	0.44	0.44	0.46	0.47*	0.49
	Nassau	51.18	43.99	40.77	42.45	44.64	44.81*	45.16
Georgia	Appling	5.71	2.60	2.10	2.38	2.47	3.04*	4.17
	Atkinson	1.89	1.50	0.58	1.58	1.58	2.02*	2.91
	Bacon	2.63	2.28	2.11	2.47	2.21	2.82*	4.04
	Ben Hill	3.71	4.92	3.34	10.97	10.98	9.84*	7.57
	Berrien	2.43	3.26	2.80	4.65	4.66	4.88*	5.33
	Bleckley	5.59	4.28	3.29	2.35	2.35	3.79*	6.66
	Brantley	1.46	1.63	1.83	1.90	1.94	1.73*	1.30
	Bryan	0.67	0.87	1.03	1.06	1.70	1.67*	1.60
	Bulloch	3.75	2.71	5.87	7.83	5.05	5.26*	5.70
	Burke	10.30	6.34	5.82	8.16	8.22	12.93*	22.34
	Camden	37.12	42.98	45.74	47.15	45.83	47.40*	50.55
	Candler	1.83	2.57	1.64	1.67	1.70	2.06*	2.79
	Charlton	6.50	1.22	1.38	1.45	0.95	1.05*	1.25
	Chatham	79.75	78.98	85.54	75.84	70.66	69.82*	68.15
	Clinch	0.85	0.72	0.65	1.03	1.04	1.17*	1.44
	Coffee	12.59	7.98	5.60	7.59	7.52	10.09*	15.23
	Crisp	3.16	3.45	5.31	10.28	10.24	9.68*	8.56
	Dodge	7.02	3.95	2.40	4.28	4.28	4.17*	3.96
	Dooly	6.30	9.45	3.18	9.25	9.25	12.39*	18.68

Table 2. Estimated ground-water pumpage from the Upper Floridan aquifer, in the coastal area of Georgia and adjacent parts of South Carolina and Florida, 1980–2000.—Continued

[Values with * are interpolated; modified from Payne and others, 2005]

State	County	Pumpage, in million gallons per day						
		1980	1985	1990	1995	1997	Sept. 1998	2000
Georgia	Echols	0.17	0.18	0.25	1.04	1.77	2.14*	2.88
	Effingham	2.26	2.06	4.98	5.98	4.42	4.49*	4.62
	Emanuel	7.34	5.30	4.18	4.51	4.53	4.43*	4.22
	Evans	0.82	0.76	1.06	1.50	1.48	1.57*	1.75
	Glascock	0.73	0.72	0.99	1.34	1.35	1.35*	1.36
	Glynn	95.40	77.84	82.02	63.68	61.61	61.45*	61.14
	Irwin	1.96	1.86	2.15	5.75	5.75	5.92*	6.25
	Jeff Davis	5.11	5.80	4.77	3.09	3.09	3.34*	3.84
	Jefferson	4.97	9.90	8.85	7.76	7.62	9.10*	12.06
	Jenkins	2.74	2.65	2.45	3.19	3.13	3.43*	4.03
	Johnson	1.37	1.81	0.92	1.83	1.83	1.93*	2.12
	Lanier	3.07	2.92	1.69	2.02	2.02	2.01*	1.97
	Laurens	4.32	4.15	4.23	5.78	5.81	6.52*	7.94
	Liberty	13.62	14.58	17.97	15.91	16.10	15.96*	15.69
	Long	0.29	0.24	0.23	0.27	0.27	0.41*	0.69
	McIntosh	0.70	1.03	0.76	1.07	1.09	1.01*	0.85
	Montgomery	0.89	1.51	0.94	2.40	2.40	2.14*	1.61
	Pierce	2.64	2.03	1.80	3.24	3.42	4.35*	6.22
	Pulaski	6.94	8.27	6.87	8.59	8.53	9.51*	11.46
	Screven	7.90	7.19	7.87	6.36	6.93	10.04*	16.24
	Tattnall	1.56	1.89	1.77	3.53	3.59	3.61*	3.66
	Telfair	3.28	4.62	3.30	6.33	6.33	5.55*	4.00
	Tift	1.89	2.19	2.61	3.95	3.80	3.72*	3.57
	Toombs	2.87	3.91	3.61	3.65	4.17	4.88*	6.30
	Treutlen	0.49	0.54	0.79	1.31	1.31	1.24*	1.10
	Turner	1.02	1.00	0.93	2.91	2.92	2.80*	2.57
	Ware	6.25	7.25	6.20	5.51	5.97	6.80*	8.45
	Washington	10.01	12.24	13.02	14.39	14.88	15.25*	16.01
	Wayne	74.54	69.80	69.27	64.89	63.59	63.55*	63.47
	Wheeler	1.60	0.83	0.61	2.22	2.22	1.84*	1.07
	Wilcox	4.06	9.84	5.40	8.43	8.43	10.53*	14.74
South Carolina	Allendale	7.84	7.84	8.31	9.44	9.85	9.76*	9.59
	Bamberg	1.99	1.99	2.09	2.52	4.04	4.80*	6.32
	Barnwell	1.15	1.15	3.32	2.91	4.90	5.77*	7.50
	Beaufort	0.85	20.80	17.48	19.56	33.58	27.77	21.44
	Colleton	0.00	0.00	0.00	0.00	0.00	0.00*	0.00
	Hampton	3.21	3.21	3.95	4.32	5.99	6.87*	8.63
	Jasper	1.25	1.16	1.97	1.31	2.13	2.54	3.34
	Total	**583.25**	**584.95**	**580.63**	**604.43**	**617.78**	**607.57**	**683.35**

Table 3. Estimated ground-water pumpage from the Lower Floridan aquifer, in the coastal area of Georgia and adjacent parts of South Carolina and Florida, 1980–2000.

[County aggregate and site-specific data were used to estimate average annual pumpage using procedures described by Taylor and others (2003). Data sources described in Payne and others (2005)]

State	County	Pumpage, in million gallons per day					
		1980	1985	1990	1995	1997	2000
Florida	Baker	0.26	0.43	0.55	0.32	0.32	0.32
	Columbia	0.00	0.00	0.00	0.00	0.00	0.00
	Duval	92.52	99.13	100.46	95.01	99.48	95.98
	Hamilton	0.00	0.00	0.00	0.00	0.00	0.00
	Nassau	2.51	2.16	2.00	2.09	2.18	2.21
Georgia	Appling	0.00	0.00	0.00	0.00	0.00	0.00
	Atkinson	0.00	0.00	0.00	0.00	0.00	0.00
	Bacon	0.00	0.00	0.00	0.00	0.00	0.00
	Ben Hill	0.21	0.39	0.38	1.30	1.30	0.59
	Berrien	0.41	0.53	0.45	0.67	0.67	0.77
	Bleckley	0.87	0.63	0.41	0.40	0.40	1.00
	Brantley	0.00	0.00	0.00	0.00	0.00	0.00
	Bryan	0.00	0.00	0.00	0.00	0.00	0.00
	Bulloch	0.23	0.20	0.16	0.31	0.32	0.32
	Burke	1.60	0.92	0.83	1.26	1.27	3.24
	Camden	0.00	0.00	0.00	0.00	0.00	0.00
	Candler	0.26	0.34	0.17	0.19	0.19	0.37
	Charlton	0.00	0.00	0.00	0.00	0.00	0.00
	Chatham	3.58	3.20	4.13	3.76	3.78	3.23
	Clinch	0.00	0.00	0.00	0.00	0.00	0.00
	Coffee	1.49	0.78	0.25	0.47	0.53	1.73
	Crisp	0.32	0.28	0.78	1.58	1.59	1.30
	Dodge	1.01	0.52	0.22	0.46	0.46	0.41
	Dooly	0.96	1.46	0.41	1.29	1.29	2.93
	Echols	0.00	0.00	0.00	0.00	0.00	0.00
	Effingham	0.02	0.01	0.03	0.04	0.03	0.03
	Emanuel	0.85	0.68	0.36	0.52	0.52	0.48
	Evans	0.05	0.04	0.05	0.06	0.06	0.09
	Glascock	0.04	0.02	0.02	0.02	0.02	0.02
	Glynn	0.00	0.00	0.00	0.00	0.00	0.00
	Irwin	0.25	0.21	0.26	0.87	0.87	0.96
	Jeff Davis	0.81	0.89	0.66	0.40	0.40	0.47
	Jefferson	0.69	1.44	1.03	0.76	0.97	1.68
	Jenkins	0.41	0.37	0.33	0.47	0.46	0.61
	Johnson	0.17	0.26	0.12	0.27	0.27	0.32
	Lanier	0.00	0.00	0.00	0.00	0.00	0.00
	Laurens	0.74	0.62	0.60	0.97	0.95	1.31
	Liberty	0.00	0.00	0.00	0.00	0.00	0.00
	Long	0.01	0.01	0.01	0.02	0.02	0.07
	McIntosh	0.00	0.00	0.00	0.00	0.00	0.00
	Montgomery	0.11	0.20	0.10	0.33	0.33	0.19
	Pierce	0.00	0.00	0.00	0.00	0.00	0.00

Table 3. Estimated ground-water pumpage from the Lower Floridan aquifer, in the coastal area of Georgia and adjacent parts of South Carolina and Florida, 1980–2000.—Continued

[County aggregate and site-specific data were used to estimate average annual pumpage using procedures described by Taylor and others (2003). Data sources described in Payne and others (2005)]

State	County	Pumpage, in million gallons per day					
		1980	1985	1990	1995	1997	2000
Georgia	Pulaski	1.11	1.31	1.09	1.31	1.35	1.81
	Screven	1.18	1.03	0.40	0.66	0.69	2.32
	Tattnall	0.06	0.09	0.08	0.28	0.28	0.15
	Telfair	0.48	0.55	0.32	0.83	0.82	0.42
	Tift	0.33	0.38	0.46	0.69	0.66	0.62
	Toombs	0.24	0.31	0.20	0.27	0.27	0.69
	Treutlen	0.06	0.05	0.06	0.12	0.12	0.11
	Turner	0.17	0.17	0.16	0.50	0.50	0.44
	Ware	0.00	0.00	0.00	0.00	0.00	0.00
	Washington	1.52	1.89	1.96	2.16	2.04	2.07
	Wayne	0.00	0.00	0.00	0.00	0.00	0.00
	Wheeler	0.21	0.10	0.06	0.34	0.34	0.14
	Wilcox	0.68	1.69	0.90	1.43	1.43	2.53
South Carolina	Allendale	0.00	0.00	0.00	0.00	0.00	0.00
	Bamberg	0.00	0.00	0.00	0.00	0.00	0.00
	Barnwell	0.00	0.00	0.00	0.00	0.00	0.00
	Beaufort	0.00	0.05	0.01	0.01	0.09	0.26
	Colleton	0.35	0.55	0.56	0.58	0.47	0.51
	Hampton	0.00	0.00	0.00	0.00	0.00	0.00
	Jasper	0.01	0.00	0.00	0.00	0.01	0.01
Total		**116.77**	**123.88**	**121.00**	**123.00**	**127.74**	**132.69**

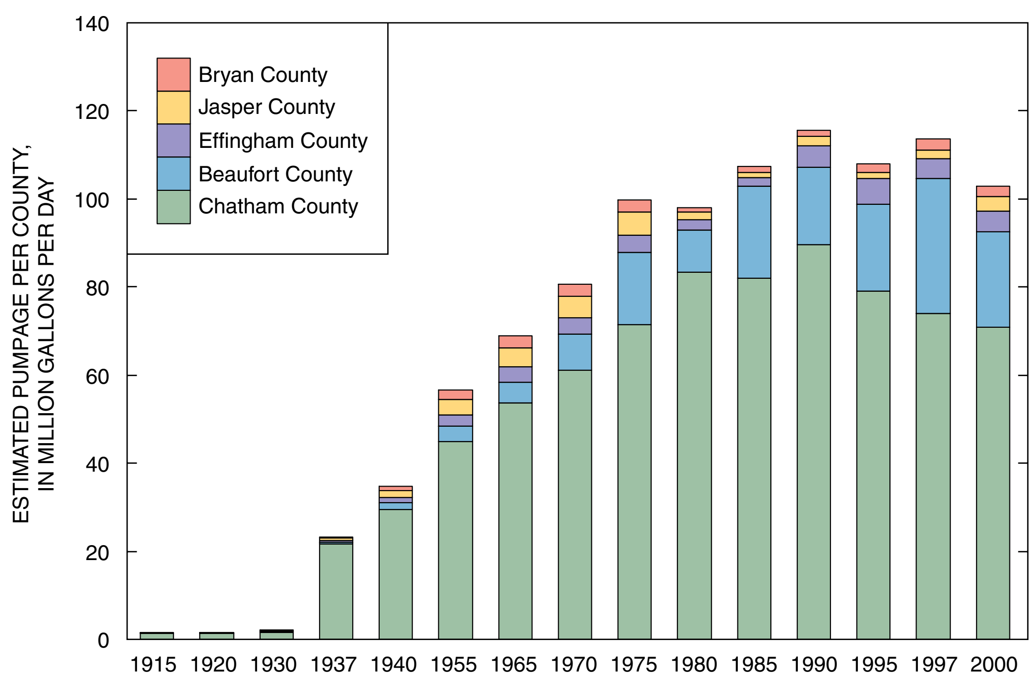

Figure 8. Estimated pumpage per county for Bryan, Chatham, and Effingham Counties, Georgia, and Beaufort and Jasper Counties, South Carolina (county locations shown in figure 1).

To determine water-level trends during 1980–2000, periodic and mean-monthly water levels in the Upper Floridan aquifer were compared and differences computed (fig. 9). In the Upper Floridan aquifer, water levels rose almost 10 ft near the center of the cone of depression in Savannah most likely because of the decrease in pumping in Chatham County during that period. In the rest of the study area, water levels declined from 1 to 20 ft (fig. 9), with the largest declines, greater than 10 ft, occurring in the western part of Chatham County. These declines correspond to a general increase in regional withdrawal from the Upper Floridan aquifer of about 100 Mgal/d, across the entire model area.

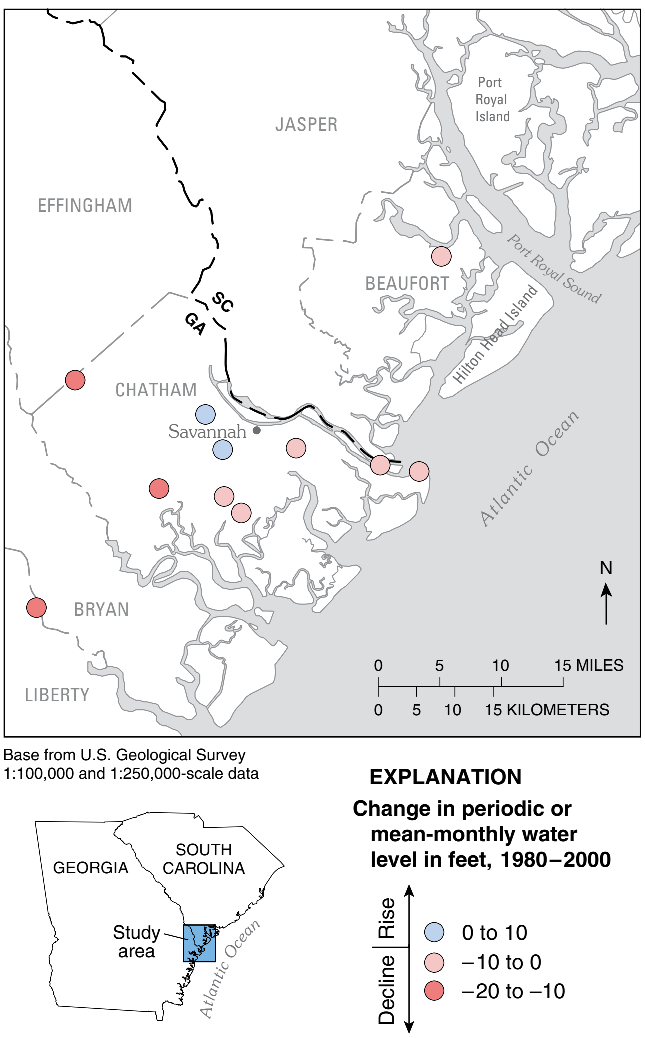

Figure 9. Change in water levels in wells in the Upper Floridan aquifer in the Savannah, Georgia–Hilton Head Island, South Carolina, area, May 1980–September 2000 (modified from Payne and others, 2005).

Salinity Distribution

The distribution of salinity in ground water in the study area is complex and indicates several possible sources and mechanisms of transport. For predevelopment conditions the distribution of salinity is uncertain, because few early data exist. An exception is at Parris Island, S.C., where shortly after water-supply wells were drilled and used for ground-water supply in the late 1800s, salinity levels in the Upper Floridan aquifer increased to an unacceptable level (Hayes, 1979).

In previous conceptual models, a predevelopment, regional, steady-state offshore freshwater-saltwater interface was postulated to extend from the coastline near Port Royal Sound, S.C., to about 70–80 mi offshore of the Georgia–Florida border (Krause and Clarke, 2001). The freshwater-saltwater interface is a subsurface zone in which freshwater and salty ground water mix through processes of mechanical dispersion and chemical diffusion. In this case, the source of saltwater is seawater or other salty surface water. The presumed configuration of this interface was based on the early presence of saltwater intrusion at Parris Island, sparse offshore water-chemistry data, an inferred extension of the onshore chloride distribution (Sprinkle, 1982), and application of the Ghyben-Herzberg principle (Reilly and Goodman, 1985). Data collected offshore of the Georgia–Florida border (Johnston and others, 1982) indicate that if a regional freshwater-saltwater interface exists, it is relatively far offshore, and likely does not contribute to saltwater intrusion in the southernmost coastal counties of Georgia or in northeastern Florida. Within the study area, Counts and Donsky (1963) used estimated predevelopment heads at Hilton Head Island, Daufuskie Island, and Cockspur Island (fig. 1), and applied the Ghyben-Herzberg principle to estimate the freshwater-saltwater interface in the Upper Floridan aquifer. The position of the predevelopment interface was estimated to be much shallower and much farther landward than indicated by post-predevelopment water-quality samples. Hence, the Ghyben-Herzberg principle probably does not apply in the study area because the saltwater-freshwater interface has not yet reached steady state, and the true present-day interface is likely much farther seaward.

Water-chemistry data collected and analyzed since predevelopment have resulted in a better definition of the present-day salinity distribution and a refinement of the conceptual model for saltwater intrusion in the Floridan aquifer system in the study area. In the confining unit above the Upper Floridan aquifer, and in overlying units, elevated salinity levels (relative to the U.S. Environmental Protection Agency [USEPA; 1994] secondary drinking water standard of 250 mg/L chloride) are observed offshore of Hilton Head Island (Falls and others, 2005b) as well as in the Savannah River channel, seaward of Savannah (Cardwell Smith, U.S. Army Corps of Engineers, written commun., 2004). These data generally show a downward decrease in salinity where vertical profiles are available, indicating that seawater is leaking downward through the confining unit in some locations.

In the Upper Floridan aquifer, the highest salinities are in the area around Parris Island and Port Royal Sound, S.C., where the aquifer is shallow and the overlying confining unit is thin. As discussed previously, shortly after wells were installed on Parris Island, S.C., ground-water salinity increased such that some wells were unusable. Hayes (1979) attributes some of the saltwater intrusion into the Upper Floridan aquifer on Parris Island, S.C., to either lateral movement or downward leakage from nearby saltwater bodies, because of breaching or thinning of the confining unit and proximity to a saltwater source. Landmeyer and Belval (1996), using data from Burt and others (1987), mapped the chloride distribution at the top and base of the Upper Floridan aquifer during 1984 in the Port Royal Sound–Hilton Head Island–Parris Island area. They interpreted a higher concentration at the base, by one or two orders of magnitude, than at the top of the aquifer. The authors noted that some of the values are from wells open to both the Upper Floridan aquifer and underlying confining unit, which generally has a higher chloride concentration.

Specific conductance monitoring at sites in southern Beaufort County since 1997 indicates areas at the northern end of Hilton Head Island, at Pinckney Island, and near the Colleton River where chloride concentration in the Upper Floridan aquifer is elevated (Robert Logan and Jack Childress, South Carolina Department of Health and Environmental Control, written commun., 2005) (appendix B, fig. B2, table B1). Chloride concentration is estimated from specific conductance using a visual best-fit approximation of data from southern Beaufort County (James E. Landmeyer, U.S. Geological Survey, written commun., 2005) (appendix B, fig. B1). These data show a spatially and temporally variable chloride concentration in the Upper Floridan aquifer. At some of these sites, a marked increase in estimated chloride concentration is observed at the base of the Upper Floridan aquifer and into the underlying confining unit (fig. 10). An increase in estimated chloride concentration through time is also observed at well BFT-0502 in the Upper Floridan aquifer (fig. 10). Recently collected samples from wells within the area of elevated chloride concentration in southern Beaufort County, analyzed for chlorofluorocarbons, indicate ages of 15–40 years for intruded saltwater (James E. Landmeyer, U.S. Geological Survey, written commun., 2005). This supports the interpretation by Back and others (1970), who used geochemical mixing analyses and C-14 dating to suggest that the Upper Floridan aquifer underlying the northern end of Hilton Head Island and Parris Island contains recently recharged ground water, whereas the part of the aquifer underlying the southern end of Hilton Head Island, where chloride concentrations are not elevated, contains older, incompletely flushed ground water. The spatial distribution of estimated chloride concentration and evidence of recent age of this ground water may indicate locations where saltwater is entering the Upper Floridan aquifer in southern Beaufort County (fig. 11).

As part of a hydrogeologic investigation of the Upper Floridan aquifer and overlying units in the area offshore of Hilton Head Island and Tybee Island and in Calibogue Sound, several wells were drilled, aquifer and confining unit sediments were sampled, ground-water levels were measured, and ground-water samples were collected and analyzed (Falls and others, 2005b). The locations of these wells generally are along the flow gradient, and cross an area where seismic data indicate that the confining unit overlying the Upper Floridan aquifer is partially eroded by paleoriver channels (Foyle and others, 2001). Samples collected at various depths from each site show decreasing concentration of chloride from the top of the confining unit downward to the top of the Upper Floridan aquifer. At one offshore site, the 8-mile site, the confining unit is notably thinner, and chloride concentrations are elevated in the confining unit and the top of the Upper Floridan aquifer, relative to the other sites (fig. 12). Geochemical data further indicate that saline water in the Upper Floridan aquifer at this site is not modern seawater, which implies a downward movement of relict saltwater into the Upper Floridan aquifer from the surficial aquifer through the thin confining unit (Falls and others, 2005b).

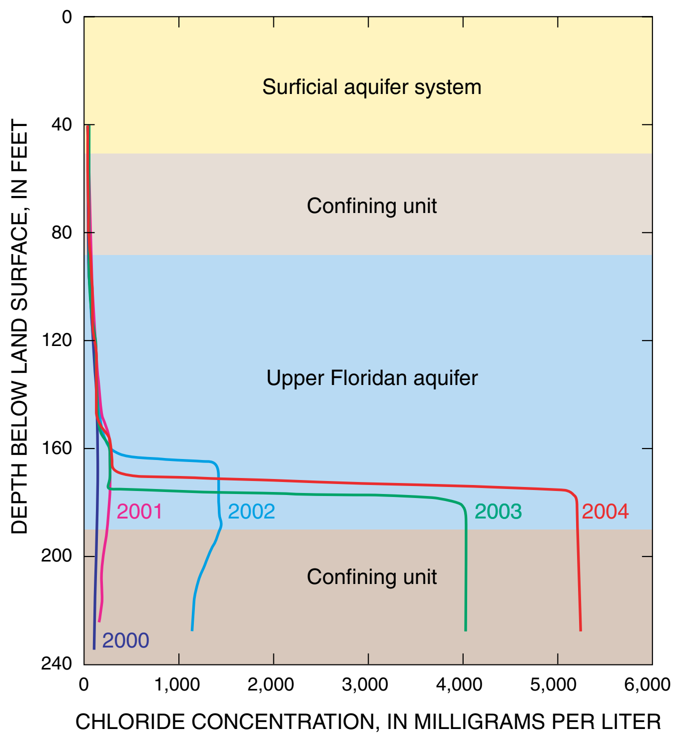

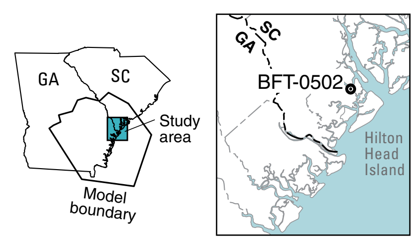

Figure 10. Estimated chloride concentration in well BFT-0502 for years 2000–2004 (data from Robert Logan, South Carolina Department of Health and Environmental Control, written commun., 2005).

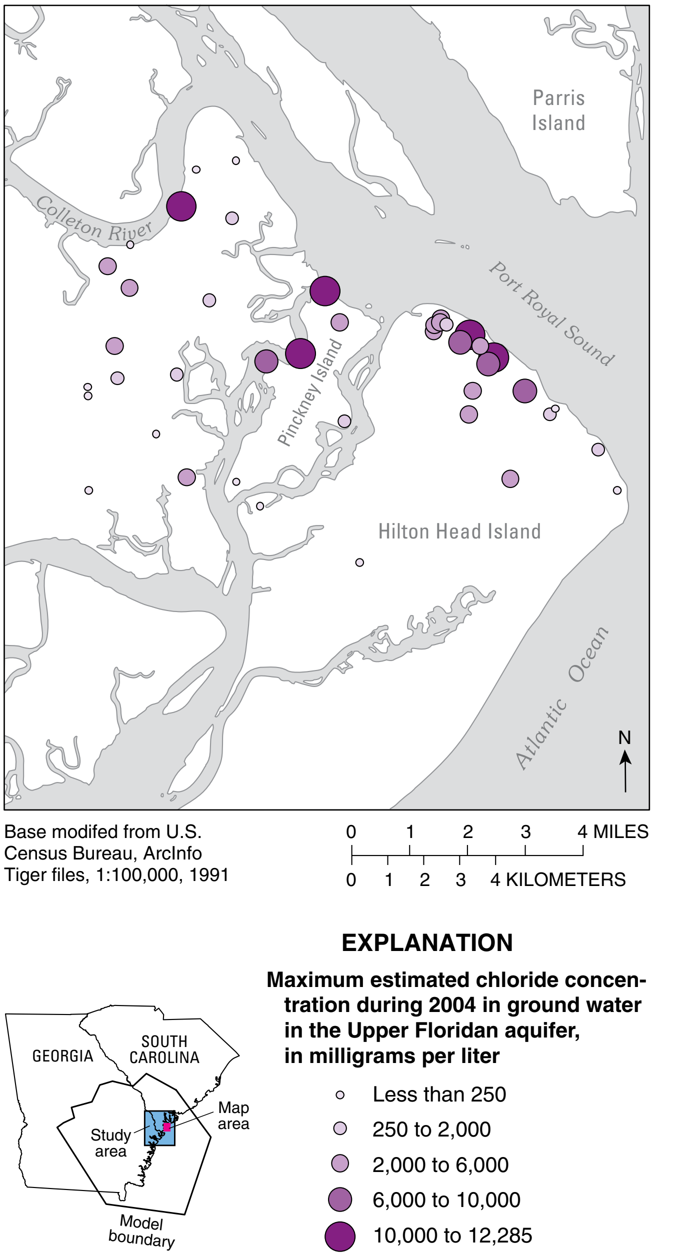

Figure 11. Maximum estimated chloride concentration in ground water in the Upper Floridan aquifer in the Hilton Head Island, South Carolina, area during 2004, estimated from specific conductance (data from Robert Logan, South Carolina Department of Health and Environmental Control, written commun., 2005).

Although fewer data exist to define the salinity distribution in the Lower Floridan aquifer, water in the Lower Floridan aquifer generally has higher salinity than water in the Upper Floridan aquifer in Chatham County and at locations in central and southern Hilton Head Island (Back and others, 1970; Clarke and others, 1990; Counts and Donsky, 1963; McCollum and Counts, 1964). In the Savannah area, salinity increases with depth from the Upper Floridan aquifer downward to the Lower Floridan aquifer and to units below; on Skidaway Island, Ga., chloride concentration in a deep Lower Floridan aquifer well increased during 1985–1987 (Clarke and others, 1990). Higher than normal fluid thermal gradients in Lower Floridan wells in the Savannah area indicate that the source of saline water at depth may be saltwater originating at greater depths (Clarke and others, 1990). Counts and Donsky (1963) noted that equivalent freshwater heads in the Lower Floridan at Cockspur Island show minimal head differential with the Upper Floridan aquifer, and suggest a low potential for upward flux of saltwater. Additionally, the lower permeability of the confining unit above the Lower Floridan aquifer makes it less likely to transport saltwater into the overlying Upper Floridan aquifer in substantial quantities. The same argument may apply to the potential of the low-permeability unit underlying the Upper Floridan aquifer on Hilton Head Island and Port Royal Sound area as a source of saltwater intrusion into the upper permeable zone.

Possible Mechanisms of Saltwater Intrusion

Three possible mechanisms of saltwater intrusion are postulated and described herein. It is likely that no single mechanism is responsible for all of the present (and potential) saltwater intrusion in the study area. Instead, a combination of some of these mechanisms may be operating at different locations and to different degrees.

> Mechanism 1: *Brackish, estuarine water or seawater moves downward along the vertical gradient, through the confining unit overlying the Upper Floridan aquifer in areas where the confining unit is thin or leaky, and laterally within the aquifer toward local pumping centers*. This confining unit is particularly thin over the Beaufort Arch. Local pumping of the Upper Floridan aquifer on Hilton Head Island and regional pumping centered at Savannah have lowered the potentiometric surface of the Upper Floridan aquifer in the study area, resulting in a downward gradient from the water table and the ocean-seafloor interface. As indicated from offshore data of Falls and others (2005b), chloride concentration decreases with depth in the confining unit, and chloride concentration in the Upper Floridan aquifer is greatest at the top (fig. 12). A pattern of decreasing chloride concentration with depth also has been observed in the Savannah River channel (Smith and McIntosh, 2005). The early history of pumping at Parris Island indicates that as soon as a downward vertical gradient was established, brackish water moved vertically downward through the confining unit into the aquifer, soon rendering the ground water unusable. After brackish estuarine water or seawater enters the Upper Floridan aquifer, either it may be diluted or it may accumulate and then move laterally along the flow gradient toward pumping centers. If the saline water is not diluted once it enters a permeable unit, density effects may result in an accumulation of the denser, more saline water at the

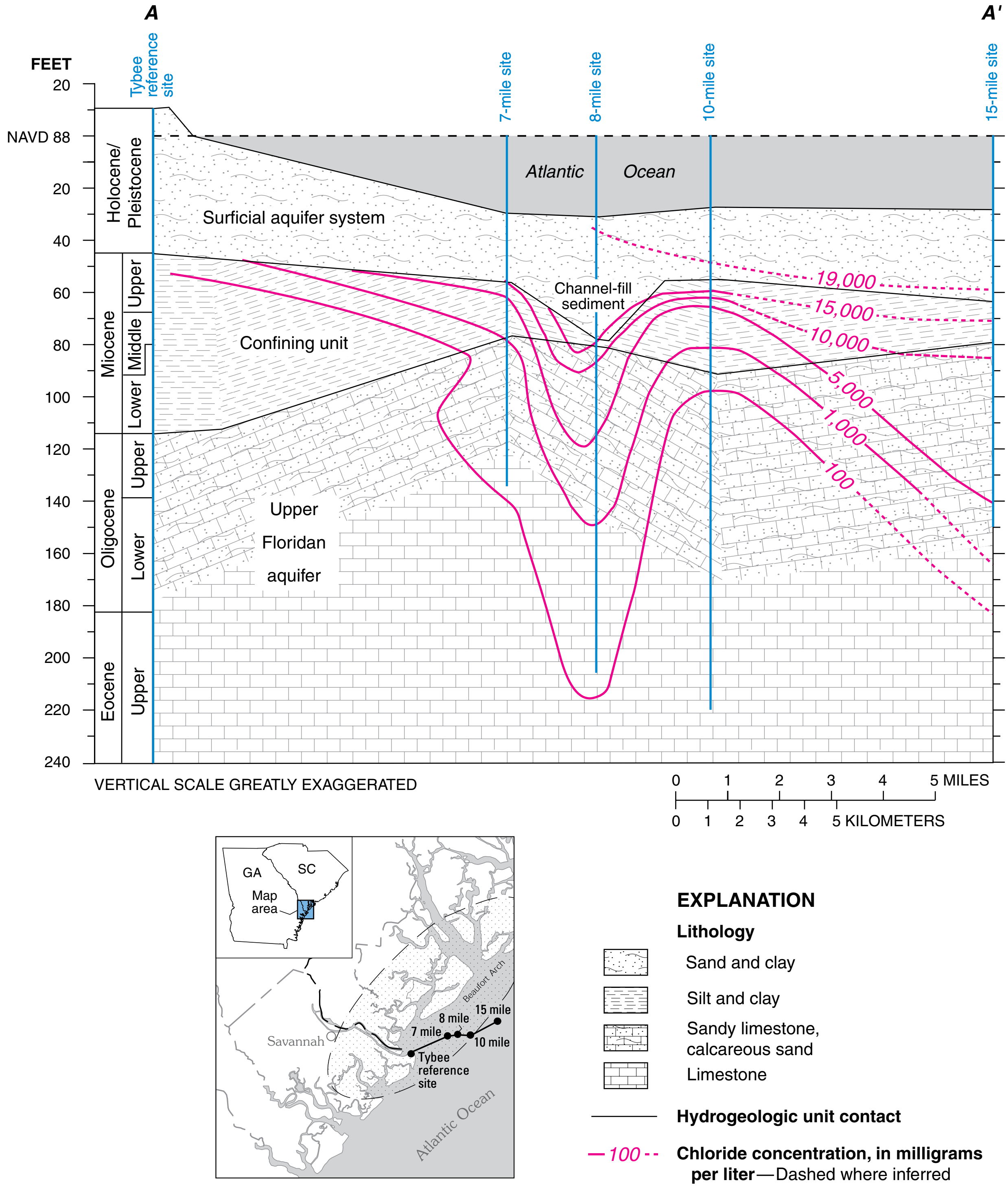

Figure 12. Hydrogeologic section A–A′ and chloride distribution from the Tybee reference site at the northern end of Tybee Island, Georgia, to the 15-mile site on the Beaufort Arch seaward of Hilton Head Island, South Carolina (modified from Falls and others, 2005b).

bottom of the permeable unit. Interpreted seismic data indicate that there are breaches in the Upper Floridan aquifer confining unit offshore of Hilton Head Island, in Calibogue Sound, at the Colleton River, and in the Beaufort and Broad Rivers (fig. 4). Seawater and brackish water overlie the aquifer at these locations. The regional potentiometric gradient is perpendicular to the contours of the cone of depression, and flow is toward Savannah on a regional scale. In addition, there are localized pumping centers on Hilton Head Island that deflect the potentiometric contours and lateral flow to these locations in the Upper Floridan aquifer. Some wells at the northern end of Hilton Head Island, at Pinckney Island, and near the Colleton River, which have been monitored for specific conductance, show an increase in salinity with depth in the Upper Floridan aquifer (Childress and Ransom, 2005).

Mechanism 2: *Saline water from the confining unit underlying the Upper Floridan aquifer may be migrating upward because of an upward hydraulic gradient.* In this case, chloride concentration would increase with depth to the base of the Upper Floridan aquifer. In the Savannah area, chloride concentration increases with depth through the Upper Floridan aquifer into the Lower Floridan aquifer. Higher-than-normal temperature gradients in deep wells and head differences between the Upper and Lower Floridan aquifers indicate an upward gradient and movement of saline waters from depth (Clarke and others, 1990). At Skidaway Island and Hutchinson Island, Ga., resistivity logs and chloride analyses of water samples collected from deep wells indicate that salinity increases with depth in the Lower Floridan aquifer, and that with time, salinity is increasing (Clarke and others, 1990). In the Hilton Head Island and Port Royal Sound area, geophysical logs and water samples collected from the deepest part of the Upper Floridan aquifer and the underlying confining unit indicate that the confining unit is saline (Burt and others, 1987). This water is possibly unflushed connate water from the previous sea-level high stand, as indicated by estimated ground-water ages of samples taken from this unit (Back and others, 1970). Vertical profiles of specific conductance at many locations near Hilton Head Island indicate an elevated chloride concentration at the base of the Upper Floridan aquifer (Childress and Ransom, 2005); however, recent age data indicate that this water is too young to be connate water (James E. Landmeyer, U.S. Geological Survey, written commun., 2005). Although the permeability of the confining unit between the Upper and Lower Floridan aquifers is unknown, it is unlikely that quantities of saltwater moving through this confining unit are large enough to result in the development of large saltwater plumes. It is possible, however, that in localized areas of high pumping rates, a substantial upward hydraulic gradient could result in localized upconing of saltwater from the confining unit into the Upper Floridan aquifer.

Mechanism 3: *Saltwater intrusion may result from the lateral movement of a proximal predevelopment, steady-state saltwater-freshwater interface in response to a pumping-induced lateral hydraulic gradient*. It has been suggested that a predevelopment interface existed in the Port Royal Sound area, and that with increases in pumping and a reversal in the hydraulic gradient, this interface started migrating along the flowpaths toward pumping centers (Krause and Clarke, 2001; Bush, 1988; Smith, 1994; Landmeyer and Belval, 1996). The presence of a predevelopment, steady-state interface is assumed in two modeling studies (Bush, 1988; Smith 1994) and used as an initial condition in both models. One of the models indicates that this interface responds rather sluggishly to the present-day stresses (Bush, 1988), whereas the other model indicates that the interface actually may be moving more rapidly and may pose an increasing potential for saltwater intrusion in the future (Smith, 1994). The presence of freshwater in the Upper Floridan aquifer offshore of Hilton Head Island (Falls and others, 2005b), however, raises doubt about the presence of the predevelopment, steady-state interface being as close to the study area as previously assumed.

Simulation of Variable-Density Ground-Water Flow and Solute Transport

Variable-density, solute-transport modeling was conducted to evaluate the conceptual model for saltwater intrusion in which salty surface water enters the Upper Floridan aquifer through localized areas in which the upper confining units are thin or absent (see “Mechanism 1” in “Possible Mechanisms of Saltwater Intrusion”). Several lines of evidence support this conceptual model: (1) the general pattern of increasing chloride concentration in the Upper Floridan aquifer; (2) seismic traces that indicate thinning of the upper confining units near two of the three apparent source areas (Foyle and others, 2001); and (3) recent ground-water dating, which indicates that much of the saltwater intruded the Upper Floridan aquifer relatively recently (James E. Landmeyer, U.S. Geological Survey, written commun., 2005). The analysis focuses on areas of observed saltwater contamination of the Upper Floridan aquifer, where sufficient data exist to calibrate the SUTRA model, specifically the northern Hilton Head Island, Pinckney Island, and Colleton River area. The model simulates the transport of saltwater through the confining unit and into the Upper Floridan aquifer by this mechanism elsewhere in the model area, as well. The paucity of data with which to calibrate the model, however, renders analysis of simulated saltwater intrusion outside of the northern Hilton Head Island–Pinckney Island–Colleton River area more speculative.

Model construction, calibration, and sensitivity are described in the following sections. Simulations were carried out through 2100 to estimate the future evolution of the chloride distribution in the Upper Floridan aquifer for several variations of the SUTRA model that account for uncertainty in the initial and boundary conditions.

In a coastal ground-water system, intrusion of saltwater into an aquifer can create gradients in fluid density that affect the flow of ground water. In the Hilton Head Island area, chloride concentrations in excess of 50 percent of seawater concentration have been observed in the Upper Floridan aquifer. Therefore, the SUTRA model described in this section is a variable-density model that accounts for the mutual interaction between the distribution of solute and the flow of ground water; the concentration of solute affects the fluid density, which affects the forces that drive ground-water flow, which in turn contributes to the transport of solute.

Model Construction

A three-dimensional, variable-density, digital ground-water flow and solute-transport model was developed for the Savannah–Hilton Head Island area, including surrounding counties and the adjacent offshore area, using the SUTRA simulator (Voss and Provost, 2002). This model was based on a regional-scale, ground-water flow model of coastal Georgia and adjacent parts of South Carolina and Florida (Payne and others, 2005), which was constructed using the USGS finite-difference ground-water flow simulator, MODFLOW-2000 (Harbaugh and others, 2000), hereinafter referred to as the MODFLOW simulator. The model is referred to as the MODFLOW model, to distinguish it from other models.

The MODFLOW model was designed to simulate steady-state regional flow characteristics of the Brunswick aquifer system, the Upper Floridan aquifer, and the Lower Floridan aquifer. The model comprises seven layers, one for each hydrogeologic unit: surficial aquifer system, Brunswick aquifer system, Upper Floridan aquifer, Lower Floridan aquifer, and intervening confining units. A combination of boundary condition types was used, including head-dependent flux at the top of the model, specified head and no-flow at the sides and bottom, and specified flux to represent wells. The MODFLOW model is calibrated to 1980 and 2000 mean-annual pumping conditions.

The SUTRA model described in this report was constructed as consistently as possible with the MODFLOW model, with some modifications to account for fundamental differences in the simulators, and others to suit better the SUTRA model's purpose and scope. The SUTRA model was used to characterize the confined ground-water flow system and chloride distribution, primarily in the Upper Floridan aquifer, and to simulate variations on a hypothetical mechanism that might contribute to observed and potential saltwater intrusion in the Upper Floridan aquifer in the Savannah–Hilton Head Island study area (fig. 1). The SutraGUI graphical modeling interface (Winston, 2000; Winston and Voss, 2004) based on Argus ONE® was used to convert spatially referenced datasets into model input datasets for both models, which facilitated conversion of the MODFLOW model to the SUTRA model. The finite-element mesh for the SUTRA model was refined in the study area and coarsened elsewhere, and the model was recalibrated to September 1998 water levels within the study area. The three-dimensional approach allowed for simulation of flow and solute transport in a hydraulically and spatially complex hydrogeologic system, and for testing of several variations of the conceptual model. To allow transient simulation of saltwater intrusion and transport, the model uses an estimated pumping history from predevelopment through the year 2000.

Model Layering

The hydrogeologic unit layering is principally unmodified from the MODFLOW model (Payne and others, 2005). There are seven simulated aquifer and confining units in the SUTRA model (fig. 13) that include the following:

- confined upper and lower water-bearing zones of the surficial aquifer system grouped together as one unit (unit 1),
- Brunswick aquifer system confining unit (unit 2),
- upper and lower Brunswick aquifers grouped together to form the Brunswick aquifer system (unit 3),
- Upper Floridan aquifer confining unit (unit 4),
- Upper Floridan aquifer (unit 5),
- Lower Floridan aquifer confining unit (unit 6), and
- Lower Floridan aquifer (unit 7).

Unit 1 comprises the confined upper and lower water-bearing zones of the surficial aquifer system. The SUTRA model does not specifically address the unconfined portion of the surficial aquifer system, because the spatial discretization of the model is generally insufficient to simulate accurately unconfined flow-system characteristics. Simulated flow in the confined surficial aquifer system is used primarily as a means to move water into and out of the deeper confined aquifers, and not to provide detailed characterization of flow in the unit.

Maps showing the altitude of the top of each unit were contoured and digitized based on published data, unpublished data, and Internet sources (appendix C). The altitude of the top of each unit was adjusted where necessary and justifiable to ensure that the surfaces did not intersect one another (see appendix C).

Although each hydrogeologic unit is assigned a specific number of element layers across the entire model area, not all hydrogeologic units are continuous across the entire model area. The distribution of the hydrogeologic units is illustrated in a schematic diagram (fig. 13) and hydrogeologic sections (fig. 14) along the approximate strike and dip of geologic formations.

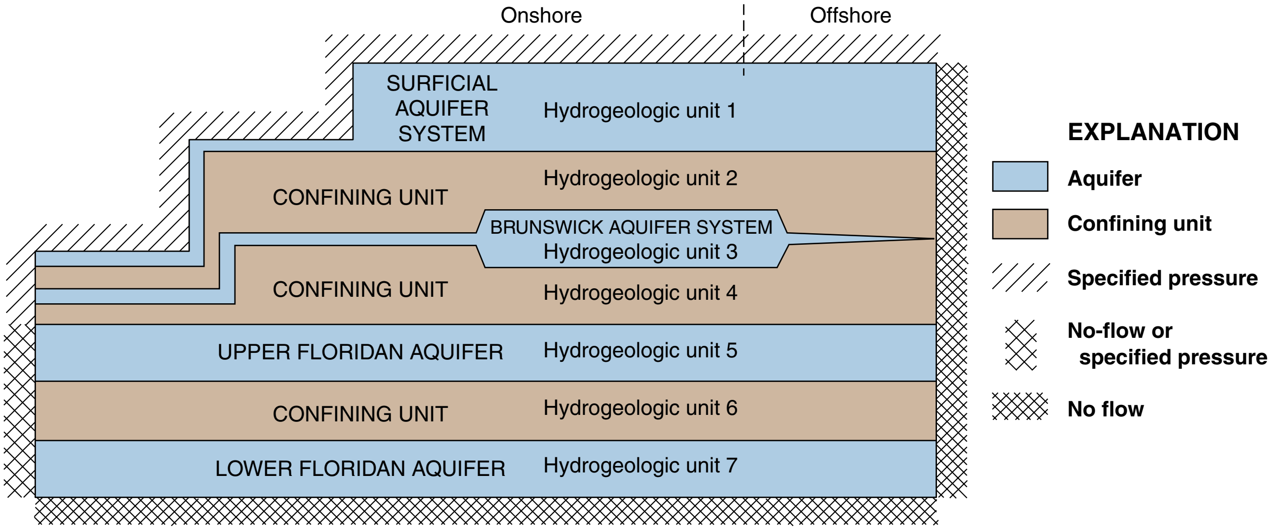

Figure 13. Schematic diagram showing layering of simulated hydrogeologic units and boundary conditions.

To simulate the "pinchout" or absence of the Brunswick aquifer system in parts of the study area, unit 3 was assigned a nominal thickness and hydraulic properties representative of the average of adjacent units 2 and 4 (figs. 13 and 14). In areas where unit 3 is absent, the Upper Floridan aquifer (unit 5) was separated from the surficial aquifer system by a composite confining unit consisting of units 2, 3, and 4. To simulate the absence of overlying units in areas where the Upper Floridan aquifer is at or near land surface, overlying hydrogeologic units were assigned a nominal thickness and the same hydraulic properties as the Upper Floridan aquifer in those areas.

Spatial Discretization

The finite-element technique used by the SUTRA simulator (Voss and Provost, 2002) requires that the simulated area be divided into discrete elements, with a node at each corner of an element. This technique allows the SUTRA model to be discretized as a three-dimensional mesh consisting of irregularly connected quadrilaterals in plan view (fig. 15). Each layer of elements is vertically aligned such that the corners of the quadrilaterals represent vertical columns of nodes. The areal extent of the SUTRA model is the same as that covered by the MODFLOW model of Payne and others (2005), but the discretization is modified to capture relevant details within the study area.

In the Savannah–Hilton Head Island study area, the finite-element mesh is refined laterally to allow more detailed representation of the pumping and head distributions, and coarsened elsewhere to minimize the number of elements and nodes, and thus the computational demands of the SUTRA model (fig. 15). The lateral discretization is further refined in selected areas where saltwater intrusion into the Upper Floridan aquifer is observed. The Upper Floridan aquifer is discretized vertically into 4 elements in the version of the SUTRA model used in the first stage of calibration (calibration to head observations) and 10 elements in the final SUTRA model that simulates solute transport; the Lower Floridan aquifer is discretized vertically into four elements. The remaining units are each discretized vertically into two elements. Along any given vertical column of nodes, the vertical spacing between nodes is uniform within each hydrogeologic unit. The SUTRA model encompasses 42,155 mi^2 and is constructed with 2,244 elements and 2,277 nodes in the horizontal dimension, and 18 elements and 19 nodes in the vertical direction in the head calibration model. The final solute-transport model comprises 4,093 elements and 4,126 nodes in the horizontal dimension, and 24 elements and 25 nodes in the vertical direction. Element sizes range from about 0.003 to 774 mi^2. The mesh was generated and modified using graphical grid-generation tools from the graphical user interface SutraGUI (Winston and Voss, 2004).

Hydraulic and Transport Properties

Permeability values used by the SUTRA simulator were transferred from hydraulic conductivity values in the MODFLOW model (Payne and others, 2005) to the SUTRA model using the relation between hydraulic conductivity and permeability

$$K_h = \frac{k\rho g}{\mu} ,$$

where K_h is hydraulic conductivity, k is permeability, ρ is fluid density, g is the gravitational constant, and μ is fluid viscosity (Freeze and Cherry, 1979). For calculating the initial permeability distribution, ρ and μ are considered constants and are given freshwater values. Initial permeability values were converted directly from hydraulic conductivity values and distributed as in the MODFLOW model. The hydraulic conductivity distribution in the MODFLOW model was based on available field data, laboratory data, potentiometric-head gradients and geologic setting (Payne and others, 2005). Hydraulic conductivity within each layer was assumed isotropic.

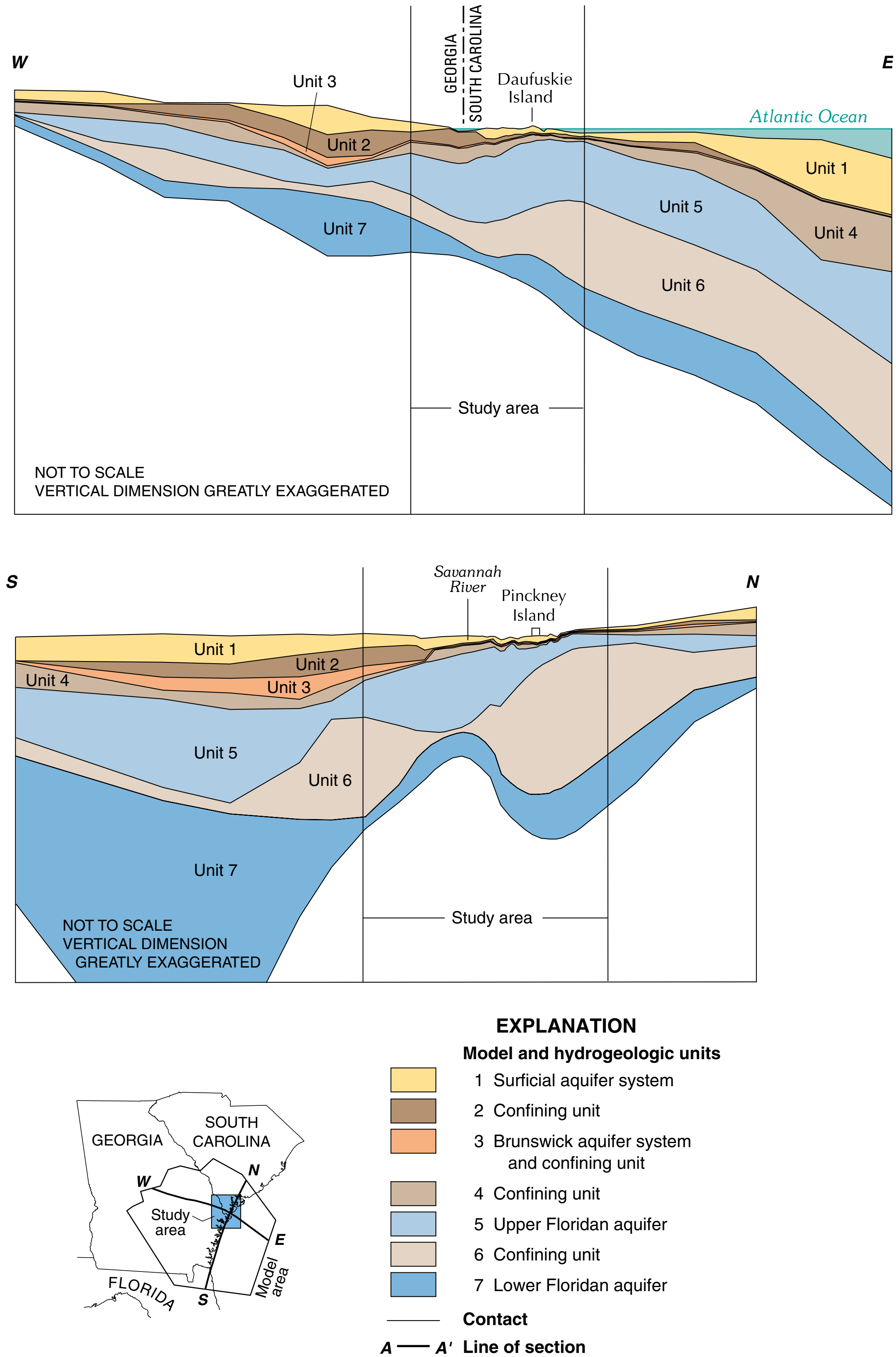

Figure 14. Hydrogeologic sections in the model area.

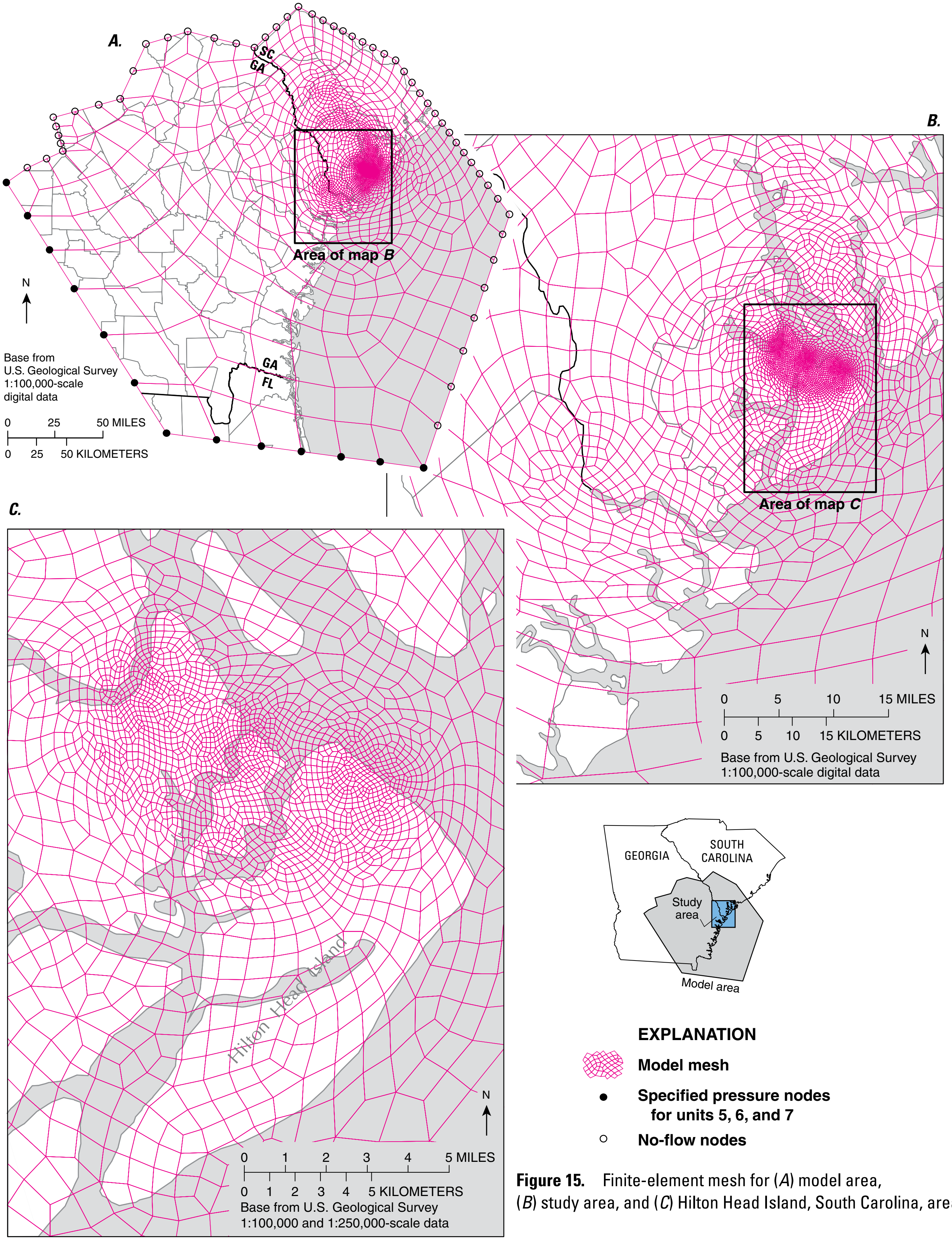

Figure 15. Finite-element mesh for (*A*) model area, (*B*) study area, and (*C*) Hilton Head Island, South Carolina, area.

In MODFLOW model hydrogeologic units 1, 6, and 7, the conductivity of each was assumed homogenous because of limited data for the surficial aquifer system, Lower Floridan confining unit, and Lower Floridan aquifer, respectively. The hydraulic conductivity for hydrogeologic units 2, 3, 4, and 5 were distributed into zones. During calibration of the MODFLOW model, values were modified where appropriate and supported by hydrogeologic information to improve model results.

During calibration of the SUTRA model, permeability zones in hydrogeologic unit 5, representing the Upper Floridan aquifer, and in hydrogeologic units 2, 3, and 4, representing the overlying confining unit, were adjusted to achieve a better match with observed heads in the study area. The resulting permeability distribution is shown in figure 16.

The compressibility of the fluid and the solid rock matrix (table 4) determine the rate at which pressures in the flow system respond to changes in the applied stresses. The compressibility of water was set to 4.47×10^{-10} $[kg/(m \cdot s^2)]^{-1}$ (kilogram per meter second squared to the negative one) (Voss and Provost, 2002). Based on a representative Upper Floridan aquifer storage coefficient of 0.0003 reported by Smith (1994), a solid matrix compressibility of 2×10^{-10} $[kg/(m \cdot s^2)]^{-1}$ was computed (appendix D). This value (about half that of water) results in a relatively incompressible porous medium in which pressures adjust rapidly to steady-state conditions.

The rate at which solute is transported is approximately inversely proportional to the effective porosity of the porous medium (appendix E). In previous modeling studies of the Savannah–Hilton Head Island area, Bush (1988) and Smith (1994) used effective porosities of 0.30 and 0.33, respectively, in the Upper Floridan aquifer, based on laboratory analyses of the porosity of core samples reported by Counts and Donsky (1963). Smith (1994) assigned an effective porosity of 0.44 to the upper confining unit based on gravimetric tests of sediment cores. The model developed in this study assigns an effective porosity of 0.33 to the surficial and Brunswick aquifer systems; 0.33 to the Upper Floridan and Lower Floridan aquifers, except as noted, and 0.44 to the confining units (table 4). Because these values are based on laboratory measurements performed on core samples, they do not necessarily reflect the fraction of pore space through which most of the solute transport occurs. In a carbonate aquifer, most of the solute transport can occur through preferential flow channels that comprise a small fraction of the total pore space of the rock *in situ* and are not represented in laboratory samples. Thus, the effective porosity that is relevant to simulating solute transport in a carbonate aquifer can be substantially less than the porosity measured from cores in the laboratory. Sensitivity of the model results to the value of the effective porosity is considered in this study.

In the Hilton Head Island area, the model layer representing the Upper Floridan aquifer corresponds to the upper permeable zone of the aquifer, which is the principal source of ground-water withdrawal in the area, and into which most of the saltwater intrusion is known to occur. Near Hilton Head Island, however, this layer includes the full thickness of the Upper Floridan aquifer, which slows the simulated rate of advective transport. To compensate for the excess aquifer volume, the porosity in parts of the Upper Floridan aquifer was decreased by about the same factor by which the aquifer thickness was overestimated. For example, in areas where the aquifer thickness was overestimated by about a factor of two, the porosity was decreased by a factor of two relative to the default value of 0.33. Figure 17 shows the zones in which the porosity of the Upper Floridan aquifer differs from the default value.

Dispersion, or spreading, of solute “occurs because of mechanical mixing during fluid advection and because of molecular diffusion” (Freeze and Cherry, 1979). In the SUTRA model developed in this study, the mechanical component of dispersion represents an averaging of processes that occur at spatial scales too small to be resolved, such as flow through individual pores, or that are too detailed to be characterized, such as flow along preferential paths such as fractures or solution channels within the porous medium. In the SUTRA simulator, longitudinal and transverse dispersivities control the rates at which solute disperses along and perpendicular to the direction of ground-water flow, respectively (Voss and Provost, 2002). The longitudinal dispersivities also influence the numerical stability of the solute-transport solution; to ensure stability, the element size in the direction of ground-water flow must be less than one-quarter the longitudinal dispersivity (Voss and Provost, 2002). Appropriate dispersivity values were determined during model calibration (table 4). The molecular diffusivity, which controls the rate of molecular diffusion of solute, was set to a representative value of 1×10^{-9} meters squared per second (m^2/s) (table 4) (Freeze and Cherry, 1979).

The concentration of seawater, expressed as the mass fraction of total dissolved solids (TDS), was set to a representative value of 0.0357 kg-TDS/kg-fluid (Voss and Provost, 2002), or 35.7 parts per thousand (ppt), which falls within the range 33 to 36 ppt reported by von Arx (1962). Freshwater was assigned a density of 1,000 kilograms per cubic meter (kg/m^3). The density of seawater was assumed to vary linearly with solute concentration at a rate of 700 kg/m^3 per unit increase in solute mass fraction (Voss and Provost, 2002), giving a seawater density of 1,024.99 kg/m^3. It was assumed that the dissolved solids in seawater are 55.04 percent by weight chloride (von Arx, 1962). Mass fraction of total dissolved solids, C, was converted to chloride concentration in milligrams per liter, $\hat{C}_{Cl}$, using the formula

$$\hat{C}_{Cl} = (550.4)\,(1000 + 700\,C)\,C,$$

which takes into account the variation of fluid density with concentration.

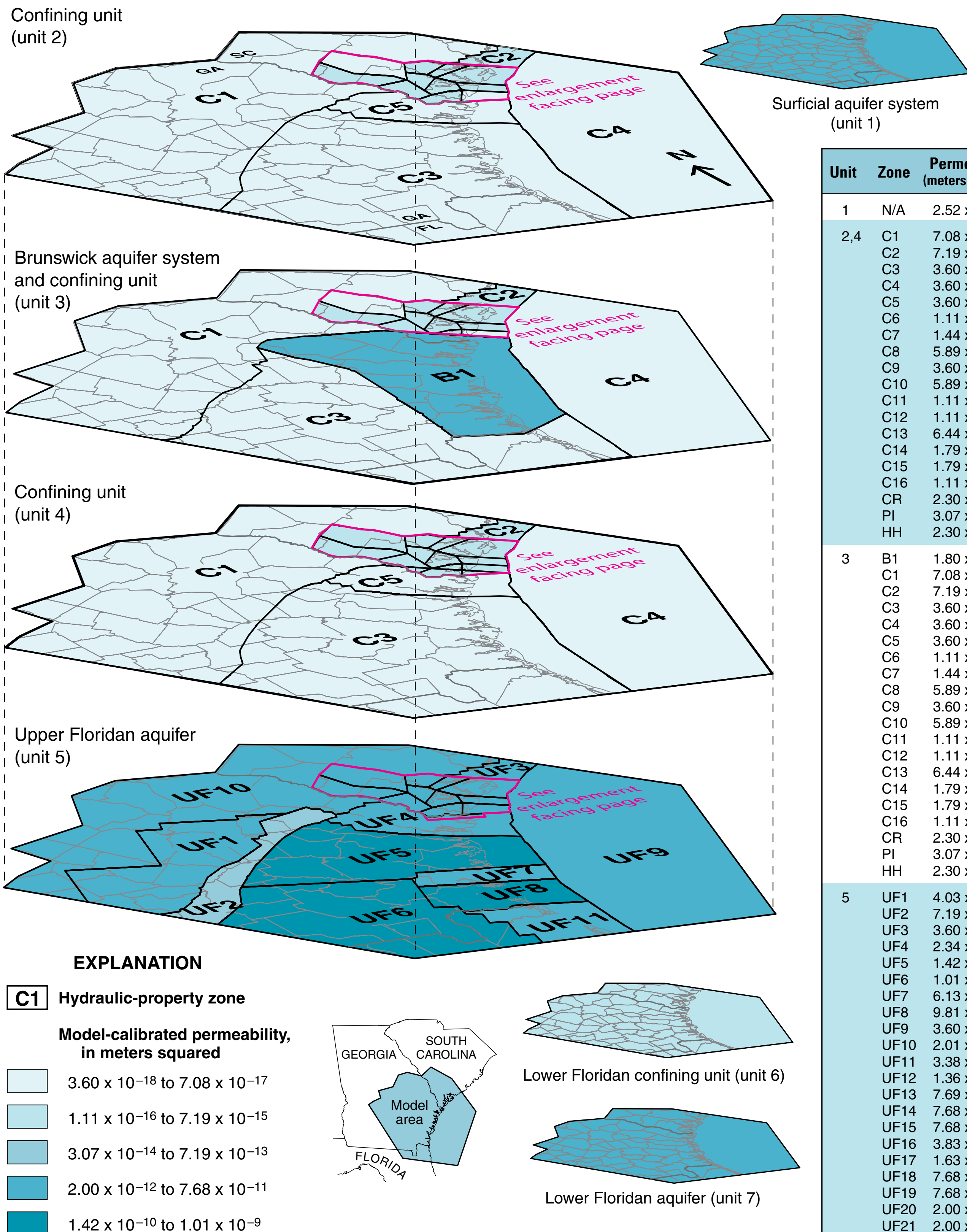

Unit	Zone	Permeability (meters squared)
1	N/A	2.52×10^{-11}
2,4	C1	7.08×10^{-17}
	C2	7.19×10^{-16}
	C3	3.60×10^{-18}
	C4	3.60×10^{-17}
	C5	3.60×10^{-17}
	C6	1.11×10^{-16}
	C7	1.44×10^{-15}
	C8	5.89×10^{-16}
	C9	3.60×10^{-17}
	C10	5.89×10^{-16}
	C11	1.11×10^{-16}
	C12	1.11×10^{-16}
	C13	6.44×10^{-17}
	C14	1.79×10^{-17}
	C15	1.79×10^{-17}
	C16	1.11×10^{-16}
	CR	2.30×10^{-13}
	PI	3.07×10^{-14}
	HH	2.30×10^{-13}
3	B1	1.80×10^{-11}
	C1	7.08×10^{-17}
	C2	7.19×10^{-16}
	C3	3.60×10^{-18}
	C4	3.60×10^{-17}
	C5	3.60×10^{-17}
	C6	1.11×10^{-16}
	C7	1.44×10^{-15}
	C8	5.89×10^{-16}
	C9	3.60×10^{-17}
	C10	5.89×10^{-16}
	C11	1.11×10^{-16}
	C12	1.11×10^{-16}
	C13	6.44×10^{-17}
	C14	1.79×10^{-17}
	C15	1.79×10^{-17}
	C16	1.11×10^{-16}
	CR	2.30×10^{-13}
	PI	3.07×10^{-14}
	HH	2.30×10^{-13}
5	UF1	4.03×10^{-12}
	UF2	7.19×10^{-13}
	UF3	3.60×10^{-11}
	UF4	2.34×10^{-11}
	UF5	1.42×10^{-10}
	UF6	1.01×10^{-9}
	UF7	6.13×10^{-11}
	UF8	9.81×10^{-10}
	UF9	3.60×10^{-11}
	UF10	2.01×10^{-11}
	UF11	3.38×10^{-11}
	UF12	1.36×10^{-11}
	UF13	7.69×10^{-12}
	UF14	7.68×10^{-11}
	UF15	7.68×10^{-11}
	UF16	3.83×10^{-11}
	UF17	1.63×10^{-11}
	UF18	7.68×10^{-11}
	UF19	7.68×10^{-11}
	UF20	2.00×10^{-12}
	UF21	2.00×10^{-12}
	UF22	2.00×10^{-12}
	UF23	7.68×10^{-11}
6	N/A	7.19×10^{-15}
7	N/A	3.60×10^{-12}

Figure 16. Distribution of permeability for model units.

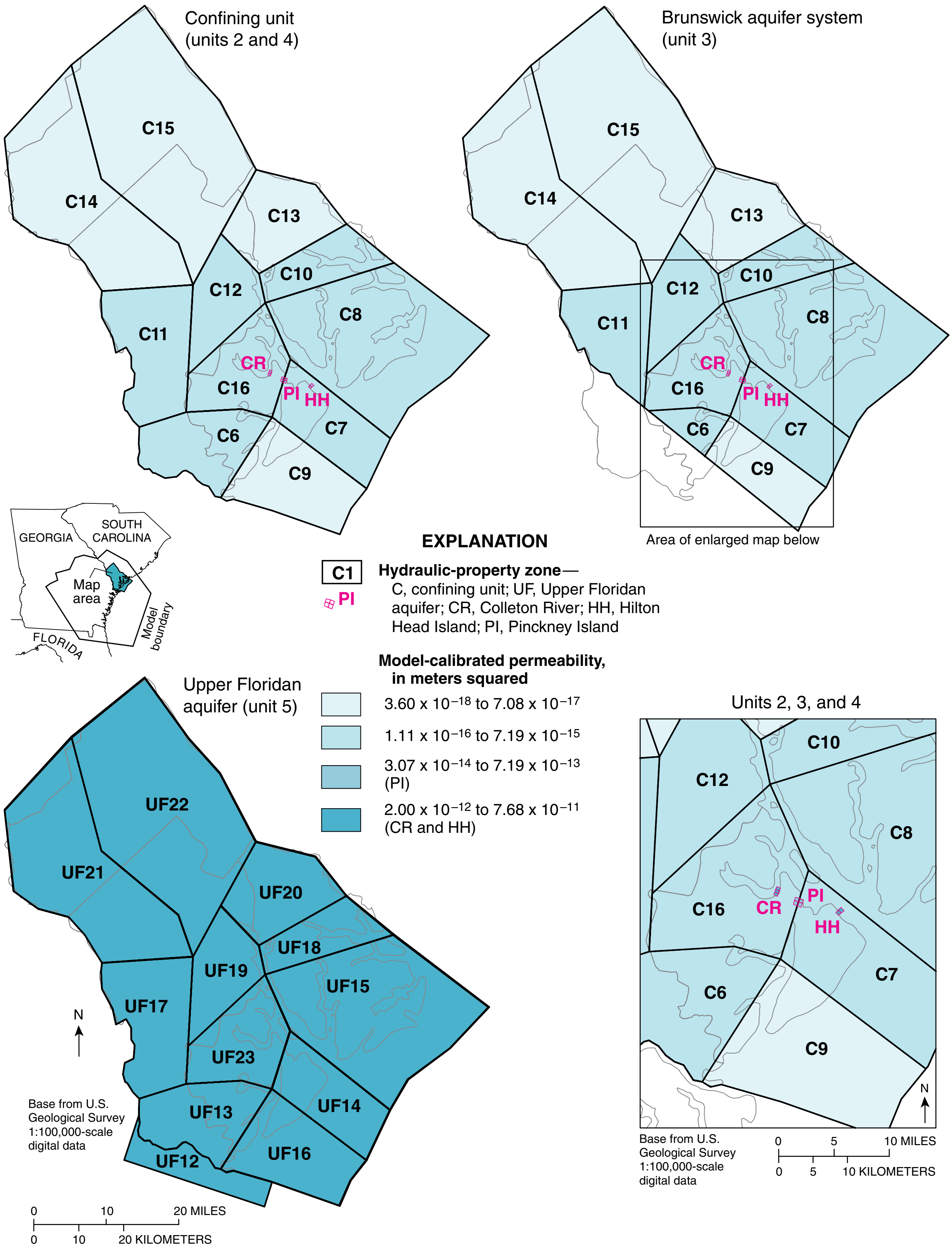

Figure 16. Distribution of permeability for model units—continued.

Table 4. Physical properties for SUTRA model.

[m, meter; m^2/s, meter squared per second; kg, kilogram; s^2, second squared; kg/m^3, kilogram per cubic meter]

Physical property	Value in calibrated model
Porosity, all aquifer units (except as specified in figure 17)	0.33 (dimensionless)
Porosity, all confining units	0.44 (dimensionless)
Longitudinal dispersivity, horizontal direction (varies by element)	135–15,000 m
Longitudinal dispersivity, vertical direction (varies by element)	0.04–158 m
Molecular diffusivity	1.0×10^{-9} m^2/s
Transverse dispersivity, horizontal direction (one-tenth of longitudinal dispersivity, horizontal direction)	13.5–1,500 m
Transverse dispersivity, vertical direction (one-tenth of longitudinal dispersivity, vertical direction)	0.004–15.8 m
Fluid compressibility	4.47×10^{-10} $[kg/(m \cdot s^2)]^{-1}$
Solid matrix compressibility	2.0×10^{-10} $[kg/(m \cdot s^2)]^{-1}$
Fluid viscosity	0.001 $kg/(m \cdot s)$
Freshwater density	1,000 kg/m^3
Rate of change in fluid density with solute mass fraction	700 kg/m^3
Solute (dissolved solids) mass fraction in seawater	0.0357 (dimensionless)

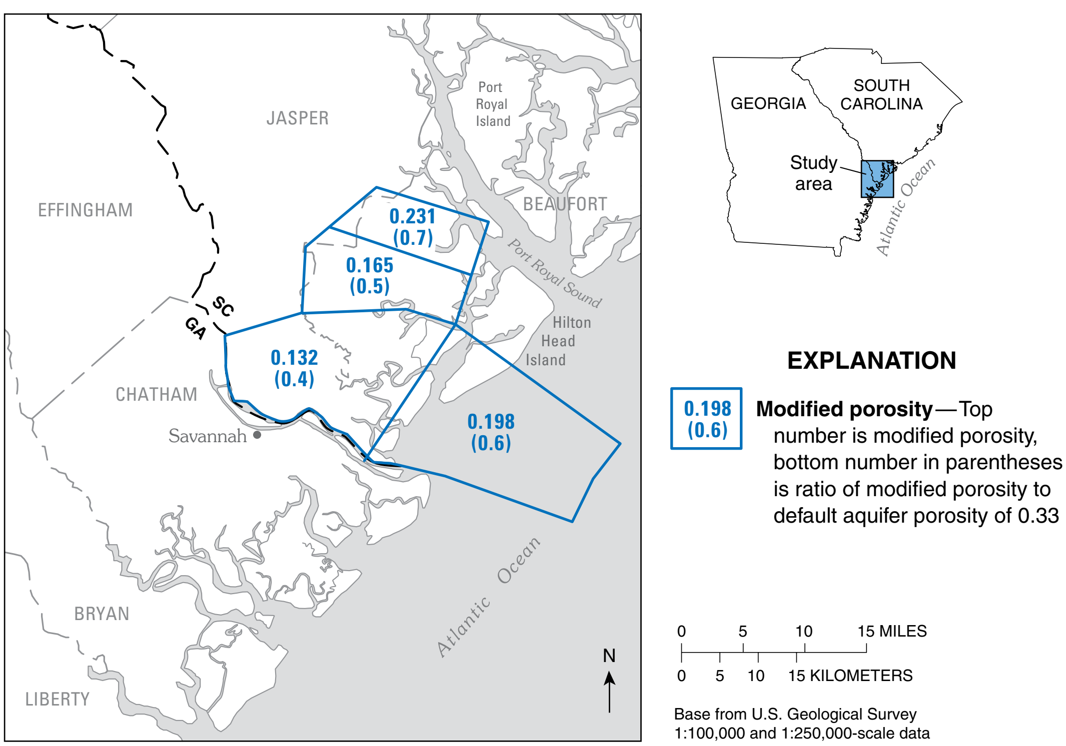

Figure 17. Areas in which the porosity of the Upper Floridan aquifer was modified to compensate for overestimated aquifer thickness.

Boundary Conditions

Boundary conditions generally are based on natural hydrologic boundaries where available; where unavailable, artificial boundaries were constructed. The SUTRA model was designed to implement the boundary conditions used by the regional flow model. Fundamental differences in the MODFLOW and SUTRA simulators resulted in different implementation of boundary conditions for some of the boundaries; care was taken, however, to make the boundaries of the SUTRA model as consistent as possible with those of the MODFLOW model. A schematic diagram of model layers and vertical boundary conditions is shown in figure 13.

Top and Bottom Boundaries

The lowermost model boundary represents no-flow conditions. Throughout the model area, this boundary corresponds to the contact between the Lower Floridan aquifer and underlying low- permeability sediments of Paleocene and older age (fig. 2).

In the MODFLOW model, the uppermost boundary was simulated using a head-dependent flux boundary condition applied to the top active cell of the model, with different controlling head and conductance parameters applied in the offshore and onshore areas (Payne and others, 2005). For the onshore area, the controlling head was the estimated water table (Peck and Payne, 2003), which was set at land-surface altitude at major streams, assuming that streams represent the intersection of the water table with land surface. The conductance term was a function of variable cell thickness, an assumed spatially constant hydraulic conductivity (which was estimated during model calibration), and the hydraulic conductivity of the active cell at the boundary. The controlling head for the offshore part of the model area was the freshwater equivalent of the saltwater head, and the conductance was assumed to be constant everywhere for simplicity. Conceptually, this boundary condition represents a source-sink boundary in the unconfined part of the surficial aquifer that recharges to and discharges from the confined, regional ground-water system. By using a source-sink boundary with resistance in the form of a conductance term, the recharge for any given model cell could be effectively limited to estimated baseflow for the model area, which is an assumed maximum value for recharge (Payne and others, 2005).

For the SUTRA model, the upper boundary condition was approximated by applying a fixed pressure at the top node of the model (appendix F). For the onshore area, an equivalent pressure was set at the top node (at land surface) assuming zero pressure at the water table and a hydrostatic pressure gradient between land surface and the water table; any water entering the model through the top node was assumed to be fresh. For the offshore area, the pressure at the top node (sea floor) was set to hydrostatic pressure that reflected the density of the overlying seawater; any water entering the model through the top node was assumed to be at seawater concentration. There is no direct and simple way in the SUTRA simulator to account for the resistance provided by the conductance term in the MODFLOW simulator's general-head boundary condition. In the offshore area, however, the conductance term of the MODFLOW model was large and did not provide much resistance, so applying a fixed pressure for the offshore area in the SUTRA model provides a similar boundary condition. In the onshore area, resistance was effectively added by modifying the permeability distributions of the Upper Floridan confining unit and Upper Floridan aquifer during calibration of the SUTRA model.

Lateral Boundaries

The lateral boundaries generally are far from the study area, and, thus, their effects on the flow system are subdued by distance. Lateral boundary conditions were selected to coincide as closely as possible with assumed natural no-flow boundaries or ground-water divides. With the exception of the Floridan aquifer system (units 5, 6, and 7), lateral boundaries for all layers are designated as no-flow and were translated directly from the MODFLOW model.

Simulated flow in the Floridan aquifer system is bounded laterally by a combination of no-flow and fixed-head boundaries (fig. 15). The northwestern boundary follows the updip extent of the Floridan aquifer system or its equivalent, as defined by Miller (1986), and is defined in both the MODFLOW and SUTRA models as a no-flow boundary. The onshore part of the northeastern boundary was assigned a no-flow boundary because it is parallel to estimated flow lines as shown on the potentiometric surface of the Upper Floridan aquifer (Ransom and White, 1999). This boundary was projected offshore and connected to the easternmost offshore boundary. The offshore boundary is located near the Florida-Hatteras shelf and assigned no-flow conditions, because sensitivity testing of the MODFLOW model indicated that the regional flow system was insensitive to the type of boundary condition used there.

To the southwest and south of the model area, there are no proximal natural hydrologic boundaries for the Floridan aquifer system, because it extends west through Georgia and Alabama and south through Florida. Additionally, a no-flow boundary parallel to estimated flow lines is not an appropriate boundary condition because potentiometric-surface maps of the Upper Floridan aquifer indicate that water levels and estimated flowpaths change with time (Johnston and others, 1980; Johnston and others, 1981; Clarke, 1987; Peck and others, 1999). Therefore, for the southwestern and southern boundaries of the MODFLOW model, a time-variable, fixed-head boundary condition was applied from the top of the Upper Floridan aquifer to the bottom of the Lower Floridan aquifer (units 5, 6, and 7) to enable simulation of changing ground-water levels. The controlling head varied spatially along the boundary according to potentiometric-head distributions derived from published maps for May 1980 (Johnston and others, 1981), May 1998 (Peck and others, 1999), and September 2000 (Peck and McFadden, 2004).

To translate these boundary conditions into the SUTRA model, a pressure was calculated from the Upper Floridan aquifer head value for each node at the top of unit 5 along this boundary. A hydrostatic pressure gradient was assumed for each vertical column of nodes, and the corresponding time-independent pressure was calculated for and assigned to each of the nodes under the top node in unit 5 along that boundary (appendix F).

Pumpage

Pumpage from predevelopment to 2000 was constructed using various data. Average daily pumpage for a given year, or month within a year, was distributed spatially for periods for which (1) the model was calibrated, (2) sufficient data coverage was available, or (3) pumpage changed substantially. These periods include 1915, 1920, 1930, 1937, 1940, 1955, 1970, 1980, 1985, 1990, 1997, September 1998, and 2000.

Pumpage data collection since the 1980s is more complete and methodical than before 1980, although not necessarily consistent between sources. Payne and others (2005) describe sources of data and methods used to distribute pumping across the model area and among aquifers. County aggregate and site-specific pumpage data were used to estimate and spatially distribute average annual pumpage for the years specified from 1980 to 2000 using procedures described by Taylor and others (2003). Site-specific pumpage data generally include permitted industrial and public-supply systems and consist of withdrawal data, permit information, and well locations. Nonsite-specific pumpage data consist of the remainder of county aggregate pumpage after the sum of site-specific pumpage for that county has been subtracted; these data may comprise agricultural, domestic, commercial, or other categories of water use for unpermitted wells. The nonsite-specific pumpage is distributed evenly across each county using a 3.1- by 3.1-mi grid, and distributed between aquifers (units 3, 5, and 7) based on the proportion of wells completed in the various aquifers in a given county. Pumpage was not assigned to unit 1, the surficial aquifer system, because there is too much uncertainty about whether the pumping would be in the unconfined part of the system, which is not simulated, or the confined part, which is simulated. For September 1998, site-specific pumpage data were available for Beaufort and Jasper Counties, S.C., and were used in the SUTRA model. For the rest of the model area, pumpage for September 1998 was calculated by linearly interpolating between values for 1997 and 2000. Per-county pumpage estimates for specific years during 1980–2000 for the model area are shown for the Upper Floridan aquifer in table 2 and for the Lower Floridan aquifer in table 3.

Counts and Donsky (1963) provided an estimate of ground-water use in the Savannah area from predevelopment to 1958. Pumpage input for a ground-water flow model in the Savannah area (Counts and Krause, 1976) provided more specific data up to 1970. Hayes (1979), Landmeyer and Belval (1996), and Smith (1994) present estimates for pre-1980s pumpage in South Carolina. Gregg and Zimmerman (1974), Wait (1965), and Wait and Gregg (1973) provided ground-water pumpage estimates for Glynn County, Ga., from the 1940s to the 1960s, although pumpage at this distance from the study area likely has little effect. Table 1 shows estimated pumpage per county for specific years before 1980. Apparent fluctuations are due to industrial shutdowns, transfer of permits to new owners, changes in reporting accuracy, gaps in reporting, and estimates from different sources for different years. For modeling purposes, pumpage was assumed insignificant in counties for which there are no pumpage estimates.

Few data exist for county pumpage distribution prior to 1980. Site-specific pumpage was distributed spatially based on available site-specific, water-use category, or county aggregate data for those counties. If known, the site-specific pumpage was applied; if industrial or public supply pumpage were known for a county, these values were evenly distributed among the known industrial and public supply sites. If only a county aggregate estimate was available, a ratio of site-specific pumpage to total pumpage, based on 1980 pumpage distribution, was calculated and applied equally to all known sites. To estimate nonsite-specific pumpage for the entire model area for a given year before 1980, the ratio of 1980 nonsite-specific to site-specific pumpage was multiplied by the total site-specific pumpage for that year. To reflect the onset of development in the Hilton Head Island area in the mid-1960s (Landmeyer and Belval, 1996), site-specific pumpage in Jasper and Beaufort Counties, S.C., was assumed to increase linearly from zero during 1965 to reported levels during 1985. The nonsite-specific pumpage was then distributed evenly across the county. Nonsite-specific pumpage was distributed among aquifers, as discussed previously.

To apply the pumpage to the SUTRA model mesh, the pumpage associated with a given well was assigned to the vertical string of nodes that lies closest to the well (as measured within the horizontal plane) and was divided equally among the nodes that lie between the top and bottom surfaces of the aquifer to which the pumpage is attributed. In Jasper and Beaufort Counties, the nonsite-specific pumpage distribution using the 3.1- by 3.1-mi grid typically is coarser than the finite-element mesh resolution. To distribute the nonsite-specific pumpage more appropriately for the fine mesh across these two counties, the nonsite-specific pumpage was totaled for each county and redistributed among the nodes of the finite-element mesh within each county in proportion to the area associated with each node. The area associated with each node was estimated by dividing the model volume associated with the node by the vertical node spacing within the aquifer. Within each county, the redistribution of nonsite-specific pumpage was performed separately for each of the three pumped aquifers: the Brunswick, the Upper Floridan, and the Lower Floridan. During simulation, the SUTRA simulator interpolates linearly through time the pumping associated with each node, because the time steps generally are shorter than the duration between years of assigned pumpage distributions. The pumpage distribution for the 1998 calibration is shown in figure 18.

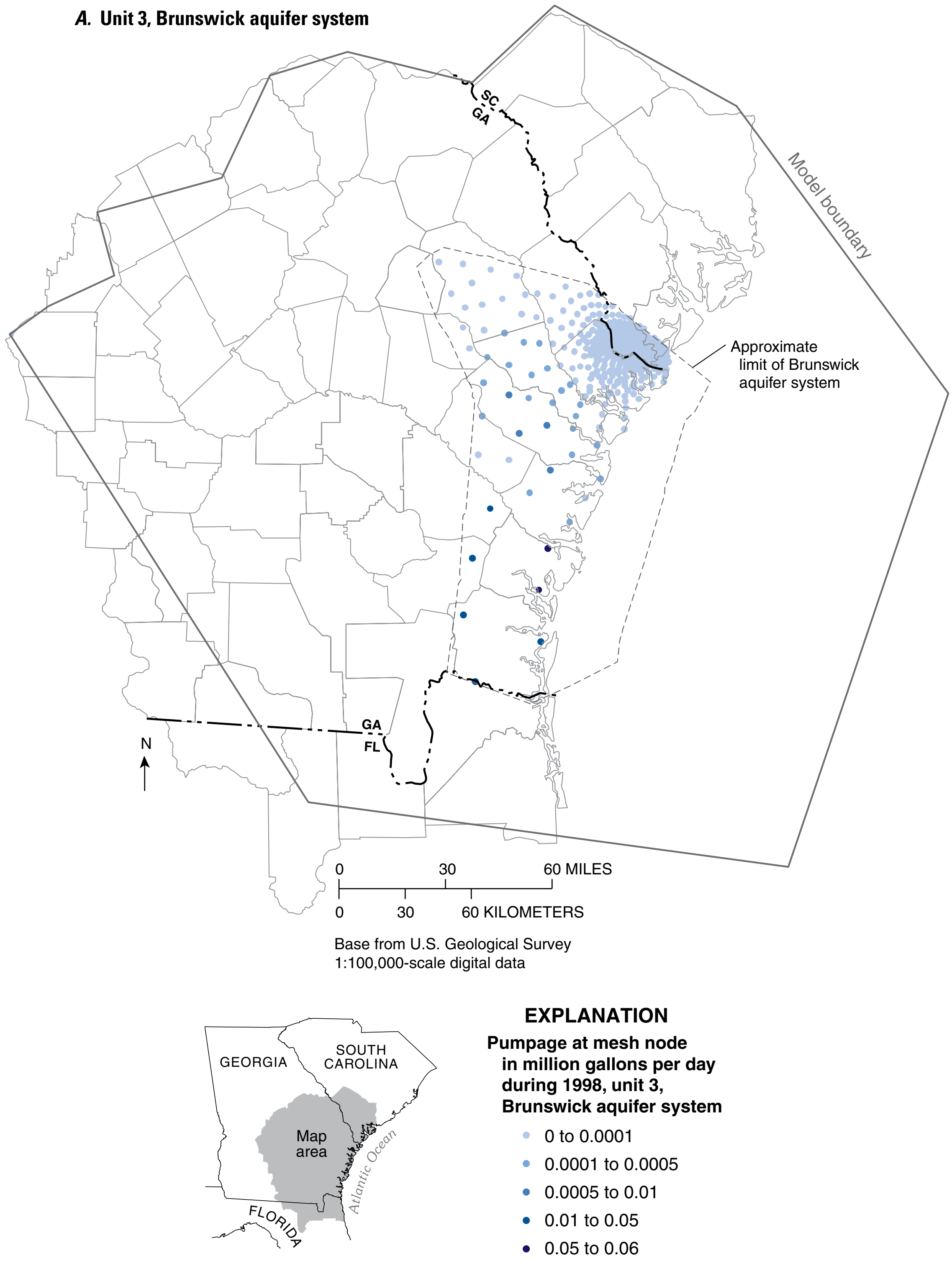

Figure 18. Distribution of ground-water pumpage by model layer, 1998, for (*A*) unit 3, Brunswick aquifer system; (*B*) unit 5, Upper Floridan aquifer (model area); (*C*) unit 5, Upper Floridan aquifer (study area); (*D*) unit 7, Lower Floridan aquifer (model area); and (*E*) unit 7, Lower Floridan aquifer (study area).

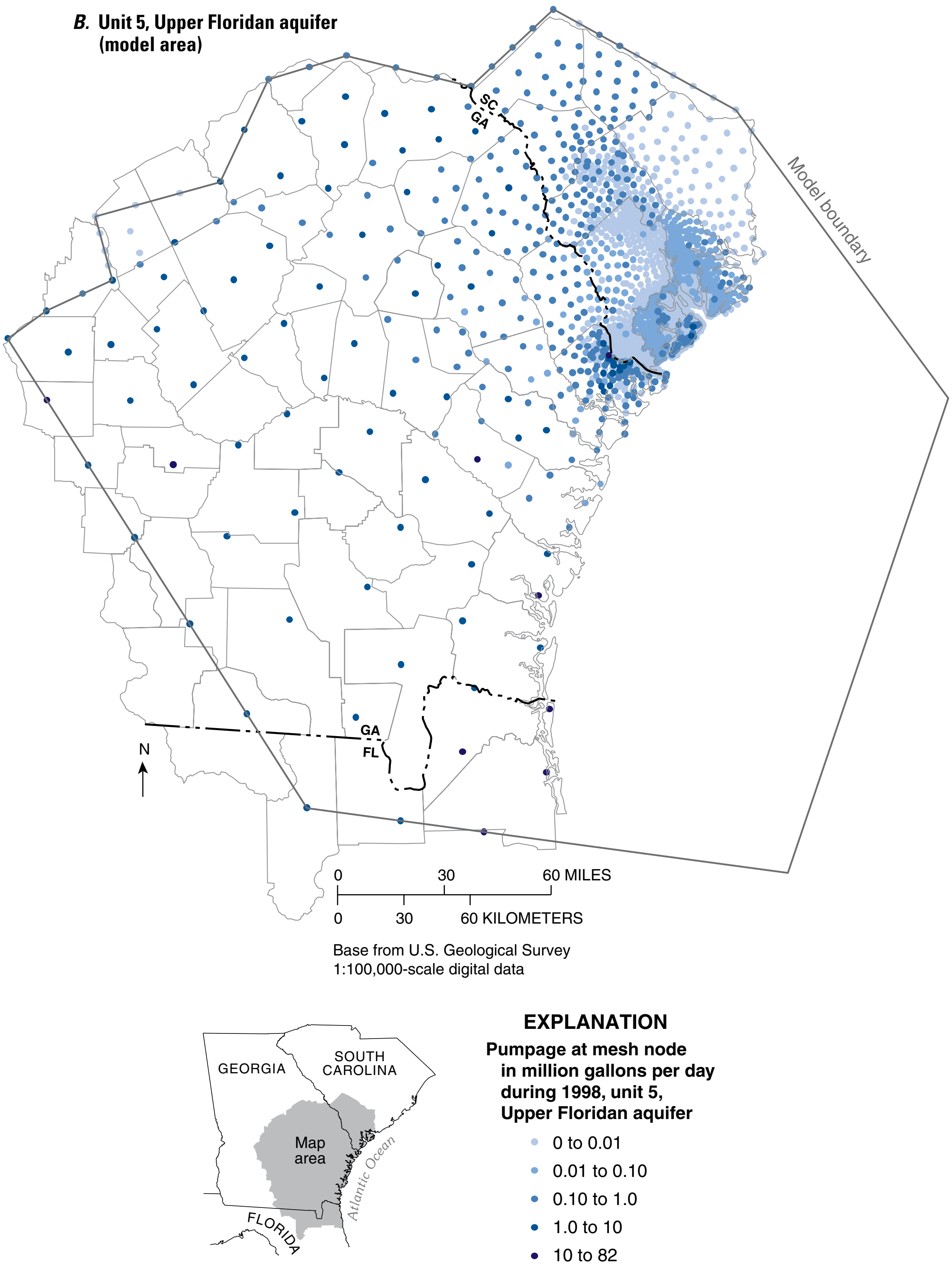

Figure 18. Distribution of ground-water pumpage by model layer, 1998, for (*A*) unit 3, Brunswick aquifer system; (*B*) unit 5, Upper Floridan aquifer (model area); (*C*) unit 5, Upper Floridan aquifer (study area); (*D*) unit 7, Lower Floridan aquifer (model area); and (*E*) unit 7, Lower Floridan aquifer (study area)—continued.

C. **Unit 5, Upper Floridan aquifer (study area)**

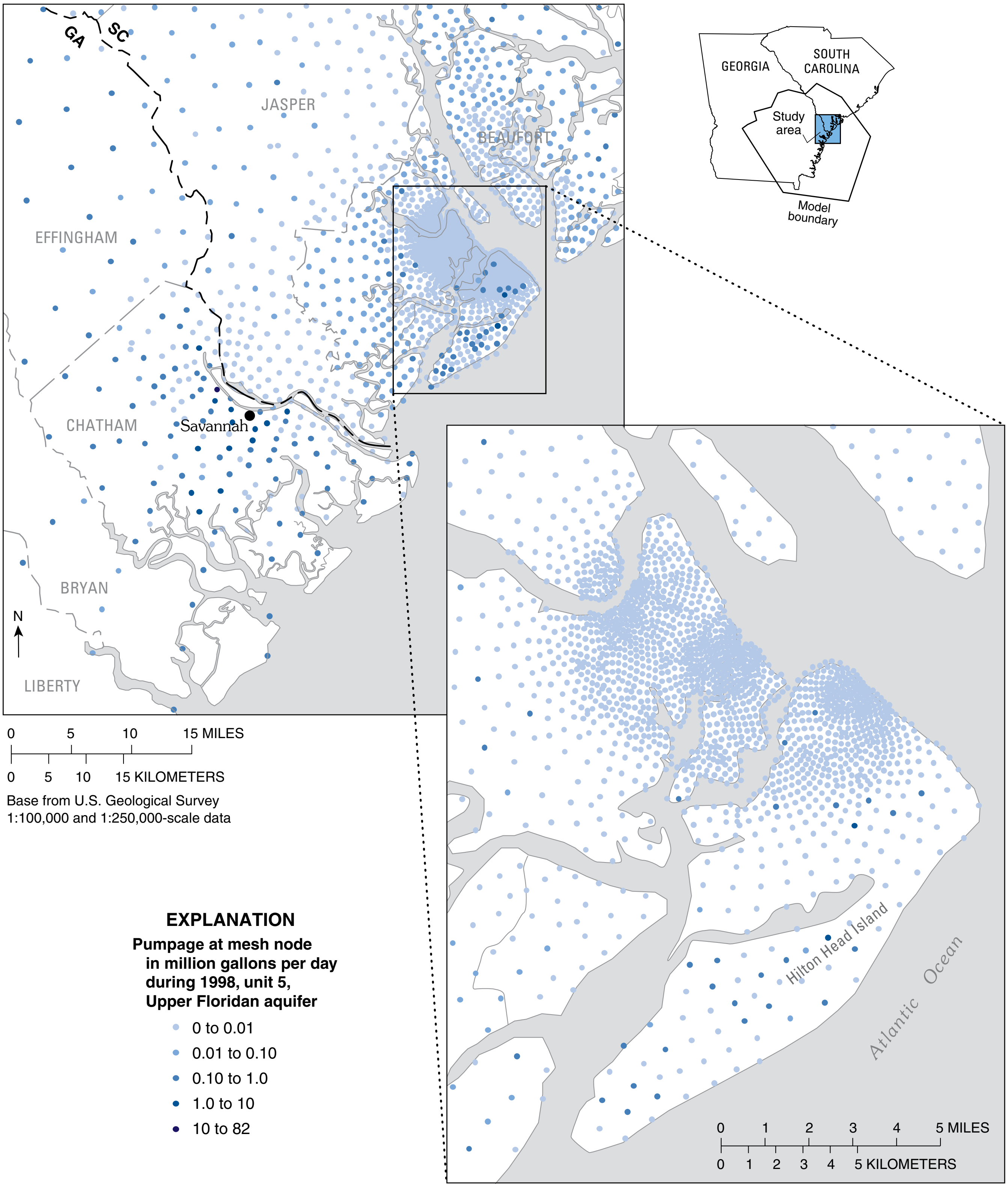

Figure 18. Distribution of ground-water pumpage by model layer, 1998, for (*A*) unit 3, Brunswick aquifer system; (*B*) unit 5, Upper Floridan aquifer (model area); (*C*) unit 5, Upper Floridan aquifer (study area); (*D*) unit 7, Lower Floridan aquifer (model area); and (*E*) unit 7, Lower Floridan aquifer (study area)—continued.

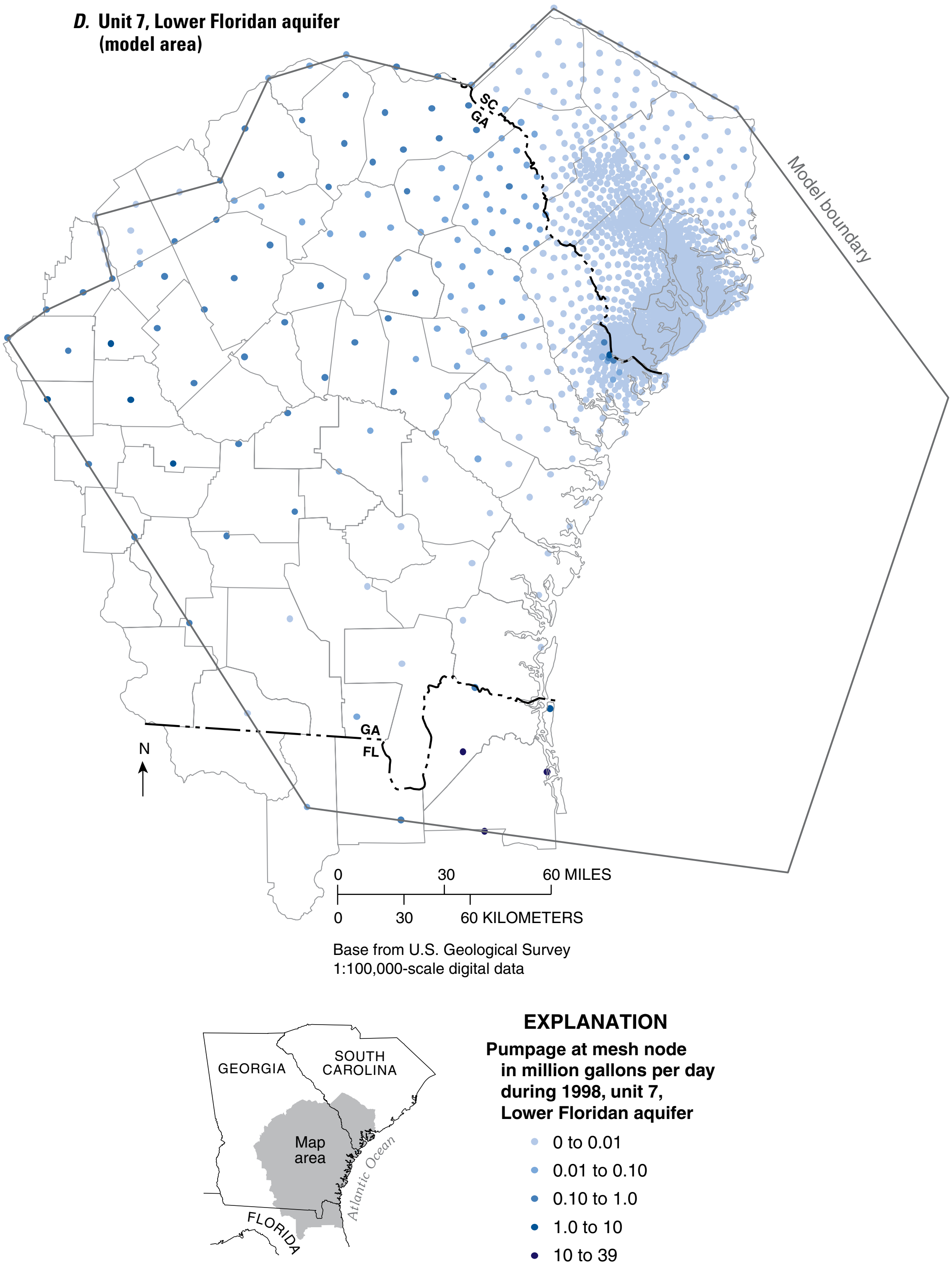

Figure 18. Distribution of ground-water pumpage by model layer, 1998, for (*A*) unit 3, Brunswick aquifer system; (*B*) unit 5, Upper Floridan aquifer (model area); (*C*) unit 5, Upper Floridan aquifer (study area); (*D*) unit 7, Lower Floridan aquifer (model area); and (*E*) unit 7, Lower Floridan aquifer (study area)—continued.

E. **Unit 7, Lower Floridan aquifer (study area)**

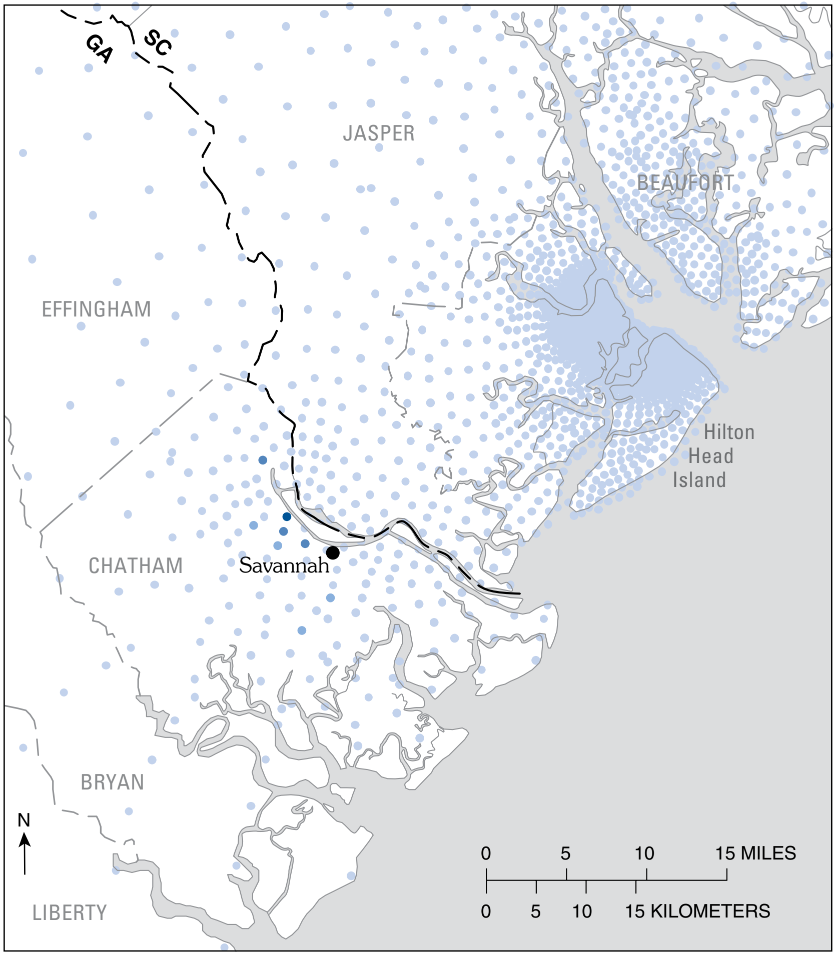

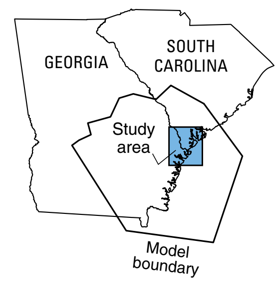

EXPLANATION

Pumpage at mesh node in million gallons per day during 1998, unit 7, Lower Floridan aquifer

- 0 to 0.01
- 0.01 to 0.10
- 0.10 to 1.0
- 1.0 to 10

Base from U.S. Geological Survey
1:100,000 and 1:250,000-scale data

Figure 18. Distribution of ground-water pumpage by model layer, 1998, for (*A*) unit 3, Brunswick aquifer system; (*B*) unit 5, Upper Floridan aquifer (model area); (*C*) unit 5, Upper Floridan aquifer (study area); (*D*) unit 7, Lower Floridan aquifer (model area); and (*E*) unit 7, Lower Floridan aquifer (study area)—continued.

Model Calibration to Observed Head ("Head Calibration") and Flow-Model Sensitivity

The SUTRA model was calibrated by first constructing a preliminary SUTRA model that was similar to the calibrated MODFLOW model of Payne and others (2005): the same boundary and hydrogeologic layering were used; a similar mesh density was used; permeability zones were the same as hydraulic conductivity zones, and values for permeability were directly translated from hydraulic conductivity values; and the controlling head values for the boundary conditions were translated into pressure values. This preliminary SUTRA model then was run for steady-state 2000 conditions, using freshwater concentration and single-density flow. Calculated pressures were translated into hydraulic head values and compared with calculated head values from the MODFLOW model. Minimal modifications were made to permeability values in the preliminary SUTRA model to ensure similarity of model results (fig. 19).

Differences in simulated head between the SUTRA and MODFLOW models may be attributable to fundamental differences in numerical methods, such as implementation of boundary conditions and calculation of flow between cells or nodes. In the MODFLOW model, a general-head boundary condition is used at the top boundary. The general-head boundary applied is a head-dependent flux boundary condition, in which the controlling head in this case is set to the water-table altitude. The flux to or from the controlling head is calculated by the MODFLOW simulator during simulation as the controlling head minus the simulated head at the top of the model multiplied by a conductance that is specified for each general-head boundary cell (Payne and others, 2005). The conductance can be expressed as a vertical hydraulic conductivity multiplied by the horizontal area of the boundary cell divided by the distance between the controlling head and the centroid of the cell. In the SUTRA model, a fixed-pressure boundary condition is applied, assuming hydrostatic conditions between land surface and the water table. Simulated heads in the Upper Floridan aquifer produced with the two simulators would differ most in places where hydrogeologic units 1 through 4 are thin or pinch out and where the Upper Floridan aquifer, hydrogeologic unit 5, is near land surface. This is likely to happen in the up-dip area of the Upper Floridan aquifer and in the Hilton Head Island–Port Royal Sound area.

In the MODFLOW simulator, vertical flow between units is calculated between cell centroids and is a function of the geometric mean of the hydraulic conductivities of adjacent cells. Where two adjacent cells are of substantially differing hydraulic conductivity, the flow between the cells is controlled by the lower hydraulic conductivity. In the MODFLOW model, each hydrogeologic unit is discretized vertically as one layer of cells. Thus, in some areas, the vertical flow between the bottom cell of the Upper Floridan confining unit and the top cell of the Upper Floridan aquifer is dominated by the hydraulic conductivity of the confining unit. In the SUTRA simulator, flow is calculated between nodes, and nodes define the top and bottom of each hydrogeologic unit, so flow between vertically adjacent nodes is controlled by the permeabilities assigned to the finite elements shared by the two nodes, all of which correspond to the same hydrogeologic unit. Thus, in the SUTRA simulator, the computation of vertical flow in the Upper Floridan aquifer is not influenced directly by the permeability of the adjacent confining units. This difference between the two simulators likely contributes to the differences in the simulated heads.

Following the initial simulations, the mesh density was increased within the study area (fig. 20), and the SUTRA model was run for steady-state conditions using only freshwater concentration. The higher-resolution SUTRA model was calibrated to match observed heads for September 1998 in Beaufort, Jasper, and Hampton Counties, S.C. (Ransom and White, 1999).

Head Calibration Method

The Upper Floridan aquifer and upper confining unit permeabilities were further subdivided into zones within the study area. The geometry of these zones and their associated permeability values were modified during calibration based on differences between simulated and observed heads, sensitivities to changes in the estimated parameters, and correlations between estimated parameters.

The calibration was performed using UCODE, the USGS computer code for inverse modeling (Poeter and Hill, 1998). UCODE seeks to minimize the sum of the squared residuals by adjusting a set of estimated parameters. In this case, the residuals were observed water levels minus simulated water levels, and the estimated parameters were values for permeability for the Upper Floridan aquifer and the overlying confining unit, which were subdivided into zones within the study area to achieve a better match between simulated and observed heads.

Parameters were estimated in selected subsets during the course of multiple UCODE runs. Based on the distribution of residuals and parameter sensitivities and correlations after each run, new parameters were introduced, existing parameters were consolidated, and different subsets of parameters were estimated until a satisfactory fit to the observations was obtained.

Head Observations

In September 1998, Ransom and White (1999) measured water levels in a network of wells open to the Upper Floridan aquifer (appendix G). The quality of the model calibration is measured by the extent to which simulated water levels match the observed water levels. The influence of each observation on the objective function is controlled by a weight that reflects the confidence in that observation. Most water-level observations were given a weight of 1 ft^{-2} (foot to the negative 2), which corresponds to a standard deviation of ±1 ft, or a 95-percent confidence interval of about ±2 ft, a value representative of the accuracies reported by Ransom and White (1999). In Hampton County, S.C., the topography is more variable than in the lower-lying coastal area, the hydrogeologic layering is poorly characterized, and the model discretization is relatively coarse.

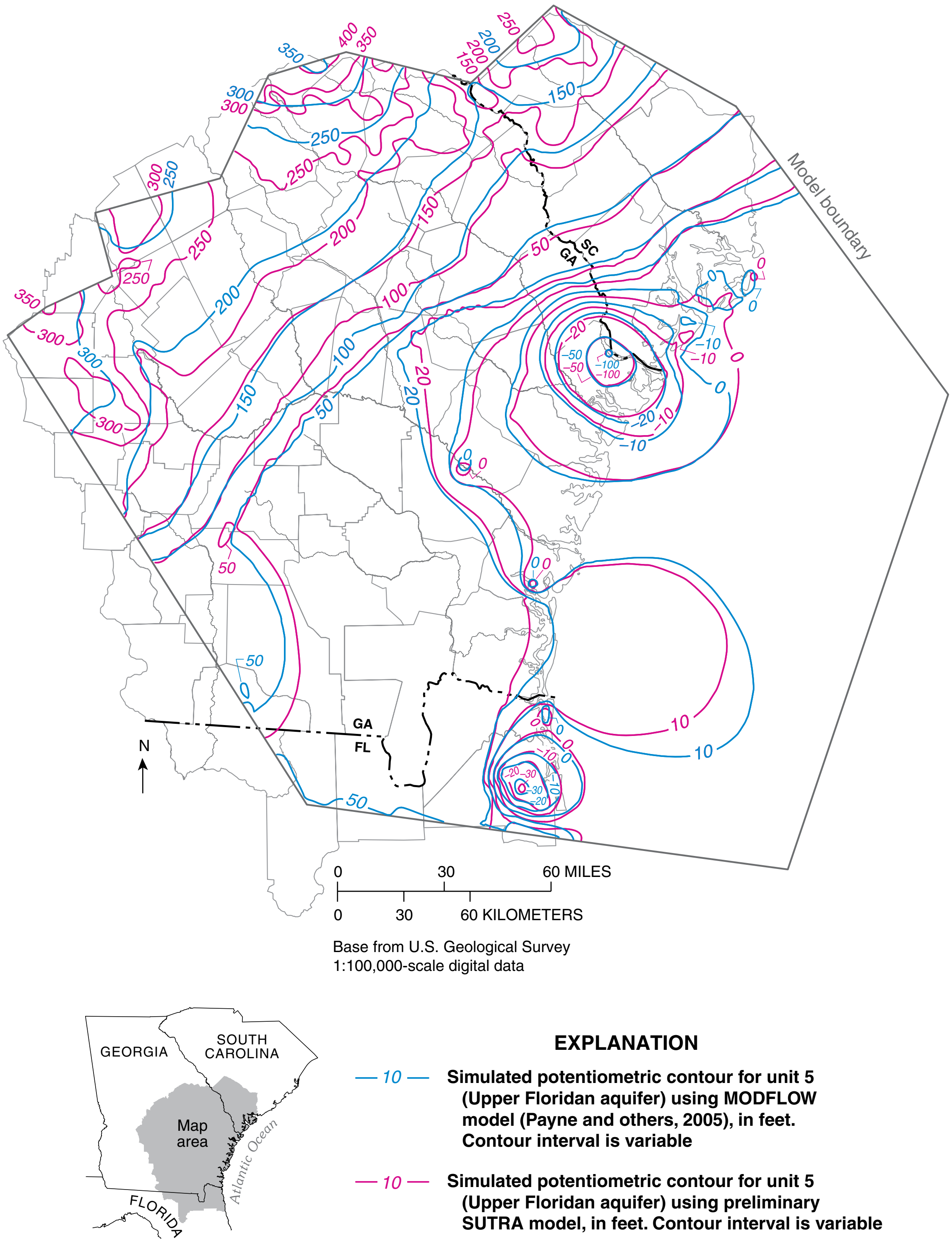

Figure 19. Simulated potentiometric surface for the Upper Floridan aquifer (unit 5) during 2000 using the calibrated MODFLOW model (Payne and others, 2005) and the preliminary SUTRA model.

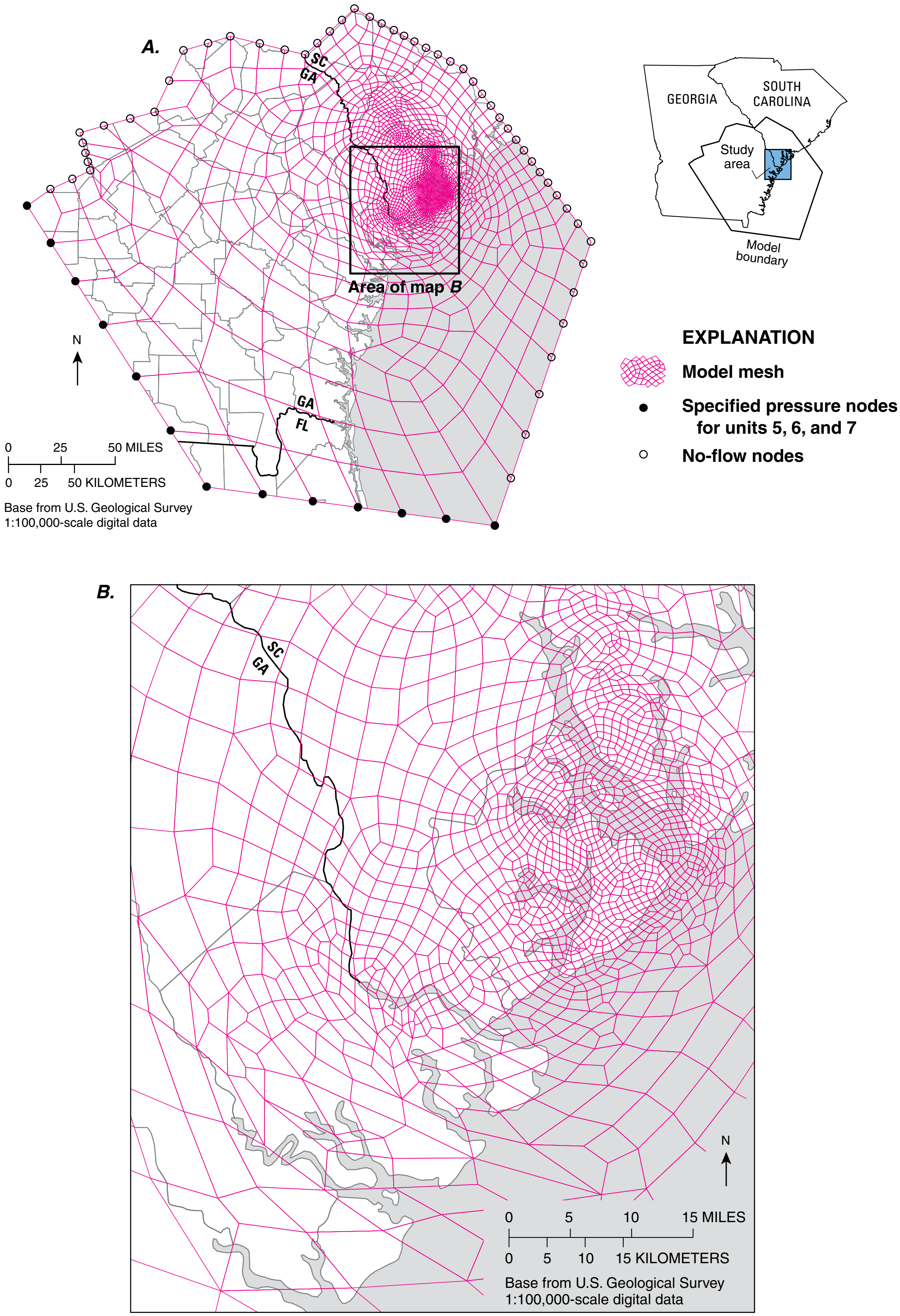

Figure 20. Mesh for calibration to September 1998 water levels for (*A*) model area and (*B*) study area.

As a result, water-level observations within Hampton County were assigned a weight of 0.04 ft^{-2}, which corresponds to a standard deviation of ±5 ft, or a 95-percent confidence interval of about ±10 ft. Observations at wells BFT-145 and BFT-420, which are in close proximity to pumping wells northwest of Port Royal Island, also were assigned weights of 0.04 ft^{-2} to reflect the uncertainty associated with the steep, local cone of depression. Throughout the report, weighted quantities are computed by multiplying unweighted values by the weighting factor, which equals square root of the weight (appendix G, table G1). For example, a weighted residual is the residual multiplied by the weighing factor assigned to the corresponding observation.

At well BFT-1814 on Hilton Head Island, reported water levels differed markedly from those at nearby wells. The observation at this well was considered unreliable and was removed from the calibration. Difficulty in achieving sufficient simulated drawdown at a group of three wells north of Port Royal Island (BFT-1806, BFT-1893, and BFT-1998) can be attributed to the proximities of these wells to potential sites of substantial local ground-water withdrawal that are not included in the pumpage database, specifically, Brays Island Plantation Golf Course and the town of Fairview, S.C. Therefore, observations at these three wells also were removed from the calibration.

The effect of salinity was not considered in using the water-level measurements as representative of hydraulic head during calibration because the September 1998 water-level observations did not include salinity measurements. If the boreholes were filled with seawater along their entire length (about 200 ft), then the amount by which equivalent freshwater head observations would be underestimated by equating these heads with measured water levels would be about 5 ft. Chloride concentrations measured in water samples collected during 1999–2004 (Childress and Ransom, 2005), however, indicate that in all but four wells (BFT-429, BFT-502, BFT-2312, and BFT-2313) salinities exceeding 10 percent seawater, where they existed, were confined to an interval less than 38 ft thick at the bottom of the sampled interval of each well. Furthermore, the maximum chloride concentration measured was about 65 percent seawater. In a 200-ft-thick column of water in which the top 162 ft are at a 10-percent seawater concentration and the bottom 38 ft are at a 65-percent seawater concentration, the additional equivalent freshwater head attributed to salinity is about 1 ft. Therefore, it is likely that in nearly all wells, the heads have been underestimated by 1 ft or less.

Head Calibration Results

Head calibration resulted in a ground-water flow model that reproduces approximately the September 1998 head distribution in the Upper Floridan aquifer. The quality of the model fit to observed data is expressed in terms of weighted residuals: observed heads minus simulated heads, multiplied by the square root of their weights. The calibrated permeability values are reported, along with linear confidence intervals, which provide an approximate measure of the likely range of values for each parameter. Correlations between parameters are also reported, and indicate the degree to which pairs of parameters can be estimated independently using the given set of observations. The sensitivity of the model to each of the estimated permeabilities is expressed in terms of composite scaled sensitivities. Finally, results of a predevelopment, steady-state simulation are compared with estimated predevelopment heads, and the steady-state assumption used during the head calibration is evaluated by performing a transient simulation from predevelopment to September 1998.

Simulated Heads and Residuals

Simulated heads in the Upper Floridan aquifer in September 1998 are shown in figure 21. The distribution of weighted residuals (observed heads minus simulated heads in the Upper Floridan aquifer, multiplied by the weighting factors) in the study area are shown in figure 22. Weighted residuals range from –5.3 to +23.4 ft, with large positive values associated with two local topographic highs. On Hilton Head Island, weighted residuals range from –4.6 to +3.1 ft.

Observed heads at 12 locations in the Upper Floridan aquifer beneath two local topographic highs, one on Port Royal Island and one on Ladies Island, are relatively close to land-surface altitude and indicate potentiometric mounds (appendix G, table G1, fig. G1). The weighted residuals range from +2.1 to +23.4 ft at these 12 points, and from –5.3 to +7.5 ft at the remaining observation points. These observations were included in the objective function for the parameter estimation runs; however, the results of attempts to calibrate the permeabilities in these areas indicate that the high heads are a local phenomenon that would require more refined permeability zones to resolve. Rather than refine these zones, the given zonation was used, and permeabilities were set such that heads surrounding (but not within) the two topographic highs were fit well by the model (fig. 22).

Weighted observed heads plotted with weighted simulated heads are shown in figure 23. With the exception of the 12 points associated with the Port Royal and Ladies Island topographic highs, the results are distributed fairly symmetrically around a line of unit slope; 93 simulated heads are above and 103 are below their corresponding observed heads.

A plot of weighted residuals and simulated heads (fig. 24) shows that, with the exception of the 12 points associated with the Port Royal Island and Ladies Island topographic highs, the spread in the distribution of residuals is relatively uniform for the range of simulated heads and is centered on the horizontal axis. The average weighted residual is +0.8 ft, and the root-mean-square error (RMSE) is 4.6 ft. Without the 12 points associated with the topographic highs, the average weighted residual is –0.08 ft, and the RMSE is 2.4 ft.

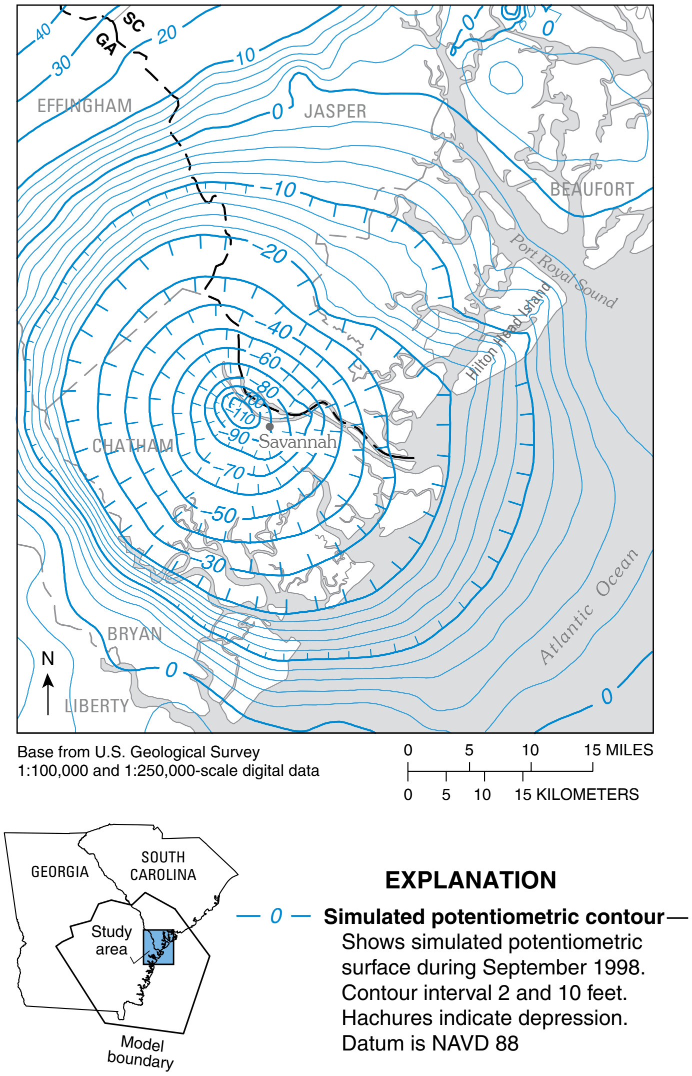

Figure 21. Potentiometric surface of the Upper Floridan aquifer for head calibration simulation in the study area, September 1998.

Calibrated Permeability Values, Confidence Intervals, and Correlations

The calibrated permeabilities in the Upper Floridan aquifer and upper confining units are shown in figure 16. Only 10 of the permeability zones were calibrated independently: C6, C7, C8, C13, C14, UF13, UF14, UF16, UF17, and UF20. Zones UF15, UF18, UF19, and UF23 were combined with zone UF14; zones UF21 and UF22 were combined with zone UF20; zone C9 was combined with zone C5; zone C10 was combined with zones C8; C11, C12, and C16 were combined with zone C6; and zone C15 was combined with zone C14.

A linear confidence interval is a measure of the uncertainty of an estimated parameter value. For example, the 95-percent confidence interval for a given parameter is the range of values within which the true value of the parameter is expected to occur with 95-percent confidence. Linear confidence intervals are computed assuming “normally distributed residuals, reasonable optimized parameter values, a satisfactory model fit, and a linear model” (Poeter and Hill, 1998). According to statistics computed by UCODE, however, residuals in this model are unlikely to be normally distributed. Additionally, the estimated permeability values depend on the particular zonation chosen, which may not be the only zonation that results in a good fit to the observed water levels. Therefore, the 95-percent linear confidence intervals reported in figure 25 should be considered approximate measures of the confidence in the estimated permeabilities.

Table 5 shows the parameter correlation matrix computed by UCODE. A high correlation (close to unity) between two different parameters indicates that the observation data are insufficient to estimate those two parameters independently. There is uncertainty because there is not a unique set of parameter values that best fits the data. To help identify parameters that are highly correlated, UCODE lists separately any correlation coefficient with an absolute value greater than or equal to 0.85. In this model, magnitudes of all of the absolute values of the correlation coefficients between distinct parameters are below 0.85, except for a value of –0.89 between parameters C14 and UF20, which are the upper confining unit and Upper Floridan permeabilities in the higher elevations, away from the main coastal pumping centers and the area of main interest (see fig. 16). The addition of flow data, such as recharge rates, within the boundaries of those zones would likely reduce the correlation between the two parameters.

Composite Scaled Sensitivities

The composite scaled sensitivity with respect to a parameter indicates the total amount of information provided by the observations (in this case, water levels) for the estimation of that parameter (Hill, 1998). During calibration, as the permeability zones and values were refined, parameters with low sensitivities for which the observations provided relatively little information were assigned fixed values or merged with other parameters. Figure 26 shows the composite scaled sensitivity for each of the final, independently estimated permeabilities. The permeabilities in zones C7, C16, and UF14, which encompass the apparent saltwater source areas, each have a composite scaled sensitivity above the median, indicating that the information content of the observations with respect to these parameters is relatively high. The smallest and largest sensitivities, associated with permeabilities in zones UF20 and C6, respectively, differ by about a factor of 11. As a rule, it is desirable for the sensitivities to differ by less than a factor of 100 to avoid problems with convergence of the regression (Poeter and Hill, 1998).

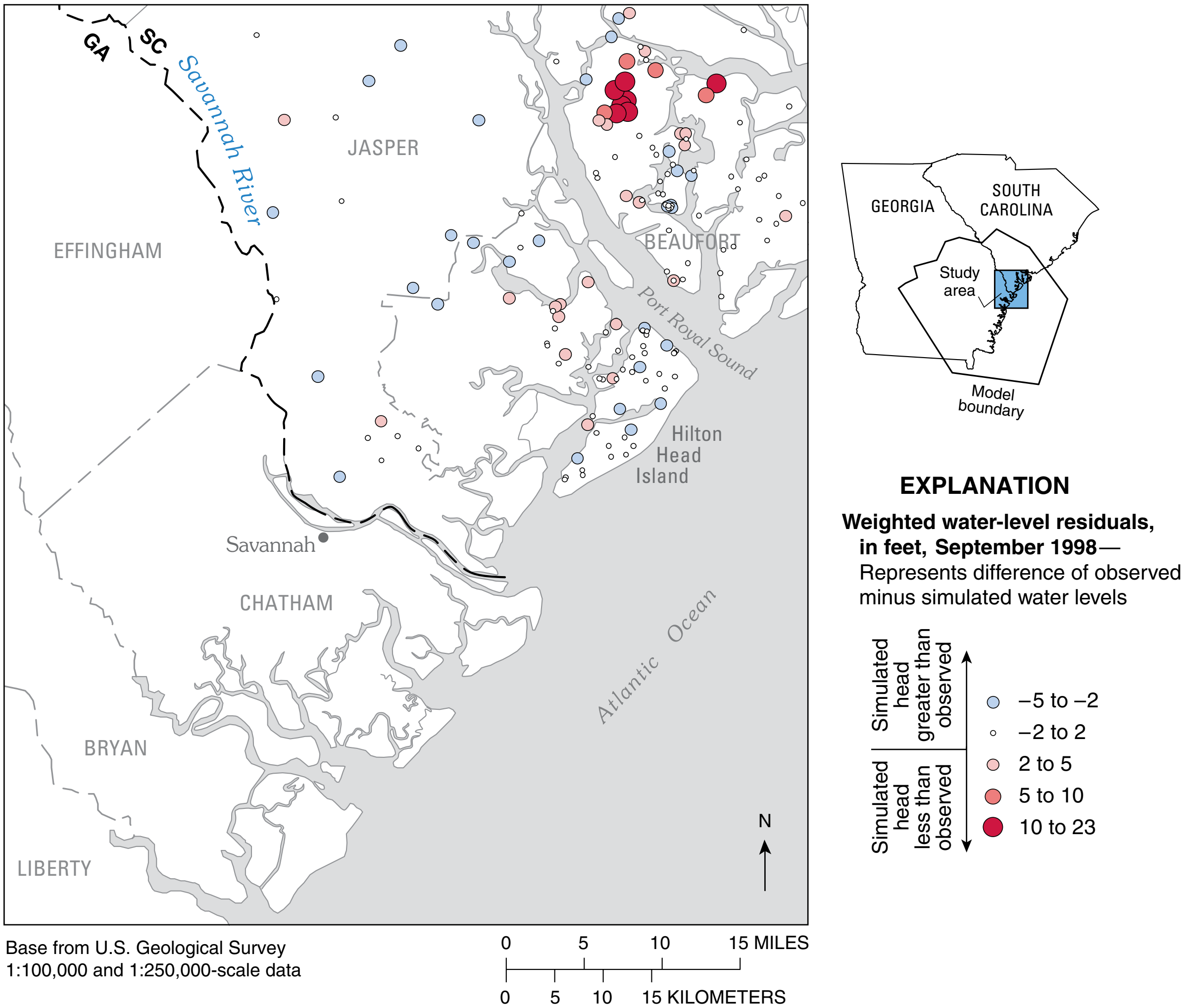

Figure 22. Weighted difference between observed and simulated water levels (residuals) for head calibration simulation in the Upper Floridan aquifer in the study area, September 1998.

Predevelopment Steady State

As a check on the calibrated model, predevelopment steady-state conditions were simulated. Figure 27 shows a comparison of simulated predevelopment heads and the estimated potentiometric surface of Johnston and others (1980), which was interpreted from sparse data and should be considered approximate. The simulated heads are generally within 10 ft of the estimated heads in Jasper and Beaufort Counties, S.C. The area of poorest agreement is in central Jasper County, where there are relatively few September 1998 head data on which to calibrate. Thus, the assumption of steady-state flow conditions in September 1998 was justified.

Evaluation of Steady-State Assumption

The calibration was performed assuming that the September 1998 head distribution was at steady state. To test this assumption, a transient run was performed, starting from predevelopment (mid-1885) and ending in mid-September 1998. The run consisted of forty 2-year time steps followed by thirty-three 1-year time steps and one 0.2068-year time step. The resulting September 1998 head distribution in the Upper Floridan aquifer is virtually identical to the corresponding steady-state distribution shown in figure 21.

Flow Budget

Computed flow-budget components include total inflow and outflow at specified pressure boundaries, and total inflow and outflow at specified fluid sources and sinks (for example, wells). For 1998 steady-state conditions, the total inflow from the specified pressure boundaries was 6.932×10^4 kilograms per second (kg/s) (1,583 Mgal/d or 2.12×10^8 cubic feet per day [ft^3/d]), and the total outflow from the specified pressure boundaries was 3.546×10^4 kg/s (810 Mgal/d or 1.08×10^8 ft^3/d). The net flow at specified pressure boundaries is 3.386×10^4 kg/s (773 Mgal/d or 1.04×10^8 ft^3/d) into the model domain. The total outflow from wells was 3.385×10^4 kg/s (773 Mgal/d or 1.03×10^8 ft^3/d). The total mass balance error is -3.691×10^{-1} kg/s (.008 Mgal/d, or 1,069 ft^3/d), which is about -5×10^{-4} percent.

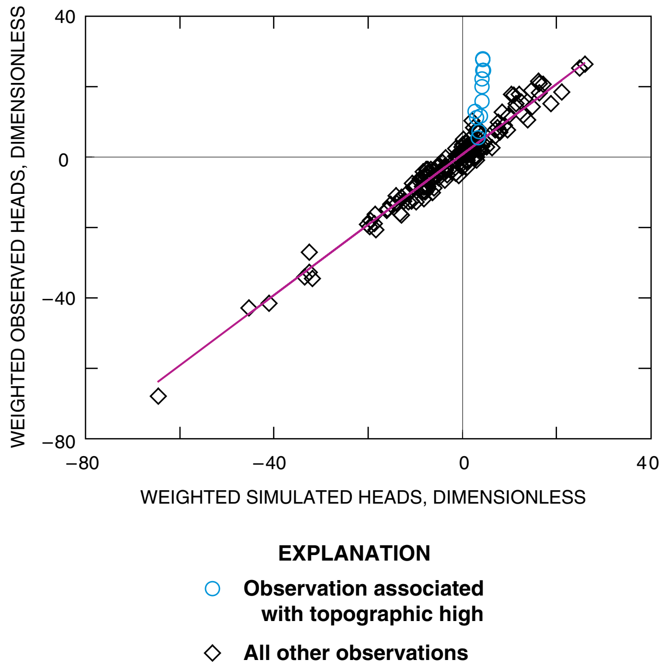

Figure 23. Weighted observed and simulated heads. (Topographic highs on Port Royal Island and Ladies Island, South Carolina, locations shown in figure G1.)

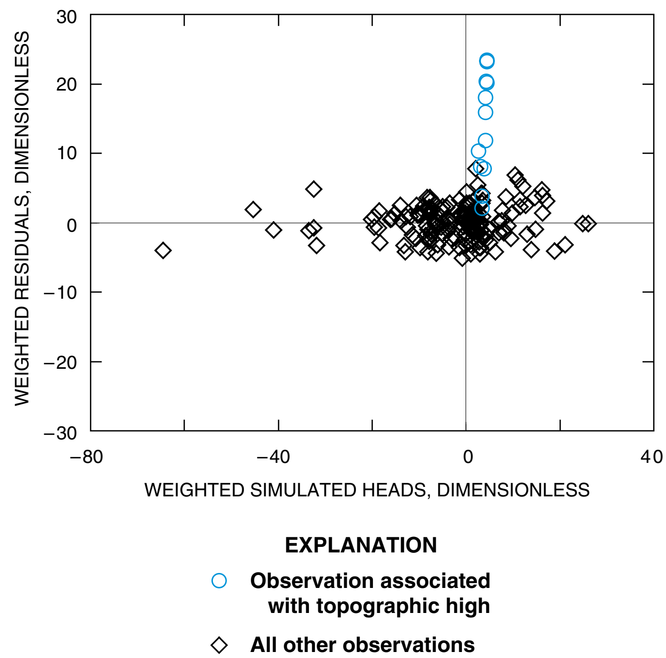

Figure 24. Weighted residuals and simulated heads. (Topographic highs on Port Royal Island and Ladies Island, South Carolina, locations shown in figure G1.)

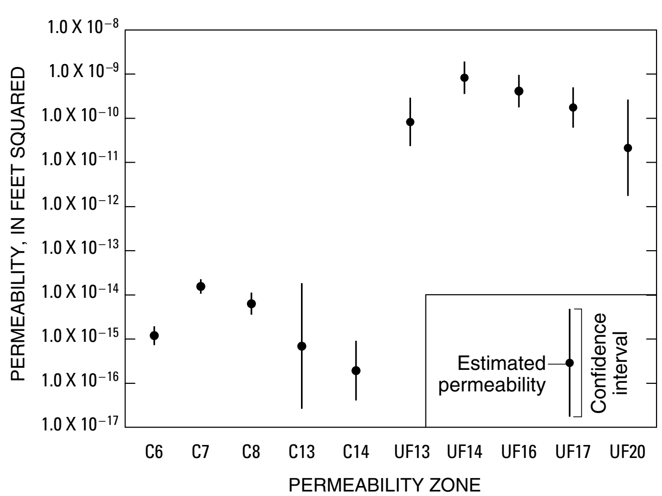

Figure 25. Ninety-five-percent linear confidence intervals for the 10 independently estimated permeabilities (see figure 16 for location of permeability zones).

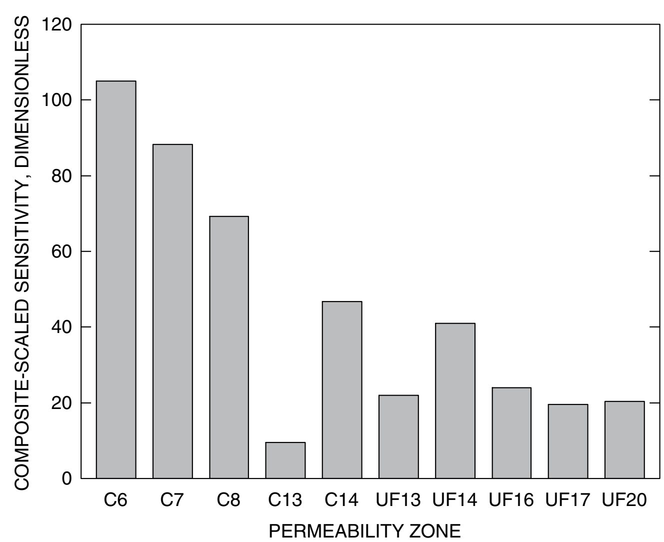

Figure 26. Composite-scaled sensitivities for the 10 independently estimated permeabilities (see figure 16 for location of permeability zones).

Table 5. Parameter correlation matrix for head calibration values.

[–, minus; values reported to two decimal places. Absolute values closer to 1.0 indicate pairs of parameter values that are less likely to be independently estimated; see figure 16 for location of permeability zones]

Perme-ability zones	C6	C7	C8	C13	C14	UF13	UF14	UF16	UF17	UF20
C6	1.00	0.08	–0.41	–0.05	–0.21	0.41	–0.44	–0.14	0.07	0.03
C7	0.08	1.00	–0.40	0.01	–0.02	0.04	–0.45	0.03	0.15	0.01
C8	–0.41	–0.40	1.00	–0.09	0.07	0.23	0.75	–0.22	–0.12	0.01
C13	–0.05	0.01	–0.09	1.00	0.49	0.00	0.06	–0.02	0.02	–0.58
C14	–0.21	–0.02	0.07	0.49	1.00	–0.05	0.14	–0.04	0.18	–0.89
UF13	0.41	0.04	0.23	0.00	–0.05	1.00	0.30	–0.19	–0.21	–0.01
UF14	–0.44	–0.45	0.75	0.06	0.14	0.30	1.00	–0.35	–0.23	–0.06
UF16	–0.14	0.03	–0.22	–0.02	–0.04	–0.19	–0.35	1.00	–0.08	0.02
UF17	0.07	0.15	–0.12	0.02	0.18	–0.21	–0.23	–0.08	1.00	–0.01
UF20	0.03	0.01	0.01	–0.58	–0.89	–0.01	–0.06	0.02	–0.01	1.00

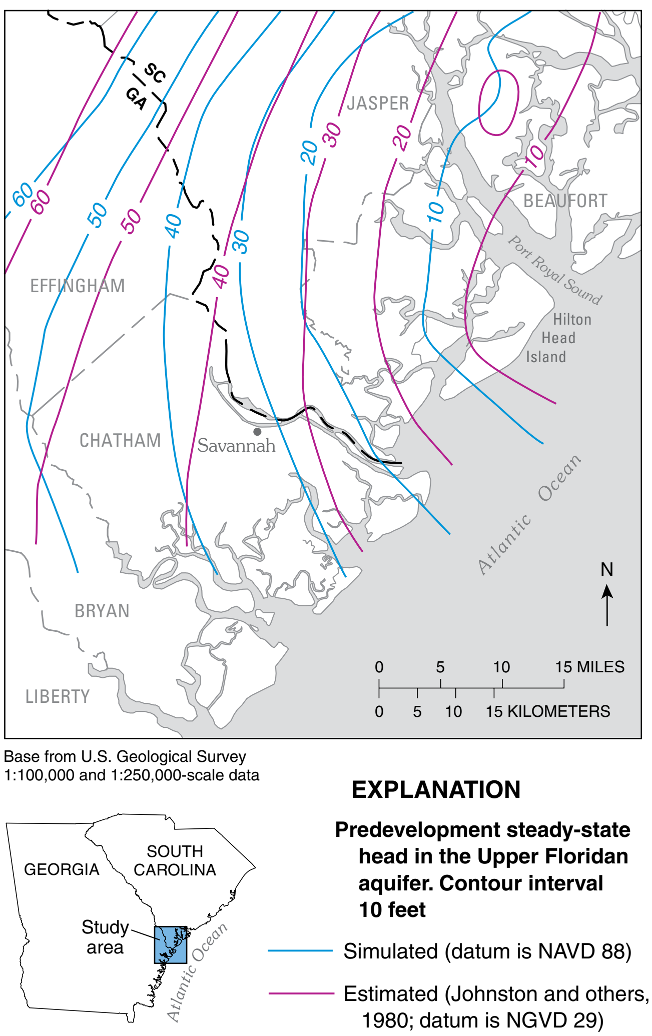

Figure 27. Comparison of simulated and estimated pre-development steady-state heads in the Upper Floridan aquifer.

Model Calibration to Observed Chloride ("Chloride Calibration") and Solute-Transport Model Sensitivity

Solute-transport simulations were performed to evaluate the hypothesis that the saltwater that has been observed in the Upper Floridan aquifer beneath the northern end of Hilton Head Island, Pinckney Island, and the Colleton River enters primarily through localized areas in which the confining units that overlie the Upper Floridan aquifer (hereinafter called the "upper confining units") are thin or absent. The flow model that resulted from the head calibration was refined and calibrated to match chloride concentrations inferred from field measurements of specific conductance (Camille Ransom III, South Carolina Department of Health and Environmental Control, written commun., 2005) by adjusting the permeability of the upper confining units in three discrete saltwater "source areas" (fig. 16, permeability zones CR [Colleton River], HH [Hilton Head], PI [Pinckney Island]). The resulting transport model, called the "Base Case," simulates the intrusion of saltwater through the overlying confining unit and into the Upper Floridan aquifer.

Sensitivity of the model results to selected physical properties, boundary conditions, and numerical controls was evaluated using perturbations of the Base Case. In addition, three variations on the Base Case are used to evaluate assumptions made regarding certain initial and boundary conditions. Variations 1 and 2 test the sensitivity of the development of the saltwater plume to the amount of salt initially present in the aquifer. Variation 3 evaluates the effect of limiting the amount of salt that is transported from the Upper Floridan aquifer to underlying units.

Chloride Calibration Method

The locations and sizes of the three source areas (fig. 16), the permeability of the upper confining units within those areas, and the longitudinal and transverse dispersivities were adjusted by trial and error until the simulated chloride distribution in the Upper Floridan aquifer gave a reasonable match to the trend in chloride distribution inferred from vertical profiles of specific conductance measured in 2000, 2002, 2003, and 2004 (appendix B, table B1; fig. 28). Simulation results computed midway between the top and bottom of the Upper Floridan aquifer, where the maximum simulated concentrations typically occur, are shown and compared with maximum measured (inferred) chloride values, which often occur at or near the bottom of the aquifer. Comparing near-maximum simulated concentrations with maximum measured concentrations was considered more appropriate than directly comparing simulated and measured concentrations at a given depth. First, the simulated concentration near the bottom of the aquifer is affected by the properties of the underlying confining unit, about which little is known. Second, there is likely discrepancy between the simulated and actual depth intervals of the Upper Floridan aquifer within each well.

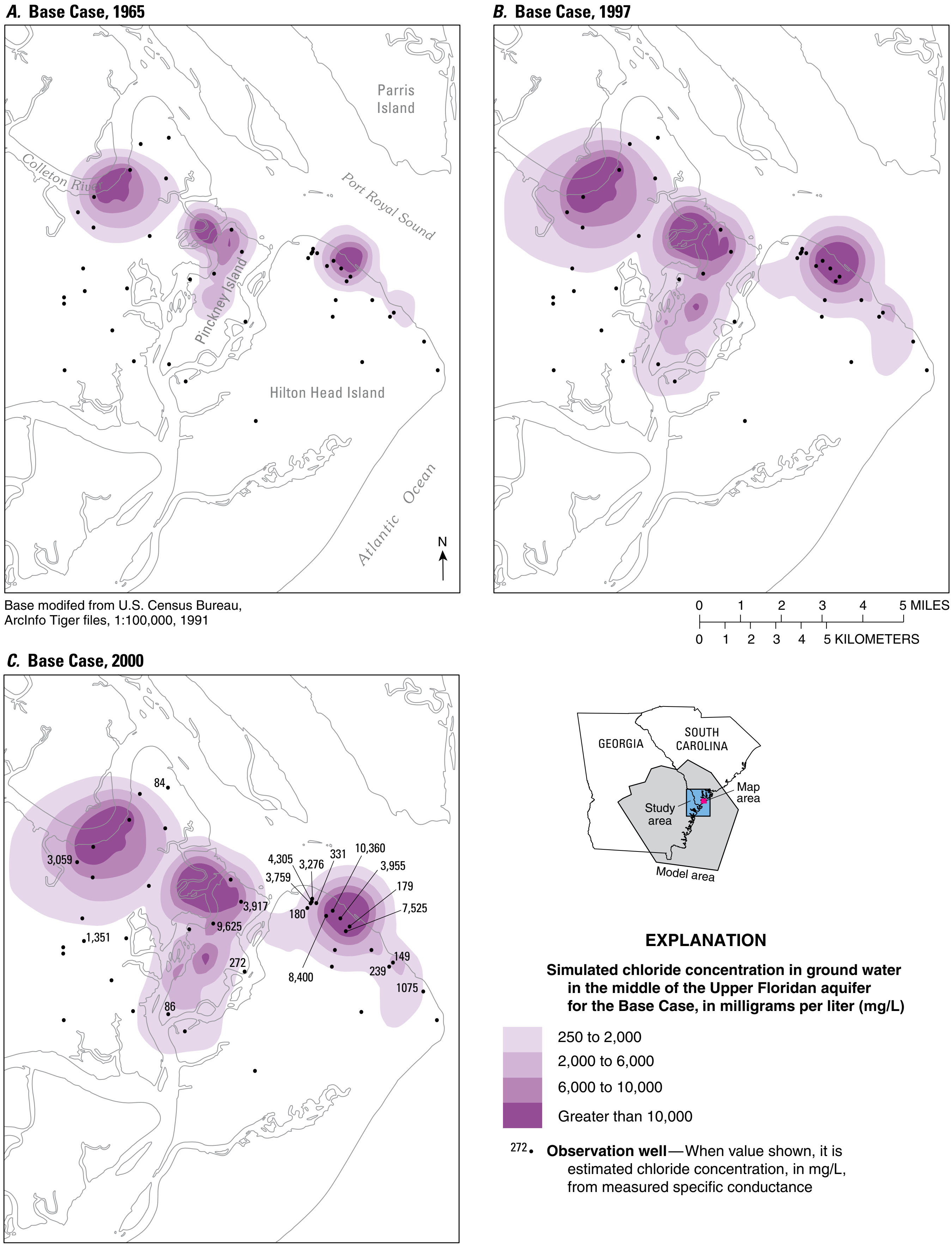

Figure 28. Simulated chloride concentration in ground water in the middle of the Upper Floridan aquifer in the Hilton Head Island, South Carolina, area for the Base Case, (*A*) 1965, (*B*) 1997, (*C*) 2000, (*D*) 2002, (*E*) 2003, (*F*) 2004.

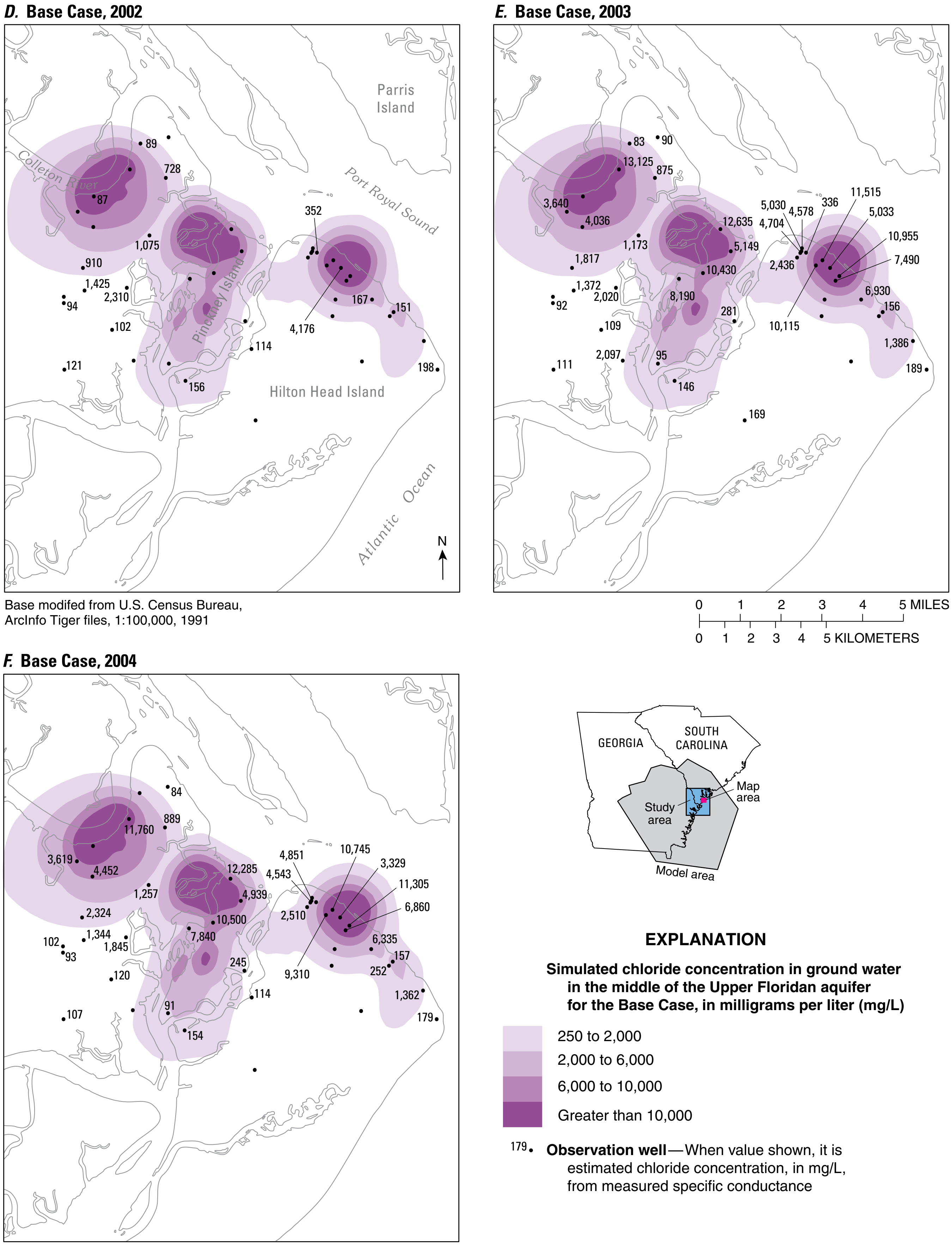

Figure 28. Simulated chloride concentration in ground water in the middle of the Upper Floridan aquifer in the Hilton Head Island, South Carolina, area for the Base Case, (*A*) 1965, (*B*) 1997, (*C*) 2000, (*D*) 2002, (*E*) 2003, (*F*) 2004—continued.

Thus, the match between simulated and measured concentrations is intended to capture the general pattern of maximum chloride concentration in the aquifer downgradient of the presumed source areas, rather than accurate vertical profiles or a detailed lateral distribution of chloride concentration. Attempts at a more detailed match were considered unjustified given the uncertainty and potential sources of error in the field data and the model (see “Model Limitations”). Simulated concentrations were evaluated at the midpoint of each year, and concentrations measured within a given year were taken to be representative of values at the midpoint of that year.

After the chloride calibration was completed, updated data became available. Appendix B summarizes these data and discusses their implications for the model calibration. Figures that illustrate the correspondence between simulated and measured chloride concentrations (figs. 28, 30–34, and 36–46) show the updated field data.

Each transient simulation begins from a steady-state flow field with no chloride initially in the subsurface, except Variation 2, which begins from the results of a transient run designed to allow salt to enter the Upper Floridan aquifer during predevelopment. Pumping after the year 2000 is assumed to remain at year-2000 levels. The interval from 1885 to 2000 was simulated by taking forty 2-year time steps (up to 1965) followed by thirty-five 1-year time steps. On each time step, the pressure (flow) field was computed using the concentration (density) field from the previous time step. Unless stated otherwise, results are presented at the midpoint of each given calendar year.

Base Case

In the Base Case simulation, the development of saltwater plumes in the Upper Floridan aquifer was simulated starting from predevelopment conditions (year 1885) in which there was assumed to be no salt initially in the subsurface. Table 4 shows the input parameter values used in the Base Case simulation.

Within the Colleton River, Pinckney Island, and Hilton Head Island source areas, upper confining units were assigned permeabilities that correspond respectively to 0.003, 0.0004, and 0.003 times the permeability of the Upper Floridan aquifer in that region. The longitudinal dispersivity in each of the coordinate directions was set to three times the theoretical minimum required for spatial stability of the transport solution (Voss and Provost, 2002) and varies with the mesh spacing. Values of longitudinal dispersivity are in the range of about 135–15,000 meters (m) in the x and y directions (within the horizontal plane) and about 0.04–158 m in the z direction (the vertical direction). The transverse dispersivity in each coordinate direction was set to one-tenth the longitudinal dispersivity in the same direction. Simulated chloride distributions for years 1965, 1997, 2000, 2002, 2003, and 2004 are shown in figure 28.

Development in the Hilton Head Island area began to expand rapidly during the mid-1960s (Landmeyer and Belval, 1996; Smith, 1994); according to the flow model that resulted from the head calibration, the zero-head contour during the mid-1960s reached the Colleton River source area as it moved northeastward as a result of increasing drawdown from pumping. The results show saltwater having penetrated the Upper Floridan aquifer despite the fact that, prior to 1965, heads in the aquifer had not yet been drawn down below sea level at the source areas (fig. 28A). Emergent wetlands, which are areas of land periodically inundated with saltwater when the tide is high, are represented in the model as potential sources of saltwater intrusion in which the water table is elevated above sea level, providing a driving force for downward flow of saltwater into the aquifer at the source areas even when the head in the aquifer is higher than sea level. An additional driving force for downward saltwater intrusion results from the greater density of seawater as compared with freshwater.

The simulated chloride distribution mirrors the general trends in the field data for 2000, 2002, 2003, and 2004, although not every detail is simulated accurately; the model results tend to underestimate the moderately high chloride concentrations observed at wells BFT-1326 and BFT-2304 (see fig. B2), which are located south of the plumes emanating from the Colleton River and Pinckney Island source areas (figs. 28C–28F). Compared with ground-water flow simulations, solute-transport simulations tend to be sensitive to the details of the distribution of hydrogeologic properties in the subsurface. It is not known whether the underestimated chloride concentrations are the result of a preferential flowpath or surface-water source area not captured by the model, or are indicative of some other saltwater-intrusion mechanism.

Solute disperses as it is advected downward through the confining units and laterally along the hydraulic gradient within the Upper Floridan aquifer. The migration of solute upgradient (northeast) of the source areas is attributed to transverse dispersion during downward flow and possibly to longitudinal dispersion during lateral flow.

Inclusion of the source areas in the transport model, which changed the permeability of the upper confining units and introduced saltwater into the system, changed the simulated head distribution and the distribution of residuals in the Upper Floridan aquifer relative to the distribution obtained during the head calibration (figs. 22 and 29; table 6). Inclusion of the source areas generally elevated heads locally in the Upper Floridan aquifer. Differences in residuals far from the source areas are likely because the results shown in figures 22 and 29 are based on different finite-element meshes. The largest differences tend to be in areas where the head gradient is steep. Inclusion of the source areas increased the root-mean-square residual by 2.1 and 3.2 ft near the Colleton River and Hilton Head Island source areas, respectively, and decreased the root-mean-square residual by 0.3 ft near the Pinckney Island source area (table 6).

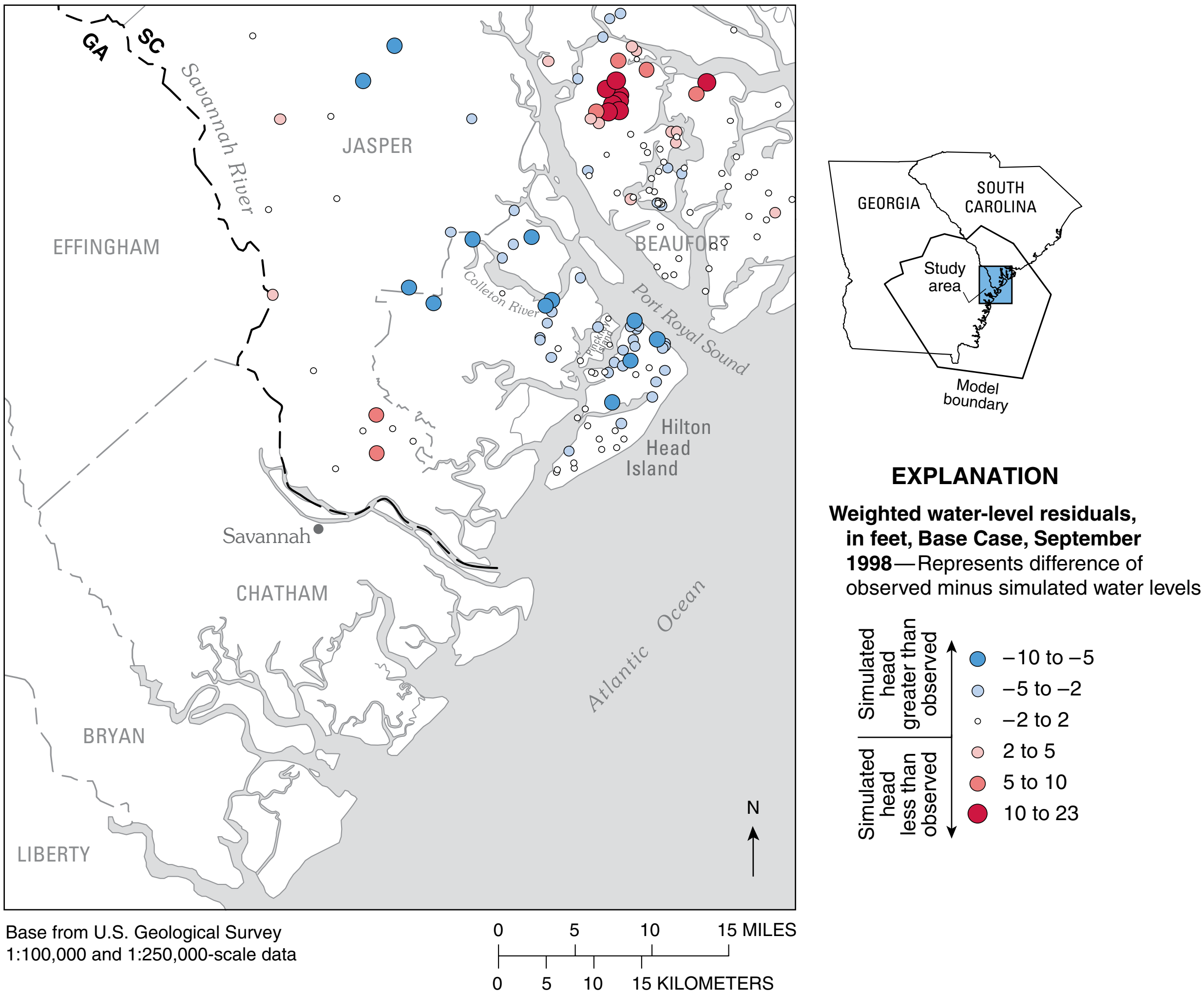

Figure 29. Weighted difference between observed and simulated water levels (residuals) for head calibration simulation in the Upper Floridan aquifer in the study area, Base Case, September 1998.

Table 6. Effect of high-permeability source areas on selected water-level residuals in the study area.

[–, minus; +, plus; values reported to one decimal place]

Source area	Wells	Minimum residual (foot)		Maximum residual (foot)		Average residual (foot)		Root-mean-square residual (foot)	
		Without source areas	With source areas	Without source areas	With source areas	Without source areas	With source areas	Without source areas	With source areas
Colleton River	BFT-493, BFT-501, BFT-502, BFT-1846	–0.7	–6.5	+3.4	–2.6	+2.1	–4.5	2.6	4.7
Hilton Head Island	BFT-315, BFT-441, BFT-787, BFT-1810, BFT-2164, BFT-2197	–3.8	–7.1	+0.3	–3.6	–1.1	–4.8	1.8	5.0
Pinckney Island	BFT-2166, BFT-2189	+2.0	–2.4	+2.6	–1.5	+2.3	–1.9	2.3	2.0

With the source areas present, all residuals within 1.2 mi of the source areas are negative; the simulated heads are consistently higher than observed heads in the Upper Floridan aquifer in that area, resulting in diminished driving forces for vertical flow through the upper confining units. To some extent, this error is mitigated by the calibration of the upper confining unit permeabilities in the source areas to match the observed evolution of the chloride distribution in the Upper Floridan aquifer; the effects of underestimated driving forces are compensated for by adjusting permeabilities to get the appropriate rate of saltwater inflow. Also, the fact that the observed water levels underestimate the equivalent freshwater head (see “Head Observations”) tends to increase the magnitude of the residuals in areas of high salinity.

Solute-Transport Model Sensitivity

Sensitivity of the solute-transport model results to selected physical properties, boundary conditions, and numerical controls was evaluated using perturbations of the Base Case. In each model run, an input parameter or group of parameters was perturbed, and results were obtained without recalibrating the model. Results compared with the Base Case for the year 2000 illustrate the effect of perturbing the model inputs.

Permeability of the Upper Confining Units in the Source Areas

The permeabilities of the confining units overlying the Upper Floridan aquifer in the three source areas (zones CR, PI, and HH, fig. 16) were each increased by a factor of two relative, to the Base Case (fig. 30). Chloride concentration in the southernmost part of the plume south of Pinckney Island decreased, possibly because of a decrease in drawdown of the Upper Floridan aquifer associated with increased hydraulic connection with the surface via the source areas.

To test the overall influence of the source areas, a model run was performed with the upper confining unit permeabilities in the source areas set to the original values that resulted from the head calibration. Even without enhanced permeability in the source areas, some saltwater still enters the Upper Floridan aquifer near each of the three source areas, although generally much less than in the Base Case (fig. 31).

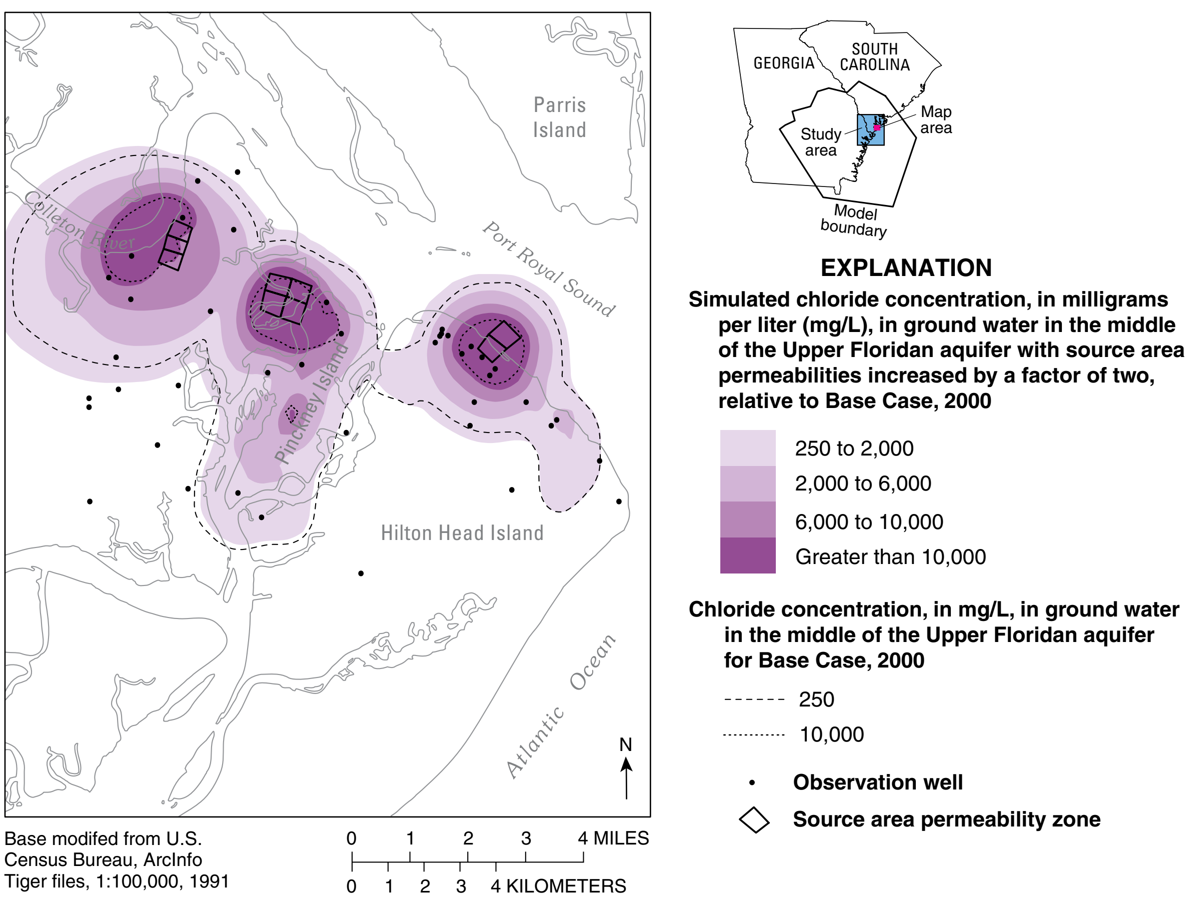

Figure 30. Simulated chloride concentration in ground water in the middle of the Upper Floridan aquifer in the Hilton Head Island, South Carolina, area with source area permeabilities increased by a factor of two, relative to Base Case, 2000.

Chloride concentration in the southernmost part of the plume south of Pinckney Island increased, possibly because of an increase in drawdown of the Upper Floridan aquifer associated with decreased hydraulic connection with the surface via the source areas. The fact that this part of the plume is a persistent feature throughout the simulations and that its presence is insensitive to the permeability of the upper confining units in the source areas indicates that development of the plume in this area is mainly a function of the local properties of the upper confining units. This area of elevated chloride concentration does not appear to be an outgrowth of the plume that emanates from the Pinckney Island source area. Rather, this area of elevated chloride concentration appears to develop from a separate source, eventually merging with the plume to the north.

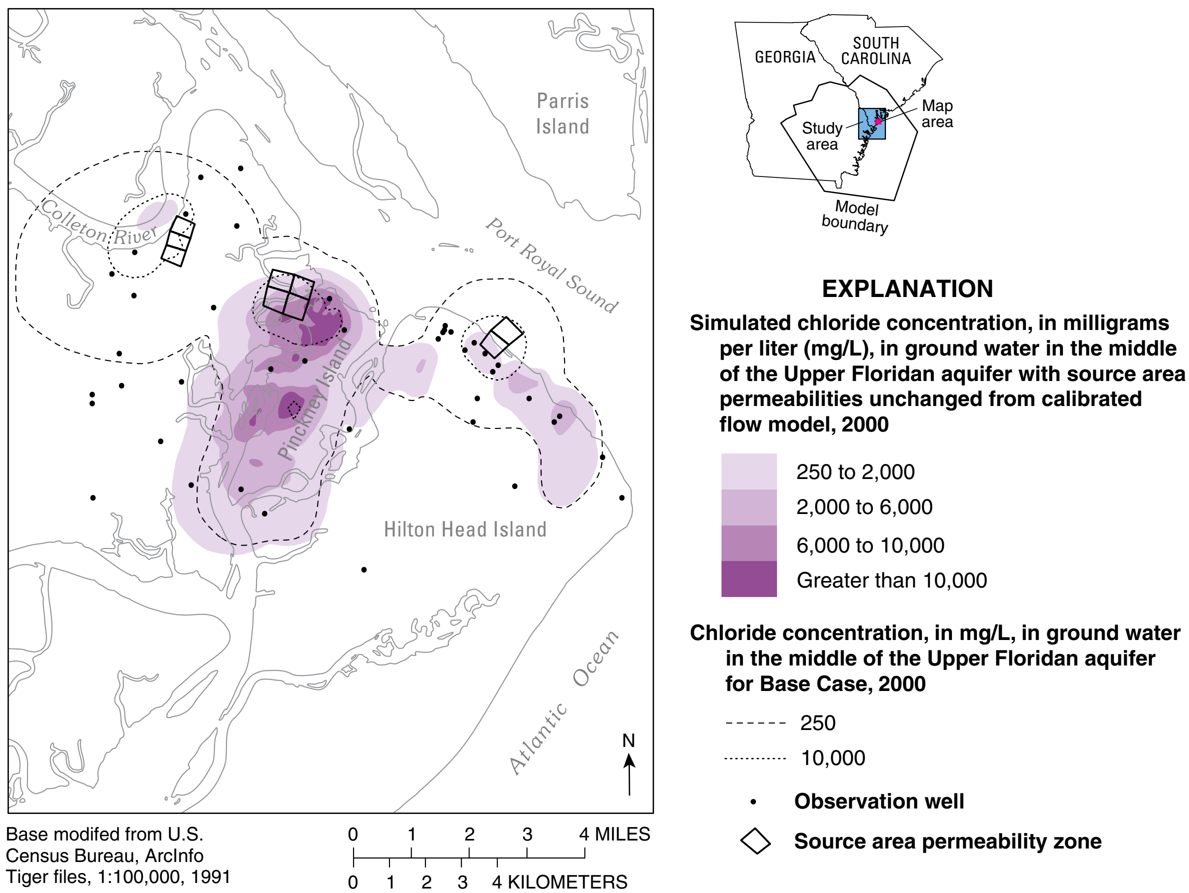

Figure 31. Simulated chloride concentration in ground water in the middle of the Upper Floridan aquifer in the Hilton Head Island, South Carolina, area with source area permeabilities unchanged from the values that resulted from calibration of the flow model to head data, 2000.

Permeability of the Upper Floridan Aquifer

The permeability of the Upper Floridan aquifer in zones UF14 and UF23 (fig. 16) was increased by a factor of two, relative to the Base Case. The greatest changes took place in the plumes emanating from the Colleton River and Pinckney Island source areas, where chloride concentrations increased slightly overall relative to the Base Case (fig. 32).

Porosity

The porosity was decreased throughout the model area by a factor of two, relative to the Base Case. The decreased porosity increases the velocity at which solute is transported, resulting in faster movement of saltwater in the aquifer relative to the Base Case (fig. 33).

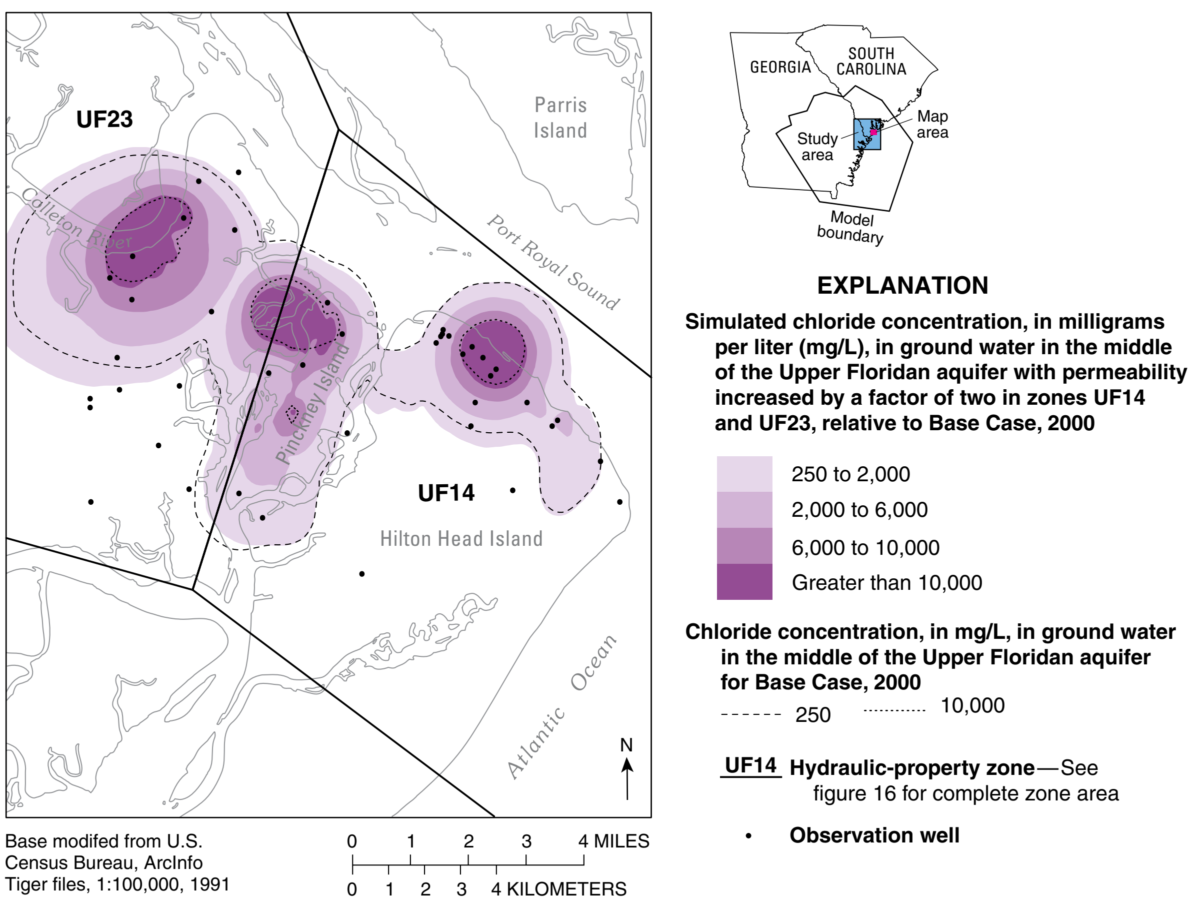

Figure 32. Simulated chloride concentration in ground water in the middle of the Upper Floridan aquifer in the Hilton Head Island, South Carolina, area with permeability increased by a factor of two in zones UF23 and UF14 (see figure 16), relative to the Base Case, 2000.

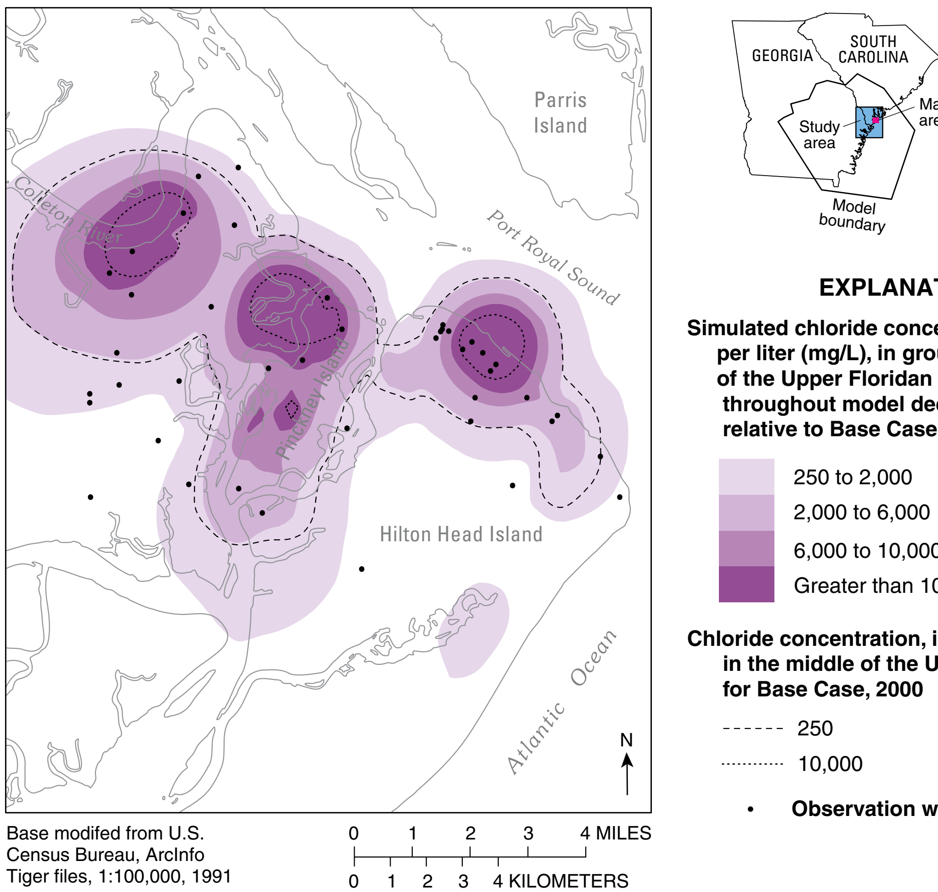

EXPLANATION

Simulated chloride concentration, in milligrams per liter (mg/L), in ground water in the middle of the Upper Floridan aquifer with porosity throughout model decreased by a factor of two, relative to Base Case, 2000

250 to 2,000
2,000 to 6,000
6,000 to 10,000
Greater than 10,000

Chloride concentration, in mg/L, in ground water in the middle of the Upper Floridan aquifer for Base Case, 2000

250
10,000

Observation well

Figure 33. Simulated chloride concentration in ground water in the middle of the Upper Floridan aquifer in the Hilton Head Island, South Carolina, area with porosity throughout the model decreased by a factor of two, relative to the Base Case, 2000.

Dispersion

The longitudinal and transverse dispersivities were increased throughout the model area by a factor of two, relative to the Base Case. The increased dispersion tends to diminish concentration gradients relative to the Base Case (fig. 34).

Surface-Water Chloride Concentration

In the Base Case model, the concentration of surface water in marine, estuarine, and emergent wetland areas was set to seawater concentration. At monitoring stations near the source areas (fig. 35), however, 25-hour continuous bottom specific-conductance measurements taken during the summer months from 1999 to 2002 (Van Dolah and others, 2002; Van Dolah and others, 2004) indicate that mean surface-water solute concentrations ranged from 82 to 99 percent seawater (table 7). To test the sensitivity of the model to the source-water chloride concentration, the chloride mass fraction of the surface-water bodies, including emergent wetlands, within the region (shown in figure 36) was set to 80 percent of seawater (0.02856 kilogram per kilogram [kg/kg]). The change affected both the source concentration and the pressure boundary condition associated with the saline surface water (fig. 36). (A model run in which only the source concentration was changed, and not the pressure boundary condition, yielded similar results.)

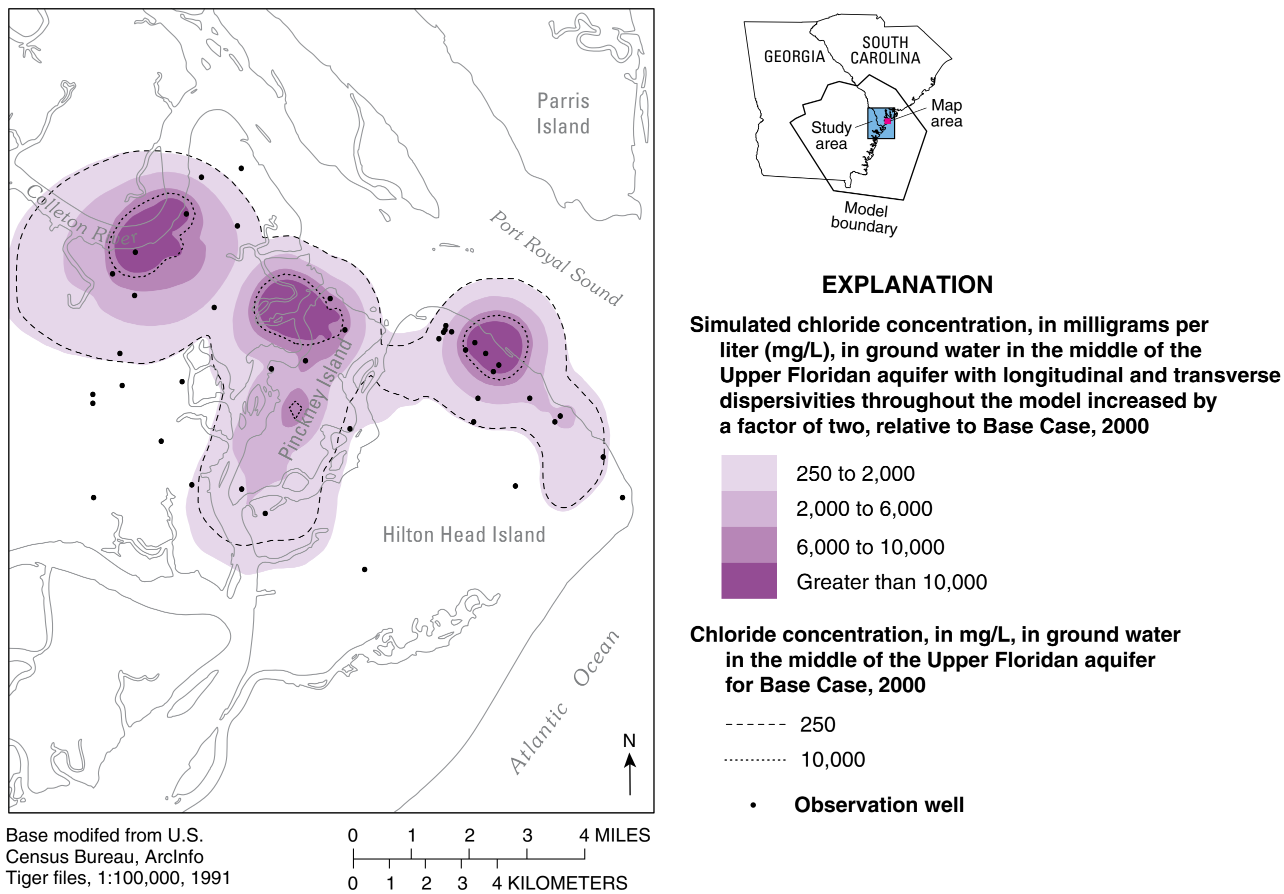

Figure 34. Simulated chloride concentration in ground water in the middle of the Upper Floridan aquifer in the Hilton Head Island, South Carolina, area with longitudinal and transverse dispersivities throughout the model increased by a factor of two, relative to the Base Case, 2000.

Table 7. Measurements of 25-hour continuous bottom salinity in open water, recorded at selected stations during the summer months from 1999 to 2002.

[ppt, parts per thousand; %, percent. Percent seawater is calculated assuming seawater salinity is 35.7 ppt. Data from Van Dolah and others, 2002, 2004]

Year	Station	Range of salinity measured (ppt)	Mean salinity (ppt)	Range of salinity measured (% seawater)	Mean salinity (% seawater)	Latitude (degree)	Longitude (degree)
1999	RO99305	29.5–30.6	30.2	83–86	85	32.30514	80.75850
	RO99325	28.1–30.2	29.2	79–85	82	32.31847	80.80146
2000	RO00024	33.7–34.1	33.9	94–96	95	32.30055	80.80145
	RO00037	34.4–35.0	34.6	96–98	97	32.29158	80.72581
2001	RO01117	31.7–32.7	32.2	89–92	90	32.24375	80.77832
2002	RO026002	33.7–34.9	34.3	94–98	96	32.20525	80.80085
	RO026018	34.9–35.3	35.1	98–99	98	32.28675	80.71152
	RO026020	25.1–34.0	30.9	72–95	87	32.22310	80.78366
	RO026023	34.8–35.4	35.2	97–99	99	32.30939	80.80363

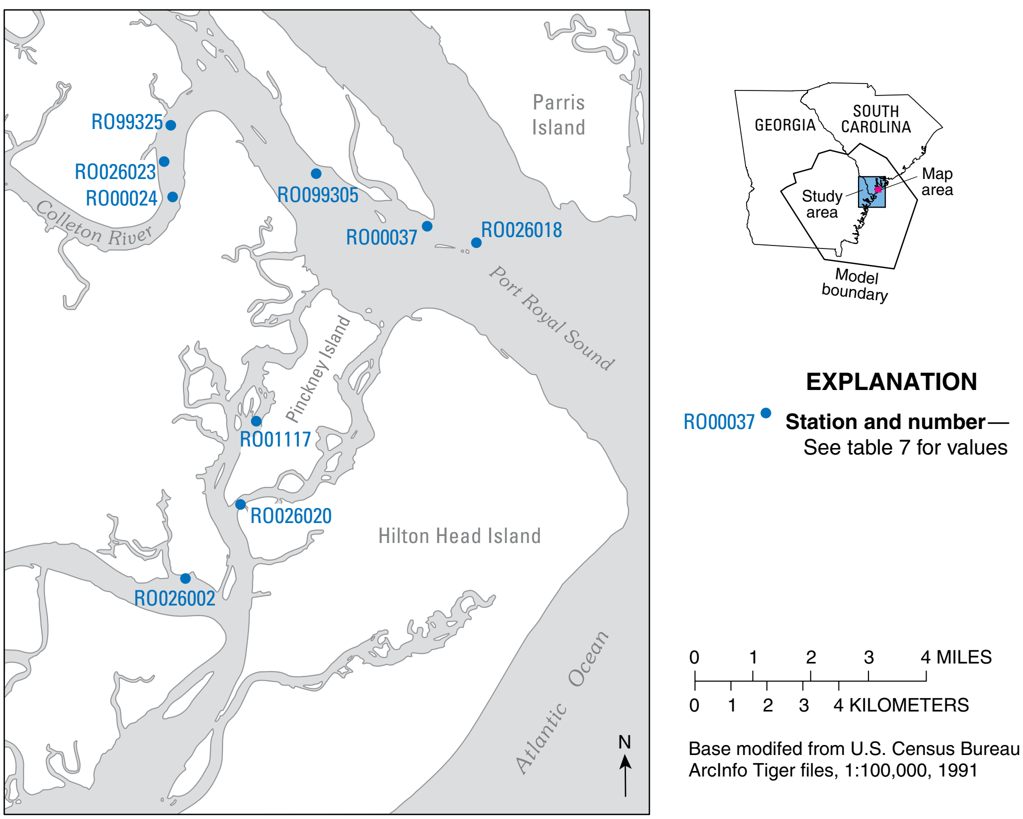

Figure 35. Stations at which 25-hour continuous bottom salinity was monitored in open water in the Hilton Head Island, South Carolina, area (Van Dolah and others, 2002, 2004).

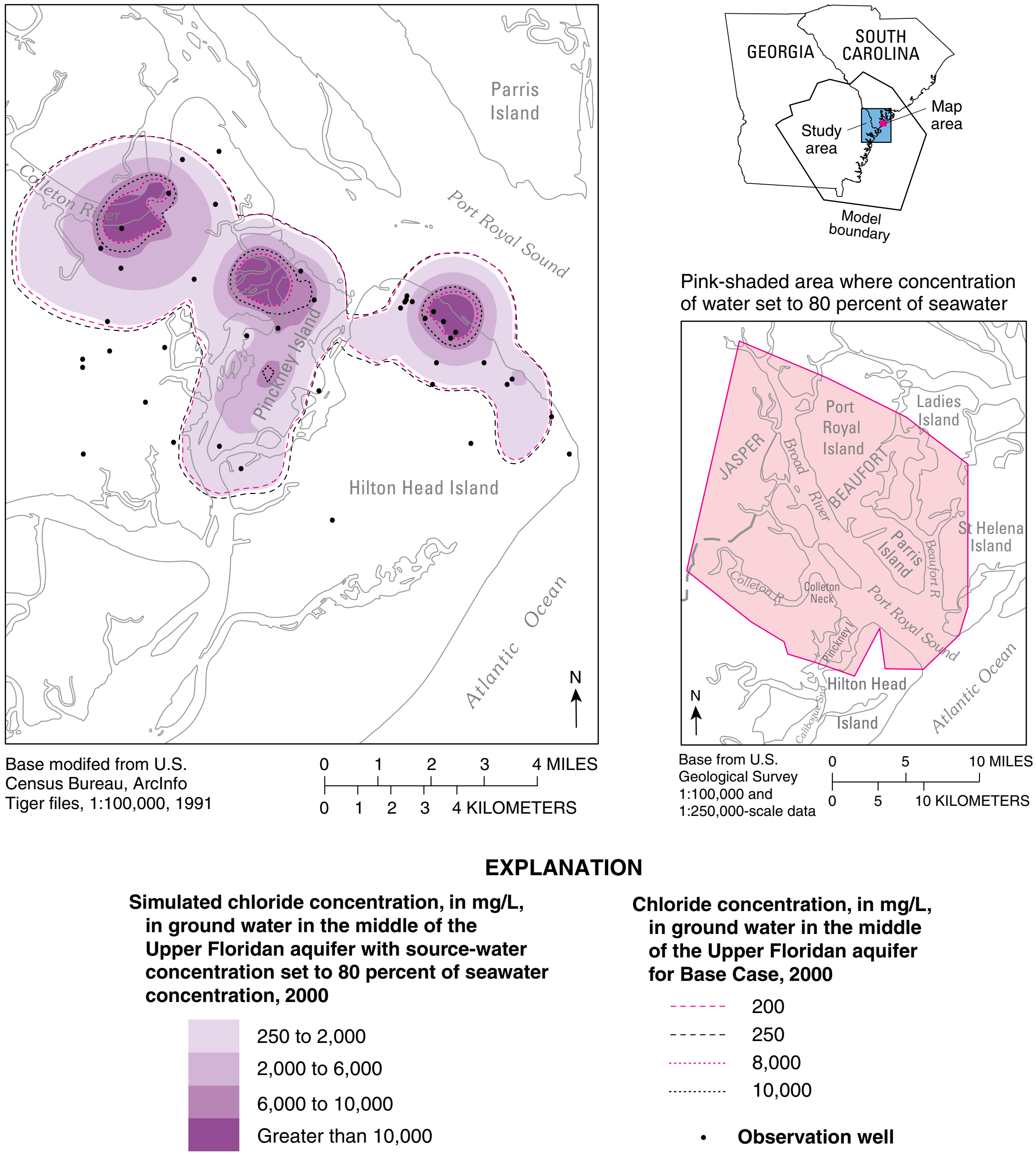

Figure 36. Simulated chloride concentration in ground water in the middle of the Upper Floridan aquifer in the Hilton Head Island, South Carolina, area with concentration of water associated with surface-water bodies and emergent wetlands (potential sources of saltwater intrusion) set to 80 percent of seawater concentration, 2000 (inset map). Reference contours are 250- and 10,000-mg/L (milligram per liter) chloride concentration for the Base Case, 2000, and 200- and 8,000-mg/L chloride concentration for 80 percent of Base Case, 2000.

If the chloride mass fractions in the Upper Floridan aquifer were a linear function of the chloride mass fraction in the source water, then the concentrations depicted in figure 36 would be equivalent to 80 percent of the chloride mass fractions computed in the Base Case. To test whether this is true, the results were redrawn with the chloride mass fractions in the Base Case scaled (prior to converting to milligrams per liter and contouring) to 80 percent of their computed values (fig. 36). The two sets of contours in figure 36 match closely, indicating that the chloride mass fraction within the plumes varies approximately linearly with the chloride mass fraction in the source water within the range 80–100 percent seawater (0.02856–0.0357 kg/kg).

To investigate the influence of fluid density (buoyancy) effects on the intrusion of saltwater at the source areas, a model run was performed with the solute acting as a tracer that enters the flow system at seawater concentration but does not increase the fluid density. The pressure boundary condition at the top surface of the model was not changed; it continued to reflect the pressure exerted by a column of seawater, which is denser than freshwater. (A similar model run in which the pressure boundary condition was changed to correspond to freshwater within the region shown in figure 36 produced very similar results.) Without the effects of fluid density, the simulated rate of saltwater intrusion is significantly less overall than in the Base Case, although substantial saltwater plumes still develop (fig. 37).

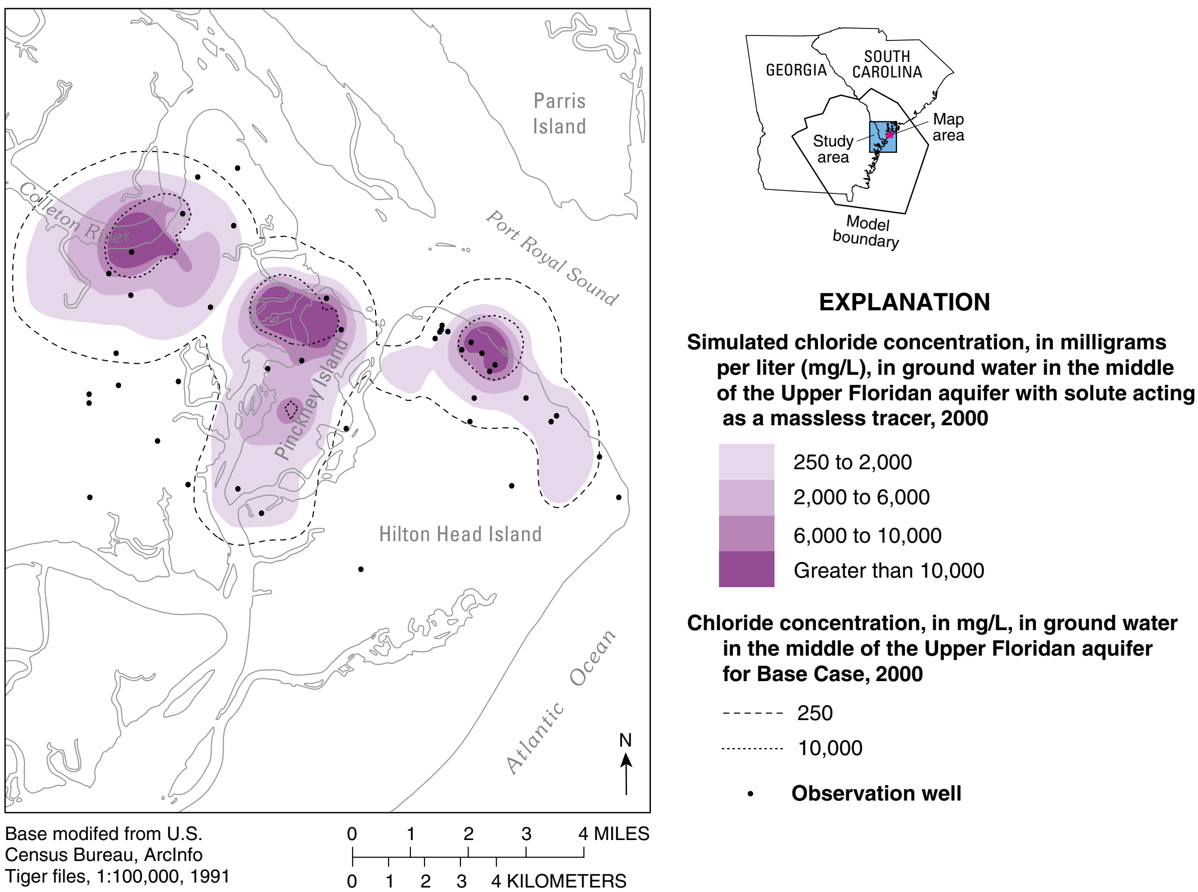

Figure 37. Simulated chloride concentration in ground water in the middle of the Upper Floridan aquifer in the Hilton Head Island, South Carolina, area with the solute acting as a massless tracer, 2000.

Spatial Discretization

The size of the finite elements near the saltwater plumes was approximately halved relative to the Base Case in each of the two horizontal dimensions. The dispersivities, which depend on element size, were adjusted to give about the same values as in the Base Case. The effect on the simulated saltwater plumes was generally small (fig. 38A). The only discernible difference occurs southeast of the Colleton River source area, where the plume is expanded, relative to the Base Case. This difference is likely due to the inclusion of additional areas of emergent wetland within the source area as a result of the different discretization.

In a separate model run, the size of the finite elements throughout the model was halved in the vertical direction relative to the Base Case. The dispersivities, which depend on element size, were adjusted to give about the same values as in the Base Case. The effect on the simulated saltwater plumes was small (fig. 38B).

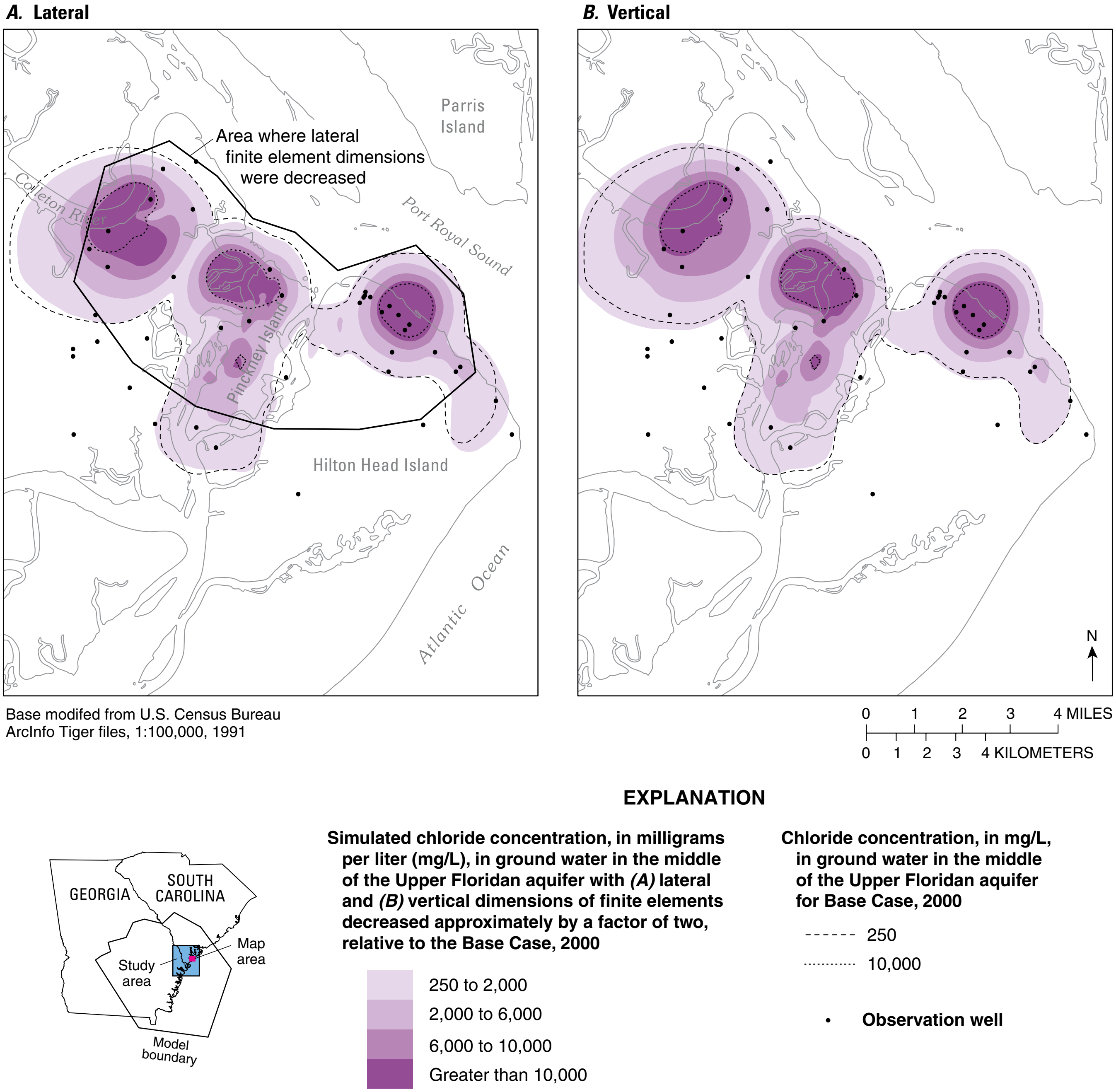

Figure 38. Simulated chloride concentration in ground water in the middle of the Upper Floridan aquifer in the Hilton Head Island, South Carolina, area with (*A*) lateral dimensions of finite elements near the simulated saltwater plumes and (*B*) vertical dimensions of finite elements decreased approximately by a factor of two, relative to the Base Case, 2000.

Temporal Discretization and Nonlinearity Iterations

To test the sensitivity of the results to the time-step size and the lag between the pressure and concentration solutions, a model run was performed in which the time-step size was halved relative to the Base Case and nonlinearity iterations were executed on each time step. The nonlinearity iterations involved alternately solving the pressure and concentration matrix problems, updating the coefficients in each problem based on the latest solutions, until the changes in solutions from one iteration to the next were less than the specified tolerances. The initial tolerances used for the pressure and concentration solutions corresponded to 0.1 ft of freshwater head and 1 percent of seawater concentration, respectively. When the nonlinearity iterations failed to converge on time-step 55 (year 1940), the time-step size was reduced to 0.25 years, the nonlinearity iteration convergence tolerance for the concentration solution was increased to 2 percent of seawater concentration, and the model run was continued from time-step 55 to completion (year 2000). The refined time stepping and the use of nonlinearity iterations made little difference in the simulated plume development relative to the Base Case (fig. 39).

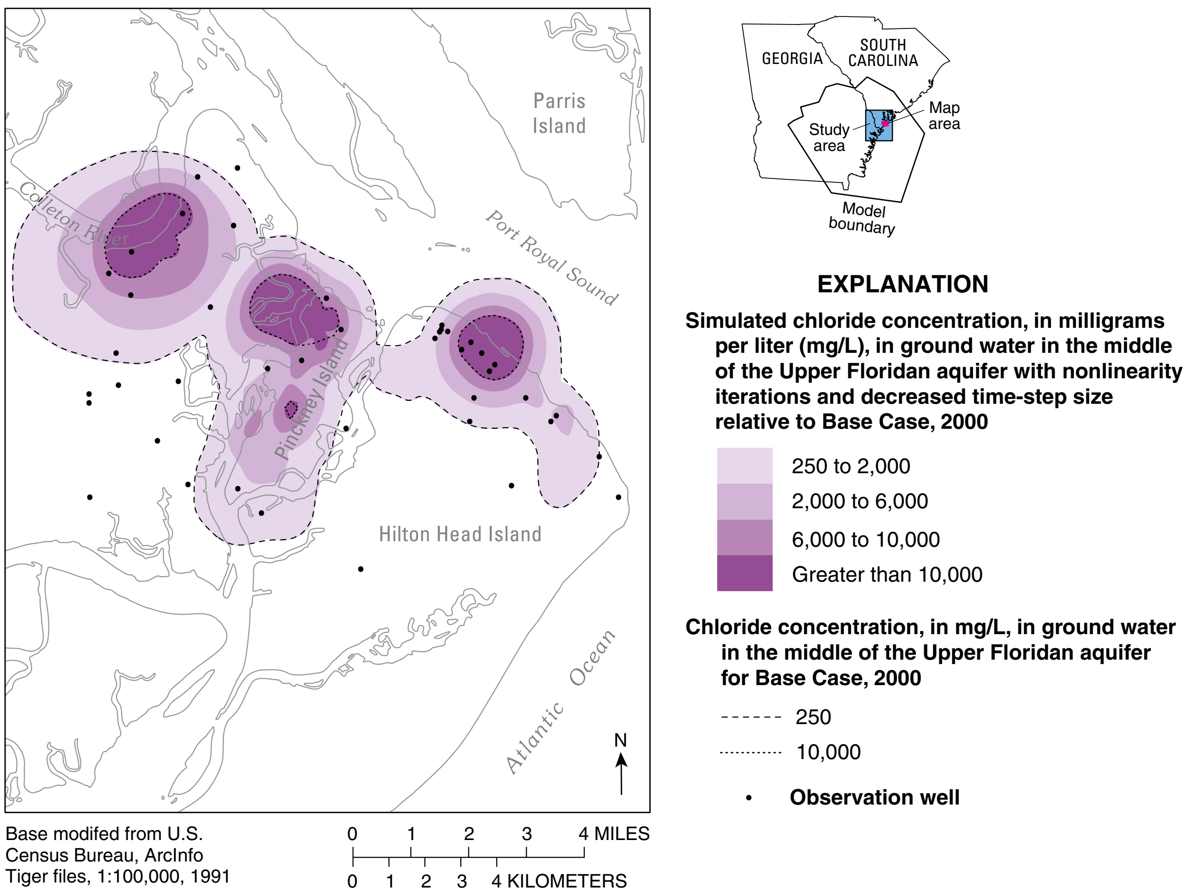

Figure 39. Simulated chloride concentration in ground water in the middle of the Upper Floridan aquifer in the Hilton Head Island, South Carolina, area with nonlinearity iterations and decreased time-step size, relative to the Base Case, 2000.

Matrix Solver Convergence Tolerances

The linear matrix equations that simulate the pressure and concentration fields were solved using iterative matrix solvers that are supplied with the SUTRA simulator. The conjugate gradient (CG) solver was used for the pressure problem, and the generalized minimum residual (GMRES) solver was used for the solute-transport (concentration) equation. Solutions to each equation were considered to be converged when the estimated errors were below the specified convergence tolerances. In the Base Case, matrix iteration tolerances of 10^{-12} and 10^{-10} were used for the pressure and concentration equations, respectively. To test the sensitivity of the results to changes in the degree of convergence of the matrix equation solutions, a model run was performed with the tolerances for the pressure and concentration equations reduced by an order of magnitude relative to the Base Case. This had an imperceptible effect on the simulated saltwater plumes.

Summary of Solute-Transport Model Sensitivity

Runs in which physical properties and boundary conditions were varied show that the solute-transport model is particularly sensitive to the value of the effective porosity, which is not well characterized in this flow system; decreasing porosity by a factor of two resulted in significantly higher chloride concentrations in the aquifer. Runs in which the spatial and temporal discretization, nonlinearity iterations, and matrix solver convergence tolerances were varied indicate that these numerical controls were chosen appropriately.

Variations on the Base Case

Three variations on the Base Case model were formulated to evaluate the effects of changing certain assumptions regarding the initial and boundary conditions. In each variation, the transport model was recalibrated so that the simulated chloride distribution in the year 2000 was similar to that obtained in the Base Case.

Variation 1: No Salt during 1965

In the Base Case simulation, a substantial quantity of saltwater enters the aquifer through the source areas prior to 1965, when heads in the aquifer are still above sea level near the source areas. During this period, driving forces for downward intrusion of saltwater are provided by parts of the source areas that simulate emergent wetlands in which the water table is specified to be above NAVD 88, and by the greater density of saltwater as compared with freshwater. Because of limitations in the accuracy and spatial resolution with which the emergent wetlands are represented in the model, and because accurate simulation of the onset of buoyancy-driven flow generally requires much finer discretization than is practical at the scale of the present model (Post and Kooi, 2003), the sensitivity of the model results to the extent of early (pre-1965) saltwater intrusion through the source areas was assessed.

This variation on the Base Case seeks to minimize the effects of early saltwater intrusion by starting the simulation from steady-state flow conditions for 1965 with no saltwater initially in the subsurface. The Base Case starts from analogous conditions for 1885. First, the model was run without recalibrating the physical properties. The simulated chloride concentration in the Upper Floridan aquifer decreased in the year 2000 relative to the Base Case (fig. 40A). The model was then recalibrated by adjusting the permeability of the upper confining units in the source areas until the plumes emanating from each of the three source areas (figs. 40B, C) were of similar extent to those obtained in the Base Case. The final upper confining unit permeabilities in the source areas were five times their respective Base Case values.

Variation 2: Predevelopment Plumes

Whereas the previous variation on the Base Case examined the effects of eliminating early intrusion of saltwater, this variation accentuates the effects of early saltwater intrusion by allowing saltwater to enter through the source areas for about 4,000 years for predevelopment conditions. The resulting flow and chloride distributions formed the initial conditions for a transient run that simulates pumping from 1885 onward, as in the Base Case.

The model run used to set up the initial conditions consisted of 75 time steps ranging from 1 to 20 years, for a total of 4,115 years of simulated time. The run was stopped at this point because the simulated time span was on the order of the time that the source areas have been inundated with seawater following the last glaciation (which reached its peak about 18,000 years ago), and because the evolution of the saltwater plumes emanating from the source areas had slowed considerably by this time. The resulting plumes are skewed to the north and east, reflecting the prevailing predevelopment hydraulic gradient (fig. 41A).

Following the predevelopment simulation, the pumping history was simulated from 1885 to 2000 (fig. 41B). The chloride distribution differs markedly from the Base Case distribution in the regions north and east of the source areas. Also, the bands of low concentration along the western and eastern shores of Hilton Head Island, which appear to a lesser degree in the initial conditions (fig. 41A) and do not seem to be directly connected with the three primary source areas, are not found in the Base Case. Along their southwestern margins, however, the evolution of the plumes emanating from the three primary source areas appears to be similar to the Base Case. For this reason, it was not considered necessary to recalibrate the permeabilities of the upper confining units in the source areas.

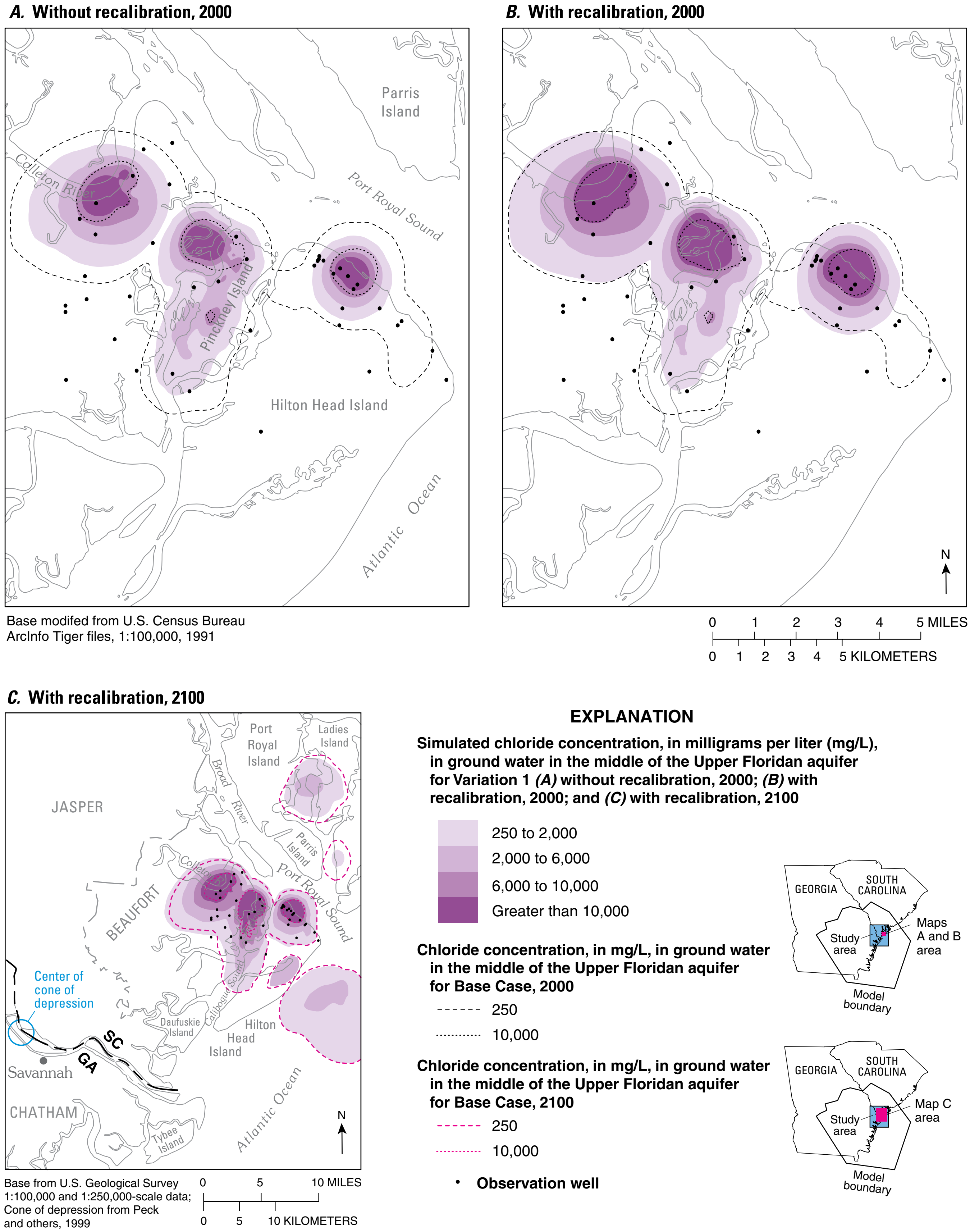

Figure 40. Simulated chloride concentration in ground water in the middle of the Upper Floridan aquifer in the Hilton Head Island, South Carolina, area for Variation 1 (*A*) without recalibration, 2000; (*B*) with recalibration, 2000; and (*C*) with recalibration, 2100.

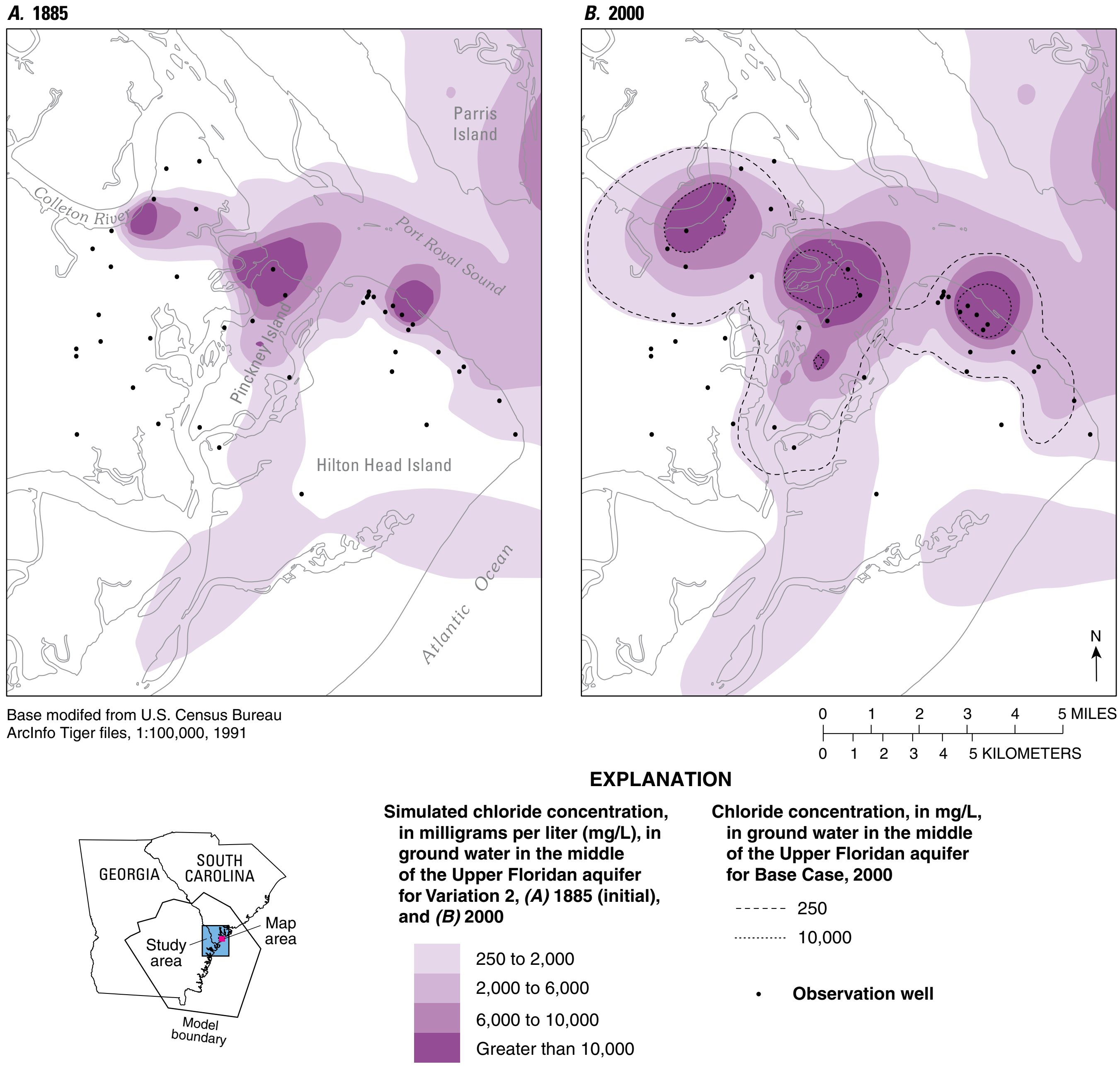

Figure 41. Simulated chloride concentration in ground water in the middle of the Upper Floridan aquifer in the Hilton Head Island, South Carolina, area for Variation 2, (*A*) 1885 (initial) and (*B*) 2000.

Variation 3: Model Truncated Below Upper Floridan Aquifer

In the Base Case simulation, substantial amounts of saltwater penetrate the units that underlie the Upper Floridan aquifer. Much of this penetration into the lower units may be caused by dispersion resulting from the large thickness and coarse vertical discretization assigned to the confining unit beneath the Upper Floridan aquifer near the source areas. Also, there is considerable uncertainty regarding the permeability and initial salinity of this confining unit and the Lower Floridan aquifer beneath it. If the permeabilities of these two units were substantially lower than assumed in the model, or if they contained relict saltwater at concentrations comparable to or greater than those found in the Upper Floridan aquifer (see “Salinity Distribution”), the movement of salt from the Upper Floridan aquifer to underlying units would be diminished or reversed relative to the rate estimated by the Base Case simulation.

To assess the effect of downward movement of salt from the Upper Floridan aquifer on the evolution of the chloride distribution within the aquifer, a variation on the Base Case was created in which the two units beneath the Upper Floridan aquifer were removed from the model, and the base of the Upper Floridan aquifer was made a no-flux boundary. In the process, the pumping associated with the Lower Floridan aquifer, which comprises a relatively small fraction of the total pumping, was also removed from the model. First, the model was run without recalibrating the physical properties. The simulated chloride concentration increased in the Upper Floridan aquifer in the year 2000, relative to the Base Case (fig. 42A). Then, the model was recalibrated by adjusting the permeabilities of the upper confining units in the source areas until the plumes emanating from each of the three source areas (fig. 42B) were of similar extent to those obtained in the Base Case. In this variation, chloride concentrations near the bottom of the aquifer were somewhat higher than those in the middle of the aquifer. Nevertheless, chloride concentrations in the middle of the aquifer were used as the basis for comparison with the Base Case. The final upper confining unit permeabilities in the Colleton River, Pinckney Island, and Hilton Head Island source areas were 0.2, 0.1, and 0.3 times their respective Base Case values.

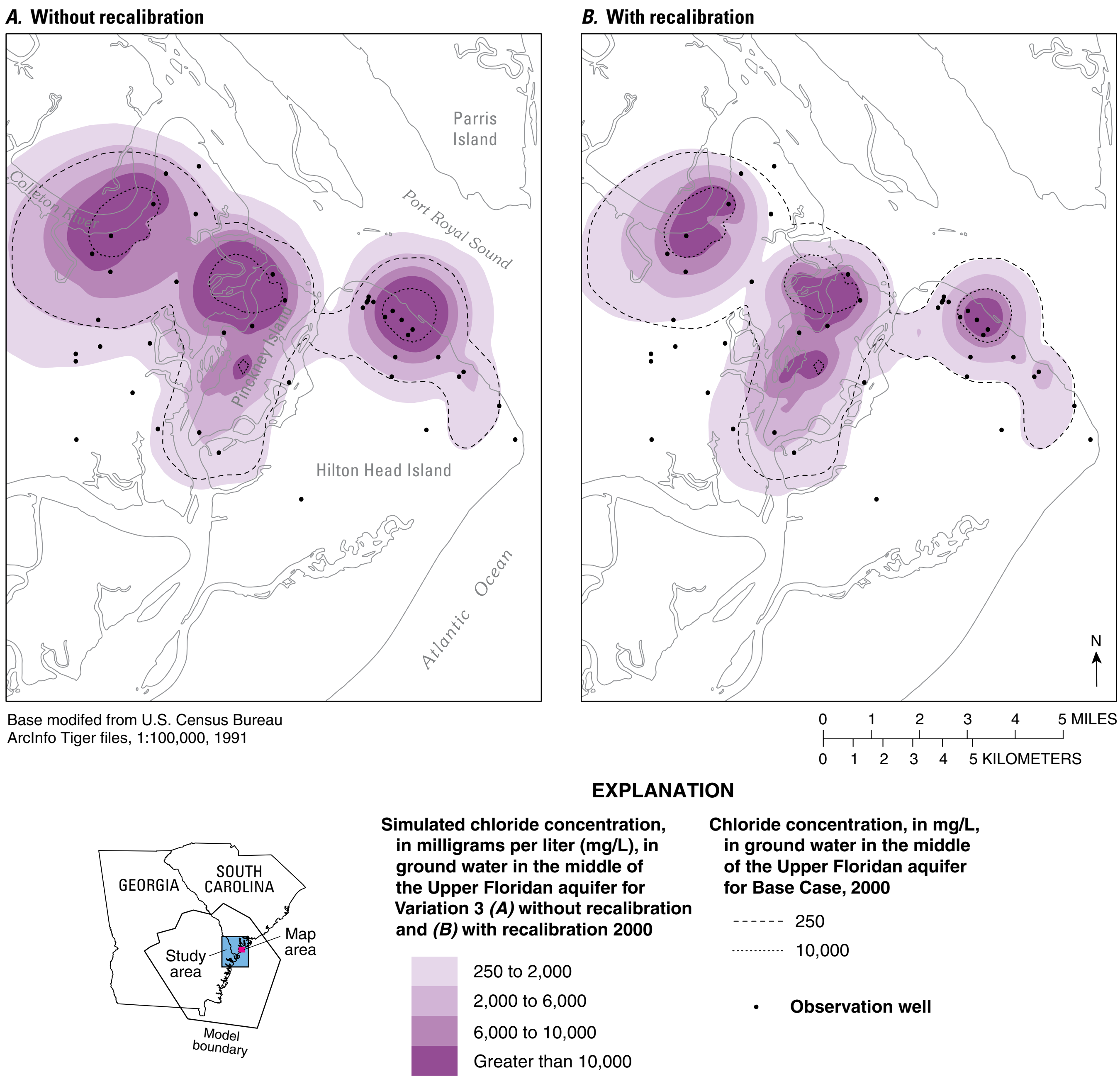

Figure 42. Simulated chloride concentration in ground water in the middle of the Upper Floridan aquifer in the Hilton Head Island, South Carolina, area for Variation 3 (*A*) without recalibration and (*B*) with recalibration, 2000.

Simulation of Future Saltwater Intrusion

For the Base Case and each of its three variations (see “Model Calibration to Observed Chloride [“Chloride Calibration”] and Transport Model Sensitivity”), the simulation was continued from 2000 to 2100 using 1-year time steps. Results are compared with the Base Case in the year 2100 to show the effects of the model variations on the predicted long-term development of the chloride distribution in the Upper Floridan aquifer. In addition, a 1,000-year transient simulation was performed using Variation 3 to estimate the effect of uncertainty in the effective porosity.

Base Case

The Base Case model predicts that, if 2000 pumping rates are maintained until 2100, the chloride plumes associated with the three source areas will continue to expand, especially southwestward, in the direction of the regional head gradient (fig. 43). At its closest point, the distance from the 250-mg/L chloride contour to the center of the Savannah cone of depression in ground-water head is about 19.8 mi during 2000 and 17.1 mi during 2100. For the 100-year interval simulated, this corresponds to an average rate of advance of the 250-mg/L chloride contour toward the center of the Savannah cone of depression of about 144 ft/yr.

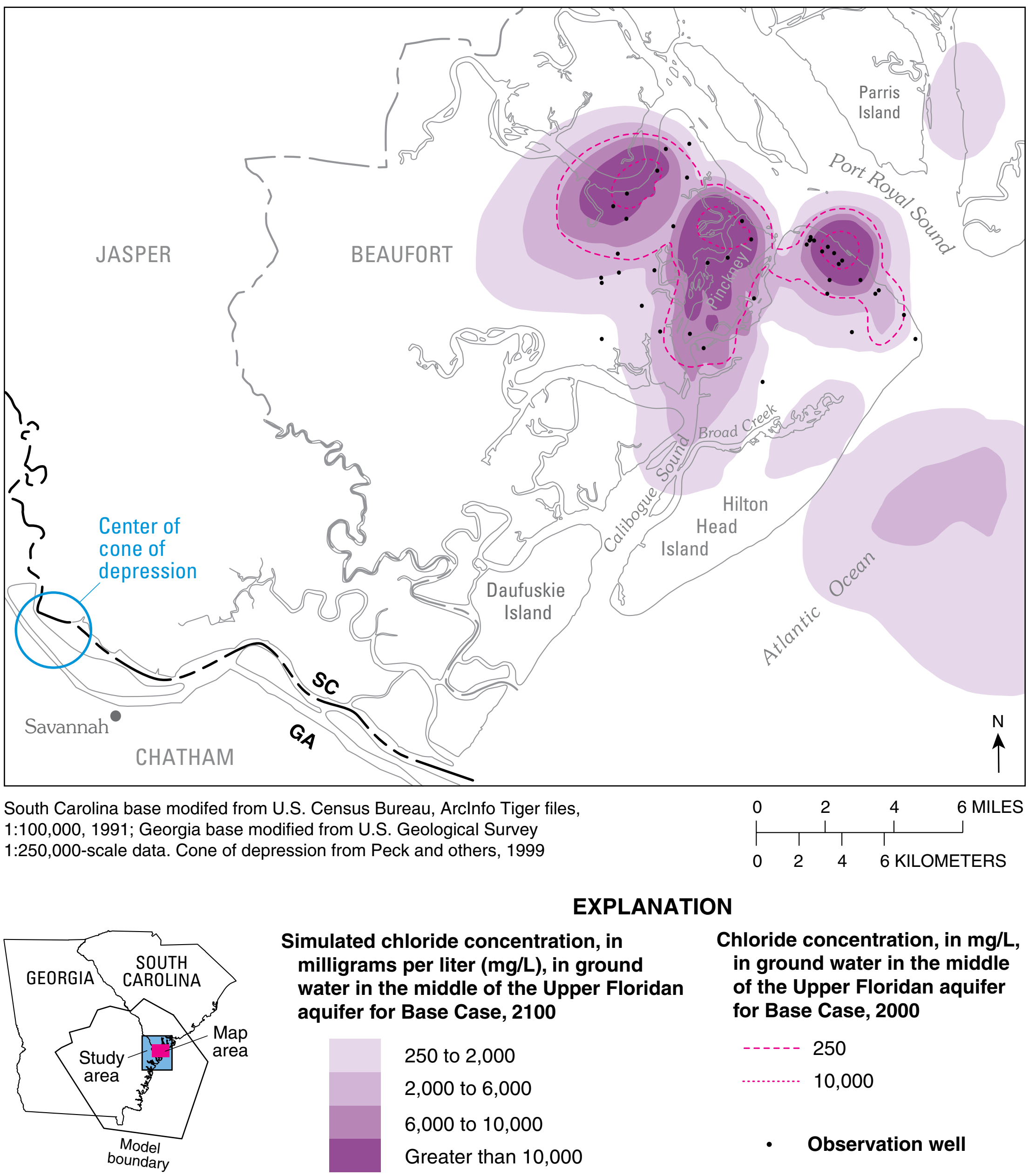

Figure 43. Simulated chloride concentration in ground water in the middle of the Upper Floridan aquifer in the Hilton Head Island, South Carolina, area for the Base Case during 2100.

Plumes also develop in areas other than the three calibrated source areas: beneath Broad Creek, offshore to the east of Hilton Head Island, and near Parris Island (fig 43). These plumes develop as saltwater leaks downward through areas where the confining unit is thin (fig. 4).

Variation 1: No Salt during 1965

For Variation 1, the simulated chloride distribution during 2100 shows only minor changes, relative to the Base Case (fig. 40C), indicating that the long-term behavior of the chloride distribution in the Upper Floridan aquifer is not very sensitive to the quantity of saltwater that intruded through the source areas prior to 1965 in the Base Case. This is reasonable in light of the fact that comparison of figures 28A and 28C indicates that most of the salt present in the aquifer during 2000 entered after 1965. At its closest point, the distance from the 250-mg/L chloride contour to the center of the Savannah cone of depression in ground-water head is approximately 16.8 mi during 2100. For the 100-year interval simulated, this corresponds to an average rate of advance of the 250-mg/L chloride contour toward the center of the Savannah cone of depression of about 160 ft/yr.

Variation 2: Predevelopment Plumes

For Variation 2, changes in the simulated chloride distribution to the south and west of the source areas during 2100, relative to the Base Case, are not large, with the exception of concentrations near the southern end of Hilton Head Island that are elevated relative to the Base Case (fig. 44).

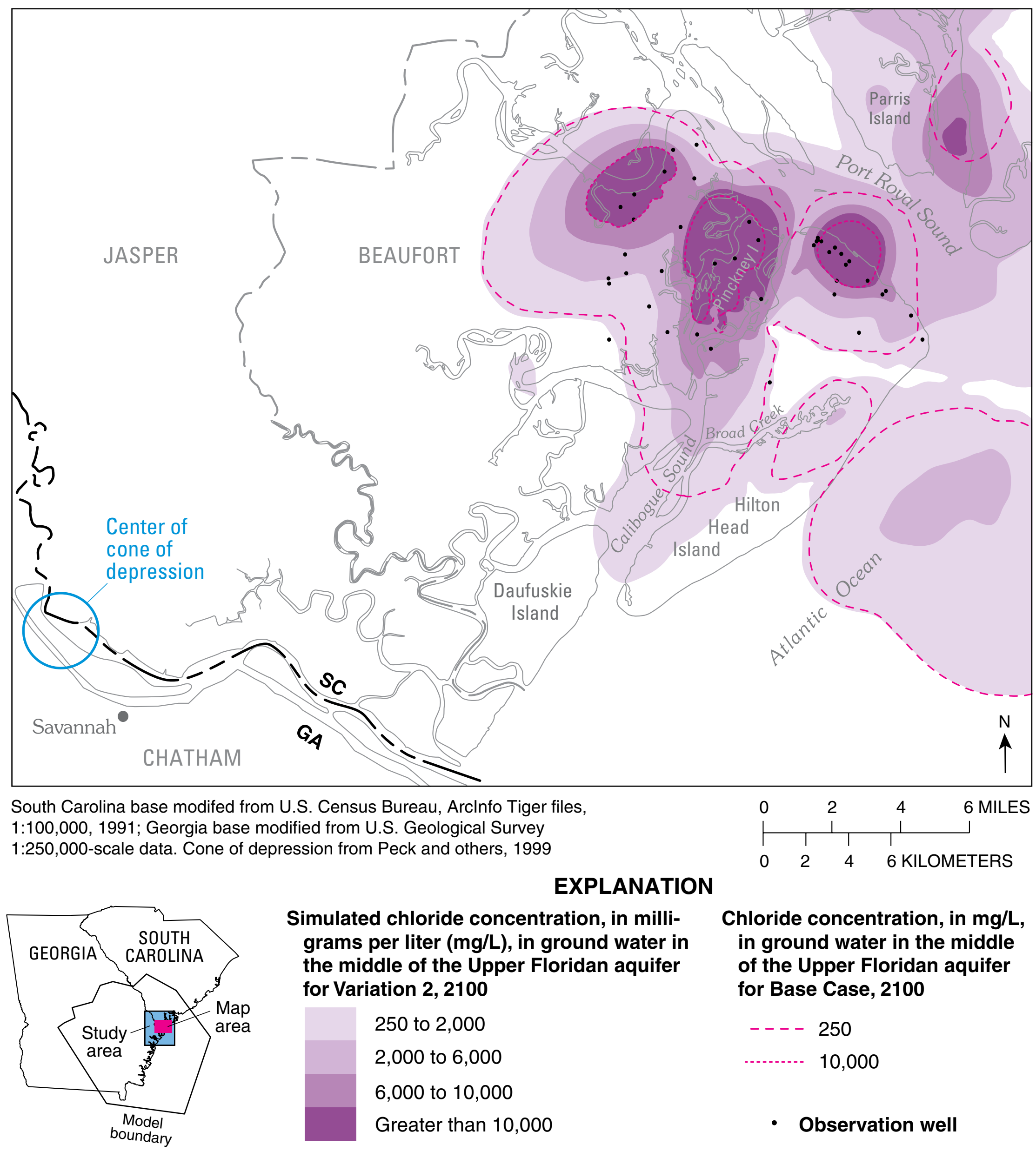

Figure 44. Simulated chloride concentration in ground water in the middle of the Upper Floridan aquifer in the Hilton Head Island, South Carolina, area for Variation 2 during 2100.

This lack of change indicates that the long-term behavior of the simulated saltwater plumes in the Upper Floridan aquifer is not very sensitive to the quantity of saltwater that may have entered the aquifer for predevelopment conditions. At its closest point, the distance from the 250-mg/L chloride contour to the center of the Savannah cone of depression in ground-water head is about 17.0 mi during 2100. For the 100-year interval simulated, this corresponds to an average rate of advance of the 250-mg/L chloride contour toward the center of the Savannah cone of depression of about 150 ft/yr.

Variation 3: Model Truncated Below Upper Floridan Aquifer

For Variation 3, the saltwater plumes for 2100 are somewhat expanded toward the southwest relative to the Base Case (fig. 45), especially in the plume emanating from the Pinckney Island source area, indicating that the long-term behavior of the chloride distribution in the Upper Floridan aquifer is moderately sensitive to the assumptions made regarding the properties of the units that underlie the Upper Floridan aquifer. At its closest point, the distance from the 250-mg/L chloride contour to the center of the Savannah potentiometric cone of depression is about 16 mi during 2100. For the 100-year interval simulated, this corresponds to an average rate of advance of the 250-mg/L chloride contour toward the center of the Savannah cone of depression of about 190 ft/yr.

Effect of Uncertainty in Porosity

In the Base Case simulation and each of the variations, porosities of 0.33 and 0.44 were assigned to the aquifers and confining units, respectively, based on median values of laboratory analyses of core samples (Smith, 1994). As discussed earlier, however, the porosity values used are at the high end of the expected range of effective porosities, and there is considerable uncertainty as to what values would best represent the transport characteristics of the subsurface in the study area. Lower effective porosity would result in faster solute transport. Therefore, it is possible that solute transport occurs faster than predicted by the model.

To assess the effect of uncertainty in the effective porosity, a simple test run was performed in which Variation 3, which resulted in the most rapid rate of plume advance of all the variations, was simulated from the year 2000 through the year 3000 using 2-year time steps. The 250-mg/L chloride contour reached the center of the Savannah potentiometric cone of depression in about the year 2800 (fig. 46); the exact time of arrival is difficult to estimate because the plumes approaching from the east merge with a small, local plume that develops at Savannah late in the simulation. Thus, with effective porosities of 0.33 and 0.44 in the aquifers and confining units, respectively, the model estimates that the plumes emanating from the primary source areas will take about 800 years (after 2000) to reach Savannah. It follows that, because the rate of solute transport is approximately inversely proportional to the porosity (appendix E), rerunning the simulation from the same initial condition during 2000 but with porosities set to one-eighth of their original values would cause the plumes to first reach Savannah in about 100 years.

The previous analysis involves extrapolation into the distant future and therefore is considered approximate. Furthermore, even if the model is accurate, the analysis provides only an upper bound on the effective porosity values that would be required to cause the 250-mg/L isochlor to reach Savannah in 100 years. This is because the analysis does not involve recalibration of the upper confining unit permeabilities in the source areas to match the observed chloride plumes during 2000–2004. Recalibration to compensate for lower porosity would result in lower permeabilities in the confining unit, which in turn would slow the rate at which saltwater enters the Upper Floridan aquifer after 2000, prolonging the time required for the 250-mg/L isochlor to reach Savannah. Thus, the analysis indicates that for the 250-mg/L isochlor to reach Savannah in 100 years or less, the effective porosity would have to be *more than* eight times lower than assumed or about 0.041 and 0.055 for the aquifers and confining units, respectively. Effective porosities of similar magnitude have been used to characterize transport in carbonate aquifers. For example, in the Biscayne aquifer in Florida, which is probably more highly karstified than the Upper Floridan aquifer in the study area, Renken and others (2005) estimated an effective porosity of 0.02–0.04, an order of magnitude smaller than had been previously assumed.

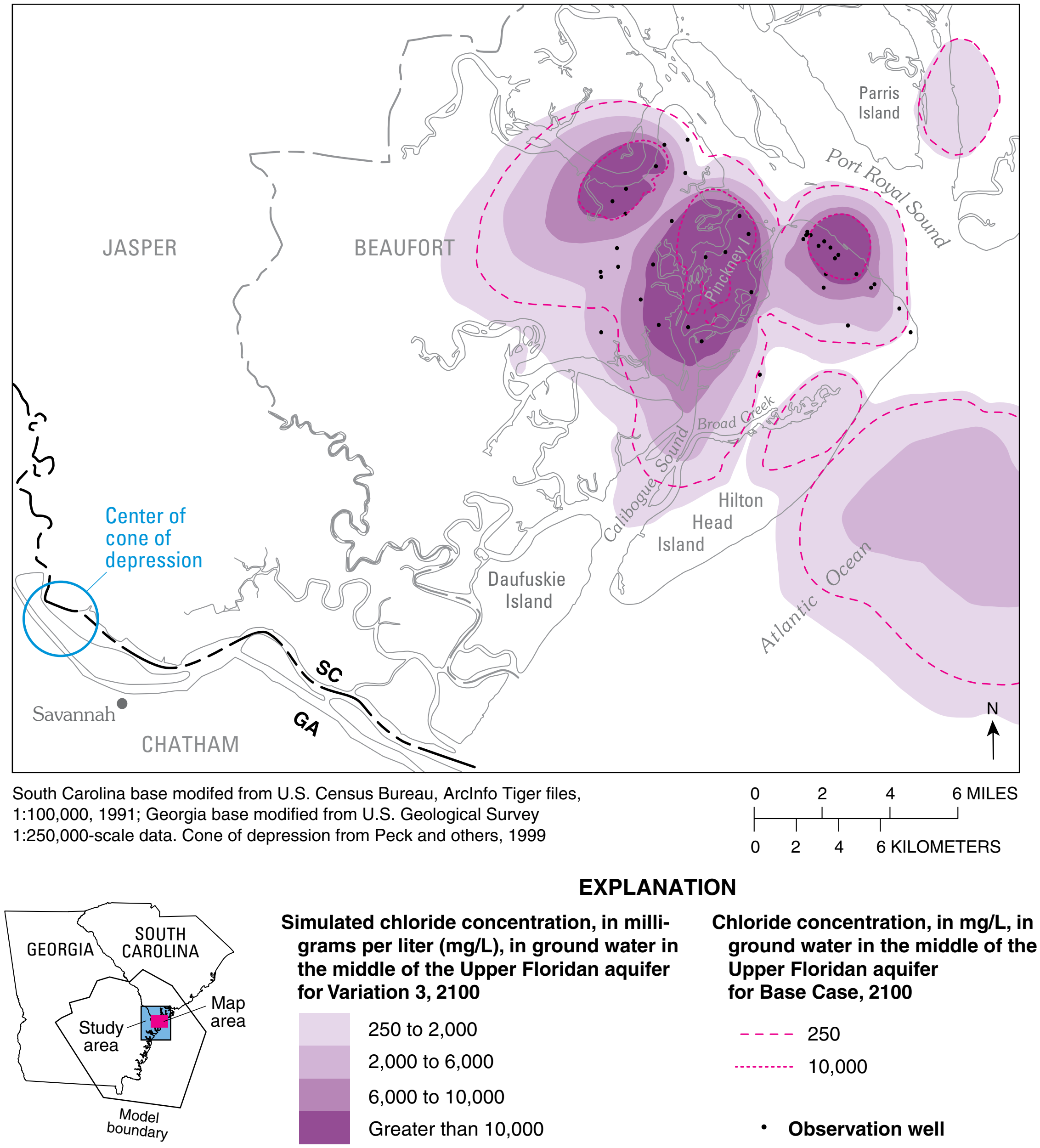

Figure 45. Simulated chloride concentration in ground water in the middle of the Upper Floridan aquifer in the Hilton Head Island, South Carolina, area for Variation 3 during 2100.

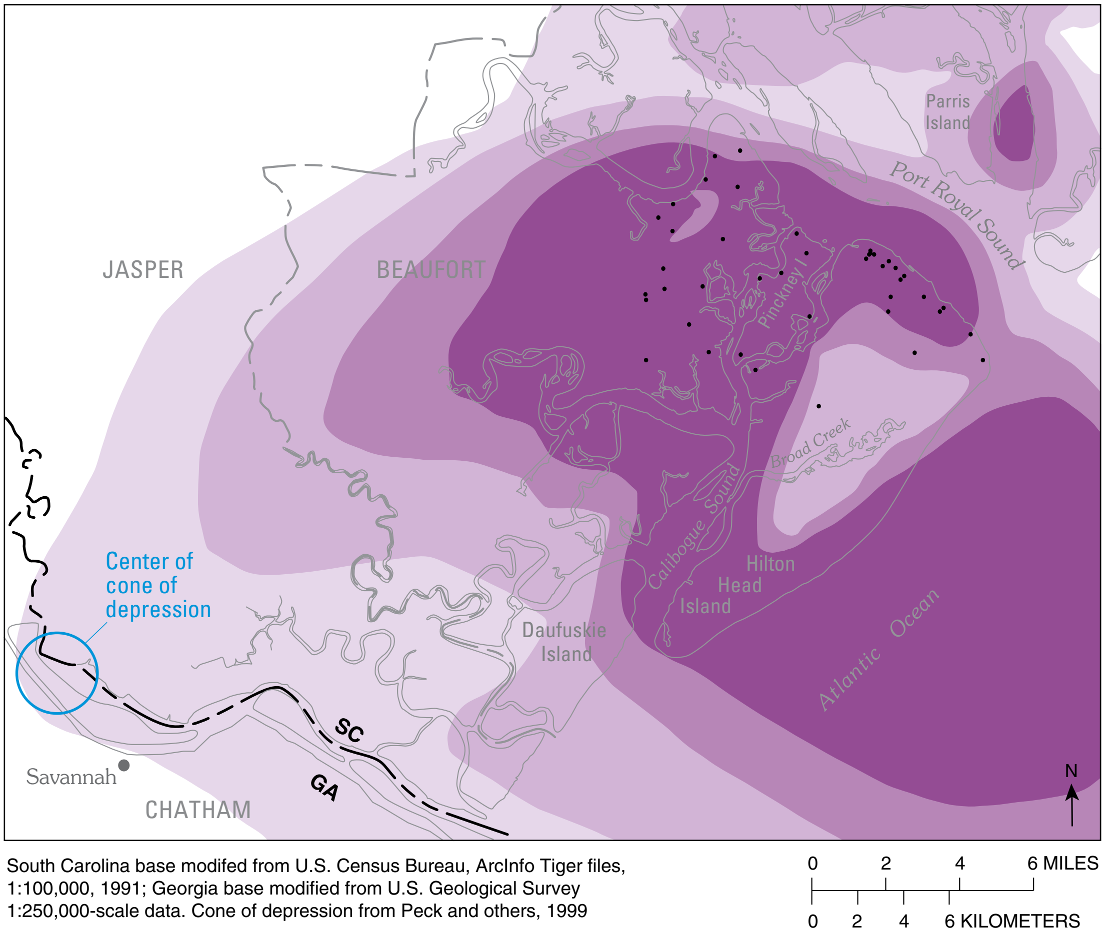

South Carolina base modifed from U.S. Census Bureau, ArcInfo Tiger files, 1:100,000, 1991; Georgia base modified from U.S. Geological Survey 1:250,000-scale data. Cone of depression from Peck and others, 1999

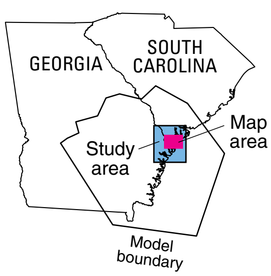

EXPLANATION

Simulated chloride concentration, in milligrams per liter, in ground water in the middle of the Upper Floridan aquifer for Variation 3, 2800

- 250 to 2,000
- 2,000 to 6,000
- 6,000 to 10,000
- Greater than 10,000

• **Observation well**

Figure 46. Simulated chloride concentration in ground water in the middle of the Upper Floridan aquifer in the Hilton Head Island, South Carolina, area for Variation 3 during 2800.

Model Limitations

Model results must be interpreted in light of uncertainties and approximations inherent in the formulation of the model. This section discusses the various potential sources of error in the model and their potential effects on the interpretation of results.

Field Data

Field observations provide a basis for the conceptual model of saltwater transport and influence the structure and properties of the mathematical model used to represent the physical system. Despite the care taken in making the field measurements, they are subject to some level of error and uncertainty, which ultimately propagates through to the model results.

The head calibration was performed based on September 1998 water-level measurements made in wells completed in the Upper Floridan aquifer. Water levels can be subject to fluctuations as nearby pumps turn on and off. Because the pumping history is not known in sufficient detail to simulate all of these fluctuations, the ability of the model to fit the water-level data is inherently limited. In addition, water levels are measured to within a limited accuracy, which is reflected in the linear confidence intervals computed for the parameters estimated during the calibration. Quantifiable components of water-level observation accuracy include land-surface altitude, accuracy of measurement, and temporal variations in water level. For the data used to calibrate this model, the largest source of error is likely temporal fluctuations. At well BFT-1810 on Hilton Head Island, water levels fluctuate up to 5 ft annually and up to 2–3 ft within a single month based on a 20-year continuous record (USGS Automated Data Processing System database).

Pumping uncertainty results from limited metering in the model area, errors in self-reporting by some users, errors in countywide estimates for several categories of water use, uncertainty from which aquifer wells are pumping, and errors in estimating an annual rate for a seasonally varying value (such as irrigation). Because the model is calibrated to simulate September 1998 conditions, and most of the pumping outside of Beaufort and Jasper Counties is based on estimated annual daily pumpage, inconsistencies in pumping rates and distribution may lead to errors in the calibration. For example, if the estimated pumping is significantly lower than actual pumping, then the calibrated permeability in an area may be too low, and the model may predict a greater response to future stresses than the system may actually demonstrate.

The solute-transport model was calibrated to chloride values inferred from specific conductance measurements made in wells open to the Upper Floridan aquifer. Inferring the chloride values introduces some error. More importantly, perhaps, is the uncertainty as to whether the measurements accurately represent conditions in the undisturbed flow system within the Upper Floridan aquifer. If any of the wells penetrate the underlying confining unit, some of the interpreted salinity may be due to connate saltwater beneath the Upper Floridan aquifer, although recently analyzed ground-water samples at some sites have a chemical signature indicating recent recharge from an overlying source area (Camille Ransom III, South Carolina Department of Health and Environmental Control, written commun., 2005). Also, vertical flow may be occurring within the boreholes, causing mixing of waters from different depths and making it difficult to interpret the measured vertical profiles of specific conductance.

Conceptual Model

Several lines of evidence support the conceptual model used as the basis for development of the solute-transport model described in this report: (1) the observed pattern of increasing chloride concentration in the Upper Floridan aquifer, which is indicative of the growth of three distinct "plumes" of saltwater; (2) seismic traces that indicate thinning of the upper confining units near two of the three apparent source areas (with no seismic data near the third apparent source area) (Foyle and others, 2001); and (3) ground-water dating that indicates that much of the saltwater intruded the Upper Floridan aquifer relatively recently (James E. Landmeyer, U.S. Geological Survey, written commun., 2005). The paucity and limited time frame of the specific conductance measurements, together with the difficulties associated with their interpretation as discussed earlier, however, leaves open the possibility that the conceptual model considered here is not the only one that might explain the observations. At the very least, it must be acknowledged that mechanisms not included in this model, such as upconing of connate saltwater from below the Upper Floridan aquifer, or transport of saltwater along preferential flowpaths in the subsurface, could be contributing to the observed pattern of saltwater intrusion.

Furthermore, this digital model was specifically designed to analyze solute transport in the Upper Floridan aquifer in areas where saltwater intrusion is known to occur—at the northern end of Hilton Head Island, at Pinckney Island, and near the Colleton River. Simulations in which present-day pumping rates are sustained into the future (to 2100) indicate other areas where the Upper Floridan confining unit is thin and saltwater may leak downward through the confining unit into the Upper Floridan aquifer, for example at Broad Creek and offshore of Hilton Head Island. Simulated rates of solute transport through the confining unit in these areas could be better constrained with specifically targeted monitoring efforts.

Geometry and Physical Properties

The model represents a simplification of the hydrogeologic structure of the subsurface. The model domain is divided into seven distinct hydrogeologic units, each of which is represented as being continuous and homogeneous across large areas. In the real system, however, these units, insofar as they can be distinguished, are commonly discontinuous and heterogeneous. In light of this simplification, the model represents a well-reasoned attempt to capture the main features that control the flow of ground water and the transport of solute.

The model presented in this report is a continuum model that does not explicitly represent processes that occur at very small spatial scales, such as within pores or individual fractures or solution channels. Rather, the model averages such effects across large volumes, as exemplified by the commonly used, though largely *ad hoc*, method of accounting for the spreading (dispersion) that occurs when solute is transported through the subsurface (Voss and Provost, 2002). Dispersivities, parameters that control the rates and directions of spreading, were adjusted, along with selected permeabilities, to fit the general trends in the observed chloride distribution. In predicting the future evolution of the chloride distribution, it was assumed that using this approach to account for dispersion, and these dispersivities in particular, would continue to represent the general spreading behavior of the solute. Furthermore, dispersivities were linked to element size, which generally increases with distance from the source areas. Thus, as the simulated solute moves away from the source areas, it is subject to greater dispersion. Qualitatively, this agrees with what is typically observed in the field: as a rule, dispersion increases as the transport reach increases. The dispersivity values that best characterize the future spreading of the solute plumes, however, are subject to considerable uncertainty.

Effective porosity of the porous medium is a major control on the rate at which solute is transported, but effective porosity is poorly characterized in this flow system. The porosity values used in this model are derived from laboratory measurements performed on core samples and, therefore, are probably at the high end of the expected range of effective porosity (see “Hydraulic and Transport Properties”). Lower values of porosity would result in faster simulated transport. The effect of porosity on the long-term evolution of the saltwater plumes was estimated using a simple approach that did not involve recalibrating the transport model (see “Effect of Uncertainty in Porosity”).

Calibration of the model to match observed water-level data resulted in revised values of permeability in the Upper Floridan aquifer and overlying confining units within the study area. As discussed earlier, uncertainty in the water-level measurements contributes to the uncertainty in the estimated permeabilities. Furthermore, although the permeabilities were estimated with the help of an optimization algorithm, the configuration of the discrete permeability zones and the final permeability values reflect informed judgments made by the modeler and may not represent the only way to fit the observed data.

The transport model was calibrated to chloride values inferred from field measurements of specific conductance. To make the chloride calibration tractable, it was performed independently of the calibration to head data, despite the fact that the presence of the highly permeable source areas perturbs the local head distribution. The locations, sizes, and upper confining unit permeabilities of the three principal source areas were adjusted by trial and error until a reasonable fit to the general trends in the evolution of the observed chloride distribution was obtained. During calibration, the evolution of the simulated chloride plumes was found to be sensitive to the locations of the source areas. The particular source areas that resulted from the calibration, however, do not necessarily represent the only way to fit the observed data.

Saline ground water typically contains a variety of chemical species whose concentrations can vary spatially and with time. In the model, dissolved solids are represented as a single species (solute) whose concentration affects the density of the fluid linearly. Seawater is assigned a total dissolved solids concentration of 0.0357 kg-solute/kg-fluid. Chloride values are inferred from the simulation results by assuming that the dissolved solids in seawater are 55.04 percent by weight chloride, and that the chloride mass fraction in the ground water varies in direct proportion to the mass fraction of total dissolved solids. This simplification is not expected to be a major source of error in the present application.

Boundary and Initial Conditions

Drawdown as a result of pumping provides much of the driving force for ground-water flow in the study area. Although the pumping history incorporated into the model is believed to take into account most of the major pumping centers, parts of the history have been constructed on the basis of incomplete records, as described earlier in this report. While it is difficult to assess the effect of uncertainties in the pumping history on the simulation results, simulated heads reasonably fit the observed heads.

Variations in water-table altitude provide another driving force for ground-water flow. In the model, the water-table altitude was set as a function of land-surface altitude, and the pressure at the top surface of the model was set to reflect the position of the water table below land surface, as described earlier in this report. The water-table altitude, and hence the pressure boundary condition at the top surface of the model, remained constant with time throughout each simulation. It is likely, therefore, that the water-table altitude assumed in the model was higher than the actual water-table altitude that existed during the drought conditions of September 1998, the period to which heads were calibrated. Nevertheless, this approximation was considered to be acceptable because the aquifer of greatest interest and the one subject to most of the pumping, the Upper Floridan aquifer, is assumed to be confined on a regional scale, and because the source areas are within and adjacent to surface-water bodies that would prevent substantial drawdown in the surficial aquifer.

Within areas of saltwater intrusion, density gradients resulting from differences in concentration also can drive flow. In the model, all potential sources of saltwater were assumed to be at seawater concentration. As was discussed earlier in this report, typical concentrations of saltwater entering at the source areas may range from 82 to 99 percent of seawater concentration. Sensitivity analysis shows that the simulated concentration in the Upper Floridan aquifer was somewhat lower when the source concentration was reduced to 80 percent of seawater concentration; the concentration in the aquifer varied nearly linearly with the source concentration. Sensitivity analysis, however, also indicates that a moderate increase in the upper confining unit permeabilities in the source areas (on the order of a factor of two) would likely compensate for the decrease in solute concentration. Results of runs performed with variations on the Base Case indicate that such moderate permeability adjustments in the source areas would probably not have a large effect on the predicted long-term evolution of the chloride distribution.

Parts of the source areas represent emergent wetlands, where the water table is above sea level, creating a driving force for downward flow of saltwater into the Upper Floridan aquifer even when heads in the aquifer are above sea level. It is assumed that the water-table altitude does not change with time; processes such as tides, which occur on time scales that are very short compared with the duration of the simulation, are not modeled. Furthermore, because the extent of the wetlands was determined from a land-use map (accessed November 4, 2004, at *http://landcover.usgs.gov/natllandcover.asp*), and because of the limited resolution of the surface-altitude data, parts of the modeled wetlands within the Colleton River source area include land-surface altitudes as high as about 9 ft above NAVD 88 and, therefore, are unlikely to be substantial sources of saltwater intrusion in the real flow system. To some extent, such errors in the downward driving force are mitigated by the calibration of the upper confining unit permeabilities in the source areas to match the observed evolution of the chloride distribution in the Upper Floridan aquifer; the effects of overestimated driving forces are compensated for by adjusting permeabilities to get the appropriate rate of saltwater inflow.

The outer boundaries of the model are sufficiently far from the study area that any reasonable modifications to the no-flux and specified-pressure conditions imposed there would be unlikely to have a great effect on the flow field within the study area. The model is likely not very sensitive to the no-flux condition imposed along the bottom surface of the model, which is the base of the Lower Floridan aquifer, because the Lower Floridan aquifer is confined above, and its extent and permeability distribution in the study area are uncertain.

Because reliable measurements of the specific conductance in the Upper Floridan aquifer in the study area prior to 1997 are lacking, there is considerable uncertainty regarding the initial conditions for the solute-transport simulations. Results indicate, however, that the simulated long-term behavior of the chloride distribution is only moderately sensitive to the initial conditions used (see Variations 1 and 2). Imposing a no-flux boundary at the base of the Upper Floridan aquifer, to prevent loss of salt to the poorly characterized underlying units, has a greater effect on the long-term chloride distribution (see Variation 3).

Numerical Approximation and Solution

The size of the finite elements, the duration of the time steps, the use of nonlinearity iterations, and the tolerances used for solution of the pressure and concentration matrix problems all can have an important influence on modeling results. Sensitivity analysis indicates that these aspects of the model were chosen appropriately for this study.

Future Predictions of Chloride Distribution

For the Base Case and each of its three variations, development of the chloride distribution was simulated through the year 2100, and the simulation of Variation 3 was continued through the year 3000 to assess the effect of uncertainty in the effective porosity. Results of these long-term simulations must be interpreted with caution because they are predicated on a particular conceptual model that may not be unique in its ability to describe the field observations and may not take into account all sources of future saltwater intrusion. In addition, these results are based on an assumed future pumping distribution and fixed water-table altitude and sea level. Finally, these results reflect, in large part, the transport of solute through areas of the model that have not been explicitly calibrated for solute transport.

Discussion

A numerical model will produce the most accurate results in areas in which the physical system is accurately characterized, and for the period for which the model is calibrated. With increasing spatial distance and time from the best characterized calibration conditions, model accuracy will decrease. Despite the limitations of the model, one of its most appropriate uses is as a tool to better understand the flow system and guide efforts to refine the conceptual model, which will result in a more accurate and reliable numerical model.

Of the three conceptual models for saltwater intrusion described previously (see “Possible Mechanisms of Saltwater Intrusion”), only the first is specifically addressed herein. This conceptual model is supported by several lines of evidence (see “Conceptual Model”), and results in a numerical model that reproduces the general trends in the observed evolution of the chloride distribution in the Upper Floridan aquifer in the area of interest. There is not enough known, however, about the hydraulic properties and salinities of the confining units overlying and underlying the Upper Floridan aquifer to quantify the possible contributions of alternative saltwater intrusion mechanisms. The conceptual model, and hence the numerical model, could be improved with estimates of field-scale permeability and salinity data for these confining units.

For the conceptual model that is tested in this study, there is considerable uncertainty in the distribution of physical properties and local boundary conditions that affect the model construction. Model results indicate that transport of saltwater in the Upper Floridan aquifer is very sensitive to effective porosity. Although there are porosity data, these data are limited to core samples and, therefore, are not likely representative of field-scale effective porosity. A better estimate of effective porosity in the Upper Floridan aquifer in the putative plume areas, through continued observation of the salinity distribution and model refinement could improve estimates of saltwater transport rates.

There is uncertainty in the lateral extent of the permeable zones in the Upper Floridan aquifer and the degree of hydraulic connection between the Upper Floridan aquifer in the Savannah, Ga., and the lower Beaufort County, S.C., areas. Conceptually, the permeable zones have been considered laterally continuous layers, which is a more applicable interpretation for siliciclastic-dominated units than carbonate units, such as the Upper Floridan aquifer. It is possible that a re-examination of available field data would elucidate the lateral extent and hydraulic connection between permeable zones.

In addition, it is uncertain to what extent the Upper Floridan aquifer is being recharged in the study area. The northern end of Hilton Head Island may be a recharge zone, but development since the 1960s may have altered the recharge rates (James E. Landmeyer, U.S. Geological Survey, oral commun., 2005). A specific estimate of recharge rates and distribution would improve the simulation of flow direction and magnitude, as well as ground-water salinity.

Continued monitoring of specific conductance, and even expansion of the network of monitoring sites within the Upper Floridan aquifer, will allow a more complete interpretation of the three-dimensional distribution of salinity in the study area, and how it is evolving with time. Expansion of the monitoring network to include the adjacent confining units may help to refine the conceptual model for saltwater intrusion in the study area.

Summary and Conclusions

In recent years, contamination of water-supply wells by saltwater near Hilton Head Island, S.C., has been a growing concern. For predevelopment conditions, the area was a regional discharge area; however, with the onset of major ground-water withdrawals in the Savannah, Ga., area and on Hilton Head Island, S.C., heads in the Upper Floridan aquifer near Hilton Head Island have declined below sea level. Numerical modeling was used to evaluate the feasibility of a conceptual model in which saline surface water intrudes vertically into the Upper Floridan aquifer through three localized “source areas,” which represent areas where the confining units overlying the aquifer are thin or absent.

The numerical model is based on a recent regional-scale ground-water flow model. The regional-scale model was refined and recalibrated in the study area to make the model suitable for local-scale solute-transport simulations.

The results of the numerical model lend support to the proposed conceptual model, because the numerical model is able to simulate plumes of saltwater in the Upper Floridan aquifer whose areal extent and range of concentrations is comparable to those observed in the study area. The model results do not preclude the possibility that other mechanisms, such as upward flow from below the Upper Floridan aquifer, may contribute to the observed saltwater contamination.

The accuracy with which the model can be expected to reproduce field measurements and predict the future evolution of the chloride distribution in the Upper Floridan aquifer in the study area is limited by the paucity of the measurements and difficulties associated with interpreting the data; the extent to which the boundary conditions, initial conditions, and hydrogeologic properties of the subsurface are characterized; and the appropriateness of the conceptual model for saltwater intrusion. Taking these factors into account, it is reasonable to interpret the model results presented herein as reproducing the general trends in the observed chloride distribution in the Upper Floridan aquifer and providing an indication of how that distribution might evolve for a conservative pumping scenario (year-2000 pumping levels maintained after 2000), given that the saltwater is assumed to intrude vertically through three localized source areas near Hilton Head Island, S.C.

The model was tested for sensitivity to various parameters and boundary and initial conditions. The evolution of the chloride plumes was found to be particularly sensitive to the effective porosity and assumptions made regarding the properties of the units underlying the Upper Floridan aquifer. Decreasing porosity by a factor of two and modifying the model to prevent downward movement of salt from the Upper Floridan aquifer to underlying units each resulted in substantially higher chloride concentrations in the aquifer.

Results show that if present-day (year-2000) pumping conditions are maintained, plumes of saltwater in the Upper Floridan aquifer will continue to expand and move toward Savannah and across Hilton Head Island. The rate of movement of the 250-mg/L (milligram per liter) isochlor and the volume of the Upper Floridan aquifer affected by saltwater intrusion is a function of the effective porosity and hydraulic conductivity of the Upper Floridan aquifer and the overlying confining units. Effective porosity is the fraction of pore space through which most of the solute transport takes place. This model parameter is poorly characterized in the study area and may be as much as an order of magnitude lower than the porosity on which these simulations are based. With the porosities of the aquifers and confining units set to 0.33 and 0.45 (the porosity of the Upper Floridan aquifer and the overlying confining units, respectively, estimated from core samples in the laboratory), the model predicts that the rate of advance of the 250-mg/L isochlor toward Savannah is between 144 and 190 feet per year between 2000 and 2100. In this case, the simulated 250-mg/L isochlor reaches the pumping center at Savannah in 800 years, and the plumes extend beneath large areas of Hilton Head Island during that time.

Lower effective porosities than those used in this model would result in an increased rate of transport, with earlier arrival of the 250-mg/L isochlor at Savannah and more rapid intrusion of saltwater into the Upper Floridan aquifer beneath Hilton Head Island. All other model input being the same, the rate of transport increases by the same factor by which porosity decreases. A change in porosity, however, would require recalibration of the model by adjusting the confining unit permeabilities in the source areas. As a result, the simulated rate of transport would increase by less than the factor by which porosity is decreased. For example, a tenfold decrease in porosity, which may be a lower limit, would result in a less than tenfold increase in the simulated rate of transport. Better understanding of current transport patterns in both the confining unit and the Upper Floridan aquifer would provide insight into the values of effective porosity and hydraulic conductivity in these formations and would allow better estimates of long-term transport times to be computed.

There is considerable uncertainty regarding the amount of salt that was present in the Upper Floridan aquifer prior to pumping. Model results indicate that plumes may have occurred along the northern shore of Hilton Head Island before development began in the mid-1960s, and lesser amounts of intrusion may have already occurred prior to the onset of pumping in 1885. Sensitivity analysis, however, shows that the long-term evolution of the plumes is not very sensitive to the amount of salt initially present in the aquifer. Moreover, results show that pumping causes accelerated expansion of the plumes towards Savannah and across Hilton Head Island.

The model provides quantitative estimates of the future evolution of the observed chloride plumes in the Upper Floridan aquifer. Uncertainty in field data, the conceptual model, the physical properties and representation of the hydrogeologic framework, and boundary and initial conditions limit the accuracy and applicability of the model, particularly in simulations projected far into the future. The model could be improved by incorporating measurements of permeability and salinity in the confining units adjacent to the Upper Floridan aquifer, better estimates of effective porosity, better characterization of the lateral extent and hydraulic connection between permeable zones, estimates of recharge at the northern end of Hilton Head Island, and data from continued monitoring of specific conductance for an expanded network of wells.

Selected References

Back, William, Hanshaw, B.B., and Rubin, Meyer, 1970, Carbon-14 ages related to occurrence of salt water, *in* Proceedings of the American Society of Civil Engineers: Journal of the Hydraulics Division, v. 96, p. 2325–2336.

Brooks, Rebekah, Clarke, J.S., and Faye, R.E., 1985, Hydrogeology of the Gordon aquifer system of east-central Georgia: Georgia Geologic Survey Information Circular 75, 41 p.

Burt, R.A., Belval, D.L., Crouch, Michael, and Hughes, W.B., 1987, Geohydrologic data from Port Royal Sound, Beaufort County, South Carolina: U.S. Geological Survey Open-File Report 86-497, 67 p.

Bush, P.W., 1988, Simulation of saltwater movement in the Floridan aquifer system, Hilton Head Island, South Carolina: U.S. Geological Survey Water-Supply Paper 2331, 19 p.

Bush, P.W., and Johnston, R.H., 1988, Ground-water hydraulics, regional flow, and ground-water development of the Floridan aquifer system in Florida, and in parts of Georgia, South Carolina, and Alabama: U.S. Geological Survey Professional Paper 1403-C, 80 p.

Charm, W.B., Nesteroff, W.D., and Valdes, Sylvia, 1969, Detailed stratigraphic description of the JOIDES cores on the continental margin off Florida: U.S. Geological Survey Professional Paper 581-D, 13 p.

Childress, J.M., and Ransom, Camille, III, 2005, Hydrogeologic data summary for the Upper Floridan aquifer, southern Beaufort County, South Carolina: South Carolina Department of Health and Environmental Control Bureau of Water Technical Report 015-05, 10 p.

Clarke, J.S., 1987, Potentiometric surface of the Upper Floridan aquifer in Georgia, 1985, and water-level trends, 1980–85: Georgia Geologic Survey Hydrologic Atlas 16, 1 sheet, scale 1:1,000,000.

Clarke, J.S., 2003, The surficial and Brunswick aquifer systems—alternative ground-water resources for coastal Georgia, in Proceedings of the 2003 Georgia Water Resources Conference, April 23–24, 2003, The University of Georgia, Hatcher, K.J., ed., Institute of Ecology, The University of Georgia, Athens, Georgia, CD–ROM, on the World Wide Web at *http://ga.water.usgs.gov/pubs/other/gwrc2003/pdf/Clarke-GWRC2003.pdf*

Clarke, J.S., Hacke, C.M., and Peck, M.F., 1990, Geology and ground-water resources of the coastal area of Georgia: Georgia Geologic Survey Bulletin 113, 106 p.

Clarke, J.S., and Krause, R.E., 2000, Design, revision, and application of ground-water flow models for simulation of selected water-management scenarios in the coastal area of Georgia and adjacent parts of South Carolina and Florida: U.S. Geological Survey Water-Resources Investigations Report 00-4084, 93 p.

Clarke, J.S., Leeth, D.C., Taylor-Harris, DáVette, Painter, J.A., and Labowski, J.L., 2004, Summary of hydraulic properties of the Floridan aquifer system in coastal Georgia and adjacent parts of South Carolina and Florida: U.S. Geological Survey Scientific Investigations Report 2004-5264, 52 p.

Clarke, J.S., and West, C.T., 1998, Simulation of ground-water flow and stream-aquifer relations in the vicinity of the Savannah River Site, Georgia and South Carolina, predevelopment through 1992: U.S. Geological Survey Water-Resources Investigations Report 98-4062, 134 p.

Counts, H.B., and Donsky, Ellis, 1963, Salt-water encroachment, geology, and ground-water resources of the Savannah area, Georgia and South Carolina: U.S. Geological Survey Water-Supply Paper 1611, 100 p.

Counts, H.B., and Krause, R.E., 1976, Digital model analysis of the principal artesian aquifer, Savannah, Georgia area: U.S. Geological Survey Water-Resources Investigations 76-133, 4 sheets.

Dale, M.W., 1995, Evaluation of the shallow aquifer, Hilton Head Island, South Carolina: South Carolina Department of Natural Resources Water Resources Division Open-File Report 2, 84 p.

Falls, W.F., Harrelson, L.G., Conlon, K.J., and Petkewich, M.D., 2005a, Hydrogeology, water quality, and water-supply potential of the Lower Floridan aquifer, coastal Georgia 1999–2002: U.S. Geological Survey Scientific Investigations Report 2005-5124, 98 p.

Falls, W.F., Ransom, Camille, III, Landmeyer, J.E., Reuber, E.J., and Edwards, L.E., 2005b, Hydrogeology, water quality, and saltwater intrusion of the Upper Floridan aquifer in the offshore area near Hilton Head Island, South Carolina, and Tybee Island, Georgia, 1999–2002: U.S. Geological Survey Scientific Investigations Report 2005-5134, 48 p.

Fanning, J.L., 2003, Water use in Georgia by county for 2000 and water-use trends for 1980–2000: Georgia Geologic Survey Information Circular 106, 176 p.

Foyle, A.M., Henry, V.J., and Alexander, C.R., 2001, The Miocene aquitard and the Floridan aquifer of the Georgia/South Carolina coast: Geophysical mapping of potential seawater intrusion sites: Georgia Geologic Survey Bulletin 132, 61 p.

Freeze, R.A., and Cherry, J.A., 1979, Groundwater: Englewood Cliffs, N.J., Prentice-Hall, Inc., 604 p.

Furlow, J.W., 1969, Stratigraphy and economic geology of the eastern Chatham County phosphate deposit: Georgia Department of Mines, Mining, and Geology Bulletin 82, 40 p.

Garza, Reggina, and Krause, R.E., 1996, Water-supply potential of major streams and the Upper Floridan aquifer in the vicinity of Savannah, Georgia: U.S. Geological Survey Water-Supply Paper 2411, 37 p.

Gawne, C.E., and Park, A.D., 1992, Water-supply potential of the middle Floridan aquifer in southern Beaufort County, South Carolina (report to the Town of Hilton Head Island Water Commission): South Carolina Water Resources Commission, Beaufort, South Carolina, 34 p.

Golder Associates, Inc., 2003, Reports on the Brunswick aquifer studies for Bryan, Chatham, Effingham, and Glynn Counties, and Ebenezer Bend: Georgia Geologic Survey Report CD-4, CD–ROM.

Gregg, D.O., and Zimmerman, E.A., 1974, Geologic and hydrologic control of chloride contamination in aquifers at Brunswick, Glynn County, Georgia: U.S. Geological Survey Water-Supply Paper 2029-D, 44 p.

Harbaugh, A.W., Banta, E.R., Hill, M.C., and McDonald, M.G., 2000, MODFLOW-2000, The U.S. Geological Survey modular ground-water model—User guide to modularization concepts and the ground-water flow process: U.S. Geological Survey Open-File Report 00-92, 121 p.

Harrelson, L.G., and Falls, W.F., 2003, Hydrogeology and aquifer tests in the Floridan aquifer system at selected sites, coastal Georgia, 2001, *in* Leeth, D.C., Clarke, J.S., Craigg, S.D., and Wipperfurth, C.J., 2003, Ground-water conditions and studies in Georgia, 2001: U.S. Geological Survey Water-Resources Investigations Report 03-4032, p. 82–87.

Hathaway, J.C., Schlee, J.S., Poag, W.C., Valentine, P.C., Weed, E.G.A., Bothner, M.H., Kohout, F.A., Manheim, F.T., Schoen, Robert, Miller, R.E., and Schultz, D.M., 1981, Summary of the 1976 Atlantic margin coring project of the U.S. Geological Survey: U.S. Geological Survey Open-File Report 81-0239, 217 p.

Hayes, L.R., 1979, The ground-water resources of Beaufort, Colleton, Hampton, and Jasper Counties, South Carolina: South Carolina Water Resources Commission Report Number 9, 91 p.

Hill, M.C., 1998, Methods and guidelines for effective model calibration: U.S. Geological Survey Water-Resources Investigations Report 98-4005, 90 p.

Hughes, W.B., Crouch, M.S., and Park, A.D., 1989, Hydrogeology and saltwater contamination of the Floridan aquifer in Beaufort and Jasper Counties, South Carolina: South Carolina Water Resources Commission Report Number 158, 52 p.

Johnston, R.H., Bush, P.W., Krause, R.E., Miller, J.A., and Sprinkle, C.L., 1982, Summary of hydrologic testing in Tertiary limestone aquifer, Tenneco offshore exploratory well—Atlantic OCS, Lease-Block 427 (Jacksonville NW 17–5): U.S. Geological Survey Water-Supply Paper 2180, 15 p.

Johnston, R.H., Healy, H.G., and Hayes, L.R., 1981, Potentiometric surface of the Tertiary limestone aquifer system, southeastern United States, May 1980: U.S. Geological Survey Open-File Report 81-486, 1 sheet, scale .

Johnston, R.H., Krause, R.E., Meyer, F.W., Ryder, P.D., Tibbals, C.H., and Hunn, J.D., 1980, Estimated potentiometric surface for the Tertiary limestone aquifer system, southeastern United States, prior to development: U.S. Geological Survey Open-File Report 80-406, 1 sheet.

Kellam, M.F., and Gorday, L.L., 1990, Hydrogeology of the Gulf Trough–Apalachicola Embayment area, Georgia: Georgia Geologic Survey Bulletin 94, 73 p.

Krause, R.E., 1982, Digital model evaluation of the predevelopment flow system of the Tertiary limestone aquifer, southeast Georgia, northeast Florida, and southern South Carolina: U.S. Geological Survey Water-Resources Investigations Report 82-173, 27 p.

Krause, R.E., and Clarke, J.S., 2001, Coastal ground water at risk—Saltwater contamination at Brunswick, Georgia, and Hilton Head Island, South Carolina: U.S. Geological Survey Water-Resources Investigations Report 01-4107, poster.

Krause, R.E., and Randolph, R.B., 1989, Hydrology of the Floridan aquifer system in southeast Georgia and adjacent parts of Florida and South Carolina: U.S. Geological Survey Professional Paper 1403-D, 65 p.

Landmeyer, J.E., and Belval, D.L., 1996, Water-chemistry and chloride fluctuation in the Upper Floridan aquifer in the Port Royal Sound area, South Carolina, 1917–93: U.S. Geological Survey Water-Resources Investigations Report 96-4102, 106 p.

McCollum, M.J., and Counts, H.B., 1964, Relation of saltwater encroachment to the major aquifer zones, Savannah area, Georgia and South Carolina: U.S. Geological Survey Water-Supply Paper 1613-D, 26 p.

Miller, J.A., 1986, Hydrogeologic framework of the Floridan aquifer system in Florida and in parts of Georgia, Alabama, and South Carolina: U.S. Geological Survey Professional Paper 1403-B, 91 p.

National Oceanic and Atmospheric Administration, 2002, Monthly station normals of temperature, precipitation, and heating and cooling degree days 1971–2000: Asheville, N.C., no. 81, 28 p.

Newcome, Roy, Jr., 2000, Results of pumping tests in the Coastal Plain of South Carolina: South Carolina Department of Natural Resources Water-Resources Open-File Report 5, 26 p.

Payne, D.F., Abu Rumman, Malek, and Clarke, J.S., 2005, Simulation of ground-water flow in coastal Georgia and adjacent parts of South Carolina and Florida—Predevelopment, 1980, and 2000: U.S. Geological Survey Scientific Investigations Report 2005-5089, 91 p., on the World Wide Web at *http://pubs.usgs.gov/sir/2005/5089/*

Peck, M.F., Clarke, J.S., Ransom, Camille, III, and Richards, C.J., 1999, Potentiometric surface of the Upper Floridan aquifer in Georgia and adjacent parts of Alabama, Florida, and South Carolina, May 1998, and water-level trends in Georgia, 1990–98: Georgia Geologic Survey Hydrologic Atlas 22, 1 sheet, scale 1:100,000, 1977–81.

Peck, M.F., and McFadden, K.W., 2004, Potentiometric surface of the Upper Floridan aquifer in the Coastal area of Georgia, September 2000: U.S. Geological Survey Open-File Report 2004-1030, on the World Wide Web at *http://pubs.usgs.gov/of/2004/1030/*

Peck, M.F., and Payne, D.F., 2003, Development of an estimated water-table map for coastal Georgia and adjacent parts of Florida and South Carolina, *in* Proceedings of the 2003 Georgia Water Resources Conference, April 23–24, 2003, The University of Georgia, Hatcher, K.J., ed., Institute of Ecology, The University of Georgia, Athens, Georgia, CD–ROM, on the World Wide Web at *http://ga.water.usgs.gov/pubs/other/gwrc2003/pdf/Peck_Payne-GWRC2003.pdf*

Poeter, E.P., and Hill, M.C., 1998, Documentation of UCODE, a computer code for universal inverse modeling: U.S. Geological Survey Water-Resources Investigations Report 98-4080, 116 p.

Post, V.E.A., and Kooi, Henk, 2003, Rates of salinization by free convection in high-permeability sediments: Insights from numerical modeling and application to the Dutch coastal area: Hydrogeology Journal, v. 11, no. 5, p. 549–559.

Priest, Sherlyn, 2004, Stream-aquifer relations in the coastal area of Georgia and adjacent parts of Florida and South Carolina: Georgia Geologic Survey Information Circular 108, 40 p.

Randolph, R.B., and Krause, R.E., 1984, Analysis of the effects of the proposed pumping from the principal artesian aquifer, Savannah, Georgia area: U.S. Geological Survey Water-Resources Investigations Report 84-4064, 26 p.

Randolph, R.B., Pernik, Maribeth, and Garza, Reggina, 1991, Water-supply potential of the Floridan aquifer system in the coastal area of Georgia—A digital model approach: Georgia Geologic Survey Bulletin 116, 30 p.

Ransom, Camille, III, and White, J.I., 1999, Potentiometric surface of the Floridan aquifer system in southern South Carolina: South Carolina Department of Health and Environmental Control, Bureau of Water Publication No. 02B-99, 1 sheet.

Reilly, T.E., and Goodman, A.S., 1985, Quantitative analysis of saltwater-freshwater relationships in ground-water systems—A historical perspective: Journal of Hydrology, v. 80, Issues 1–2, p. 125–160.

Renken, R.A., Cunningham, K.J., Zygnerski, M.R., Wacker, M.A., Shapiro, A.M., Harvey, R.W., Metge, D.W., Osborn, C.L., and Ryan, J.N., 2005, Assessing the vulnerability of a municipal well field to contamination in a karst aquifer: Environmental and Engineering Geoscience, v. 11, no. 4, p. 319–331.

Scholle, P.A., 1979, Geological studies of the COST GE-1 well, United States south Atlantic outer continental shelf area: U.S. Geological Survey Circular 800, 114 p.

Seager, M.K., 1989, A SLAP for the Masses, *in* Parallel Supercomputing: Methods, Algorithms, and Applications, Carey, G.F., ed.: Wiley, p. 135–155.

Smith, B.S., 1988, Ground-water flow and saltwater encroachment in the Upper Floridan aquifer, Beaufort and Jasper Counties, South Carolina: U.S. Geological Survey Water-Resources Investigations Report 87-4285, 61 p.

Smith, B.S., 1994, Saltwater movement in the Upper Floridan aquifer beneath Port Royal Sound, South Carolina: U.S. Geological Survey Water-Supply Paper 2421, 40 p.

Smith, H.C., and McIntosh, M.G., 2005, Assessment of saltwater migration through the Upper Floridan confining unit in the Savannah Harbor area, *in* Proceedings of the 2005 Georgia Water Resources Conference, April 25–27, 2005, The University of Georgia, Hatcher, K.J., ed., Institute of Ecology, the University of Georgia, Athens, Georgia, CD–ROM.

Sprinkle, C.L., 1982, Chloride concentration in water from the upper permeable zone of the Tertiary limestone aquifer system, southeastern United States: U.S. Geological Survey Water-Resources Investigations Open-File Report 81-1103, 1 sheet.

Steele, W.M., and McDowell, R.J., 1998, Permeable thickness of the Miocene upper and lower Brunswick aquifers, coastal area, Georgia: Georgia Geologic Survey Information Circular 103, 34 p.

Taylor, D.A., Painter, J.A., and Payne, D.F., 2003, Development of a water-use database for use in coastal region ground-water models, Georgia, South Carolina, and Florida, 1980–2000, *in* Proceedings of the 2003 Georgia Water Resources Conference, April 23–24, 2003, The University of Georgia, Hatcher, K.J., ed., Institute of Ecology, The University of Georgia, Athens, Georgia, CD–ROM, on the World Wide Web at *http://ga.water.usgs.gov/pubs/other/gwrc2003/pdf/Taylor-GWRC2003.pdf*

U.S. Environmental Protection Agency, 1994, Drinking water regulations and health advisories: EPA report no. 822-R-94-001.

Van Dolah, R.F., Jutte, P.C., Riekerk, G.H.M., Levisen, M.V., Crowe, S.E., Lewitus, A.J, Chestnut, D.E., McDermott, W., Beardon, D., and Fulton, M.H., 2004, The condition of South Carolina's estuarine and coastal habitats during 2001–2002: South Carolina Marine Resources Division Technical Report No. 100, 70 p.

Van Dolah, R.F., Jutte, P.C., Riekerk, G.H.M., Levisen, M.V., Zimmerman, L.E., Jones, J.D., Lewitus, A.J., Chestnut, D.E., McDermott, W., Bearden, D., Scott, G.I., and Fulton, M.H., 2002, The condition of South Carolina's estuarine and coastal habitats during 1999–2000: South Carolina Marine Resources Division, Technical Report No. 90, 132 p.

von Arx, W.S., 1962, An Introduction to Physical Oceanography: Reading, Massachusetts, Addison-Wesley Publishing Company, 422 p.

Voss, C.I., 1984, A finite-element simulation model for saturated-unsaturated, fluid-density-dependent ground-water flow with energy transport or chemically-reactive single-species solute transport: U.S. Geological Survey Water Resources Investigations Report 84-4369, 409 p.

Voss, C.I., and Provost, A.M., 2003 Version of 2002, SUTRA: A model for saturated-unsaturated, variable-density ground-water flow with solute or energy transport: U.S. Geological Survey Water-Resources Investigations Report 02-4231, 250 p.

Waddell, M.G., 1989, A geological approach to modeling the movement of ground water in the shallow aquifer in the vicinity of the Burton recharge area, Beaufort, South Carolina: Phase I: South Carolina Water Resources Commission Report Number 165, 23 p.

Wait, R.L., 1965, Geology and occurrence of fresh and brackish ground water in Glynn County, Georgia: U.S. Geological Survey Water-Supply Paper 1613-E, 94 p.

Wait, R.L., and Davis, M.E., 1986, Configuration and hydrology of the pre-Cretaceous rocks underlying the Southeastern Coastal Plain aquifer system: U.S. Geological Survey Water-Resources Investigations Report 86-4010, 1 sheet, scale 1:2,000,000.

Wait, R.L., and Gregg, D.O., 1973, Hydrology and chloride contamination of the principal artesian aquifer in Glynn County, Georgia: Georgia Department of Natural Resources Hydrologic Report, 93 p.

Warren, M.A., 1944, Artesian water in southeastern Georgia: Georgia Geologic Survey Bulletin No. 49, 140 p.

Weems, R.E., and Edwards, L.E., 2001, Geology of Oligocene, Miocene, and younger deposits in the coastal area of Georgia: Georgia Geologic Survey Bulletin 131, 124 p.

Winston, R.B., 2000, Graphical user interface for MODFLOW, Version 4: U.S. Geological Survey Open-File Report 00-315, 27 p.

Winston, R.B., and Voss, C.I., 2004, SutraGUI—A graphical user interface for SUTRA, a model for ground-water flow with solute or energy transport: U.S. Geological Survey Open-File Report 03-285, 114 p.

Appendix A. Modifications to SUTRA Code

The ground-water flow and solute-transport simulation code used in this work is based on the U.S. Geological Survey code SUTRA Version 2D3D.1. The main changes made in adapting the code for this work are described below. A complete listing of the FORTRAN source code is archived in accordance with U.S. Geological Survey policy and is available upon request.

Irregular Three-Dimensional Meshes

SUTRA Version 2D3D.1 requires that three-dimensional (3D) finite-element meshes be logically rectangular (Voss and Provost, 2002). To allow the use of irregular 3D meshes, the code was modified as follows.

Subroutine PTRSET, which sets up arrays needed to specify the structure of the matrices in the global flow and transport matrix equations, was modified to use SLAP column format instead of SLAP triad format (Seager, 1989). In SLAP column format, non-zero matrix entries are stored for each column of the matrix, with the diagonal entry listed first, followed by the remaining non-zero entries in the column. Arrays PMAT and UMAT hold the flow and transport matrices, respectively, with columns stored consecutively. Array IA holds the row index of each non-zero entry. Array JA holds the offset into the PMAT, UMAT, and IA arrays for the beginning of each column. The modified version of PTRSET sets up IA and JA by first creating a linked list of neighboring nodes for each node in the mesh, then transferring the linked lists to arrays IA and JA in SLAP column format. The coding for the subroutine is listed in its entirety below:

```
      SUBROUTINE PTRSET()
      USE ALLARR
      USE PTRDEF
      IMPLICIT DOUBLE PRECISION (A-H,O-Z)
      COMMON /DIMS/ NN,NE,NIN,NBI,NCBI,NB,NBHALF,NPBC,NUBC,
     1   NSOP,NSOU,NBCN
      COMMON /DIMX/ NWI,NWF,NWL,NELT,NNNX,NEX,N48
      COMMON /DIMX2/ NELTA, NNVEC, NDIMIA, NDIMJA
C
C.....SET UP POINTER ARRAYS IA AND JA THAT SPECIFY MATRIX STRUCTURE IN
C        "SLAP COLUMN" FORMAT.  FOR EACH NODE, CONSTRUCT A LINKED LIST
C        OF NEIGHBORING NODES.  HLIST(K) POINTS TO THE HEAD OF THE LIST
C        FOR NODE K.  THEN, TRANSFER THE LISTS TO ARRAYS IA AND JA.
C
C.....ALLOCATE HLIST AND LLIST, AND INITIALIZE LIST LENGTHS TO ZERO.
      ALLOCATE(LLIST(NN), HLIST(NN))
      DO 490 I=1,NN
         ALLOCATE(HLIST(I)%PL)
         LLIST(I) = 0
  490 CONTINUE
C.....LOOP THROUGH INCIDENCE LIST.
      DO 500 L=1,NE
      DO 500 IL=1,N48
         IC = IN((L-1)*N48+IL)
      DO 500 JL=1,N48
         JC = IN((L-1)*N48+JL)
C.......INSERT NEIGHBOR JC IN LIST FOR NODE IC IN ASCENDING ORDER.
C           (IF DUPLICATE OR SELF-NEIGHBOR, SKIP IT.)
         IF (JC.EQ.IC) THEN
C..........SKIP SELF-NEIGHBOR.
            GOTO 500
         ELSE IF (LLIST(IC).EQ.0) THEN
C..........PLACE FIRST LIST ENTRY AT HEAD.
            HLIST(IC)%PL%NODNUM = JC
            GOTO 498
         ELSE
C..........INSERT INTO LIST, OR SKIP IF DUPLICATE.
```

```
            ALLOCATE(DENTPV)
            DENTPI => DENTPV
            DENTPV%NENT => HLIST(IC)%PL
            DO 495 K=1,LLIST(IC)
               DENT => DENTPV%NENT
               IF (JC.EQ.DENT%NODNUM) THEN
                  DEALLOCATE(DENTPI)
                  GOTO 500
               ELSE IF (JC.LT.DENT%NODNUM) THEN
                  ALLOCATE(DENTNW)
                  DENTNW%NODNUM = JC
                  DENTNW%NENT => DENT
                  IF (K.EQ.1) THEN
                     HLIST(IC)%PL => DENTNW
                  ELSE
                     DENTPV%NENT => DENTNW
                  END IF
                  DEALLOCATE(DENTPI)
                  GOTO 498
               END IF
               DENTPV => DENT
  495       CONTINUE
C...........APPEND TO TAIL.
            ALLOCATE(DENTNW)
            DENTNW%NODNUM = JC
            DENT%NENT => DENTNW
            DEALLOCATE(DENTPI)
         END IF
  498    LLIST(IC) = LLIST(IC) + 1
  500 CONTINUE
C.....COMPUTE THE ARRAY DIMENSION NELT AND ALLOCATE ARRAY IA.
      NELT = 0
      DO 600 I=1,NN
  600    NELT = NELT + LLIST(I) + 1
      NDIMIA = NELT
      ALLOCATE(IA(NDIMIA))
C.....TRANSFER THE LINKED LISTS TO ARRAYS IA AND JA IN SLAP COLUMN
C        FORMAT.  DEALLOCATE POINTERS AS THEY ARE TRANSFERRED.
      JASTRT = 1
      DO 660 I=1,NN
         JA(I) = JASTRT
         IA(JASTRT) = I
         DENT => HLIST(I)%PL
         DO 650 K=1,LLIST(I)
            IA(JASTRT + K) = DENT%NODNUM
            DENTPV => DENT
            DENT => DENT%NENT
            DEALLOCATE(DENTPV)
  650    CONTINUE
         JASTRT = JASTRT + LLIST(I) + 1
  660 CONTINUE
      JA(NN + 1) = NELT + 1
      DEALLOCATE(HLIST, LLIST)
C
      RETURN
      END
```

The call to subroutine PTRSET was moved from subroutine SUTRA to the main program, SUTRA_MAIN, to facilitate allocation of the required pointers. Declarations of allocatable arrays were moved from the main program, SUTRA_MAIN, to a new module, ALLARR:

```
      MODULE ALLARR
      IMPLICIT NONE
      LOGICAL ALLO1, ALLO2, ALLO3
      DOUBLE PRECISION, DIMENSION(:,:), ALLOCATABLE ::
     1   PMAT, UMAT
      DOUBLE PRECISION, DIMENSION(:), ALLOCATABLE ::
     1   PITER, UITER, PM1, DPDTITR, UM1, UM2, PVEL, SL, SR, X, Y, Z,
     2   VOL, POR, CS1, CS2, CS3, SW, DSWDP, RHO, SOP, QIN, UIN, QUIN,
     3   QINITR, RCIT, RCITM1
      DOUBLE PRECISION, DIMENSION(:), ALLOCATABLE ::
     1   PVEC, UVEC
      DOUBLE PRECISION, DIMENSION(:), ALLOCATABLE ::
     1   ALMAX, ALMIN, ATMAX, ATMIN, VMAG, VANG1,
     2   PERMXX, PERMXY, PERMYX, PERMYY, PANGL1
      DOUBLE PRECISION, DIMENSION(:), ALLOCATABLE ::
     1   ALMID, ATMID, VANG2, PERMXZ, PERMYZ,
     2   PERMZX, PERMZY, PERMZZ, PANGL2, PANGL3
      DOUBLE PRECISION, DIMENSION(:), ALLOCATABLE ::
     1   PBC, UBC, QPLITR
      DOUBLE PRECISION, DIMENSION(:,:), ALLOCATABLE ::
     1   GXSI, GETA, GZET
      DOUBLE PRECISION, DIMENSION(:), ALLOCATABLE ::
     1   FWK ,B
      INTEGER, DIMENSION(:), ALLOCATABLE ::
     1   IN, IQSOP, IQSOU, IPBC, IUBC,
     2   IOBS, NREG, LREG, IWK, IA, JA
      TYPE OBSDAT
         CHARACTER*40 :: NAME
         INTEGER :: L
         DOUBLE PRECISION :: X, Y, Z
         DOUBLE PRECISION :: XSI, ETA, ZET
      END TYPE OBSDAT
      TYPE (OBSDAT), DIMENSION (:), ALLOCATABLE :: OBSPTS
C
      END MODULE ALLARR
```

The definition of TYPE OBSDAT is discussed below in the context of generalized observation points.

Module PTRDEF was created to define pointers and arrays needed by PTRSET:

```
      MODULE PTRDEF
      IMPLICIT NONE
C.....DEFINE DERIVED TYPE LNKLST (LINKED LIST) WITH TWO COMPONENTS:
C        NODNUM (NODE NUMBER) AND NENT (POINTER TO NEXT ENTRY).
      TYPE LNKLST
         INTEGER :: NODNUM
         TYPE (LNKLST), POINTER :: NENT
      END TYPE LNKLST
C.....DECLARE DENT, DENTPV, DENTPI, AND DENTNW AS GENERAL-PURPOSE
C        POINTERS OF TYPE LNKLST.
      TYPE (LNKLST), POINTER :: DENT, DENTPV, DENTPI, DENTNW
C.....DEFINE DERIVED TYPE IPOINT WITH ONE COMPONENT: A POINTER, PL,
C        OF TYPE LNKLST.
      TYPE IPOINT
```

```
            TYPE (LNKLST), POINTER :: PL
         END TYPE IPOINT
      C.....DECLARE HLIST, AN ARRAY OF POINTERS THAT WILL POINT TO THE HEAD
      C        OF THE LINKED LIST OF NEIGHBORS FOR EACH NODE.
         TYPE (IPOINT), ALLOCATABLE :: HLIST(:)
      C.....DECLARE ARRAY LLIST.
         INTEGER, DIMENSION(:), ALLOCATABLE :: LLIST
      C
         END MODULE PTRDEF
```

Subroutine TRISET and all calls to TRISET were rendered obsolete and were removed.

Subroutine BC, which incorporates specified-pressure and specified-temperature or specified-concentration boundary conditions into the global flow and transport matrix equations, was modified to store and access matrices in SLAP column format instead of SLAP triad format. Variable IMID, which, for a given row, represents the index of the diagonal entry in the matrix array, is set to the row number, I, when the DIRECT solver is being used, and to JA(I) when an iterative solver is being used:

```
      IF (KSOLVP.EQ.0) THEN
         IMID = I
      ELSE
         IMID = JA(I)
      END IF
```

The changes to subroutine BC described previously necessitated passing array JA through the argument list. Changes made to subroutine NODAL, which adds cell-wise terms and fluid mass and solute mass or energy source terms to the global flow and transport matrix equations, were exactly analogous to those made to subroutine BC.

Subroutine GLOTRI, which assembles results of element-wise integrations into the global flow and transport matrix equations, was renamed GLOCOL and modified to store and access matrices in SLAP column format instead of SLAP triad format. IB is the current row number, JB is the current column number, and M is the index of entry (IB, JB) in the matrix array. Within the p-matrix assembly loop, the calculation of JB and M was modified to read as follows:

```
      JB = IN(JJ)
      MBEG = JA(JB)
      MEND = JA(JB + 1) - 1
      DO 9060 MM=MBEG,MEND
         IF (IB.EQ.IA(MM)) THEN
            M = MM
            GOTO 9100
         END IF
 9060 CONTINUE
```

The DO loop above searches the section of array IA that contains the row indices for non-zero matrix entries in column JB. When a match is found with the current row number, IB, M is set to the corresponding index in the matrix array. An exactly analogous change was made in the U-matrix assembly loop. The changes to subroutine GLOTRI described above necessitated passing arrays IA and JA through the argument list. All references to arrays NBI27 and MIOFF, which were used to store information related to logically rectangular meshes, were removed from the code.

Generalized Observation Points

SUTRA Version 2D3D.1 outputs computed pressure, concentration or temperature, and saturation only at model nodes (corners of finite elements). The code was modified as follows to allow output of the aforementioned quantities at any point or points, called “generalized observation points,” within the model domain.

In module ALLARR (listed earlier), a new data type OBSDAT was defined. It has the following components: NAME, a character variable of length 40 that holds the name of the observation point; L, an integer variable that holds the number of the finite element that contains the observation point; X, Y, and Z, double-precision variables that hold the global coordinates of the observation point; and XSI, ETA, and ZETA, double-precision variables that hold the local coordinates of the observation point. Allocatable array OBSPTS, which is of type OBSDAT, was introduced to hold name and location data for all of the observation points, replacing array IOBS.

The input format for dataset 8D of the INP (main input) file was modified to allow generalized observation points and to allow the user to control the output format in the OBS (observation output) file. In addition to accepting node numbers to identify observation points, the modified code accepts generalized observation points of the form

```
('<NAME>'  <X-COORD>  <Y-COORD>  <Z-COORD>)
```

where <NAME> is the name of the observation point, and <X-COORD>, <Y-COORD>, and <Z-COORD> are its global coordinates. For example,

```
('JAS-80'  237383.700655054  1012336.79593972  -111.313)
```

specifies a point named "JAS-80" at global coordinates (X, Y, Z) = (237383.700655054, 1012336.79593972, –111.313). A new input parameter, NOBLIN, which specifies the number of observation points to be listed across the page in the OBS file, was also added to dataset 8D.

In subroutine INDAT1, code was added to read in and parse observation points from the INP (main input) file:

```
C.....INITALIZE LINE NUMBER AND OBSERVATION COUNT.
      NLINE = 0
      NOBCNT = 0
C.....READ A LINE.
10    CALL READIF(K1, INTFIL, ERRCOD)
      NLINE = NLINE + 1
      LENIF = LEN_TRIM(INTFIL)
C.....PARSE ANY NUMBERS THAT PRECEDE THE FIRST GENERALIZED
C        OBSERVATION POINT ON THIS LINE.
      M2 = 0
      M3 = M2 + SCAN(INTFIL(M2+1:LENIF),"(")
      IF (M3.EQ.M2) M3 = LENIF + 1
      IFDUM = INTFIL(M2+1:M3-1)
      CALL PRSWDS(IFDUM, " ", 0, WORD, NFLDS)
      IF (NLINE.EQ.1) THEN
C.......IF THIS IS THE FIRST LINE, READ AND/OR SET THE OBSERVATION
C          PRINT CYCLE, NOBCYC, AND THE NUMBER OF OBSERVATION POINTS
C          ACROSS A LINE OF OUTPUT, NOBLIN.  SET NFNOT SUCH THAT
C          THESE PARAMETERS ARE LATER SKIPPED WHEN ACTUAL OBSERVATION
C          NODE NUMBERS ARE BEING READ.
         IF (NFLDS.EQ.1) THEN
            READ(IFDUM,*,IOSTAT=INERR(1)) NOBCYC
            NOBLIN = 0
            NFNOT = 1
         ELSE
            READ(IFDUM,*,IOSTAT=INERR(1)) NOBCYC, NOBLIN
            IF (NOBLIN.LT.0) THEN
               NFNOT = 2
            ELSE
               NOBLIN = 0
               NFNOT = 1
            END IF
         END IF
         NOBLIN = -NOBLIN
      ELSE
C.......IF THIS IS NOT THE FIRST LINE, NOBCYC AND NOBLIN DO NOT
C          APPEAR.  SET NFNOT=0 SO THAT NO FIELDS ARE SKIPPED WHEN
C          OBSERVATION NODE NUMBERS ARE BEING READ.
         NFNOT = 0
      END IF
C.....READ ANY OBSERVATION NODE NUMBERS THAT PRECEDE THE FIRST
C        GENERALIZED OBSERVATION POINT ON THIS LINE.  END OF LIST
```

```
C        IF NODE NUMBER IS ZERO.
      NFACT = NFLDS - NFNOT
      ALLOCATE(CNODES(NFACT))
      READ(IFDUM,*,IOSTAT=INERR(1)) (NDUM,K=1,NFNOT),
     1   (CNODES(K),K=1,NFACT)
      DO 40 K=1,NFACT
         NOBCNT = NOBCNT + 1
         OBSPTS(NOBCNT)%NAME = "NODE_" // ADJUSTL(CNODES(K))
         WRITE(IFDUM,*) CNODES(K)
         READ(IFDUM,*) OBSPTS(NOBCNT)%L
         IF (CNODES(K).EQ."0") THEN
            DEALLOCATE(CNODES)
            GOTO 300
         END IF
   40 CONTINUE
      DEALLOCATE(CNODES)
C.....IF END OF LINE, READ NEXT LINE.
      IF (M3.GT.LENIF) GOTO 10
C.....PARSE ANY REMAINING GENERALIZED OBSERVATION POINTS AND
C        OBSERVATION NODE NUMBERS ON THIS LINE.
      M1 = M3
      DO 100 M=1,LENIF
C.......FIND AND PARSE NEXT GENERALIZED OBSERVATION POINT.  STORE
C           ITS NAME AND (X, Y, Z) COORDINATES IN COMPONENTS OF
C           OBSPTS.
         M2 = M1 + SCAN(INTFIL(M1+1:LENIF),")")
         NOBCNT = NOBCNT + 1
         IF (N48.EQ.8) THEN
            READ(INTFIL(M1+1:M2-1),*,IOSTAT=INERR(1))
     1         OBSPTS(NOBCNT)%NAME, OBSPTS(NOBCNT)%X,
     2         OBSPTS(NOBCNT)%Y, OBSPTS(NOBCNT)%Z
         ELSE
            READ(INTFIL(M1+1:M2-1),*,IOSTAT=INERR(1))
     1         OBSPTS(NOBCNT)%NAME, OBSPTS(NOBCNT)%X,
     2         OBSPTS(NOBCNT)%Y
         END IF
         IF (INERR(1).NE.0) PRINT *,"Error reading gen obs pt!"
C.......FIND AND PARSE NEXT SERIES OF OBSERVATION NODE NUMBERS.
C           CONVERT EACH INTO A GENERALIZED OBSERVATION POINT NAMED
C           "NODE_nnn", WHERE "nnn" IS THE NODE NUMBER.  STORE
C           ITS NAME IN COMPONENT %NAME OF OBSPTS.  THE (X, Y, Z)
C           COORDINATES WILL LATER BE READ FROM THE LIST OF NODAL
C           COODINATES.  END OF LIST IF NODE NUMBER IS ZERO.
         M3 = M2 + SCAN(INTFIL(M2+1:LENIF),"(")
         IF (M3.EQ.M2) M3 = LENIF + 1
         IFDUM = INTFIL(M2+1:M3-1)
         CALL PRSWDS(IFDUM, " ", 0, WORD, NFLDS)
         ALLOCATE(CNODES(NFLDS))
         READ(IFDUM,*,IOSTAT=INERR(1)) (CNODES(K),K=1,NFLDS)
         DO 80 K=1,NFLDS
            NOBCNT = NOBCNT + 1
            OBSPTS(NOBCNT)%NAME = "NODE_" // ADJUSTL(CNODES(K))
            WRITE(IFDUM,*) CNODES(K)
            READ(IFDUM,*) OBSPTS(NOBCNT)%L
            IF (CNODES(K).EQ."0") THEN
               DEALLOCATE(CNODES)
```

```
                GOTO 300
             END IF
 80       CONTINUE
          DEALLOCATE(CNODES)
          IF (M3.GT.LENIF) GOTO 10
          M1 = M3
100    CONTINUE
300    IF (NOBLIN.EQ.0) NOBLIN = NOBCNT - 1
```

The changes described above necessitated passing array OBSPTS through the argument list and declaring a character variable IFDUM of length 1,000 and an allocatable array CNODES of character type and length 40 to temporarily store observation node numbers.

In the main program, SUTRA_MAIN, code was added to determine the element number and local coordinates for each observation point:

```
C.....LOOK UP COORDINATES FOR OBSERVATION POINTS THAT ARE NODES.
      DO 710 K=1,NOBS
         IF (OBSPTS(K)%NAME(1:5).EQ."NODE_") THEN
            I = OBSPTS(K)%L
            OBSPTS(K)%X = X(I)
            OBSPTS(K)%Y = Y(I)
            IF (N48.EQ.8) OBSPTS(K)%Z = Z(I)
         END IF
  710 CONTINUE
C
C.....FIND THE ELEMENT EACH OBSERVATION POINT IS IN.  IN COMPONENTS OF
C        OBSPTS, OVERWRITE NODE NUMBERS AND GLOBAL COORDINATES WITH
C        ELEMENT NUMBERS AND LOCAL COORDINATES.
      DO 900 K=1,NOBS
         XK = OBSPTS(K)%X
         YK = OBSPTS(K)%Y
         IF (N48.EQ.8) ZK = OBSPTS(K)%Z
         DO 800 LL=1,NE
            IF (N48.EQ.8) THEN
               CALL FINDL3(X,Y,Z,IN,LL,XK,YK,ZK,XSI,ETA,ZET,INOUT)
            ELSE
               CALL FINDL2(X,Y,IN,LL,XK,YK,XSI,ETA,INOUT)
            END IF
            IF (INOUT.EQ.1) THEN
               L = LL
               GOTO 820
            END IF
  800    CONTINUE
         PRINT *, "ERROR: Element not found for ", OBSPTS(K)%NAME(1:15)
         STOP
  820    OBSPTS(K)%L = L
         OBSPTS(K)%XSI = XSI
         OBSPTS(K)%ETA = ETA
         IF (N48.EQ.8) OBSPTS(K)%ZET = ZET
  900 CONTINUE
```

For each observation point, the routine loops over all elements in the mesh, calling subroutine FINDL3 (for 3D) or FINDL2 (for 2D), which in turn solves for the local coordinates of the observation point with respect to the current element. If the local coordinates are all between –1.001 and +1.001, the observation point is considered to be within the current element. Subroutine FINDL3, which is relevant to the 3D meshes used in this work, is listed below:

```
      SUBROUTINE FINDL3(X,Y,Z,IN,LL,XK,YK,ZK,XSI,ETA,ZET,INOUT)
C     ADAPTED FROM SUTRAPLOT SUBROUTINE ITER3D.
```

```
C
      IMPLICIT DOUBLE PRECISION (A-H, O-Z)
      COMMON /DIMS/ NN, NE
      DIMENSION IN(NE*8)
      DIMENSION X(NN), Y(NN), Z(NN)
      DATA TOL /0.001/, ITRMAX /25/, EPSILON /0.001/
C
C.....DEFINE OPE = (1. + EPSILON) FOR CONVENIENCE.
      OPE = 1D0 + EPSILON
C
C.....SET CORNER COORDINATES.
      M0 = (LL - 1)*8
      X1 = X(IN(M0+1))
      X2 = X(IN(M0+2))
      X3 = X(IN(M0+3))
      X4 = X(IN(M0+4))
      X5 = X(IN(M0+5))
      X6 = X(IN(M0+6))
      X7 = X(IN(M0+7))
      X8 = X(IN(M0+8))
      Y1 = Y(IN(M0+1))
      Y2 = Y(IN(M0+2))
      Y3 = Y(IN(M0+3))
      Y4 = Y(IN(M0+4))
      Y5 = Y(IN(M0+5))
      Y6 = Y(IN(M0+6))
      Y7 = Y(IN(M0+7))
      Y8 = Y(IN(M0+8))
      Z1 = Z(IN(M0+1))
      Z2 = Z(IN(M0+2))
      Z3 = Z(IN(M0+3))
      Z4 = Z(IN(M0+4))
      Z5 = Z(IN(M0+5))
      Z6 = Z(IN(M0+6))
      Z7 = Z(IN(M0+7))
      Z8 = Z(IN(M0+8))
C
C.....CALCULATE COEFFICIENTS.
      AX = +X1+X2+X3+X4+X5+X6+X7+X8
      BX = -X1+X2+X3-X4-X5+X6+X7-X8
      CX = -X1-X2+X3+X4-X5-X6+X7+X8
      DX = -X1-X2-X3-X4+X5+X6+X7+X8
      EX = +X1-X2+X3-X4+X5-X6+X7-X8
      FX = +X1-X2-X3+X4-X5+X6+X7-X8
      GX = +X1+X2-X3-X4-X5-X6+X7+X8
      HX = -X1+X2-X3+X4+X5-X6+X7-X8
      AY = +Y1+Y2+Y3+Y4+Y5+Y6+Y7+Y8
      BY = -Y1+Y2+Y3-Y4-Y5+Y6+Y7-Y8
      CY = -Y1-Y2+Y3+Y4-Y5-Y6+Y7+Y8
      DY = -Y1-Y2-Y3-Y4+Y5+Y6+Y7+Y8
      EY = +Y1-Y2+Y3-Y4+Y5-Y6+Y7-Y8
      FY = +Y1-Y2-Y3+Y4-Y5+Y6+Y7-Y8
      GY = +Y1+Y2-Y3-Y4-Y5-Y6+Y7+Y8
      HY = -Y1+Y2-Y3+Y4+Y5-Y6+Y7-Y8
      AZ = +Z1+Z2+Z3+Z4+Z5+Z6+Z7+Z8
      BZ = -Z1+Z2+Z3-Z4-Z5+Z6+Z7-Z8
```

```
      CZ = -Z1-Z2+Z3+Z4-Z5-Z6+Z7+Z8
      DZ = -Z1-Z2-Z3-Z4+Z5+Z6+Z7+Z8
      EZ = +Z1-Z2+Z3-Z4+Z5-Z6+Z7-Z8
      FZ = +Z1-Z2-Z3+Z4-Z5+Z6+Z7-Z8
      GZ = +Z1+Z2-Z3-Z4-Z5-Z6+Z7+Z8
      HZ = -Z1+Z2-Z3+Z4+Z5-Z6+Z7-Z8
C
C.....INITIAL GUESS OF ZERO FOR XSI, ETA, AND ZETA.
      XSI=0.0
      ETA=0.0
      ZET=0.0
C
C.....ITERATION LOOP TO SOLVE FOR LOCAL COORDINATES.
C
      DO 800 I=1,ITRMAX
C
         F10 = AX - 8.*XK + BX*XSI + CX*ETA + DX*ZET + EX*XSI*ETA
     1        + FX*XSI*ZET + GX*ETA*ZET + HX*XSI*ETA*ZET
         F20 = AY - 8.*YK + BY*XSI + CY*ETA + DY*ZET + EY*XSI*ETA
     1        + FY*XSI*ZET + GY*ETA*ZET + HY*XSI*ETA*ZET
         F30 = AZ - 8.*ZK + BZ*XSI + CZ*ETA + DZ*ZET + EZ*XSI*ETA
     1        + FZ*XSI*ZET + GZ*ETA*ZET + HZ*XSI*ETA*ZET
         FP11 = BX + EX*ETA + FX*ZET + HX*ETA*ZET
         FP12 = CX + EX*XSI + GX*ZET + HX*XSI*ZET
         FP13 = DX + FX*XSI + GX*ETA + HX*XSI*ETA
         FP21 = BY + EY*ETA + FY*ZET + HY*ETA*ZET
         FP22 = CY + EY*XSI + GY*ZET + HY*XSI*ZET
         FP23 = DY + FY*XSI + GY*ETA + HY*XSI*ETA
         FP31 = BZ + EZ*ETA + FZ*ZET + HZ*ETA*ZET
         FP32 = CZ + EZ*XSI + GZ*ZET + HZ*XSI*ZET
         FP33 = DZ + FZ*XSI + GZ*ETA + HZ*XSI*ETA
C
         S11 = FP22*FP33 - FP32*FP23
         S12 = FP21*FP33 - FP31*FP23
         S13 = FP21*FP32 - FP31*FP22
         CF12 = -F20*FP33 + F30*FP23
         CF34 = -F20*FP32 + F30*FP22
         CF43 = -CF34
         CF56 = -F30*FP21 + F20*FP31
C
         DETXSI = -F10*S11 - FP12*CF12 + FP13*CF34
         DETETA = FP11*CF12 + F10*S12 + FP13*CF56
         DETZET = FP11*CF43 - FP12*CF56 - F10*S13
         DETERM = FP11*S11 - FP12*S12 + FP13*S13
         DELXSI = DETXSI/DETERM
         DELETA = DETETA/DETERM
         DELZET = DETZET/DETERM
C
         XSI = XSI + DELXSI
         ETA = ETA + DELETA
         ZET = ZET + DELZET
C
C.......STOP ITERATING IF CHANGE IN XSI, ETA, AND ZETA < TOL.
         IF ((ABS(DELXSI).LT.TOL).AND.(ABS(DELETA).LT.TOL).AND.
     1       (ABS(DELZET).LT.TOL)) GOTO 900
C
```

```
  800 CONTINUE
C
C.....ITERATONS FAILED TO CONVERGE.  SET INOUT = 99 AND RETURN.
      INOUT = 99
      GOTO 1000
C
C.....ITERATIONS CONVERGED.  IF POINT IS INSIDE THE ELEMENT,
C        SET INOUT = 1.  IF OUTSIDE, SET INOUT = 0.
  900 INOUT = 1
      IF ((ABS(XSI).GT.OPE).OR.(ABS(ETA).GT.OPE).OR.(ABS(ZET).GT.OPE))
     1   INOUT = 0
C
 1000 RETURN
      END
```

Subroutine OUTOBS, which writes observation output to file, was modified extensively. In SUTRA Version 2D3D.1, OUTOBS writes observation data directly to the sequential-access OBS file as they are generated. In the modified code, because of the option to output a limited number of observation points across the page, the observation data are first stored in a temporary, direct-access file called “SUTRA.OBD.” This is performed by the following portion of subroutine OUTOBS:

```
C........WRITE HEADER INFORMATION
         LR = 1
         WRITE(KOBD,'(40(A1))',REC=LR) (TITLE1(I),I=1,40)
         LR = LR + 1
         WRITE(KOBD,'(40(A1))',REC=LR) (TITLE1(I),I=41,80)
         LR = LR + 1
         WRITE(KOBD,'(40(A1))',REC=LR) (TITLE2(I),I=1,40)
         LR = LR + 1
         WRITE(KOBD,'(40(A1))',REC=LR) (TITLE2(I),I=41,80)
         LR = LR + 1
         IF (KTYPE(2).GT.1) THEN
            IF (KTYPE(2).EQ.3) THEN
               CTYPE2 = "BLOCKWISE MESH"
            ELSE
               CTYPE2 = "REGULAR MESH  "
            END IF
            WRITE(KOBD,16,REC=LR) KTYPE(1),CTYPE2
            LR = LR + 1
            WRITE(KOBD,17,REC=LR) NN1,NN2,NN3,NN
            LR = LR + 1
         ELSE IF (KTYPE(2).EQ.1) THEN
            CTYPE2 = "LAYERED MESH  "
            WRITE(KOBD,16,REC=LR) KTYPE(1),CTYPE2
            LR = LR + 1
            WRITE(KOBD,17,REC=LR) NLAYS,NNLAY,0,NN
            LR = LR + 1
         ELSE
            CTYPE2 = "IRREGULAR MESH"
            WRITE(KOBD,16,REC=LR) KTYPE(1),CTYPE2
            LR = LR + 1
            WRITE(KOBD,17,REC=LR) 0,0,0,NN
            LR = LR + 1
         END IF
   16    FORMAT(I1,1X,A14)
   17    FORMAT(4(1X,I9))
         WRITE(KOBD,'(I9)',REC=LR) KTMAX
         LR = LR + 1
```

```
         WRITE(KOBD,'(A8,2(1X,A13))',REC=LR) HORP,TORC1,TORC2
         LR = LR + 1
         DO 20  KT=1, KTMAX
            WRITE(KOBD,'(I8,1X,1PE13.6)',REC=LR) ITT(KT),TT(KT)
            LR = LR + 1
            WRITE(KOBD,'(3(1X,I9))',REC=LR) ISHORP(KT),ISTORC(KT),
     1         ISSATU(KT)
            LR = LR + 1
   20    CONTINUE
         NOBS = NOBSN - 1
         NOBREM = MOD(NOBS,NOBLIN)
         NSETS = NOBS/NOBLIN
         IF (NOBREM.NE.0) NSETS = NSETS + 1
         WRITE(KOBD,'(3(1X,I9))',REC=LR) NSETS, NOBLIN, NOBREM
         LR = LR + 1
         LR0 = LR
         JJ0 = 0
         DO 100 NS=1,NSETS
            IF ((NS.EQ.NSETS).AND.(NOBREM.NE.0)) THEN
               NOBL = NOBREM
            ELSE
               NOBL = NOBLIN
            END IF
            JJ1 = JJ0 + 1
            JJ2 = JJ0 + NOBL
            DO 45 JJ=JJ1,JJ2
               WRITE(KOBD,'(A40)',REC=LR) OBSPTS(JJ)%NAME
               LR = LR + 1
               WRITE(KOBD,40,REC=LR) OBSPTS(JJ)%X,OBSPTS(JJ)%Y,
     1            OBSPTS(JJ)%Z
   40          FORMAT(3(1X,1PE14.7))
               LR = LR + 1
   45       CONTINUE
            DO 50 KT=1,KTMAX*NOBL
               WRITE(KOBD,"(/)",REC=LR)
               LR = LR + 1
   50       CONTINUE
            JJ0 = JJ0 + NOBL
  100    CONTINUE
C
C........DEALLOCATE LOCAL ARRAYS.
         DEALLOCATE(TT,ITT,ISTORC,ISHORP,ISSATU)
C
         ONCOBD = .TRUE.
      ENDIF
C
C.....IF NO OBSERVATIONS, RETURN.
      IF (NOBSN-1.EQ.0) RETURN
C
C.....WRITE OBSERVATIONS.
      IF ((IT.EQ.0).OR.((IT.EQ.1).AND.(ISSTRA.EQ.1))) THEN
         TOUT = TSTART
         KTDONE = 0
      ELSE
         TOUT = TSEC
      END IF
```

```
      LR = LR0
      JJ0 = 0
      DO 1000 NS=1,NSETS
         IF ((NS.EQ.NSETS).AND.(NOBREM.NE.0)) THEN
            NOBL = NOBREM
         ELSE
            NOBL = NOBLIN
         END IF
         LR = LR + (2 + KTDONE)*NOBL
         DO 995 JJ=JJ0+1,JJ0+NOBL
            WRITE(KOBD,990,REC=LR) PUSW(OBSPTS(JJ)%L,
     1         OBSPTS(JJ)%XSI,OBSPTS(JJ)%ETA,OBSPTS(JJ)%ZET,
     2         PVEC,UVEC,IN,LREG)
  990       FORMAT(A45)
            LR = LR + 1
  995    CONTINUE
         LR = LR + (KTMAX - KTDONE - 1)*NOBL
         JJ0 = JJ0 + NOBL
 1000 CONTINUE
```

Subroutine OUTOBS calls function PUSW to evaluate the pressure, concentration or temperature, and saturation at observation points using the trilinear basis functions on which SUTRA is based:

```
      FUNCTION PUSW(L,XLOC,YLOC,ZLOC,PVEC,UVEC,IN,LREG)
      IMPLICIT DOUBLE PRECISION (A-H, O-Z)
      CHARACTER*45 PUSW
      DIMENSION FX(8),FY(8),FZ(8),F(8)
      DIMENSION PVEC(NN),UVEC(NN)
      DIMENSION IN(NIN),LREG(NE),KTYPE(2)
      COMMON /CONTRL/ GNUP,GNUU,UP,DTMULT,DTMAX,ME,ISSFLO,ISSTRA,
     1   ITCYC,NPCYC,NUCYC,NPRINT,IREAD,ISTORE,NOUMAT,IUNSAT,KTYPE
      COMMON /DIMS/ NN,NE,NIN,NBI,NCBI,NB,NBHALF,NPBC,NUBC,
     1   NSOP,NSOU,NBCN
C
      IF (KTYPE(1).EQ.2) THEN
C.....2D MESH
C........EVALUATE BASIS FUNCTIONS
         XF1=1.D0-XLOC
         XF2=1.D0+XLOC
         YF1=1.D0-YLOC
         YF2=1.D0+YLOC
         FX(1)=XF1
         FX(2)=XF2
         FX(3)=XF2
         FX(4)=XF1
         FY(1)=YF1
         FY(2)=YF1
         FY(3)=YF2
         FY(4)=YF2
         DO 20 I=1,4
   20       F(I)=0.250D0*FX(I)*FY(I)
C........EVALUATE P AND U
         P=0.D0
         U=0.D0
         DO 2000 IL=1,4
            II=(L-1)*4 +IL
            I=IN(II)
```

```
            P=P+PVEC(I)*F(IL)
            U=U+UVEC(I)*F(IL)
 2000    CONTINUE
C........EVALUATE SW
         IF ((IUNSAT.EQ.2).AND.(P.LT.0D0)) THEN
            CALL UNSAT(SW,DSWDPG,RELK,P,LREG(L))
         ELSE
            SW=1.0D0
         END IF
C........WRITE RESULTS TO STRING
         WRITE(UNIT=PUSW,FMT="(3(1PE15.7))") P, U, SW
      ELSE
C.....3D MESH
C........EVALUATE BASIS FUNCTIONS
         XF1=1.D0-XLOC
         XF2=1.D0+XLOC
         YF1=1.D0-YLOC
         YF2=1.D0+YLOC
         ZF1=1.D0-ZLOC
         ZF2=1.D0+ZLOC
         FX(1)=XF1
         FX(2)=XF2
         FX(3)=XF2
         FX(4)=XF1
         FX(5)=XF1
         FX(6)=XF2
         FX(7)=XF2
         FX(8)=XF1
         FY(1)=YF1
         FY(2)=YF1
         FY(3)=YF2
         FY(4)=YF2
         FY(5)=YF1
         FY(6)=YF1
         FY(7)=YF2
         FY(8)=YF2
         FZ(1)=ZF1
         FZ(2)=ZF1
         FZ(3)=ZF1
         FZ(4)=ZF1
         FZ(5)=ZF2
         FZ(6)=ZF2
         FZ(7)=ZF2
         FZ(8)=ZF2
         DO 30 I=1,8
   30       F(I)=0.125D0*FX(I)*FY(I)*FZ(I)
C........EVALUATE P AND U
         P=0.D0
         U=0.D0
         DO 3000 IL=1,8
            II=(L-1)*8 +IL
            I=IN(II)
            P=P+PVEC(I)*F(IL)
            U=U+UVEC(I)*F(IL)
 3000    CONTINUE
C........EVALUATE SW
```

```
            IF ((IUNSAT.EQ.2).AND.(P.LT.0D0)) THEN
               CALL UNSAT(SW,DSWDPG,RELK,P,LREG(L))
            ELSE
               SW=1.0D0
            END IF
C........WRITE RESULTS TO STRING
            WRITE(UNIT=PUSW,FMT="(3(1PE15.7))") P, U, SW
         END IF
         END
```

At the end of the run, the observation data are transcribed by subroutine CPYOBS from the temporary file to the OBS file in the desired format:

```
      SUBROUTINE CPYOBS()
      CHARACTER OBSNAM*40,FRMT*80,FRMT2*80,BLANKS*20
      CHARACTER TITLE1A*40,TITLE1B*40,TITLE2A*40,TITLE2B*40
      CHARACTER HORP*8,TORC1*13,TORC2*13,CTYPE2*14
      LOGICAL OBSREC
      COMMON /FUNITS/ K00,K0,K1,K2,K3,K4,K5,K6,K7,KOBD
      COMMON /OBS/ NOBSN,NTOBS,NOBCYC,NOBLIN
      COMMON /OBSL/ OBSREC
      ALLOCATABLE TT(:),ITT(:),ISHORP(:),ISTORC(:),ISSATU(:)
      ALLOCATABLE OBSP(:),OBSU(:),OBSS(:)
      ALLOCATABLE OBSNAM(:),OBSX(:),OBSY(:),OBSZ(:)
      DATA BLANKS /"                    "/
C
C.....READ HEADER INFORMATION.
      LR = 1
      READ(KOBD,'(A40)',REC=LR) TITLE1A
      LR = LR + 1
      READ(KOBD,'(A40)',REC=LR) TITLE1B
      LR = LR + 1
      READ(KOBD,'(A40)',REC=LR) TITLE2A
      LR = LR + 1
      READ(KOBD,'(A40)',REC=LR) TITLE2B
      LR = LR + 1
      READ(KOBD,16,REC=LR) MDIM,CTYPE2
      LR = LR + 1
      READ(KOBD,17,REC=LR) NN1,NN2,NN3,NN
      LR = LR + 1
   16 FORMAT(I1,1X,A14)
   17 FORMAT(4(1X,I9))
      READ(KOBD,'(I9)',REC=LR) KTMAX
      LR = LR + 1
      READ(KOBD,'(A8,2(1X,A13))',REC=LR) HORP,TORC1,TORC2
      LR = LR + 1
      ALLOCATE(TT(KTMAX),ITT(KTMAX))
      ALLOCATE(ISHORP(KTMAX),ISTORC(KTMAX),ISSATU(KTMAX))
      DO 200 KT=1,KTMAX
         READ(KOBD,'(I8,1X,1PE13.6)',REC=LR) ITT(KT),TT(KT)
         LR = LR + 1
         READ(KOBD,'(3(1X,I9))',REC=LR) ISHORP(KT),ISTORC(KT),ISSATU(KT)
         LR = LR + 1
200   CONTINUE
      READ(KOBD,'(3(1X,I9))',REC=LR) NSETS, NOBLIN, NOBREM
      LR = LR + 1
      ALLOCATE (OBSNAM(NOBLIN),OBSX(NOBLIN),OBSY(NOBLIN),OBSZ(NOBLIN))
```

```
      ALLOCATE(OBSP(NOBLIN),OBSU(NOBLIN),OBSS(NOBLIN))
C
C.....WRITE HEADER INFORMATION.
         WRITE(K7,50) TITLE1A, TITLE1B, TITLE2A, TITLE2B
         IF ((CTYPE2(1:7).EQ.'REGULAR').OR.
     1        (CTYPE2(1:9).EQ.'BLOCKWISE')) THEN
            IF (MDIM.EQ.3) THEN
               WRITE(K7,51) MDIM,CTYPE2,NN1,NN2,NN3,NN," Nodes"
            ELSE
               WRITE(K7,52) MDIM,CTYPE2,NN1,NN2,NN," Nodes"
            END IF
         ELSE IF (CTYPE2(1:7).EQ.'LAYERED') THEN
            WRITE(K7,52) MDIM,CTYPE2,NN1,NN2,NN," Nodes"
         ELSE
            WRITE(K7,54) MDIM,CTYPE2,NN," Nodes"
         END IF
         WRITE(K7,60) "OBSERVATION POINT RESULTS",
     1      KTMAX, HORP, TORC1, "Sat"
         DO 20  KT=1, KTMAX
            WRITE(K7,61) ITT(KT), TT(KT), ISHORP(KT),
     1         ISTORC(KT), ISSATU(KT)
   20    CONTINUE
         WRITE(K7,'("## "/"## ",77("="))')
   50    FORMAT("## ", 2(A40),
     1         /"## ", 2(A40),
     2         /"## ")
   51    FORMAT("## ", I1, "-D, ", A, 5X,
     1                "(", 2(I9, ")*("), I9, ") = ", I9, A,
     2         /"## ")
   52    FORMAT("## ", I1, "-D, ", A, 17X,
     1                "(", I9, ")*(", I9, ") = ", I9, A,
     2         /"## ")
   54    FORMAT("## ", I1, "-D, ", A, 43X, I9, A,
     1         /"## ")
   60    FORMAT("## ", 77("="),
     4         /"## ", A, 24X, I9, " Time steps printed",
     5         /"## ", 77("="),
     6         /"## ",
     7         /"##  Time steps", 27X,
     8                "[Latest time step computed]",
     9         /"## in this file    Time (sec)", 9X,A5, 10X,A4, 11X,A3,
     T         /"## ", 12("-"), 3X, 12("-"), 1X, 3(3X, 12("-")) )
   61    FORMAT("## ", 3X, I8, 3X, 1PE13.6, 3(7X, I8))
C
C.....PROCESS THE OBSERVATIONS.
      DO 300 NS=1,NSETS
C
         IF ((NS.EQ.NSETS).AND.(NOBREM.NE.0)) THEN
            NOBL = NOBREM
         ELSE
            NOBL = NOBLIN
         END IF
C
C.......READ OBSERVATION POINT NAMES AND COORDINATES.
         DO 220 JJ=1,NOBL
ccc               print *,ns,jj,nobl  ! kluge
```

```
            READ(KOBD,'(A40)',REC=LR) OBSNAM(JJ)
            LR = LR + 1
            READ(KOBD,215,REC=LR) OBSX(JJ),OBSY(JJ),OBSZ(JJ)
  215       FORMAT(3(1X,1PE14.7))
            LR = LR + 1
  220    CONTINUE
C
C........WRITE HEADER.
         WRITE(FRMT,"(A,I9,A)") '("## "/"## ",24X,',
     1      NOBLIN,"(4X,3(A)))"
         WRITE(K7,FRMT)
     1     (BLANKS(1:(44-LEN_TRIM(OBSNAM(JJ)))/2),
     2      TRIM(OBSNAM(JJ)),
     3      BLANKS(1:44-LEN_TRIM(OBSNAM(JJ))-
     4              (44-LEN_TRIM(OBSNAM(JJ)))/2), JJ=1,NOBL)
         WRITE(FRMT2,"(A,I9,A)") '("## ",24X,',NOBL,
     1      "(:3X,1X,A14,2A15))"
         WRITE(K7,FRMT2) ('---------------',JJ=1,3*NOBL)
         WRITE(FRMT,"(A,I9,A)") '("## ",25X,',NOBL,
     1      "(:2X,'(',2(1PE14.7,','),1PE14.7,')'))"
         WRITE(K7,FRMT) (OBSX(JJ),OBSY(JJ),OBSZ(JJ), JJ=1,NOBL)
         WRITE(K7,FRMT2) ('---------------',JJ=1,3*NOBL)
         WRITE(FRMT,"(A,I9,A)") '("## ","Time Step",5X,"Time (sec)",',
     1      NOBL,"(:10X,A,2X,A,5X,'Saturation'))"
         WRITE(K7,FRMT) (HORP, TORC2, JJ=1,NOBL)
C
C........READ AND WRITE OBSERVATIONS.
         DO 248 KT=1,KTMAX
            DO 246 JJ=1,NOBL
               READ(KOBD,242,REC=LR) OBSP(JJ),OBSU(JJ),OBSS(JJ)
  242          FORMAT(3(1PE15.7))
               LR = LR + 1
  246       CONTINUE
            WRITE(FRMT,"(A,I9,A)") "(3X,I9,1PE15.7,",NOBL,
     1         "(3X,3(1PE15.7)))"
            WRITE(K7,FRMT) ITT(KT),TT(KT),
     1         (OBSP(JJ),OBSU(JJ),OBSS(JJ), JJ=1,NOBL)
  248    CONTINUE
C
  300 CONTINUE
      GOTO 500
C
C.....ERROR HANDLING.
  400 PRINT *, "*** Error reading temporary direct access file ***"
      STOP
C.....WRITE MESSAGES, DEALLOCATE ARRAYS, AND RETURN.
  500 IF (OBSREC) THEN
         WRITE (*,502)
         WRITE (K00,502)
  502    FORMAT (1X,"*** OBSERVATION RECOVERY COMPLETED ",
     1      "SUCCESSFULLY ***")
      END IF
      WRITE(K7,512)
  512 FORMAT ("##"/"## *** OBSERVATION OUTPUT IS COMPLETE ***")
      DEALLOCATE(TT,ITT)
      DEALLOCATE(OBSNAM,OBSX,OBSY,OBSZ)
```

```
      DEALLOCATE(OBSP,OBSU,OBSS)
      RETURN
      END
```

Subroutine PRSWDS, which parses the character string STRING into individual words delimited by one or more of the single-character delimiter DELIM and/or blanks, was modified to simply compute the number of words, NWORDS, if the maximum number of words to parse, NWMAX, is set to zero. Additional changes were made to streamline the code.

```
      SUBROUTINE PRSWDS(STRING, DELIM, NWMAX, WORD, NWORDS)
      CHARACTER*(*) STRING, WORD(NWMAX)
      CHARACTER DELIM*1, DELIM2*2
C
C.....DEFINE SET OF DELIMITERS (SPACE PLUS USER-SPECIFIED CHARACTER)
      DELIM2 = " " // DELIM
C
C.....COMPUTE LENGTH OF STRING WITHOUT TRAILING BLANKS
      LSTRNG = LEN_TRIM(STRING)
C
C.....INITIALIZE WORD LIST AND COUNTERS
      DO 50 I=1,NWMAX
         WORD(I) = ""
   50 CONTINUE
      NWORDS = 0
      M2 = 0
C
  300 CONTINUE
C.....FIND THE NEXT CHARACTER THAT IS NOT A DELIMITER
      M1L = VERIFY(STRING(M2+1:LSTRNG),DELIM2)
      IF (M1L.EQ.0) RETURN
      M1 = M2 + M1L
C
  400 CONTINUE
C.....FIND THE NEXT CHARACTER THAT IS A DELIMITER
      M2L = SCAN(STRING(M1+1:LSTRNG),DELIM2)
      IF (M2L.EQ.0) THEN
         M2 = LSTRNG + 1
      ELSE
         M2 = M1 + M2L
      END IF
C
  500 CONTINUE
C.....STORE THE LATEST WORD FOUND
      NWORDS = NWORDS + 1
      IF (NWMAX.GT.0) WORD(NWORDS) = STRING(M1:M2-1)
C
C.....IF END OF STRING NOT REACHED AND NUMBER OF WORDS IS LESS THAN
C        THE MAXIMUM ALLOWED, CONTINUE PARSING
      IF ((M2.LT.LSTRNG).AND.((NWORDS.LT.NWMAX).OR.(NWMAX.EQ.0)))
     1   GOTO 300
C
      RETURN
      END
```

The termination sequence, the section of code that deallocates arrays and closes files at the conclusion of a model run, was moved from the main program, SUTRA_MAIN, to a new subroutine, TERSEQ. A call to subroutine CPYOBS was added to TERSEQ to transfer observation data from "SUTRA.OBD" to the OBS file.

Time-Dependent Pumping

Time-dependent pumping was programmed in subroutine BCTIME. Annualized pumping rates for a series of years are read from files, and pumping at intermediate times is interpolated linearly from the available data. Each file contains data for a particular year and is in the format required by dataset 17 of the INP (main input) file. Pumping is assumed to be uniformly zero in mid-1885 (predevelopment) and to remain at year-2000 levels after 2000. To implement the scheme described above, the following changes were made to subroutine BCTIME.

Arrays PYR and PMPFIL, which hold the times and filenames for the available data, are initialized in a DATA statement:

```
      data (pyr(npf),pmpfil(npf),npf=0,npfmax+1)
     1   /1885.5,     'dummy',
     1    1915.5,     '1915_pumping.inp17',
     1    1920.5,     '1920_pumping.inp17',
     1    1930.5,     '1930_pumping.inp17',
     1    1937.5,     '1937_pumping.inp17',
     1    1940.5,     '1940_pumping.inp17',
     1    1955.5,     '1955_pumping.inp17',
     1    1965.5,     '1965_pumping.inp17',
     1    1970.5,     '1970_pumping.inp17',
     1    1975.5,     '1975_pumping.inp17',
     1    1980.5,     '1980_pumping.inp17',
     1    1985.5,     '1985_pumping.inp17',
     1    1990.5,     '1990_pumping.inp17',
     1    1995.5,     '1995_pumping.inp17',
     1    1997.5,     '1997_pumping.inp17',
     1    1998.7068,  '1998_Sept_pumping.inp17',
     2    2000.5,     '2000_pumping.inp17',
     3    2000.5,     '2000_pumping.inp17'/
      save npf, pyri, pyrf
```

The SAVE statement preserves the values of NPF, the number of the last data file read, and PYRI and PYRF, the initial and final times of the current interpolation period, between calls to BCTIME.

The portion of BCTIME that reads and interpolates the pumping data and sets the corresponding boundary conditions is listed below:

```
      if (it.eq.1) then
        print *, 'NOTE: Pumping node list checking removed for ',
     1      'the sake of hhi-off/sav-off runs !!!!!!!!!'
        do 452 npf1=npfmax,0,-1
           if (year.ge.pyr(npf1)) then
              npf = npf1
              goto 453
           end if
452     continue
        print *, 'Starting year, ', year, ', predates ', pyr(0), ' !!!'
453     continue
        pyrf = pyr(npf)
        if (npf.eq.0) then
          do 454 iqp=1,nsopi
            i=iqsop(iqp)
            if (i.lt.0) then
               qinf(-i) = 0.
               uinf(-i) = 0.
            end if
454       continue
        else
          open (unit=88, file=pmpfil(npf), status='old')
          do 455 iqp=1,nsopi
```

```
            i=iqsop(iqp)
            if (i.lt.0) then
               qinf(-i) = 0.
               uinf(-i) = 0.
            end if
455       continue
          do 456 iqr=1,nsopi
             read(88,*,err=457,end=457) ir, qr
             if (ir.eq.0) goto 457
             if (ir.lt.0) then
                qinf(-ir) = qr
                uinf(-ir) = 0.
             end if
456       continue
457       continue
          close(88)
        end if
      end if
c
      if (year.ge.pyrf) then
         npf = npf + 1
         pyri = pyrf
         pyrf = pyr(npf)
         open (unit=88, file=pmpfil(npf), status='old')
         do 468 iqp=1,nsopi
            i=iqsop(iqp)
            if (i.lt.0) then
               qini(-i) = qinf(-i)
               uini(-i) = uinf(-i)
               qinf(-i) = 0.
               uinf(-i) = 0.
            end if
468      continue
         do 470 iqr=1,nsopi
            read(88,*,err=471,end=471) ir, qr
            if (ir.eq.0) goto 471
            if (ir.lt.0) then
               qinf(-ir) = qr
               uinf(-ir) = 0.
            end if
470      continue
471      continue
         close(88)
      end if
c
      wt = (year - pyri)/(pyrf - pyri)
      print *, "wt = ", wt
      print *, "( ", pyri, " - ", pyrf, " )"
      cwt = 1d0 - wt
      DO 600 IQP=1,NSOPI
      I=IQSOP(IQP)
      IF(I) 500,600,600
  500 CONTINUE
C     NOTE: A FLOW AND TRANSPORT SOLUTION MUST OCCUR FOR ANY
C           TIME STEP IN WHICH QIN( ) CHANGES.
C     QIN(-I) =   ((            ))
```

```
            qin(-i) = cwt*qini(-i) + wt*qinf(-i)
      C     NOTE: A TRANSPORT SOLUTION MUST OCCUR FOR ANY
      C           TIME STEP IN WHICH UIN( ) CHANGES.
      C     UIN(-I) =   ((          ))
            uin(-i) = cwt*uini(-i) + wt*uinf(-i)
        600 CONTINUE
```

Arrays QINI and QINF store the pumping rates at the beginning and end of each pumping period and are passed through the argument list of BCTIME. Analogous arrays UINI and UINF, which store solute concentrations, were defined for the sake of generality but were not required for the present application.

Time-Step Cycling

To facilitate temporal discretization appropriate for the present application, the criterion for identifying time steps on which the time-step size changes was modified throughout the code from

```
IF (MOD(JT,ITCYC).EQ.0 .AND. JT.GT.1) DELTK=DELTK*DTMULT
```

to

```
IF (MOD(JT-1,ITCYC).EQ.0 .AND. JT.GT.1) DELTK=DELTK*DTMULT
```

where JT is the current time-step number, ITCYC is the number of time steps in a time-step change cycle, DELTK is the time-step size, and DTMULT is the time-step size multiplier. ITCYC and DTMULT are input parameters in dataset 6 of the INP (main input) file.

Other Changes

Several additional changes were made that are not directly relevant to the functioning of the code in the present application. The modified code allows input data to be “inserted” into the INP (main input) and ICS (initial conditions) files from separate files. This feature was not used in the present application. New mesh types were defined for the sake of postprocessing. They do not affect the way in which SUTRA formulates and processes the ground-water flow and transport model. Finally, error handling—how SUTRA responds to errors encountered while input data are being read or during a model run—was updated.

Appendix B. Observed Specific Conductance Measurements and Estimated Chloride Concentration

Specific conductance data were collected using a Hydrolab® Mini-Sonde 4a. The monitor was moved incrementally along the open interval of a well bore and a specific-conductance reading was taken at each depth (Camille Ransom III, South Carolina Department of Health and Environmental Control, oral commun., 2004). The result for any given well is a vertical profile of specific conductance through the water column. The data are summarized in table B1.

To estimate chloride concentration from specific-conductance values, a linear function relating the properties was used (fig. B1). This function is a visual fit to data collected in the Upper Floridan aquifer in southern Beaufort County, S.C. (James E. Landmeyer, U.S. Geological Survey, written commun., 2005).

After the chloride calibration was completed, updated locations of chloride observation wells became available (Robert Logan and Jack Childress, South Carolina Department of Health and Environmental Control, written commun., 2005; fig. B2). For most wells, the change in location was minor. In general, the largest changes in location occurred for wells in the area of the northern Hilton Head Island plume. Despite the changes, it was not deemed necessary to recalibrate the model.

Chloride measurements made in wells BFT-2401 and BFT-2402 in 2004 were not included during the chloride calibration. Subsequent comparison shows, however, that the general pattern of salinity simulated in the Base Case is consistent with these field data (fig. 28).

Chloride measurements made in well BFT-1591 in 2004 were not available at the time of the chloride calibration. The model results clearly underestimate the chloride concentration at this well. Because well BFT-1591 is somewhat removed from the apparent source of the northern Hilton Head Island plume, it is not clear whether the chloride observed in this well is part of that plume, or whether it comes from another source.

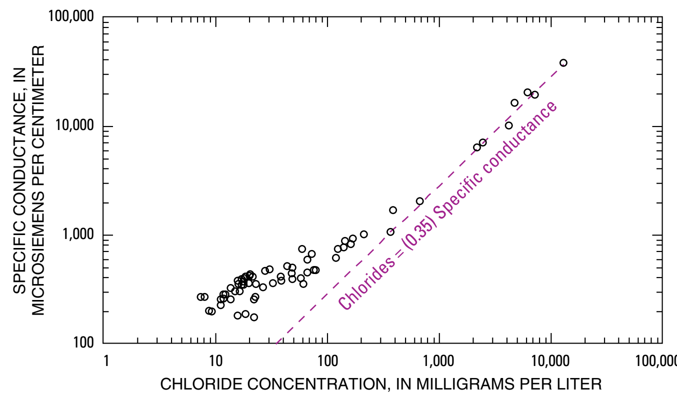

Figure B1. Relation between specific conductance and chloride concentration in the Upper Floridan aquifer, southern Beaufort County, South Carolina (data from James E. Landmeyer, U.S. Geological Survey, written commun., 2005).

Table B1. Estimated chloride concentration values used to calibrate solute transport model..

[mS/cm, millisiemens per centimeter; mg/L, milligrams per liter; ft, feet; %, percent; –, below NAVD 88; see figure B2 for well location. In general, parentheses indicate that the highest concentrations sampled were located at the bottom of the sampling interval. Single parentheses indicate that the interval over which concentration was greater than 50% of the maximum concentration was within 10 ft of the maximum depth sampled. Double parentheses indicate that the interval over which concentration was greater than 50% of the maximum concentration was within 5 ft of the maximum depth sampled. Data from Robert Logan, South Carolina Department of Health and Environmental Control, written commun., 2005]

Well identifier	Date	Maximum specific conductance (mS/cm)	Maximum chloride concentration (mg/L)	Elevation of sampling interval (altitude NAVD 88, ft)
BFT-315	7/18/00	0.947	(331)	–93.94 to –171.94
	5/1/02	1.005	((352))	–93.94 to –171.84
	1/23/03	0.96	336	–33.94 to –171.84
BFT–358	6/5/02	0.269	94	–30 to –323.8
	7/15/03	0.263	92	–50 to –323.8
	3/3/04	0.265	93	–50 to –324.5
BFT-429	9/12/02	2.6	910	–19 to –279
	7/15/03	5.19	1,817	–19 to –279
	3/4/04	6.64	2,324	–19 to –279
BFT-493	4/25/02	0.249	87	–52.7 to –69.1
BFT-500	3/3/04	0.292	102	–29 to –298
BFT-502	7/15/03	11.53	4,036	–17 to –204.5
	3/3/04	12.72	4,452	–17 to –205.5

Table B1. Estimated chloride concentration values used to calibrate solute transport model.—Continued

[mS/cm, millisiemens per centimeter; mg/L, milligrams per liter; ft, feet; %, percent; –, below NAVD 88; see figure B2 for well location. In general, parentheses indicate that the highest concentrations sampled were located at the bottom of the sampling interval. Single parentheses indicate that the interval over which concentration was greater than 50% of the maximum concentration was within 10 ft of the maximum depth sampled. Double parentheses indicate that the interval over which concentration was greater than 50% of the maximum concentration was within 5 ft of the maximum depth sampled. Data from Robert Logan, South Carolina Department of Health and Environmental Control, written commun., 2005]

Well identifier	Date	Maximum specific conductance (mS/cm)	Maximum chloride concentration (mg/L)	Elevation of sampling interval (altitude NAVD 88, ft)
BFT-787	5/2/02	0.477	167	–76.6 to –157.6
	2/28/03	19.8	(6,930)	–89 to –223.8
	1/28/04	18.1	(6,335)	–39 to –224
BFT-1326	7/21/00	3.86	1,351	–76.5 to –174.9
	6/5/02	4.07	1,425	–26.5 to –175
	8/27/03	3.92	1,372	–26.5 to –175
	1/16/04	3.84	1,344	–26.5 to –175
BFT-1689	7/25/00	0.241	84	–90.84 to –190.84
	2/19/03	0.257	90	–40.84 to –192.64
	1/11/04	0.241	84	–40.84 to –192.64
BFT-1810	2/9/00	9.36	3,276	–37.42 to –185.42
	3/19/03	13.08	4,578	–37.42 to –185.42
BFT-1814	7/20/00	3.07	(1,075)	–89.16 to –219.16
	8/28/03	3.96	(1,386)	–39.16 to –217.86
	2/5/04	3.89	(1,362)	–39.16 to –218.66
BFT-1822	3/2/03	0.484	169	–40.4 to –234
BFT-1846	7/19/00	8.74	3,059	–37.77 to –165.27
	8/1/03	10.4	3,640	–37.77 to –165.57
	1/16/04	10.34	3,619	–37.77 to –165.57
BFT-2162	7/21/00	0.682	239	–106.23 to –208.43
	3/10/04	0.72	252	–36.23 to –207.33
BFT-2163	7/25/00	0.425	149	–106.03 to –206.33
	6/6/02	0.432	151	–36.03 to –206.33
	1/27/03	0.445	156	–36.03 to –206.33
	3/10/04	0.449	157	–36.03 to –206.73
BFT-2164	7/18/00	0.515	180	–110 to –177
	2/27/03	6.96	2,436	–100 to –214.4
	2/10/04	7.17	2,510	–50 to –214.3
BFT-2165	7/20/00	0.245	86	–86.52 to –187.62
	8/28/03	0.272	95	13.48 to –186.62
	1/11/04	0.259	91	–36.52 to –187.82
BFT-2166	8/17/00	27.5	9,625	–90.65 to –198.75
	8/29/03	29.8	10,430	–40.65 to –200.25
	3/2/04	30	10,500	–40.65 to –199.75
BFT-2187	7/24/00	21.5	((7,525))	–100 to –211.1
	2/27/03	21.4	((7,490))	–40 to –210.8
	2/11/04	19.6	((6,860))	–40 to –211.4
BFT-2188	7/18/00	24	((8,400))	–110 to –211.4
	1/24/03	28.9	(10,115)	–50 to –216
	2/1/04	26.6	(9,310)	–50 to –215.7
BFT-2189	8/17/00	11.19	3,917	–84.6 to –173.3
	7/14/03	14.71	(5,149)	–84.6 to –174.6
	2/27/04	14.11	4,939	–34.6 to –176
BFT-2190	8/17/00	0.778	272	–90.44 to –179.94
	7/14/03	0.803	281	–90.44 to –180.44
	2/27/04	0.7	245	–40.44 to –180.44
BFT-2196	7/18/00	12.3	4,305	–95.8 to –192.7
	1/20/03	14.37	5,030	–35.8 to –192.7
	2/10/04	13.86	4,851	–35.8 to –195.6
BFT-2197	7/18/00	10.74	3,759	–94.08 to –194.68
	1/23/03	13.44	4,704	–34.08 to –194.78
	2/10/04	12.98	4,543	–34.08 to –195.08

Table B1. Estimated chloride concentration values used to calibrate solute transport model.—Continued

[mS/cm, millisiemens per centimeter; mg/L, milligrams per liter; ft, feet; %, percent; –, below NAVD 88; see figure B2 for well location. In general, parentheses indicate that the highest concentrations sampled were located at the bottom of the sampling interval. Single parentheses indicate that the interval over which concentration was greater than 50% of the maximum concentration was within 10 ft of the maximum depth sampled. Double parentheses indicate that the interval over which concentration was greater than 50% of the maximum concentration was within 5 ft of the maximum depth sampled. Data from Robert Logan, South Carolina Department of Health and Environmental Control, written commun., 2005]

Well identifier	Date	Maximum specific conductance (mS/cm)	Maximum chloride concentration (mg/L)	Elevation of sampling interval (altitude NAVD 88, ft)
BFT-2198	7/23/00	11.3	((3,955))	–110 to –207.5
	6/6/02	11.93	((4,176))	–50 to –208.1
	1/26/03	14.38	((5,033))	–50 to –208.1
	2/11/04	9.51	((3,329))	–50 to –208.4
BFT-2200	7/24/00	0.51	179	–90.96 to –185.56
	2/27/03	31.3	(10,955)	–30.96 to –204.06
	3/4/04	32.3	(11,305)	–30.96 to –204.06
BFT-2201	7/18/00	29.6	10,360	–95.55 to –201.75
	1/24/03	32.9	11,515	–35.55 to –201.35
	2/11/04	30.7	10,745	–35.55 to –203.75
BFT-2299	4/20/02	2.08	728	–47.3 to –140.7
	8/27/03	2.5	875	–9.3 to –154.9
	1/16/04	2.54	889	–9.3 to –152.9
BFT-2300	4/30/02	3.07	1,075	–45.94 to –133.34
	5/15/03	3.35	1,173	–6.84 to –150.44
	1/11/04	3.59	1,257	–6.84 to –150.34
BFT-2301	2/20/03	37.5	13,125	–64.62 to –144.62
	1/16/04	33.6	11,760	–34.62 to –144.62
BFT-2302	4/30/02	0.237	83	–41.68 to –146.88
	2/20/02	0.254	89	–56.98 to –162.98
	1/16/03	0.238	83	–56.98 to –162.98
BFT-2303	4/22/02	0.292	102	–56.71 to –154.71
	2/24/03	0.312	109	–81.81 to –180.31
	1/20/04	0.342	120	–31.81 to –180.31
BFT-2304	4/22/02	6.6	2,310	–62.06 to –163.66
	8/27/03	5.77	2,020	13.84 to –183.66
	1/20/04	5.27	1,845	–36.16 to –183.16
BFT-2307	4/23/02	0.347	121	–47.55 to –183.95
	7/15/03	0.316	111	–68.65 to –205.65
	2/25/04	0.306	107	–38.65 to –206.15
BFT-2308	4/23/02	0.566	198	–91.93 to –187.23
	2/24/03	0.539	189	–108.13 to –204.13
	2/5/04	0.51	179	–38.13 to –204.33
BFT-2310	8/28/03	5.99	2,097	9.81 to –186.69
BFT-2312	7/14/03	23.4	8,190	–90.98 to –202.48
	3/2/04	22.4	7,840	–40.98 to –203.18
BFT-2313	7/14/03	36.1	12,635	–84.96 to –187.46
	2/27/04	35.1	12,285	–34.96 to –194.76
BFT-2314	4/18/02	0.445	156	–76.84 to –199.44
	3/9/03	0.417	146	–90.74 to –214.04
	1/20/04	0.441	154	–40.74 to –213.74
BFT-2315	4/19/02	0.327	114	–66.41 to –173.31
	2/25/04	0.326	114	–35.41 to –200.41
BFT-2401	3/4/04	16.3	((5,705))	–25 to –230.8
BFT-2402	3/4/04	12.61	4,414	–25 to –249

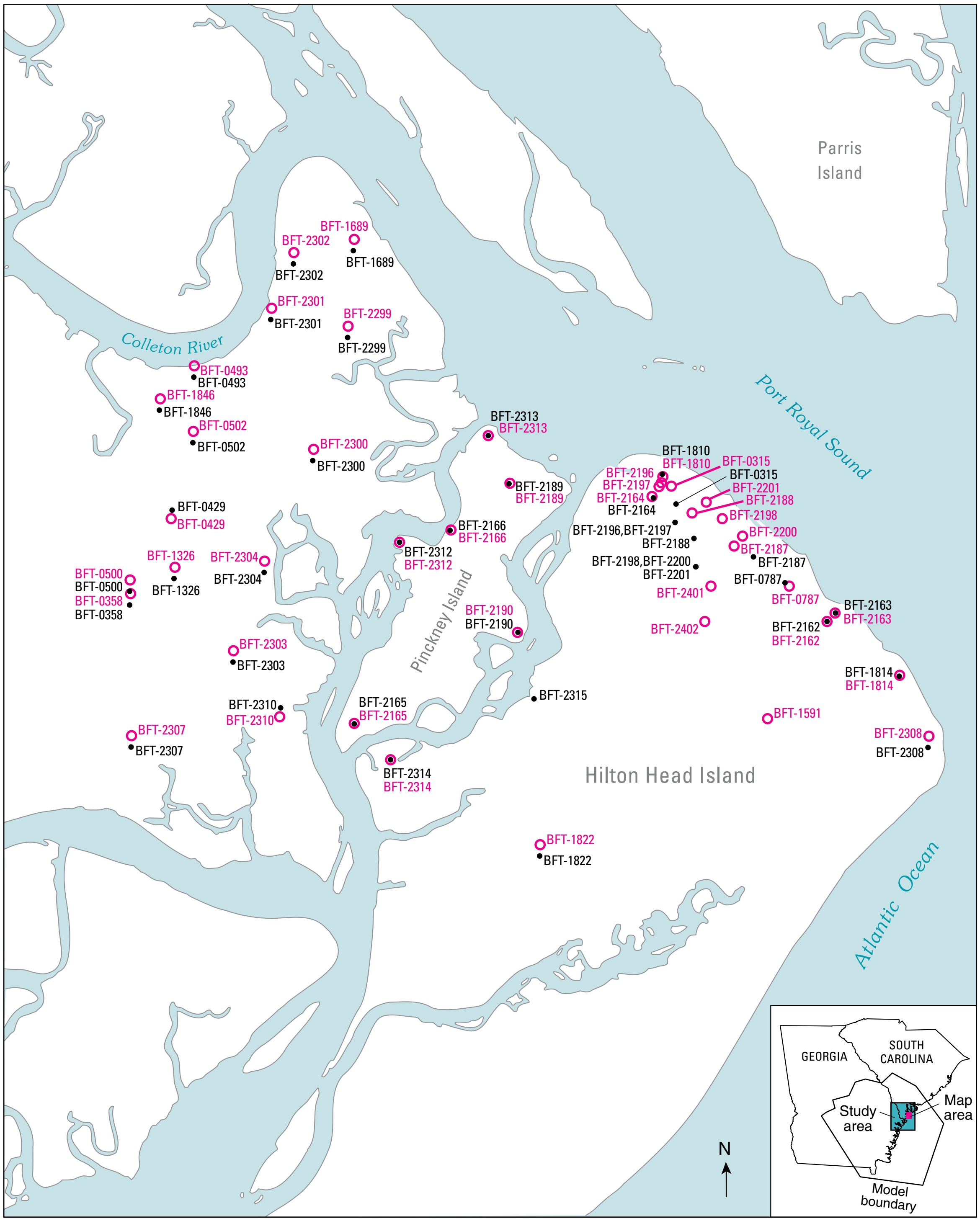

Base modifed from U.S. Census Bureau
ArcInfo Tiger files, 1:100,000, 1991

0 1 2 3 MILES
0 1 2 3 KILOMETERS

EXPLANATION

- • BFT-1822 **Well used for model calibration and identification**
- ○ BFT-1822 **Updated well location and identification**

Figure B2. Location of wells in the Hilton Head Island, South Carolina, area used in calibration of solute transport (data and locations from Robert Logan and Jack Childress, South Carolina Department of Health and Environmental Control, written commun., 2005).

Appendix C. Altitude of Top and Bottom Surfaces of Hydrogeologic Units

The top surfaces of each of the hydrogeologic units used in the model (as well as the bottom of the Floridan aquifer system) were generated using point data from a variety of sources. Publications used to construct hydrogeologic unit surfaces include: Brooks and others (1985), Charm and others (1969), Clarke and others (1990), Falls and others (2005a), Foyle and others (2001), Hathaway and others (1981), Kellam and Gorday (1990), Miller (1986), Scholle (1979), and Steele and McDowell (1998). Other unpublished data were received from Anthony Foyle (Georgia Southern University, Applied Coastal Research Laboratory, written commun., 2002), Joseph Gellici (South Carolina Department of Natural Resources, written commun., 2002), and Harold Gill (Jordan Jones and Goulding, written commun., 2001). Internet sources of data include National Elevation Dataset (accessed January 24, 2000, at *http://ned.usgs.gov*), and National Geophysical Data Center Coastal Relief Model (accessed January 10, 2001, at *http://www.ngdc.noaa.gov/mgg/coastal/coastal.html*).

These surfaces were constrained by a fundamental requirement of the model that the surfaces not intersect. The data available to define each of these surfaces, the control points, differed in number and distribution for each surface. Therefore, it was not possible to construct the nonintersecting surfaces by mapping thicknesses of the units. The procedure to generate surfaces appropriate for the model was as follows:

1. for each hydrogeologic unit, a surface was generated by interpolating between available control points for that surface;
2. each surface was sampled at the center points of the regional MODFLOW flow-model grid cells;
3. differences between sampled hydrogeologic surfaces were calculated to determine where these surfaces intersected; and
4. for cases in which surfaces crossed, a series of calculations was made to redefine the surfaces such that no surfaces intersected.

To rectify intersecting surfaces, a general hierarchy of surfaces was established, based on quantity and distribution of control points. For example, the most well-defined surface is the top surface of unit 1, which is defined by land-surface altitude and bathymetry raster data (NAVD 88). Where the top surface of another unit intersected the top surface of unit 1, the other surface was set to an elevation at least 5 ft lower than the top of unit 1. In some cases, certain surfaces were better constrained than others in some areas, and more poorly constrained in other areas. In such cases, intersecting surfaces were locally rectified.

The resulting surfaces do not intersect each other, and represent appropriate relative thicknesses of aquifer and confining units where known. Outside of areas where the hydrogeologic unit surfaces are well defined by control data, artifacts of the rectification process may result in unrealistic topography. These areas of unrealistic topography, however, generally have little effect on the model and model results. For example, figure C4 shows an alignment of contours for the top of unit 4 that mimics the shape of the simulated extent of the Brunswick aquifer system (fig. 16, zone B1). This alignment is inconsequential because unit 3 pinches out at the edge of this area (fig. 13) and uniform permeability is assigned to units 2, 3, and 4, because they represent a single confining unit. Unrealistic topographies may also appear in offshore areas (for example, fig. C2). Because there is little control on the hydrogeologic unit surfaces in these areas, and because they are removed from the study area, any additional adjustments would serve primarily aesthetic purposes and, thus, was deemed not necessary for the purpose of modeling.

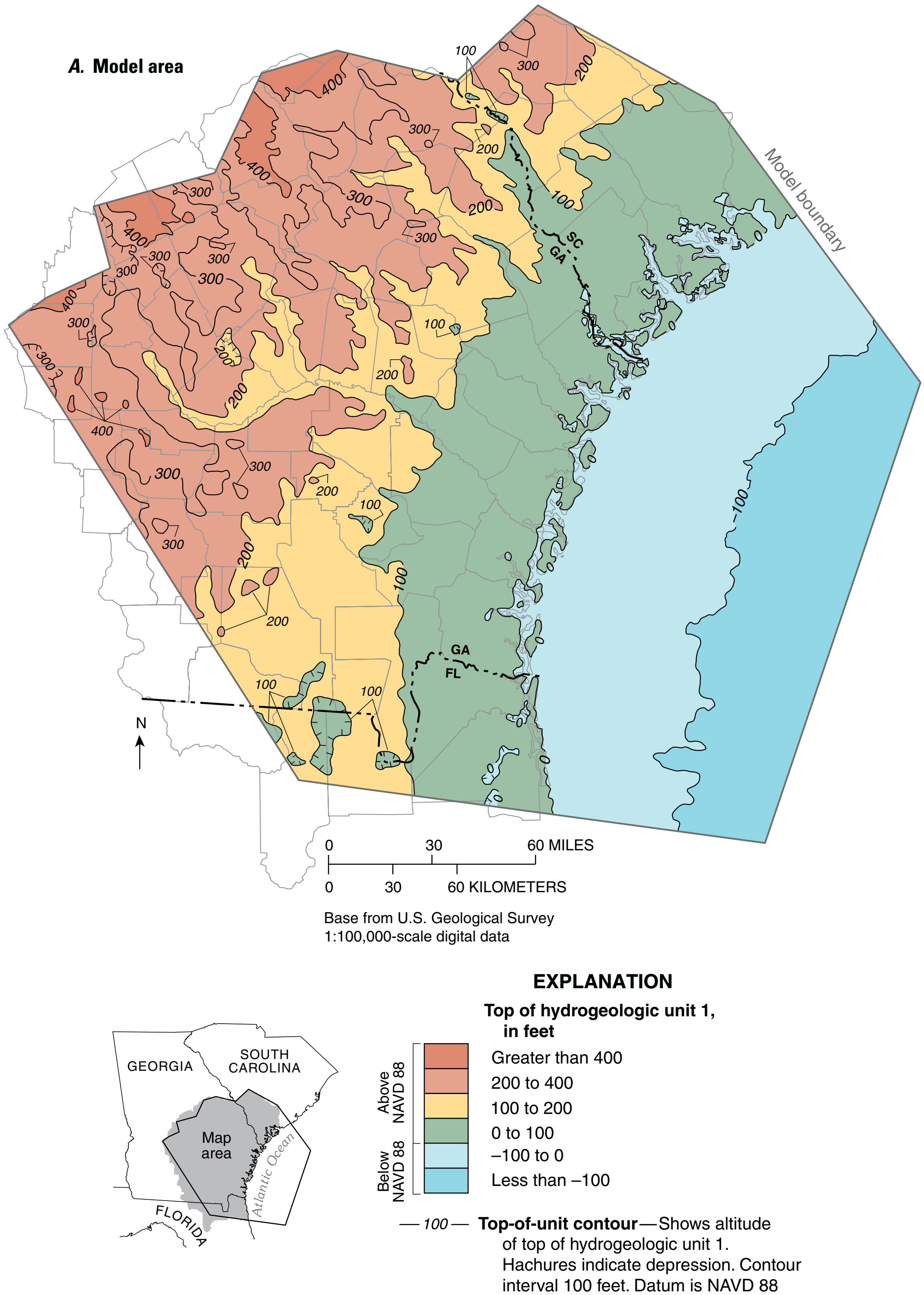

Figure C1. Altitude of top of hydrogeologic unit 1 for (*A*) model area and (*B*) study area. This represents land surface and bathymetry.

***B.* Study area**

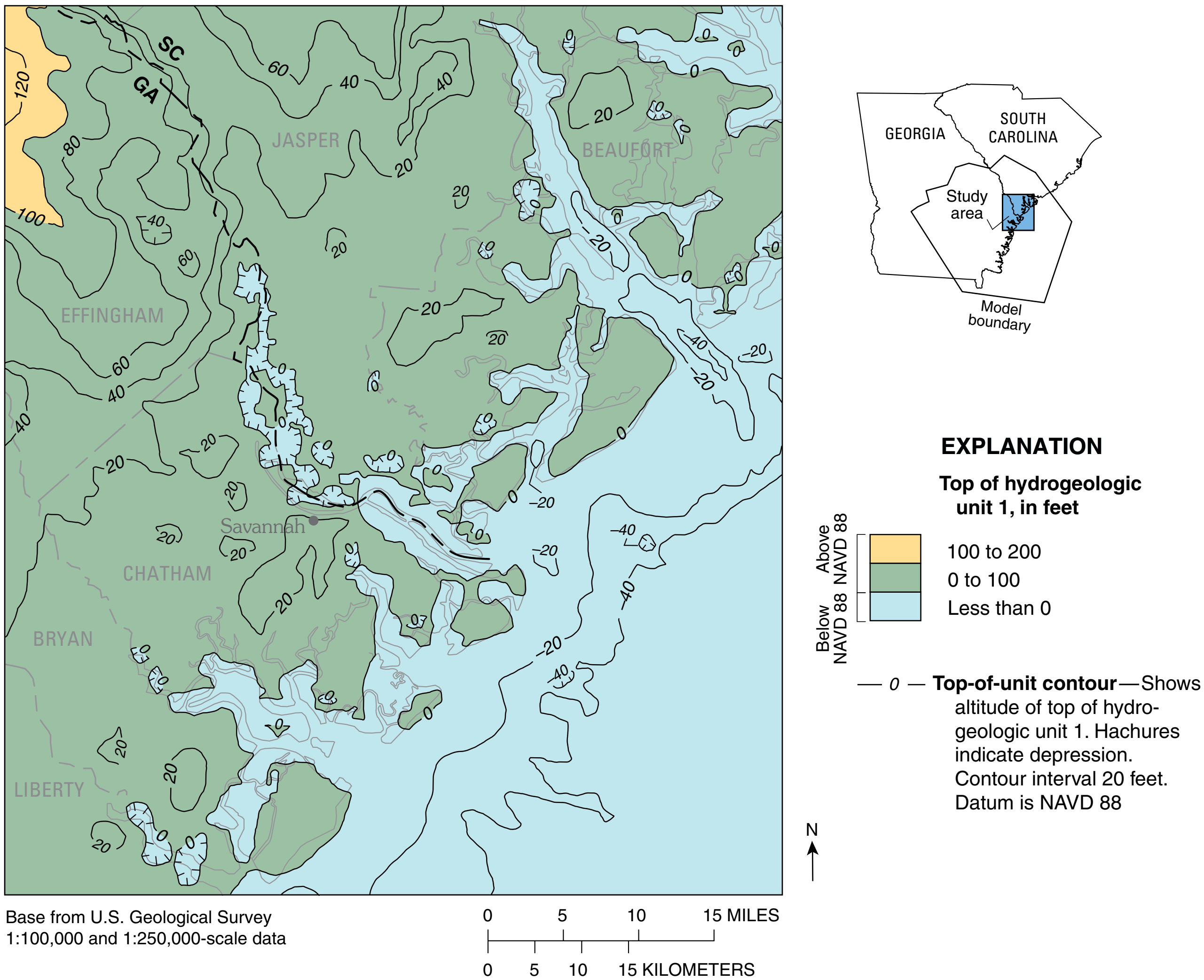

Figure C1. Altitude of top of hydrogeologic unit 1 for (*A*) model area and (*B*) study area. This represents land surface and bathymetry—continued.

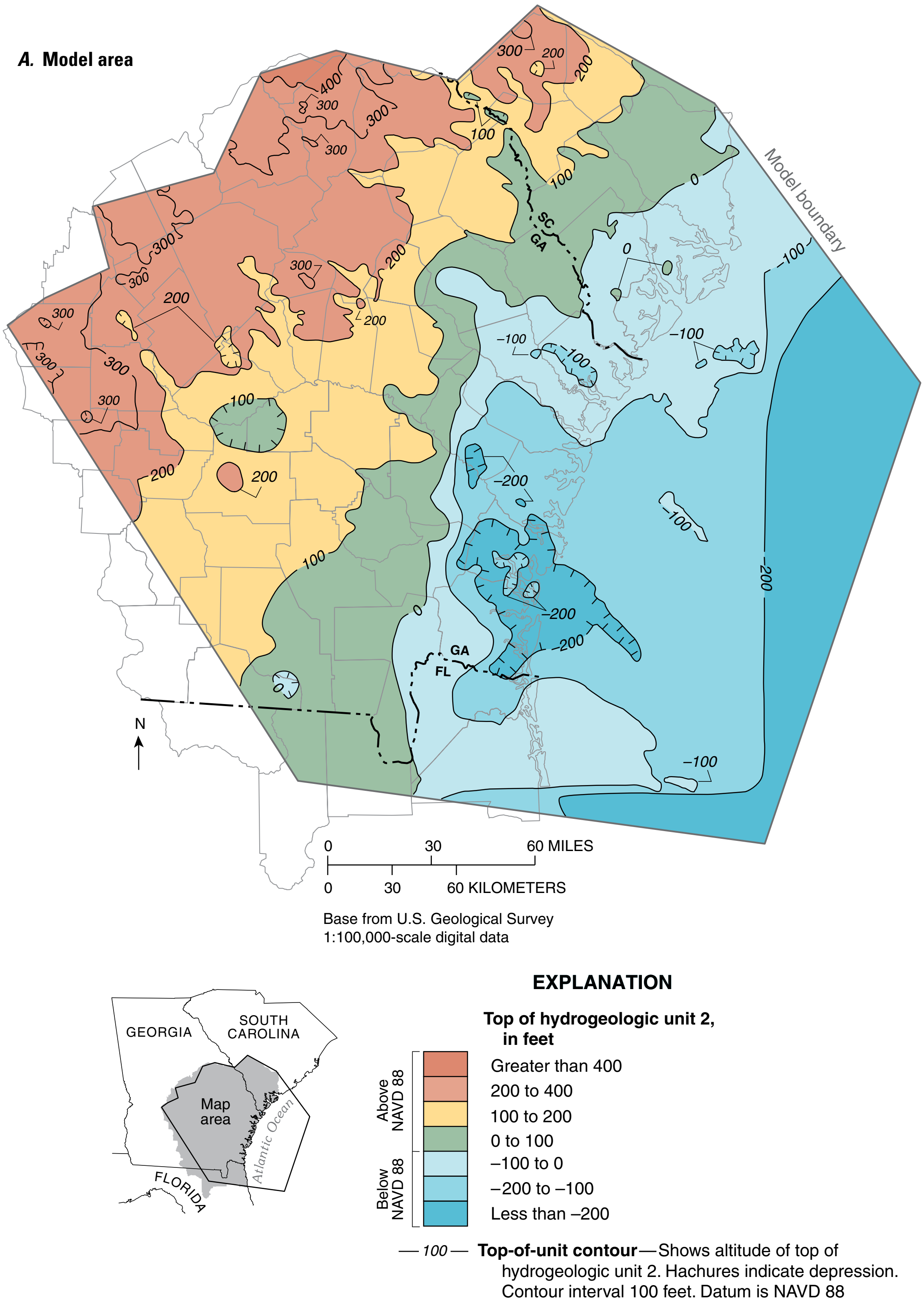

Figure C2. Altitude of top of hydrogeologic unit 2 for (*A*) model area and (*B*) study area. This represents the top of the Upper Floridan confining unit.

***B.* Study area**

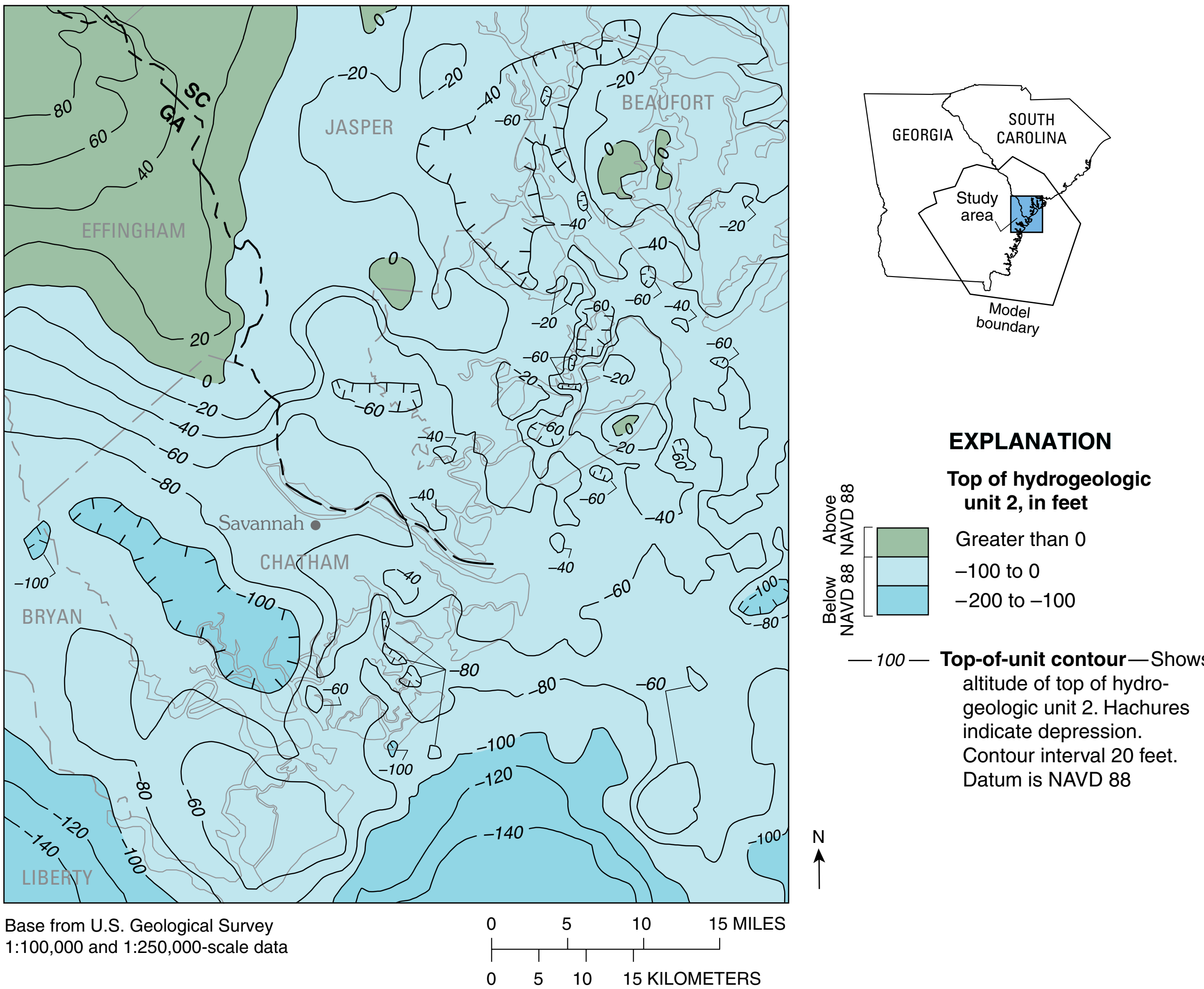

Figure C2. Altitude of top of hydrogeologic unit 2 for (*A*) model area and (*B*) study area. This represents the top of the Upper Floridan confining unit—continued.

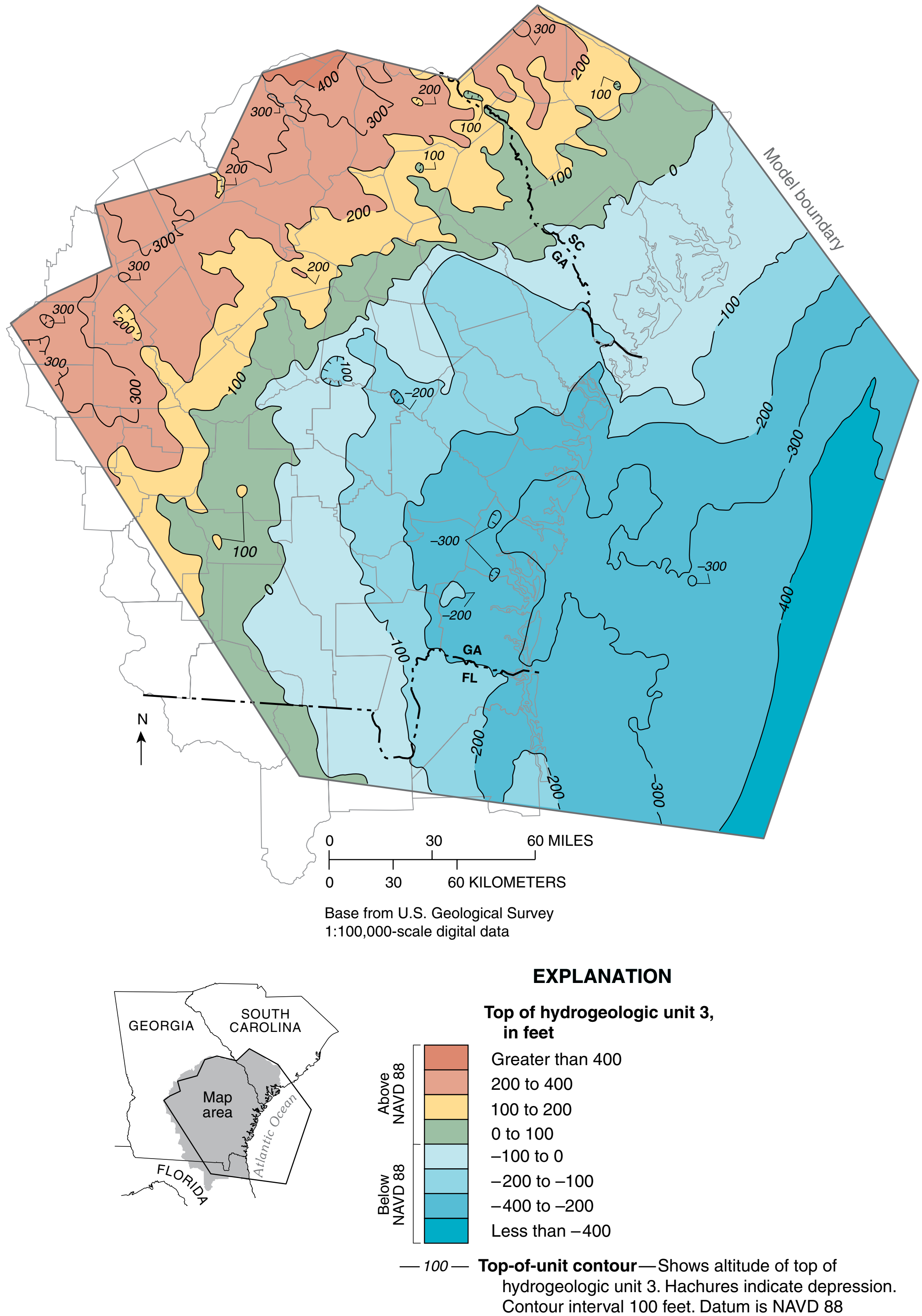

Figure C3. Altitude of top of hydrogeologic unit 3 for model area.

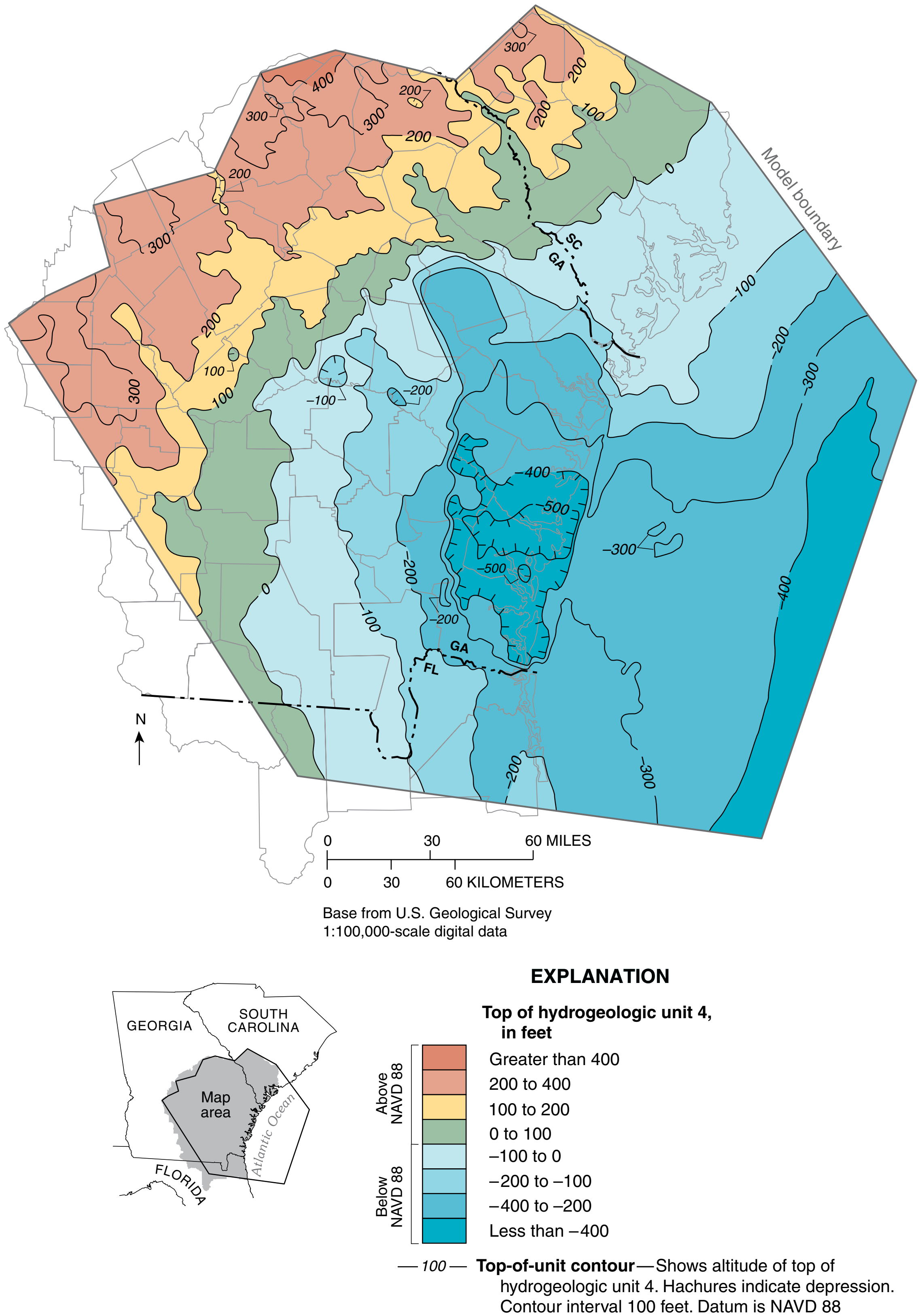

Figure C4. Altitude of top of hydrogeologic unit 4 for model area.

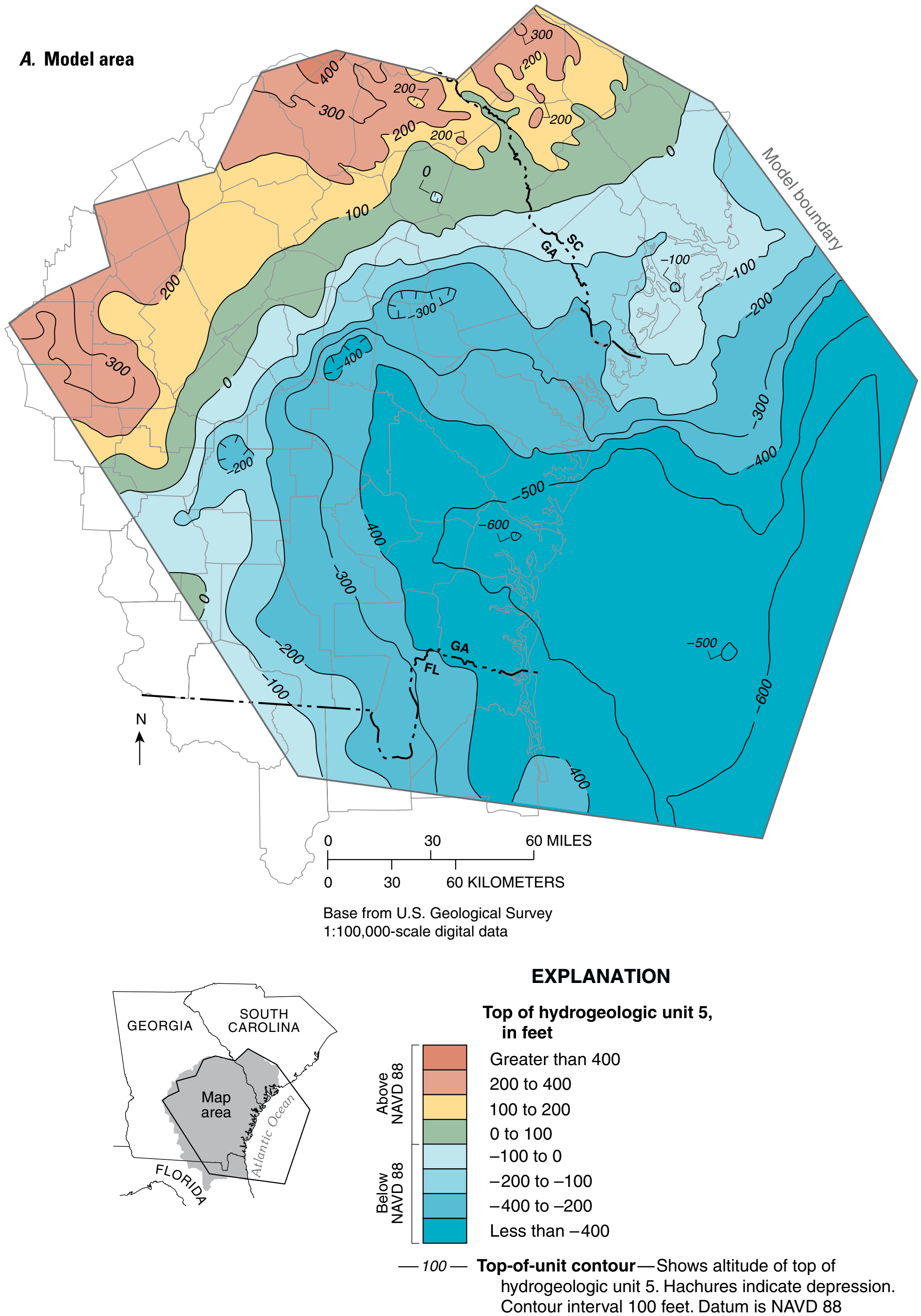

Figure C5. Altitude of top of hydrogeologic unit 5 for (*A*) model area, and (*B*) study area. This represents the top of the Upper Floridan aquifer.

***B.* Study area**

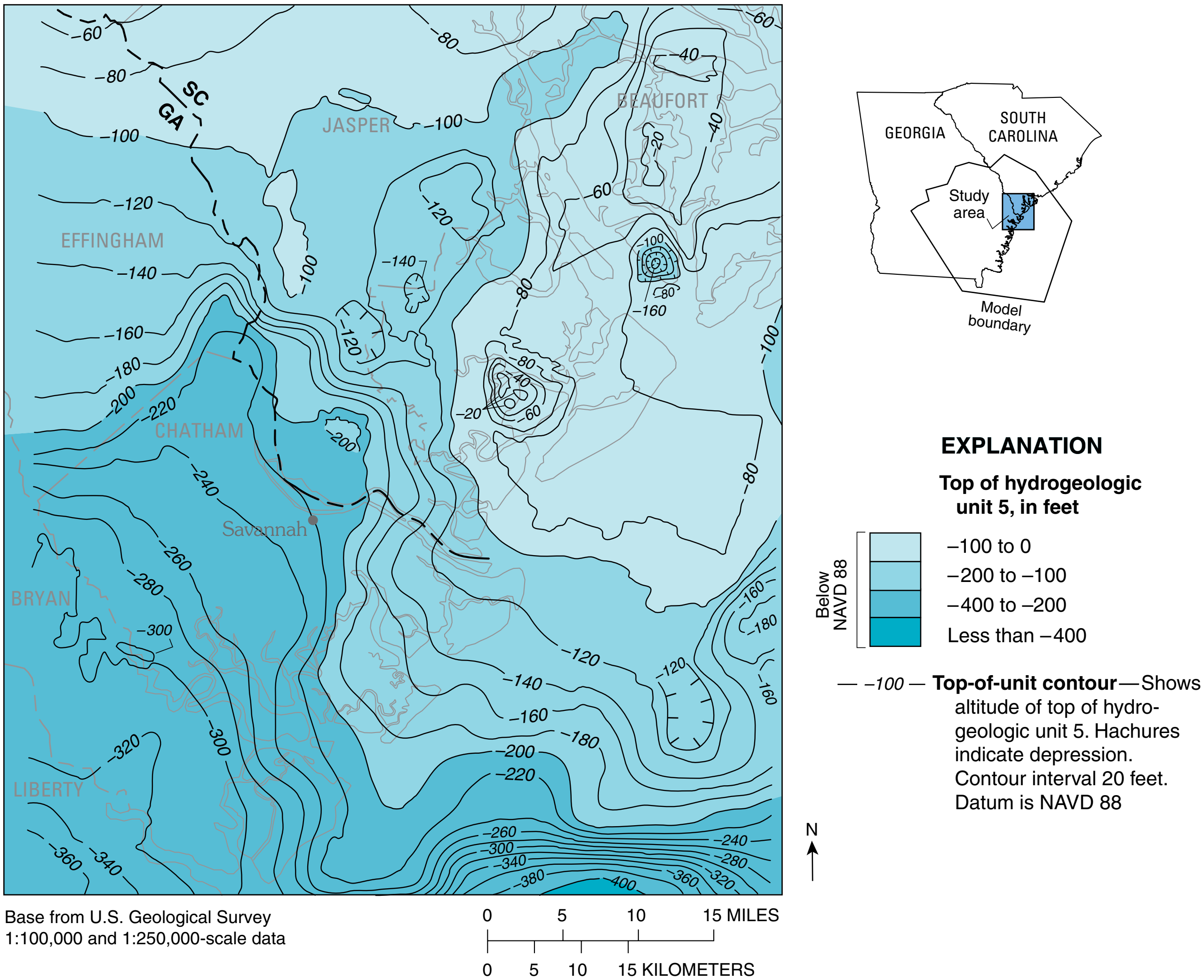

Figure C5. Altitude of top of hydrogeologic unit 5 for (*A*) model area, and (*B*) study area. This represents the top of the Upper Floridan aquifer—continued.

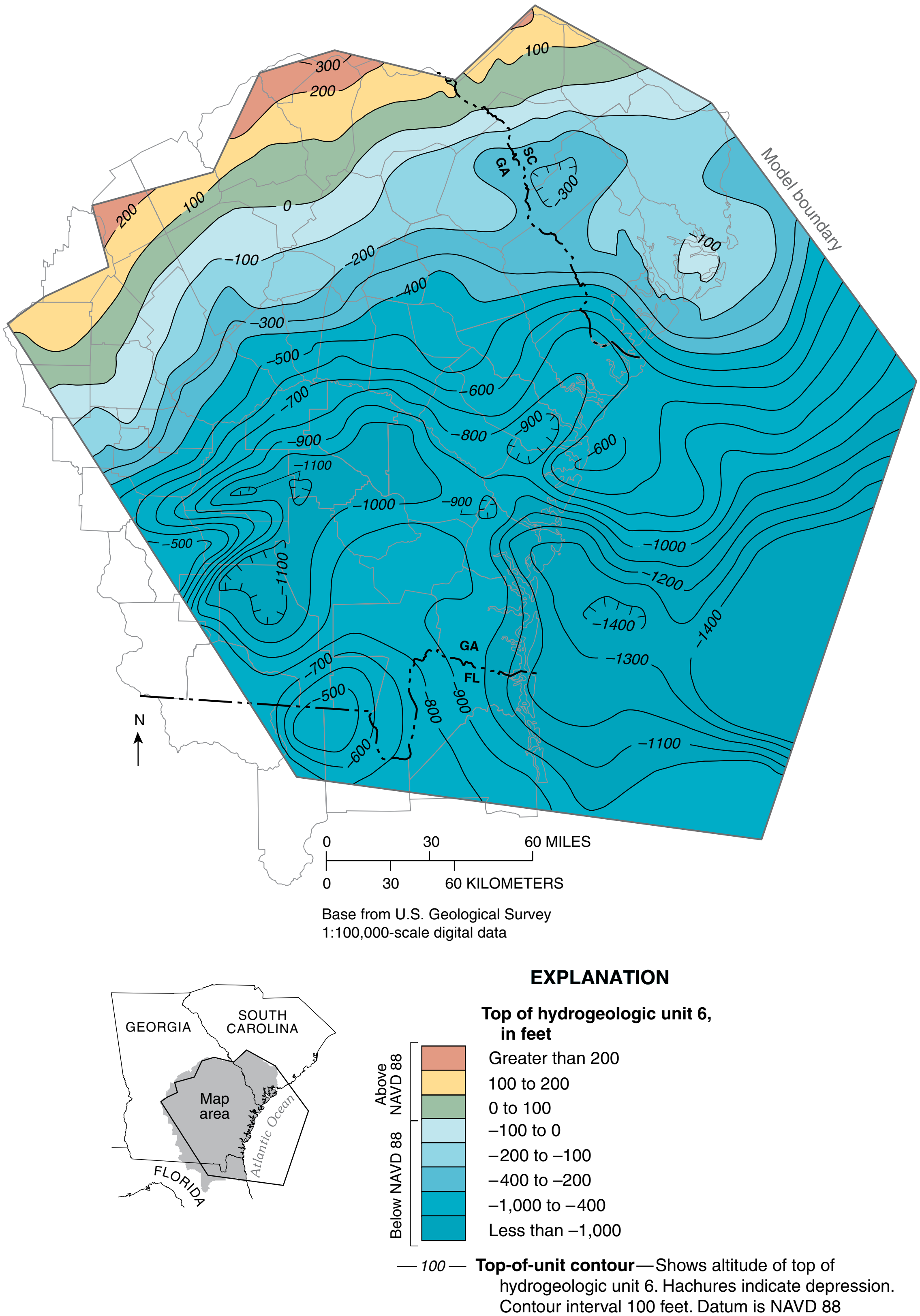

Figure C6. Altitude of top of hydrogeologic unit 6 for model area.

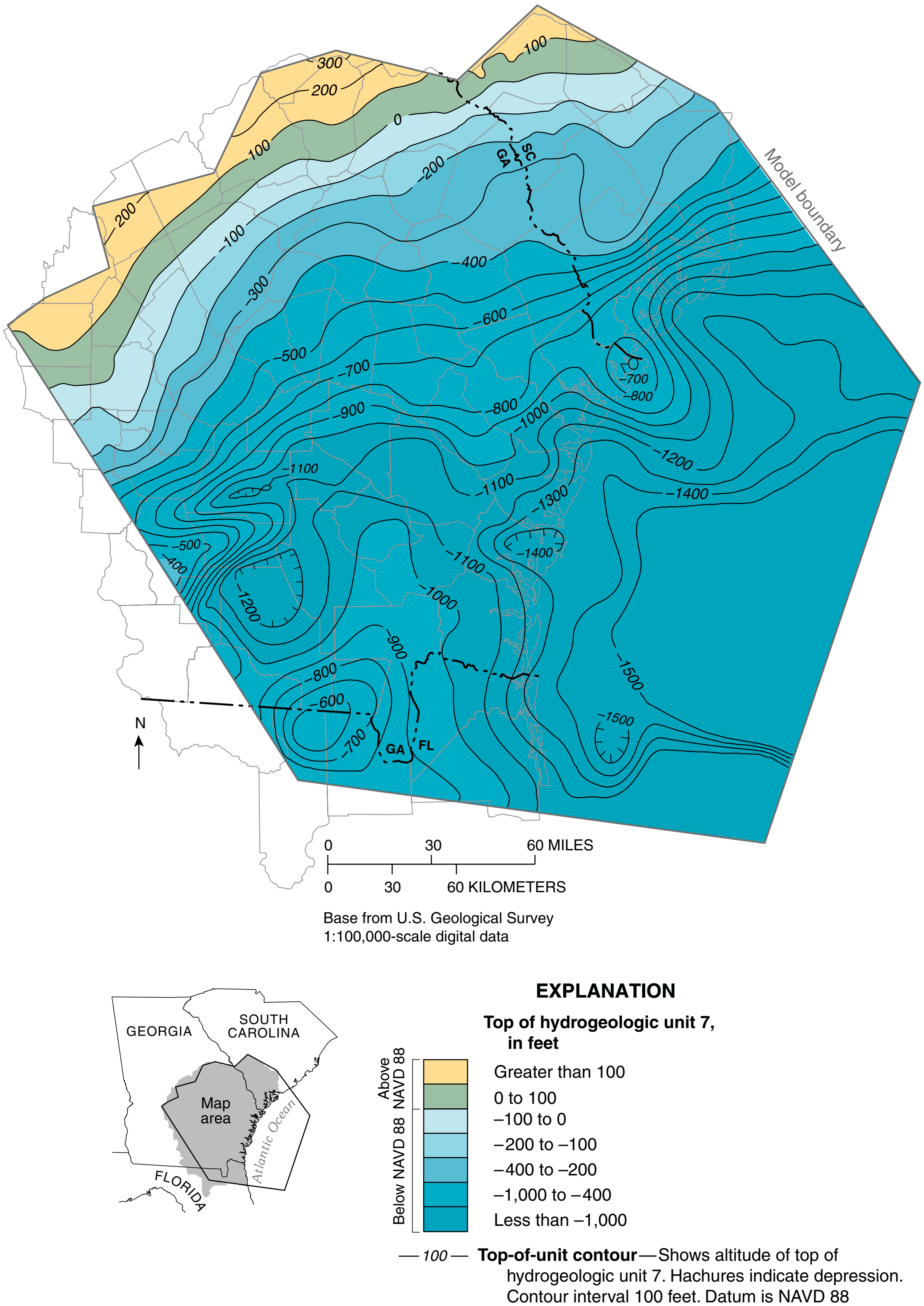

Figure C7. Altitude of top of hydrogeologic unit 7 for model area.

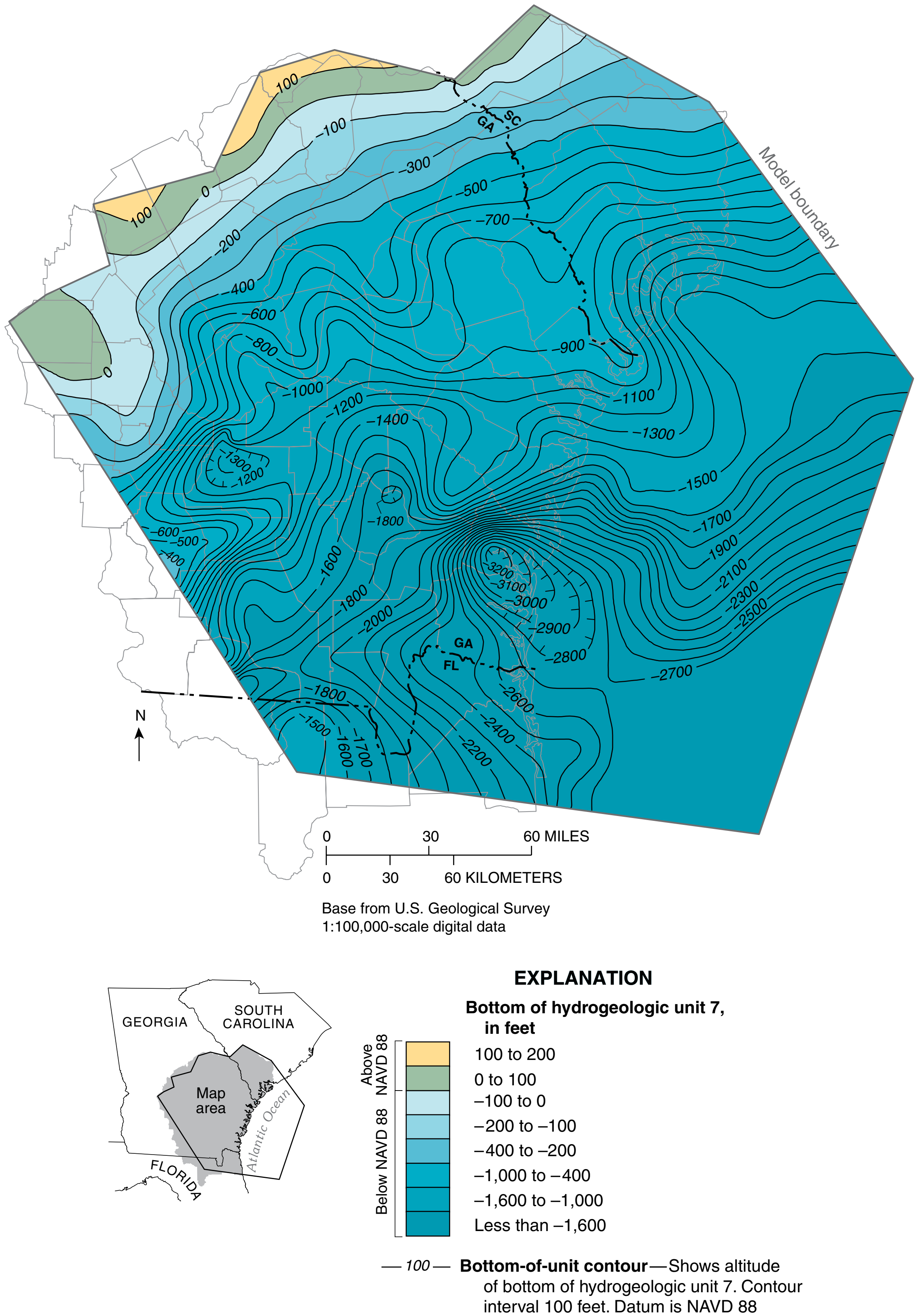

Figure C8. Altitude of bottom of hydrogeologic unit 7 for model area.

Appendix D. Solid Matrix Compressibility

The storage coefficient, the volume of water released from storage per unit change in head, is given by (Voss and Provost, 2003; Smith, 1994)

$$S = \rho g b S_{0p} = 0.0003, \tag{D1}$$

where

ρ = fluid density ≈ 1,000 kg/m^3 (kilogram per cubic meter)
g = acceleration of gravity = 9.81 m/s^2 (meter per second squared)
b = aquifer thickness,
S_{0p} = specific pressure storativity.

The specific pressure storativity is, in turn, given by (Voss and Provost, 2003)

$$S_{0p} = (1 - \varepsilon)\alpha + \varepsilon\beta, \tag{D2}$$

where

ε = porosity,
α = solid matrix compressibility,
β = fluid compressibility ≈ 4.47×10^{-10} (kg/(m·s^2))$^{-1}$ (kilogram per meter second squared to the negative one).

Substituting (D2) into (D1) and solving for α gives

$$\alpha = [(S/\rho g b) - \varepsilon\beta]/(1 - \varepsilon). \tag{D3}$$

Using representative values of $\varepsilon = 0.33$ and $b = 100$ meters for the study area in (D3) results in a solid matrix compressibility of about 2×10^{-10} (kg/(m·s^2))$^{-1}$.

This page left blank intentionally.

Appendix E. Effect of Porosity on Rate of Transport

For fully saturated flow in the absence of solute adsorption, production, or decay, the equation that describes solute transport in SUTRA is (Voss and Provost, 2003)

$$\varepsilon\rho(\partial C/\partial t) + \varepsilon\rho\underline{v}\cdot\nabla C - \nabla\cdot[\varepsilon\rho(D_m\underline{\underline{I}} + \underline{\underline{D}})\cdot\nabla C] = Q_p(C^* - C), \quad \text{(E1)}$$

where

$$\underline{v} = -(\underline{\underline{k}}/\varepsilon\mu)\cdot(\nabla p - \rho\underline{g}) \quad \text{(E2)}$$

is the fluid velocity, and

ε = porosity,

ρ = fluid density,

∇ = gradient symbol

C = mass fraction of solute,

D_m = molecular diffusivity,

$\underline{\underline{I}}$ = identity tensor,

$\underline{\underline{D}}$ = dispersion tensor,

Q_p = fluid mass source,

C^* = solute mass fraction of fluid mass source,

$\underline{\underline{k}}$ = permeability tensor,

μ = fluid viscosity,

p = pressure, and

$\underline{g}$ = gravity vector.

According to (E2), the fluid velocity, which appears in the second term of (E1), is inversely proportional to porosity. The dispersion tensor, which appears in the third term of (E1), is proportional to the fluid velocity (Voss and Provost, 2003) and is therefore also inversely proportional to porosity. Thus, if the porosity were scaled by a uniform factor ϕ throughout the model, ε, $\underline{v}$, and $\underline{\underline{D}}$ would be replaced respectively by $\phi\varepsilon$, $\underline{v}/\phi$, and $\underline{\underline{D}}/\phi$ in (E1), which could then be rearranged to read

$$\rho(\partial C/\partial t') + \varepsilon\rho\underline{v}\cdot\nabla C - \nabla\cdot[\varepsilon\rho(\phi D_m\underline{\underline{I}} + \underline{\underline{D}})\cdot\nabla C] = Q_p(C^* - C), \quad \text{(E3)}$$

where $t' = t/\phi$. Equation (E3) is identical to (E1) except that time has been scaled by ϕ and the molecular diffusivity is premultiplied by ϕ. If molecular diffusion is negligible compared with mechanical dispersion, then (E3) shows that multiplying the porosity by a factor of ϕ changes the rate of solute transport by a factor of $1/\phi$.

Multiplying the longitudinal dispersivity for flow in the horizontal plane near the primary source areas (67.5 meters) by the flow velocity estimated from the rate of advance of the 250-mg/L (milligram per liter) chloride contour toward Savannah (40 meter per year ≈ 1.3×10^{-6} m^2/s (meter squared per second), gives a representative magnitude of about 1×10^{-4} m^2/s for mechanical dispersion. This is five orders of magnitude greater than the molecular diffusivity, 1×10^{-9} m^2/s, so molecular diffusion is negligible compared with mechanical dispersion, and the rate of solute transport is inversely proportional to porosity.

Appendix F. Distribution of Specified Pressure Applied at Model Boundaries

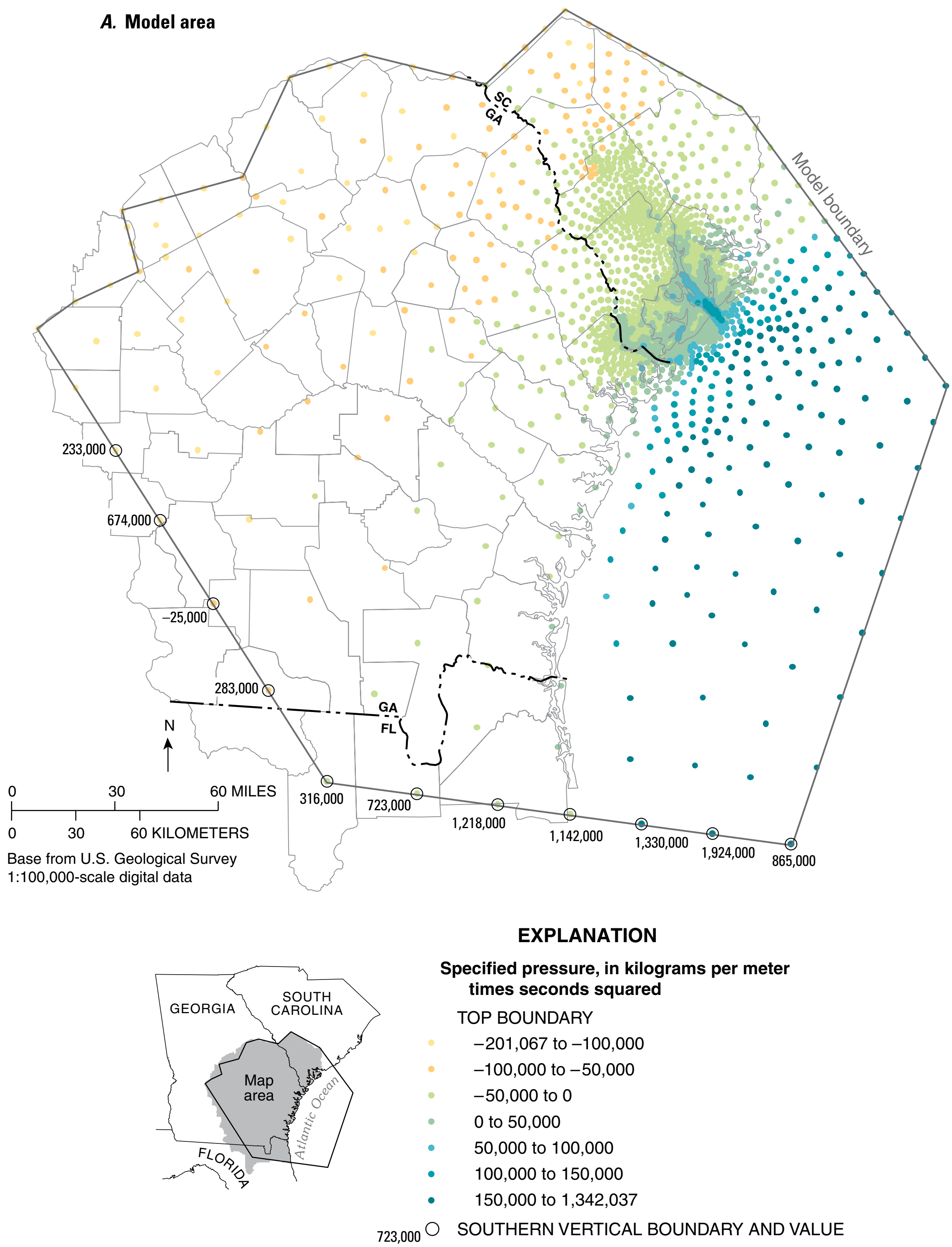

Figure F1. Specified pressure applied to nodes at top boundary (colored symbols) and at top of hydrogeologic unit 5 (Upper Floridan aquifer) at southern vertical boundary (open circles with values) for (*A*) model area and (*B*) study area.

***B.* Study area**

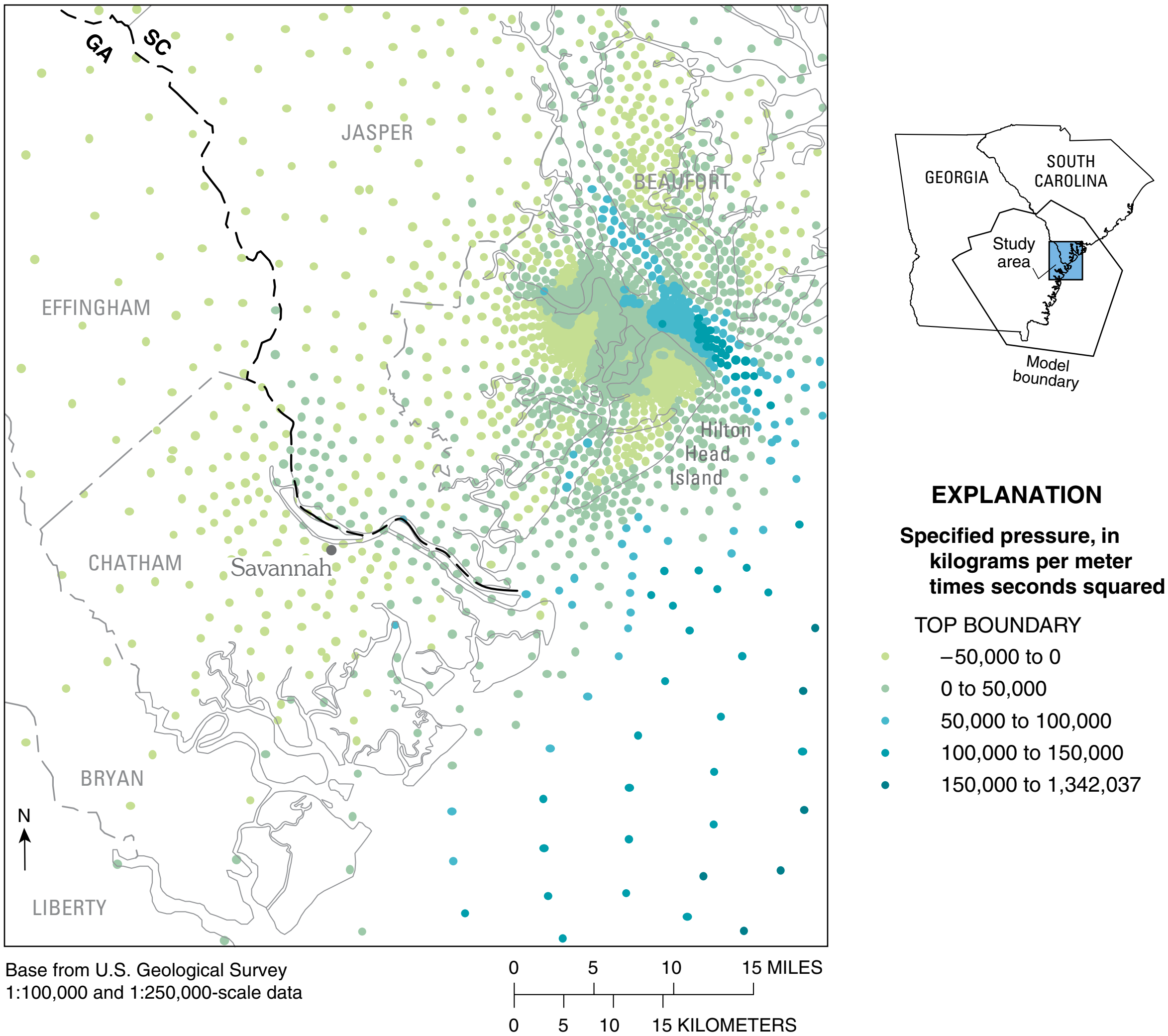

Figure F1. Specified pressure applied to nodes at top boundary (colored symbols) and at top of hydrogeologic unit 5 (Upper Floridan aquifer) at southern vertical boundary (open circles with values) for (*A*) model area and (*B*) study area–continued.

Appendix G. Observed and Simulated Water Levels

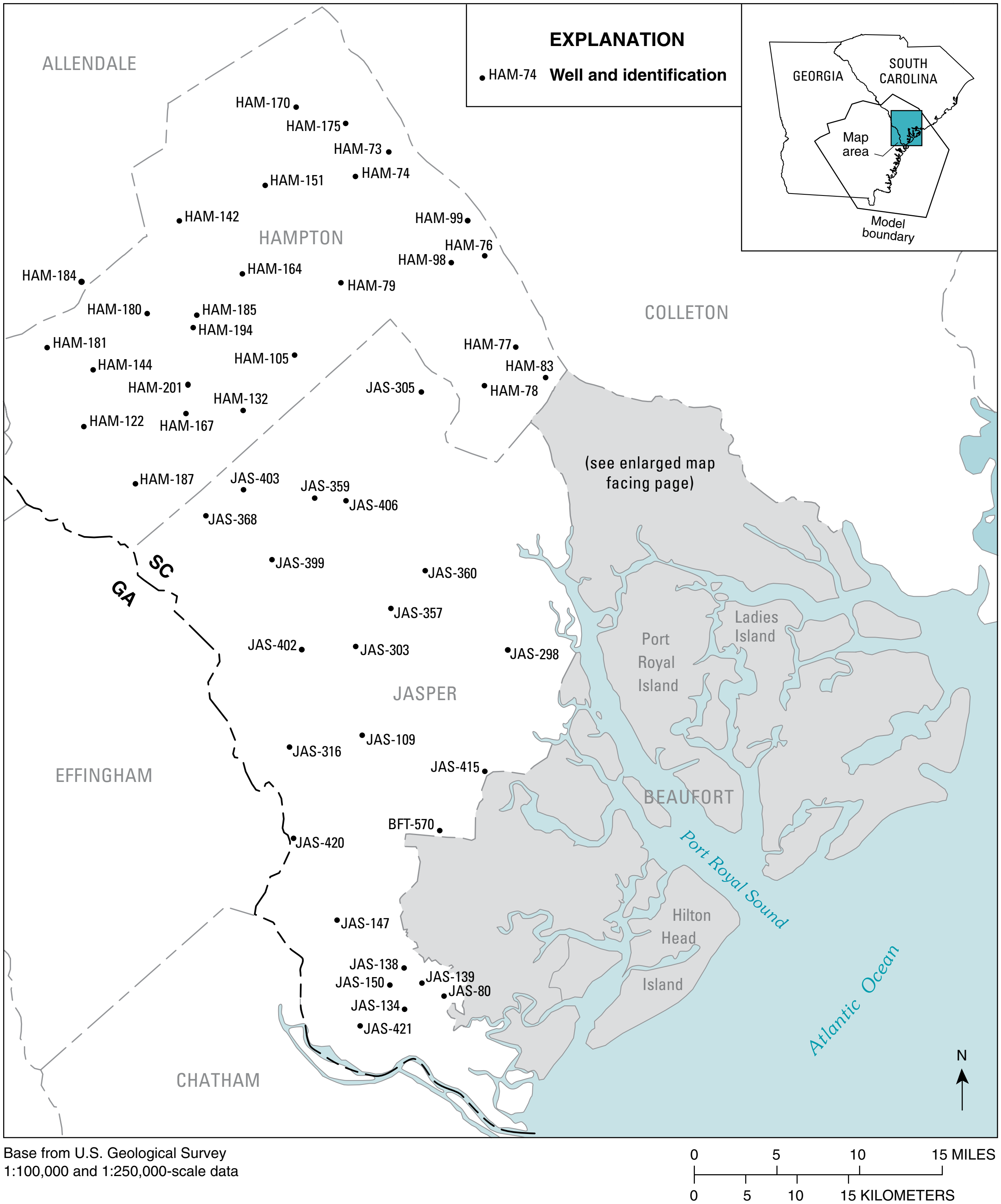

Base from U.S. Geological Survey
1:100,000 and 1:250,000-scale data

Figure G1. Location of wells in Beaufort, Hampton, and Jasper Counties, South Carolina, used for September 1998 simulation (data from Robert Logan, South Carolina Department of Health and Environmental Control, written commun., 2005).

Figure G1. Location of wells in Beaufort, Hampton, and Jasper Counties, South Carolina, used for September 1998 simulation (data from Robert Logan, South Carolina Department of Health and Environmental Control, written commun., 2005)–continued.

Table G1. Measured and simulated water levels, weighted and unweighted residuals (measured minus simulated water level), September 1998.

[ft, feet. Values in bold indicate wells associated with topographic highs on Port Royal and Ladies Islands (see text). Measured water levels reported to a maximum of two decimal places. Simulated water levels and residuals reported to two decimal places. Data from Ransom and White, 1999]

County	Well identifier	Date of water-level measurement	Measured water level (ft)	Assigned weighting factor (ft^{-1})	Weighted water level, dimensionless	Simulated water level (ft), head calibration	Residual (ft), head calibration	Weighted residual (ft), head calibration	Simulated water level (ft), Base Case	Residual (ft), Base Case	Weighted residual (ft), Base Case
Beaufort	BFT-101	09/17/98	–13.19	1	–13.19	–11.17	–2.02	–2.02	–11.44	–1.75	–1.75
	BFT-118	09/15/98	0.40	1	0.40	1.99	–1.59	–1.59	2.50	–2.10	–2.10
	BFT-121	**09/14/98**	**22.20**	**1**	**22.20**	**4.17**	**18.03**	**18.03**	**4.34**	**17.86**	**17.86**
	BFT-124	**09/14/98**	**27.61**	**1**	**27.61**	**4.38**	**23.23**	**23.23**	**4.47**	**23.14**	**23.14**
	BFT-133	09/14/98	1.73	1	1.73	1.54	0.18	0.18	–0.18	1.90	1.90
	BFT-145	09/15/98	–21.56	0	–4.31	–9.86	–11.69	–2.34	–2.15	–19.41	–3.88
	BFT-154	09/19/98	–6.45	1	–6.45	–4.68	–1.77	–1.77	–3.34	–3.11	–3.11
	BFT-181	09/15/98	0.02	1	0.02	–0.90	0.92	0.92	–0.03	0.05	0.05
	BFT-198	09/14/98	6.28	1	6.28	3.67	2.61	2.61	3.51	2.77	2.77
	BFT-301	09/16/98	–12.28	1	–12.28	–7.88	–4.40	–4.40	–6.66	–5.62	–5.62
	BFT-315	09/18/98	–3.67	1	–3.67	–3.17	–0.50	–0.50	–1.01	–2.67	–2.67
	BFT-331	09/16/98	2.37	1	2.37	0.23	2.14	2.14	0.90	1.47	1.47
	BFT-337	09/17/98	–11.50	1	–11.50	–13.75	2.25	2.25	–13.46	1.96	1.96
	BFT-346	09/17/98	–20.14	1	–20.14	–19.27	–0.87	–0.87	–20.10	–0.04	–0.04
	BFT-358	09/18/98	–9.20	1	–9.20	–10.01	0.81	0.81	–7.72	–1.48	–1.48
	BFT-374	09/21/98	–8.60	1	–8.60	–9.48	0.88	0.88	–7.58	–1.01	–1.01
	BFT-392	09/14/98	0.08	1	0.08	3.12	–3.04	–3.04	3.56	–3.49	–3.49
	BFT-420	09/15/98	–19.27	0.2	–3.85	–31.62	12.35	2.47	–2.92	–16.35	–3.27
	BFT-429	09/18/98	–7.31	1	–7.31	–8.78	1.46	1.46	–5.58	–1.73	–1.73
	BFT-430	09/15/98	–0.08	1	–0.08	–0.84	0.76	0.76	–0.26	0.18	0.18
	BFT-435	09/17/98	–15.17	1	–15.17	–15.52	0.35	0.35	–15.23	0.06	0.06
	BFT-436	09/17/98	–13.53	1	–13.53	–13.54	0.01	0.01	–13.17	–0.36	–0.36
	BFT-437	09/17/98	–13.04	1	–13.04	–12.16	–0.88	–0.88	–11.80	–1.24	–1.24
	BFT-439	09/17/98	–21.20	1	–21.20	–18.07	–3.12	–3.12	–17.98	–3.22	–3.22
	BFT-441	09/18/98	–4.81	1	–4.81	–4.69	–0.12	–0.12	–2.82	–1.99	–1.99
	BFT-449	09/15/98	0.32	1	0.32	0.14	0.18	0.18	–0.88	1.20	1.20
	BFT-452	09/17/98	3.00	1	3.00	0.36	2.64	2.64	–0.31	3.31	3.31
	BFT-455	09/15/98	0.52	1	0.52	–0.09	0.61	0.61	–0.92	1.45	1.45
	BFT-456	09/15/98	–0.07	1	–0.07	0.01	–0.08	–0.08	–0.76	0.69	0.69
	BFT-459	09/15/98	–0.14	1	–0.14	–1.13	1.00	1.00	–0.10	–0.04	–0.04
	BFT-461	09/16/98	7.33	0.2	1.47	18.53	–11.20	–2.24	19.63	–12.30	–2.46
	BFT-471	09/15/98	–0.62	1	–0.62	3.17	–3.79	–3.79	3.16	–3.78	–3.78
	BFT-476	09/15/98	–0.94	1	–0.94	–0.20	–0.74	–0.74	0.59	–1.53	–1.53
	BFT-486	09/16/98	–9.14	1	–9.14	–5.73	–3.40	–3.40	–3.73	–5.41	–5.41
	BFT-488	09/15/98	3.63	1	3.63	0.99	2.64	2.64	1.20	2.43	2.43
	BFT-493	09/16/98	–5.48	1	–5.48	–7.50	2.01	2.01	–2.21	–3.27	–3.27
	BFT-497	09/15/98	1.24	1	1.24	0.83	0.41	0.41	0.64	0.61	0.61
	BFT-500	09/19/98	–8.79	1	–8.79	–9.96	1.17	1.17	–7.59	–1.20	–1.20
	BFT-501	09/16/98	–3.95	1	–3.95	–7.40	3.44	3.44	–1.89	–2.07	–2.07
	BFT-502	09/23/98	–4.55	1	–4.55	–7.97	3.42	3.42	–3.74	–0.81	–0.81

Table G1. Measured and simulated water levels, weighted and unweighted residuals (measured minus simulated water level), September 1998.—Continued

[ft, feet. Values in bold indicate wells associated with topographic highs on Port Royal and Ladies Islands (see text). Measured water levels reported to a maximum of two decimal places. Simulated water levels and residuals reported to two decimal places. Data from Ransom and White, 1999]

County	Well identifier	Date of water-level measurement	Measured water level (ft)	Assigned weighting factor (ft^{-1})	Weighted water level, dimensionless	Simulated water level (ft), head calibration	Residual (ft), head calibration	Weighted residual (ft), head calibration	Simulated water level (ft), Base Case	Residual (ft), Base Case	Weighted residual (ft), Base Case
Beaufort	BFT-559	09/14/98	6.84	1	6.84	3.88	2.96	2.96	3.75	3.09	3.09
	BFT-563	09/15/98	2.99	1	2.99	1.50	1.49	1.49	1.85	1.14	1.14
	BFT-564	09/15/98	1.65	1	1.65	0.67	0.98	0.98	1.05	0.60	0.60
	BFT-565	09/15/98	0.31	1	0.31	–0.15	0.46	0.46	0.43	–0.12	–0.12
	BFT-566	09/15/98	1.40	1	1.40	0.31	1.09	1.09	0.83	0.57	0.57
	BFT-570	09/22/98	–17.00	1	–17.00	–12.58	–4.42	–4.42	–11.92	–5.08	–5.08
	BFT-600	09/15/98	3.62	1	3.62	1.20	2.42	2.42	1.53	2.09	2.09
	BFT-651	09/17/98	–6.13	1	–6.13	–6.25	0.12	0.12	–5.34	–0.79	–0.79
	BFT-652	09/18/98	–5.20	1	–5.20	–6.87	1.67	1.67	–6.33	1.13	1.13
	BFT-668	09/17/98	–13.21	1	–13.21	–9.45	–3.76	–3.76	–9.17	–4.03	–4.03
	BFT-676	09/15/98	–6.63	1	–6.63	–7.45	0.82	0.82	–6.38	–0.25	–0.25
	BFT-696	09/17/98	–6.23	1	–6.23	–7.85	1.62	1.62	–7.49	1.26	1.26
	BFT-697	09/18/98	–5.84	1	–5.84	–5.00	–0.84	–0.84	–3.32	–2.53	–2.53
	BFT-704	09/17/98	–15.56	1	–15.56	–15.81	0.24	0.24	–15.54	–0.02	–0.02
	BFT-709	09/17/98	–16.69	1	–16.69	–18.13	1.44	1.44	–18.50	1.81	1.81
	BFT-744	09/17/98	–13.88	1	–13.88	–14.96	1.08	1.08	–14.78	0.90	0.90
	BFT-747	09/17/98	–18.52	1	–18.52	–19.20	0.67	0.67	–19.88	1.36	1.36
	BFT-750	09/17/98	–19.28	1	–19.28	–18.32	–0.96	–0.96	–18.81	–0.47	–0.47
	BFT-767	09/17/98	–8.97	1	–8.97	–7.80	–1.17	–1.17	–6.43	–2.54	–2.54
	BFT-771	09/18/98	–6.81	1	–6.81	–6.24	–0.58	–0.58	–5.20	–1.62	–1.62
	BFT-779	09/17/98	–6.69	1	–6.69	–6.40	–0.30	–0.30	–5.50	–1.19	–1.19
	BFT-782	**09/15/98**	**13.02**	**1**	**13.02**	**2.67**	**10.34**	**10.34**	**2.59**	**10.42**	**10.42**
	BFT-787	09/18/98	–7.08	1	–7.08	–3.33	–3.75	–3.75	–1.71	–5.37	–5.37
	BFT-798	**09/14/98**	**19.97**	**1**	**19.97**	**4.13**	**15.84**	**15.84**	**3.98**	**15.99**	**15.99**
	BFT-801	09/14/98	7.72	1	7.72	3.68	4.04	4.04	3.55	4.17	4.17
	BFT-805	09/17/98	–10.99	1	–10.99	–11.60	0.61	0.61	–11.30	0.31	0.31
	BFT-844	09/16/98	–8.64	1	–8.64	–7.13	–1.51	–1.51	–5.26	–3.38	–3.38
	BFT-976	09/15/98	0.20	1	0.20	0.64	–0.44	–0.44	0.77	–0.57	–0.57
	BFT-982	09/15/98	0.44	1	0.44	1.35	–0.92	–0.92	1.56	–1.12	–1.12
	BFT-985	09/18/98	–10.65	1	–10.65	–6.04	–4.61	–4.61	–5.08	–5.57	–5.57
	BFT-1210	09/15/98	–12.96	1	–12.96	–10.44	–2.52	–2.52	–0.48	–12.48	–12.48
	BFT-1212	09/16/98	–4.98	1	–4.98	–1.16	–3.82	–3.82	1.75	–6.73	–6.73
	BFT-1239	09/17/98	–11.94	1	–11.94	–12.55	0.61	0.61	–12.81	0.87	0.87
	BFT-1247	09/15/98	0.59	1	0.59	1.00	–0.41	–0.41	1.27	–0.69	–0.69
	BFT-1288	09/15/98	0.31	1	0.31	0.65	–0.34	–0.34	1.00	–0.69	–0.69
	BFT-1306	**09/14/98**	**11.71**	**1**	**11.71**	**3.89**	**7.82**	**7.82**	**4.25**	**7.46**	**7.46**
	BFT-1311	09/14/98	9.96	1	9.96	2.42	7.54	7.54	2.15	7.80	7.80
	BFT-1330	09/19/98	–6.55	1	–6.55	–8.70	2.15	2.15	–6.55	0.01	0.01
	BFT-1417	09/15/98	2.33	1	2.33	2.26	0.07	0.07	2.09	0.25	0.25
	BFT-1452	09/21/98	–7.96	1	–7.96	–10.28	2.32	2.32	–8.27	0.31	0.31

Table G1. Measured and simulated water levels, weighted and unweighted residuals (measured minus simulated water level), September 1998.—Continued

[ft, feet. Values in bold indicate wells associated with topographic highs on Port Royal and Ladies Islands (see text). Measured water levels reported to a maximum of two decimal places. Simulated water levels and residuals reported to two decimal places. Data from Ransom and White, 1999]

County	Well identifier	Date of water-level measurement	Measured water level (ft)	Assigned weighting factor (ft^{-1})	Weighted water level, dimensionless	Simulated water level (ft), head calibration	Residual (ft), head calibration	Weighted residual (ft), head calibration	Simulated water level (ft), Base Case	Residual (ft), Base Case	Weighted residual (ft), Base Case
Beaufort	**BFT-1489**	**09/15/98**	**11.18**	**1**	**11.18**	**3.09**	**8.09**	**8.09**	**3.12**	**8.06**	**8.06**
	BFT-1496	09/15/98	2.55	1	2.55	2.46	0.09	0.09	2.16	0.39	0.39
	BFT-1513	09/15/98	1.20	1	1.20	2.64	–1.45	–1.45	2.21	–1.01	–1.01
	BFT-1515	09/14/98	4.46	1	4.46	3.79	0.66	0.66	3.64	0.82	0.82
	BFT-1526	09/15/98	2.72	1	2.72	2.61	0.11	0.11	2.38	0.34	0.34
	BFT-1527	09/15/98	2.93	1	2.93	2.40	0.53	0.53	2.08	0.85	0.85
	BFT-1540	09/15/98	1.89	1	1.89	1.54	0.35	0.35	1.40	0.49	0.49
	BFT-1548	09/15/98	3.03	1	3.03	2.13	0.90	0.90	1.99	1.05	1.05
	BFT-1554	09/15/98	1.08	1	1.08	–0.08	1.16	1.16	0.39	0.69	0.69
	BFT-1588	09/15/98	–5.95	1	–5.95	–7.39	1.45	1.45	–6.39	0.45	0.45
	BFT-1592	09/15/98	2.34	1	2.34	1.47	0.87	0.87	1.53	0.80	0.80
	BFT-1604	09/15/98	–3.19	1	–3.19	0.32	–3.50	–3.50	0.21	–3.40	–3.40
	BFT-1605	09/15/98	3.53	1	3.53	2.70	0.84	0.84	2.34	1.19	1.19
	BFT-1609	09/15/98	2.82	1	2.82	1.62	1.20	1.20	1.10	1.72	1.72
	BFT-1611	09/16/98	–0.43	1	–0.43	3.35	–3.79	–3.79	3.45	–3.89	–3.89
	BFT-1635	09/16/98	–10.36	1	–10.36	–8.25	–2.11	–2.11	–6.41	–3.95	–3.95
	BFT-1689	09/16/98	–2.63	1	–2.63	–4.67	2.04	2.04	–1.03	–1.60	–1.60
	BFT-1701	09/15/98	0.42	1	0.42	1.80	–1.39	–1.39	2.08	–1.67	–1.67
	BFT-1709	09/14/98	4.44	1	4.44	1.69	2.75	2.75	15.91	–11.47	–11.47
	BFT-1714	09/14/98	2.99	1	2.99	3.45	–0.46	–0.46	3.57	–0.59	–0.59
	BFT-1717	09/14/98	2.19	1	2.19	3.51	–1.33	–1.33	3.69	–1.50	–1.50
	BFT-1718	09/14/98	3.36	1	3.36	3.39	–0.02	–0.02	3.53	–0.17	–0.17
	BFT-1727	**09/14/98**	**7.22**	**1**	**7.22**	**3.45**	**3.77**	**3.77**	**3.85**	**3.37**	**3.37**
	BFT-1728	**09/14/98**	**15.90**	**1**	**15.90**	**4.11**	**11.79**	**11.79**	**4.39**	**11.51**	**11.51**
	BFT-1731	**09/14/98**	**5.43**	**1**	**5.43**	**3.33**	**2.10**	**2.10**	**3.80**	**1.63**	**1.63**
	BFT-1732	**09/14/98**	**24.56**	**1**	**24.56**	**4.43**	**20.13**	**20.13**	**4.53**	**20.03**	**20.03**
	BFT-1733	09/14/98	7.94	1	7.94	2.74	5.20	5.20	2.32	5.62	5.62
	BFT-1734	09/14/98	2.69	1	2.69	2.15	0.54	0.54	1.58	1.11	1.11
	BFT-1736	09/15/98	–1.82	1	–1.82	0.03	–1.85	–1.85	0.77	–2.59	–2.59
	BFT-1742	09/17/98	–10.43	1	–10.43	–7.58	–2.86	–2.86	–7.06	–3.38	–3.38
	BFT-1743	09/14/98	–5.80	1	–5.80	–0.46	–5.34	–5.34	–0.11	–5.69	–5.69
	BFT-1744	09/17/98	–8.86	1	–8.86	–7.03	–1.84	–1.84	–6.24	–2.63	–2.63
	BFT-1748	09/17/98	–3.96	1	–3.96	–7.04	3.08	3.08	–6.18	2.21	2.21
	BFT-1752	09/15/98	0.83	1	0.83	0.78	0.06	0.06	0.70	0.13	0.13
	BFT-1773	09/15/98	3.15	1	3.15	3.34	–0.19	–0.19	3.30	–0.16	–0.16
	BFT-1810	09/18/98	–5.39	1	–5.39	–2.93	–2.47	–2.47	–0.95	–4.45	–4.45
	BFT-1840	09/16/98	–1.40	1	–1.40	–1.17	–0.23	–0.23	–0.14	–1.26	–1.26
	BFT-1841	09/16/98	1.90	1	1.90	–1.17	3.07	3.07	–0.14	2.04	2.04
	BFT-1846	09/18/98	–8.84	1	–8.84	–8.19	–0.65	–0.65	–4.05	–4.79	–4.79
	BFT-1867	09/17/98	1.04	1	1.04	0.00	1.05	1.05	0.59	0.45	0.45

Table G1. Measured and simulated water levels, weighted and unweighted residuals (measured minus simulated water level), September 1998.—Continued

[ft, feet. Values in bold indicate wells associated with topographic highs on Port Royal and Ladies Islands (see text). Measured water levels reported to a maximum of two decimal places. Simulated water levels and residuals reported to two decimal places. Data from Ransom and White, 1999]

County	Well identifier	Date of water-level measurement	Measured water level (ft)	Assigned weighting factor (ft^{-1})	Weighted water level, dimensionless	Simulated water level (ft), head calibration	Residual (ft), head calibration	Weighted residual (ft), head calibration	Simulated water level (ft), Base Case	Residual (ft), Base Case	Weighted residual (ft), Base Case
Beaufort	**BFT-1925**	**09/14/98**	**24.72**	**1**	**24.72**	**4.37**	**20.35**	**20.35**	**4.53**	**20.19**	**20.19**
	BFT-1950	**09/14/98**	**27.84**	**1**	**27.84**	**4.41**	**23.43**	**23.43**	**4.51**	**23.33**	**23.33**
	BFT-1969	09/15/98	–2.02	1	–2.02	1.34	–3.35	–3.35	1.63	–3.65	–3.65
	BFT-1970	09/15/98	0.13	1	0.13	1.42	–1.29	–1.29	1.71	–1.58	–1.58
	BFT-1971	09/15/98	2.13	1	2.13	1.47	0.65	0.65	1.76	0.36	0.36
	BFT-1972	09/15/98	0.41	1	0.41	1.38	–0.98	–0.98	1.67	–1.26	–1.26
	BFT-1974	09/15/98	0.03	1	0.03	1.44	–1.42	–1.42	1.73	–1.70	–1.70
	BFT-1975	09/15/98	–1.24	1	–1.24	1.39	–2.62	–2.62	1.68	–2.91	–2.91
	BFT-1976	09/15/98	0.70	1	0.70	1.48	–0.78	–0.78	1.76	–1.06	–1.06
	BFT-1977	09/15/98	–3.37	1	–3.37	1.36	–4.72	–4.72	1.66	–5.03	–5.03
	BFT-1985	09/16/98	1.63	1	1.63	3.78	–2.15	–2.15	3.83	–2.20	–2.20
	BFT-1987	09/15/98	0.18	1	0.18	0.69	–0.50	–0.50	1.20	–1.02	–1.02
	BFT-1994	09/16/98	2.25	1	2.25	3.54	–1.29	–1.29	3.64	–1.39	–1.39
	BFT-1996	09/15/98	2.13	1	2.13	1.94	0.19	0.19	2.18	–0.05	–0.05
	BFT-2000	09/15/98	1.28	1	1.28	2.50	–1.23	–1.23	2.72	–1.45	–1.45
	BFT-2007	09/15/98	4.10	1	4.10	3.04	1.06	1.06	3.24	0.86	0.86
	BFT-2038	09/23/98	–16.54	1	–16.54	–13.01	–3.53	–3.53	–12.13	–4.41	–4.41
	BFT-2050	09/18/98	–4.90	1	–4.90	–3.51	–1.39	–1.39	–2.38	–2.52	–2.52
	BFT-2051	09/15/98	4.64	1	4.64	0.47	4.17	4.17	1.04	3.60	3.60
	BFT-2052	09/18/98	–4.68	1	–4.68	–5.66	0.98	0.98	–4.38	–0.31	–0.31
	BFT-2162	09/16/98	–4.80	1	–4.80	–3.43	–1.36	–1.36	–2.30	–2.49	–2.49
	BFT-2163	09/16/98	–4.24	1	–4.24	–3.29	–0.95	–0.95	–2.14	–2.10	–2.10
	BFT-2164	09/16/98	–3.20	1	–3.20	–3.19	–0.01	–0.01	–1.21	–1.99	–1.99
	BFT-2165	09/16/98	–5.87	1	–5.87	–7.25	1.39	1.39	–5.77	–0.09	–0.09
	BFT-2166	09/15/98	–1.90	1	–1.90	–3.85	1.95	1.95	–1.50	–0.40	–0.40
	BFT-2189	09/15/98	–0.64	1	–0.64	–3.25	2.61	2.61	–1.00	0.36	0.36
	BFT-2190	09/15/98	–3.32	1	–3.32	–4.99	1.67	1.67	–3.72	0.40	0.40
	BFT-2197	09/18/98	–3.06	1	–3.06	–3.40	0.34	0.34	–1.26	–1.80	–1.80
Hampton	HAM-73	09/18/98	56.80	0.2	11.36	66.43	–9.63	–1.93	65.95	–9.15	–1.83
	HAM-74	09/18/98	75.89	0.2	15.18	64.70	11.19	2.24	63.67	12.21	2.44
	HAM-76	09/18/98	32.92	0.2	6.58	41.50	–8.58	–1.72	43.96	–11.04	–2.21
	HAM-77	09/18/98	11.81	0.2	2.36	27.07	–15.26	–3.05	27.82	–16.01	–3.20
	HAM-78	09/18/98	13.09	0.2	2.62	22.83	–9.74	–1.95	22.85	–9.76	–1.95
	HAM-79	09/18/98	43.06	0.2	8.61	46.38	–3.32	–0.66	46.39	–3.34	–0.67
	HAM-83	09/18/98	8.23	0.2	1.65	21.91	–13.68	–2.74	22.75	–14.52	–2.90
	HAM-98	09/18/98	35.56	0.2	7.11	41.77	–6.21	–1.24	43.27	–7.71	–1.54
	HAM-99	09/18/98	36.56	0.2	7.31	49.25	–12.69	–2.54	49.37	–12.81	–2.56
	HAM-105	09/17/98	39.37	0.2	7.87	39.18	0.18	0.04	39.63	–0.26	–0.05
	HAM-122	09/14/98	56.40	0.2	11.28	50.57	5.83	1.17	50.37	6.04	1.21
	HAM-132	09/17/98	27.78	0.2	5.56	36.36	–8.58	–1.72	35.40	–7.62	–1.52

Table G1. Measured and simulated water levels, weighted and unweighted residuals (measured minus simulated water level), September 1998.—Continued

[ft, feet. Values in bold indicate wells associated with topographic highs on Port Royal and Ladies Islands (see text). Measured water levels reported to a maximum of two decimal places. Simulated water levels and residuals reported to two decimal places. Data from Ransom and White, 1999]

County	Well identifier	Date of water-level measurement	Measured water level (ft)	Assigned weighting factor (ft^{-1})	Weighted water level, dimensionless	Simulated water level (ft), head calibration	Residual (ft), head calibration	Weighted residual (ft), head calibration	Simulated water level (ft), Base Case	Residual (ft), Base Case	Weighted residual (ft), Base Case
Hampton	HAM-142	09/18/98	104.96	0.2	20.99	82.14	22.82	4.56	84.00	20.96	4.19
	HAM-144	09/14/98	69.24	0.2	13.85	58.80	10.44	2.09	58.65	10.59	2.12
	HAM-151	09/18/98	91.91	0.2	18.38	74.82	17.09	3.42	75.25	16.66	3.33
	HAM-164	09/17/98	74.09	0.2	14.82	58.76	15.32	3.07	59.56	14.52	2.91
	HAM-167	09/17/98	47.72	0.2	9.54	39.88	7.84	1.57	39.41	8.31	1.66
	HAM-170	09/18/98	101.58	0.2	20.32	87.19	14.39	2.88	87.96	13.62	2.72
	HAM-175	09/17/98	69.76	0.2	13.95	75.62	–5.86	–1.17	73.55	–3.79	–0.76
	HAM-180	09/14/98	87.06	0.2	17.41	62.02	25.03	5.01	61.51	25.54	5.11
	HAM-181	09/14/98	50.52	0.2	10.10	71.18	–20.65	–4.13	69.71	–19.19	–3.84
	HAM-184	09/14/98	101.90	0.2	20.38	83.28	18.62	3.73	81.76	20.14	4.03
	HAM-185	09/14/98	85.95	0.2	17.19	56.40	29.54	5.91	55.38	30.56	6.11
	HAM-187	09/14/98	36.55	0.2	7.31	36.71	–0.16	–0.03	35.09	1.45	0.29
	HAM-194	09/14/98	87.26	0.2	17.45	54.05	33.20	6.64	52.13	35.13	7.03
	HAM-201	09/17/98	61.38	0.2	12.28	44.08	17.30	3.46	43.84	17.54	3.51
Jasper	JAS-80	09/14/98	–33.11	1	–33.11	–32.16	–0.95	–0.95	–33.89	0.78	0.78
	JAS-109	09/17/98	–6.43	1	–6.43	–5.70	–0.73	–0.73	–6.02	–0.41	–0.41
	JAS-134	09/17/98	–43.29	1	–43.29	–44.98	1.69	1.69	–47.65	4.36	4.36
	JAS-138	09/17/98	–27.56	1	–27.56	–32.16	4.60	4.60	–33.80	6.24	6.24
	JAS-139	09/17/98	–34.60	1	–34.60	–33.19	–1.41	–1.41	–34.94	0.34	0.34
	JAS-147	09/17/98	–35.02	1	–35.02	–31.52	–3.50	–3.50	–33.96	–1.06	–1.06
	JAS-150	09/17/98	–41.88	1	–41.88	–40.64	–1.24	–1.24	–43.38	1.50	1.50
	JAS-298	09/17/98	–2.83	1	–2.83	–0.12	–2.71	–2.71	0.46	–3.29	–3.29
	JAS-303	09/14/98	0.70	1	0.70	1.03	–0.33	–0.33	1.33	–0.63	–0.63
	JAS-305	09/14/98	20.07	0.2	4.01	25.70	–5.63	–1.13	26.06	–6.00	–1.20
	JAS-316	09/17/98	–9.55	1	–9.55	–6.95	–2.60	–2.60	–8.47	–1.08	–1.08
	JAS-357	09/14/98	–1.40	1	–1.40	3.29	–4.69	–4.69	4.81	–6.21	–6.21
	JAS-359	09/14/98	18.01	1	18.01	21.43	–3.42	–3.42	21.16	–3.15	–3.15
	JAS-360	09/14/98	2.21	1	2.21	6.61	–4.40	–4.40	7.38	–5.17	–5.17
	JAS-368	09/14/98	24.82	1	24.82	25.22	–0.40	–0.40	24.35	0.47	0.47
	JAS-399	09/14/98	17.81	1	17.81	16.64	1.18	1.18	16.23	1.58	1.58
	JAS-402	09/14/98	7.56	1	7.56	3.54	4.02	4.02	2.90	4.66	4.66
	JAS-403	09/14/98	25.93	1	25.93	26.31	–0.38	–0.38	25.97	–0.04	–0.04
	JAS-406	09/14/98	14.82	1	14.82	19.11	–4.29	–4.29	18.43	–3.61	–3.61
	JAS-415	09/17/98	–10.35	1	–10.35	–7.75	–2.60	–2.60	–6.84	–3.51	–3.51
	JAS-420	09/17/98	–19.64	1	–19.64	–19.86	0.22	0.22	233.50	–253.10	–253.10
	JAS-421	09/17/98	–68.40	1	–68.40	–64.22	–4.18	–4.18	–69.03	0.63	0.63

Manuscript approved for publication, February 24, 2006
Prepared by USGS Georgia Water Science Center
Edited by Patricia L. Nobles
Graphics by Caryl J. Wipperfurth
For more information concerning the research in this report, contact
Georgia Water Science Center, Atlanta,
telephone 770-903-9100